Identification and characterization of Adenosine A_{2A} heteromers in the CNS

Identificació i caracterització d'heteròmers d'Adenosina A_{2A} al SNC

Marc Brugarolas Campillos

UNIVERSITAT DE BARCELONA

FACULTAT DE BIOLOGIA
DEPARTAMENT DE BIOQUÍMICA I BIOLOGIA MOLECULAR

Identification and characterization of Adenosine A_{2A} heteromers in the CNS.

Identificació i caracterització d'heteròmers d'Adenosina A_{2A} al SNC.

Memòria presentada pel Llicenciat en Biologia

Marc Brugarolas Campillos

per a optar al grau de Doctor per la Universitat de Barcelona.

Aquesta tesi s'ha adscrit al Departament de Bioquímica i Biologia Molecular de la Universitat de Barcelona, dins del programa de doctorat de Biomedicina.

El treball experimental i la redacció de la present memoria han estat realitzats per Marc Brugarolas Campillos sota la direcció del Dr. Rafael Franco Fernández i del Dr. Vicent Casadó Burillo.

Dr. Rafael Franco Fernández

Dr. Vicent Casadó Burillo

Marc Brugarolas Campillos
Barcelona, setembre del 2013.

INDEX

LIST OF ABBREVIATIONS

[^{3}H]: ^{3}H-labeled

[^{35}S]: ^{35}S-labelled

2-AG: 2-Arachidonoylglycerol

5-HT_{2B}R: 5- hydroxytryptamine (serotonin) receptor 2B

A_1R: Adenosine A_1 receptor

A_{2A}R: Adenosine A_{2A} receptor

A_{2A}^{A374}R: Adenosine receptor A_{2A} with a mutation in the position 374 of a serine to an alanine.

A_3R: Adenosine A_3 receptor

AC: Adenylyl cyclase

ADA: Adenosine deaminase

ADP: Adenosine diphosphate

Ala: Alanine

α-MEM: α-Modification of minimum essential medium.

AMP: Adenosine monophosphate

AMPA: α-amino-3-hydroxy-5-methyl-4-isoxazolepropionic acid

ANOVA: Analysis of variance

ATP: Adenosine triphosphate

B_{50}: Concentration competing 50% of radioligand binding

BAY-59-3074: 3-[2-Cyano-3-(trifluoromethyl) phenoxy] phenyl 4, 4, 4-trifluoro-1-butanesulfonic acid ester

BCA: Bicinchoninic acid assay

BDNF: Brain-derived neurotrophic factor

BiLFC: Bimolecular fluorescence complementation

BRET: Bioluminescence resonance energy transfer

BSA: Bovine serum albumin

CADO: 2-Chloro-adenosine

Ca^{2+}: Calcium

cAMP: Cyclic adenosine monophosphate

CB_1R: Cannabinoid CB_1 receptor

CCPA: 2-Chloro-N-cyclopentyladenosine

cDNA: Cyclic deoxyribonucleic acid

CDS: Cellular dielectric spectroscopy

CGS 21680: 4-[2-[[6-Amino-9-(N-ethyl-β-D-ribofuranuronamidosyl)-9H-purin-yl]amino]ethyl]benzenepropanoic acid hydrochloride

CHDI: Curing Huntington's disease initiative

CHO: Chinese hamster ovary cells

ChTx: Cholera toxin

cm: Centimeter

CNS: Central nervous system

CP 55,940: (-)-*cis*-3-[2-Hydroxy-4-(1,1-dimethyl-heptyl)phenyl]-*trans*-4-(3-hydroxypropyl)cyclohexanol

CPA: (N^6-Cyclopentyladenosine)

CREB: cAMP response element-binding protein

cRluc: C-terminus renilla luciferase

Cy3: Cyanine 3

cYFP: C-terminus yellow fluorescent protein

D_2R: Dopamine D_2 receptor

DAG: Diacylglycerol

DARPP-32: Dopamine- and cyclic AMP-regulated phosphoprotein of 32 kDa

DAT: Dopamine transporter

D_{CB}: Dimer cooperativity index for the competing ligand B

ddH_2O: Double distilled water

Δ^9-THC: Δ^9-tetrahydrocannabinol

DGL: Diacylglycerol lipase

DMEM: Dulbeco's modified Eagle's medium

DMSO: Dimethyl-sulfoxyde

DNA: Deoxyribonucleic acid

DPCPX: 8-Cyclophenyl-1,3-dipropylxantine

DTT: Dithiothreitol

ECL: Extracellular

EDTA: Ethylenediaminetetraacetic acid

eGFP: Enhanced green fluorescent protein

Elk1: ETS domain-containing protein 1

EMCCD: Electron multiplying charge-coupled device

EMG: Electromyographic

ER: Endoplasmic reticulum

ERK: Extracellular signal-regulated kinases

ETS: E-twenty six transcription factor

EYFP: Enhanced yellow fluorescent protein

FAD: Flavin adenine dinucleotide

FAAH: Fatty acid amide hydrolase

FBS: Foetal Bovine Serum

Fig.: Figure

FITC: Fluorescein isothiocyanate

FRAP: Fluorescence recovery after photobleaching

FRET: Förster resonance energy transfer

FSH: Follicle-stimulating hormone

GABA: *Gamma*-aminobutyric acid

GABAergic: *Gamma*-Aminobutyric-acidergic

GAT: *Gamma*-aminobutyric acid transporter

GDP: Guanosine-5'-diphosphate

GEF: Guanine nucleotide exchange factor

GFAP: Glial fibrillary acidic protein

GFP: Green fluorescent protein

GPCR: G-protein coupled receptor

Gpe: Globus pallidus external segment

Gpi: Globus pallidus internal segment

GRK: G-protein receptor kinase

GTP: Guanosine-5'-triphosphate

GTP-γ-S: Guanosine-5'-O-gamma-thiophosphate

H: Hour

HBSS: Hank's balanced salt solution

HD: Huntington's disease

HEPES: 4-(2-Hydroxyethyl)-1-piperazineethanesulfonic acid

HEK: Human embryonic kidney cells

HPLC: High-performance liquid chromatography

HTS: High-throughput screening

HU210: (6aR, 10aR)-9-(Hydroxymethyl)-6,6-dimethyl-3-(2-methyloctan-2-yl)-6a, 7, 10,

10a -tetrahydrobenzo [c]chromen-1-ol

IC_{50}: Half maximal inhibitory concentration

ICL: Intracellular

i.e.: id est, for example

IgG: Immunoglobulin G

I.P.: Intraperitoneal

JNK: c-Jun N-terminus kinase

KO: Knock out

K^+: Potassium

K_D: Dissociation constant

K_M: Michaelis constant

KW 6002: (E)-1,3-diethyl-8-(3,4-dimethoxystyryl)-7-methyl-3,7-dihydro-1H-purine-2,6-dione

L-DOPA: L-3,4-dihydroxyphenylalanine

L-VDCC: L-type voltage dependent channels

MAPK: Mitogen-activated protein kinase

mBU: Milli BRET units : net BRET X 1000

MEK: MAPK kinase

$mGluR_1$: Type I metabotropic glutamate receptor

μm: Micro meter

μM: Micro molar

$\mu m^2/s$: Micro square meters per second

Min: Minute

ms: Milliseconds

MSD: Mean square displacement

MSK1: Mitogen- and stress-activated protein kinase-1

MSN: Medium spiny neurons

MSX 2: (E)-3-(3-hydroxypropyl)-8-[2-(3-methoxyphenyl)vinyl]-7-methyl-1-prop-2-ynyl-3,7.dihydropurine-2,6-dione

MSX 3: (E)-phosphoric acid mono-(3-{8-[2-(3-methoxyphenyl)vinyl]-7-methyl-2,6-dioxo-1-prop-2-ynyl-1,2,6,7-tetrahydropurin-3-yl}propyl) ester disodium salt

NaCl: Sodium chloride

NAD^+: Aldehyde dehydrogenase

$NADP^+$: 2-Oxoaldehyde dehydrogenase

nM: Nano molar

nm: Nano meter

NMDA: N-methyl-D-aspartate

NR2B: Glutamate [NMDA] receptor subunit epsilon-2 or NMDA receptor subtype 2B

nRluc: N-terminus renilla luciferase

nYFP: N-terminus yellow fluorescent protein

OR: Opioid receptor

PBP: Periplasmic binding protein

PBS: Phosphate buffered saline

PCC: Power correlation coefficient

PD: Parkinson's disease

PEI: Polyethylenimine

PET: Positron emission tomography

PFA: Paraformaldehyde

PI3K: Phosphoinositide 3-kinase

PKA: Protein kinase A

PKC: Protein kinase C

PLC: Phospholipase C

PM: Plasma membrane

PoliQ: Poliglutamine

PP-1: Protein phosphatase-1

PTx: Pertussis toxin

QA: Quinolinic acid

PVDF: Polyvinylidene fluoride

RAMP: Receptor activity modifying proteins

RET: Resonance energy transfer

Rluc: Renilla luciferase

RMS: Root mean square

Rp-cAMP: Rp-cyclic 3',5'-hydrogen phosphorothioate adenosine triethylammonium salt

R-PIA: R-phenyl-isopropyladenosine

RSK: Ribosomal s6 kinase

S: Second

S1P: Sphingosine-1-phosphate

S.C.: Subcutaneous

SCH 420814: 2-(2-furanyl)-7-[2-[4-[4-(2-methoxyethoxy)phenyl]-1-piperazinyl]ethyl]-7H-pyrazolo[4,3-e][1,2,4]-triazolo[1,5-c]pyrimidin-5-amine

SCH 442416: 2-(2-Furanyl)-7-[3-(4-methoxyphenyl)propyl]-7H-pyrazolo [4.3- e] [1,2,4] triazolo [1,5-c] pyrimidin-5-amine

SCH 58261: [2-(2-furanyl)-7-(2-phenylethyl)-7H-pyrazolo [4,3-e][1,2,4]triazolo[1,5-c]pyrimidin-5-amine]

SDS: Sodium dodecyl sulfate

SDS-PAGE: Sodium dodecyl sulfate polyacrylamide gel electrophoresis

SEM: Standard error of the mean

Ser: Serine

SKF 89976A: hydrochloride [1-(4,4-diphenil-3-butenyl)-3-piperidinecarboxylic acid hydrochloride]

SNc: Substantia nigra pars compacta

SNr: Substantia nigra pars reticulata

SPT: Single particle tracking

SRET: Sequential resonance energy transfer

STN: Subthalamic nucleus

THC: Tetrahydrocannabinol

TIRF: Total internal reflection fluorescence

TM: Transmembrane

TMD: Transmembrane domains

Tris: Tris(hydroxymethyl)aminomethane

TRITC: Tetramethylrhodamine isothiocyanate

TR-FRET: Time-resolved FRET

TRK: Tyrosine kinase receptor

TSH: Thyroid-stimulating hormone

TWEEN: Polysorbate

U73122: 1-[6[[(17-β)-3-methoxyestra-1,3,5(10)-trien-17-yl]amino]hexyl]-1H-pyrrole-2,5-dione

VER 7835: 2-amino-6-(furan-2-yl)-N-(thiophen-2-ylmethyl)-9H-purine-9-carboxamide

VTA: Ventral tegmental area

WIN-55,212-2: (R)-(+)-[2, 3- Dihydro-5-methyl-3-(4-morpholinylmethyl) pyrrolo [1, 2, 3 – de]- 1, 4 – benzoxazin-6-yl]-1-napthalenylmethanone

YFP: Yellow fluorescent protein

I. INTRODUCTION

1. G-protein coupled receptors.

G-protein coupled receptors (GPCR) or seven transmembrane domain receptors (7-TM) are the biggest protein superfamily and the most versatile group of membrane receptors involved in signal transduction. In humans, more than 1% of the genome codes for more than a thousand of these proteins, 90% of which are expressed in the Central Nervous System (CNS) (George et al., 2002; Gudermann et al., 1997).

The chemical diversity of the endogenous ligands for these receptors is wide and include amines, peptides, glucoproteins, lipids, nucleotides and ions (Kolakowski, 1994). Environment stimuli perception is also mediated by GPCR such as light, taste and smell (Figure 1). It has been estimated that half of the modern drugs target these receptors (Flower, 1999). These drugs only target a small proportion of the GPCR superfamily and the potential finding of new drug therapies in this field is still very large.

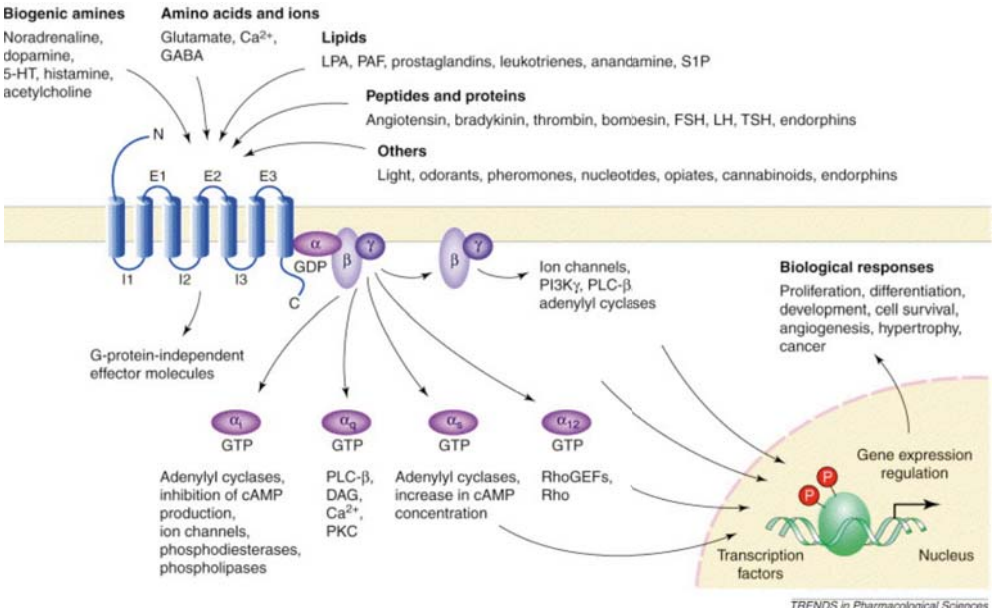

Figure 1. GPCR endogenous ligands and signaling mechanisms. A wide variety of ligands use GPCR to stimulate cytoplasmic and nuclear targets through heterotrimeric G-protein-dependent and –independent pathways. Such signaling pathways regulate key biological functions such as cell proliferation, cell survival and angiogenesis (Marinissen and Gutkind, 2001).

1.1. GPCR function and structure.

GPCR have seven transmembrane domains (TMs). These TMs are between 25 and 35 consecutive amino acids that show a relatively high degree of hydrophobicity and form a recognizable and an intra-extracellular stimuli transmission-capable unit. You can find the protein N-terminus in the extracellular space whereas the C-terminus is inside the cell. The first GPCR crystal structure appeared in 2000 (Palczewski et al., 2000) and it was the high definition structure of bovine rhodopsin. With a resolution of 2.3 Å, it was confirmed that the α-helical transmembrane domains (TMD) rearranged in a closely packed bundle forming the transmembrane receptor core. The seven transmembrane helices are connected by six alternating intracellular (ICL) and extracellular (ECL) loops (Figure 1). In the last 12 years, more than 75 structures of 18 different family A GPCR have been determined in complex with ligands of varied pharmacology, peptides, antibodies and G-protein (Venkatakrishnan et al., 2013).

The correct integration and orientation of the polypeptide is done in the endoplasmic reticulum (ER) and the α-helices are stabilized inside the lipid bilayer due to the molecule hydrophobicity, facing the polar residues to the receptor core, minimizing the hydrophobic interactions with the bilayer. Finally, in a second stage, the functional tertiary structure is formed by the specific interactions between helices leading to the ring-shape compact structure of the transmembrane domains.

Another characteristic of the GPCR is its interaction with a heterotrimeric G-protein, a guanine nucleotide-exchanging unit, from which most of the receptor signaling will be directed. As shown in Figure 1, some signaling mechanisms are dependent on the receptor-G-protein interaction: after the receptor activation there is a conformational change that is transmitted to the G-protein α-subunit (G_α), which exchanges a GDP nucleotide for a GTP. This provokes that the G_α subunit bound to GTP dissociates from the receptor and

from the βγ dimer ($G_{\beta\gamma}$) (Marinissen and Gutkind, 2001). The two resulting subunits, G_{α} bound to GTP and $G_{\beta\gamma}$ are capable of activate or modulate different cellular signaling pathways such as adenylate cyclase activation or inhibition, phospholipase activation or potassium and calcium channel activity regulation (Hamm, 1998).

However, GPCR action mechanisms are complex and some years ago was proved that GPCR can produce signals independently of G-protein (Daaka et al., 1998; Lefkowitz, 1998). It has been suggested that agonist-induced receptor phosphorylation through G-protein receptor kinases (GRK) and the subsequent arrestin and surface receptor recruiting are not only important mechanisms for decreasing the signaling capacity of the receptor but also play a key role in switching the receptor from G-protein-coupled-dependent signaling pathways to G-protein-independent signaling cascades normally associated with growth factor receptors (Ferguson, 2001; Krupnick and Benovic, 1998; Luttrell and Lefkowitz, 2002; Woehler and Ponimaskin, 2009).

The exposure of GPCR to agonists often results in a rapid attenuation of receptor responsiveness. This receptor desensitization process is the consequence of a combination of different mechanisms. These mechanisms include the receptor uncoupling from the heterotrimeric G-proteins in response to receptor phosphorylation (Ferguson, 2001; Hausdorff et al., 1989; Lohse et al., 1990), the internalization of cell surface receptors to various intracellular compartments (Hermans et al., 1997; Marchese et al., 2008; Trejo et al., 1998), and the down-regulation of the total number of receptors in the cell. The latter of the three is accomplished through mechanisms to reduce receptor mRNA and protein synthesis, as well as the lysosomal degradation of pre-existing receptors (Jockers et al., 1999; Pak et al., 1999). The time range over which these processes occur is from seconds (phosphorylation) to minutes (endocytosis) and hours (down-regulation of surface receptors) and the amount of receptor desensitization varies from the complete termination of receptor signaling, as observed in the visual and olfactory systems, to the attenuation of agonist potency and

maximal responsiveness, such as observed for the β_2-adrenergic receptor (Sakmar, 1998). The different receptor desensitization is regulated by a number of factors concerning the receptor structure and cellular environment.

The most rapid means by which GPCR are uncoupled from heterotrimeric G-proteins is through the covalent modification of the receptor through its phosphorylation by intracellular kinases (Figure 2). It is generally accepted that both second messenger-dependent protein kinases (cAMP-dependent protein kinase A and protein kinase C) and GRK phosphorylate serine and threonine residues within the intracellular loops and carboxyl-terminal tails of GPCR (Krupnick and Benovic, 1998; Lefkowitz et al., 1993). Second-messenger dependent protein kinases not only phosphorylate agonist-activated GPCR, but also indiscriminately phosphorylate receptors that have not been exposed to agonist (Hausdorff et al., 1989). In contrast, GRK family members selectively phosphorylate agonist-activated receptors, thereby promoting the binding of cytosolic cofactor proteins called arrestins, which uncouple the receptor from heterotrimeric G-proteins (Kang et al., 2013; Kendall and Luttrell, 2009; Lohse et al., 1990; Luttrell and Gesty-Palmer, 2010).

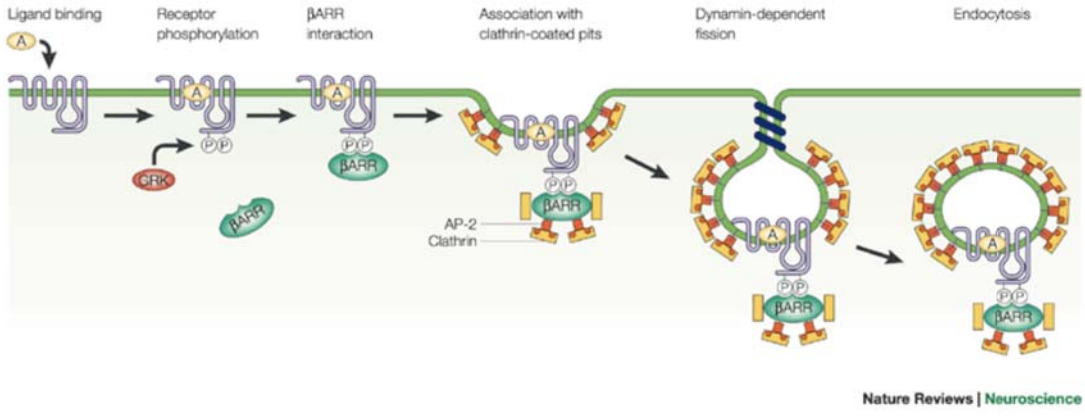

Figure 2. Desensitization and internalization model proposed for the GPCR. After agonist (A) binding to GPCR, GRK phosphorylate residues in the third intracellular loop and carboxyl tail of GPCR, leading to the recruitment of β-arrestins (βARR). The β-arrestins recruit clathrin and the AP-2 complex, which target GPCR for clathrin-mediated endocytosis (Pierce and Lefkowitz, 2001).

GPCR internalization following agonist-administration is a commonly observed response. Over the years, numerous reports have addressed the role of receptor recruitment in desensitization and resensitization. Indeed, trafficking of an uncoupled receptor to endosomal compartments allows dephosphorylation and recycling of the receptor to the cell surface (Krueger et al., 1997). This is in contrast to receptor down-regulation observed after prolonged agonist exposure, which leads to targeting of the receptors to degradation pathways (Böhm et al., 1997). Once internalized, receptors are targeted to recycling or degradation pathways. GRK and β-arrestins appear to be key regulatory molecules for receptor internalization since these proteins have been shown to interact with components of the clathrin-coated vesicle pathway (Figure 2). Nevertheless, not all GPCRs necessarily internalize in a β-arrestin-/clathrin-dependent manner but may also be internalized through alternative endocytic pathways. Some GPCRs have been found in cholesterol rich plasma membrane structures termed caveolae (Burgueño et al., 2003a; Chun et al., 1994; Huang et al., 1997). These domains are also known as signaling domains, but appear to contain proteins involved in the formation of vesicles such as dynamin. Finally, some receptors seem to use a third alternative endocytic pathway. No coat or adaptor proteins have been identified for the generation of these vesicles (Claing et al., 2000). However, GPCR desensitization and endocytosis can act as molecular switches coupling GPCR to alternative signal transduction pathways. β-Arrestins not only function in the molecular switch required for GPCR desensitization and internalization, but also act as scaffolds to transduce and compartmentalize the alternative signals. In fact, β-arrestins have the ability to interact with a variety of endocytic and signaling proteins such as c-SRC (Luttrell et al., 1999), MAPK and Raf (DeFea et al., 2000).

1.2. GPCR classification.

GPCR do not share any overall sequence homology, the only common feature to all GPCR is the presence of seven transmembrane-spanning α-helical segments connected by alternating intracellular and extracellular loops. Two cysteine residues conserved in most GPCR (one in ECL1 and one in ECL2), form a disulfide bond, which is presumed to be important for the packaging and stabilization of a restricted number of conformations of these seven transmembrane domains (Baldwin, 1994; Probst et al., 1992). Aside from wide sequence variations, GPCRs differ in the length and function of their intracellular N-terminus domain, their intracellular C-terminus domain, and the six alternating ICL and ECL.

GPCRs have been classified based on several systems. One of the oldest is the Kolakowski system (Kolakowski, 1994), in which GPCR are grouped in six families (A-F) according to its structure and genetic characteristics. In Figure 3 are represented the three biggest families: A, B and C. The rest of smaller families are D, E (yeast pheromone receptors) and F, constituted by four cAMP receptors from *Dictoyostelium discoideum* (Kolakowski, 1994).

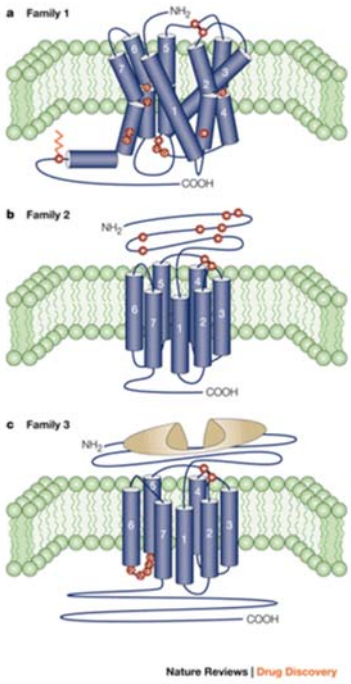

Figure 3. Schematic representation of the biggest GPCR families. The transmembrane domains are drawn in blue and the conserved residues are the red spheres.

Family A is by far the biggest and most studied. It contains 90% of all the GPCR such as rhodopsin and a lot of hormone and neurotransmitter receptors. There is a low homology among these receptors and is concentrated in certain key very conserved amino acidic residues, a fact that suggests that these residues are essential for the structure and function of the receptors. The only amino acid residue conserved among all family A receptors is the arginine in the Asp-Arg-Tyr (DRY) motif, which is located on the cytoplasmic side of the third transmembrane domain (Probst et al., 1992) and is believed to be involved in G-protein activation. A lot of receptors from this family have a palmiloylated cysteine in the C-terminus tail that is used for anchoring the receptor to the membrane. The ligands are usually bound to these receptors through a cavity formed by the transmembrane domains, although in some cases this interactions takes place in the extracellular loops and in the N-terminus tail (George et al., 2002; Jacoby et al., 2006). The receptors studied in this thesis belong to this family.

Family B receptor includes approximately 20 different hormone and neuropeptide receptors, such as vasoactive intestinal peptide, calcitonin and glucagon. Except for the disulfide bond connecting the ECL1 and ECL2, family B receptors do not contain any structural features in common with family A. The DRY motif is absent. The most prominent characteristic of family B receptors is a long (of approximately 100 residues) extracellular N-terminus that contains several cysteine residues (George et al., 2002; Jacoby et al., 2006), presumably forming a network of bisulfide bridges (Ulrich et al., 1998).

Family C receptors' main characteristic is an exceptionally long N-terminus tail (500 to 600 amino acids). This family includes metabotropic glutamate, GABA, and calcium receptors among others. Similarly to the previous families, family C receptor contains two putative disulfide bonds in ECL1 and ECL2, but do not share any conserved residues. Each receptor in the family C possesses a very large extracellular domain that shares a low but significant sequence similarity to bacterial periplasmic binding proteins (PBP). In addition, these receptors have a short and highly conserved ICL3. As a consequence of the crystallographic studies performed with glutamate metabotropic receptor bound to glutamate, it has been proposed that the ligand binding to these receptors takes place in its extracellular N-terminus tail (Conn and Pin, 1997; O'Hara et al., 1993).

The A-F GPCR classification is widely accepted, however, after performing the first phylogenetic study of the entire superfamily of GPCR a more accurate classification was proposed (Fredriksson et al., 2003). According to this classification method, also known as GRAFS, human GPCR can be divided into five families that share a common evolutionary origin: glutamate, rhodopsin, adhesion, frizzled/taste2 and secretin. The old A, B, C family system is compatible with the new system (Attwood and Findlay, 1994), although the two others are not included.

1.3. Signaling pathways.

GPCR owe their name to the interaction with heterotrimeric G-proteins, constituted of α (39-46 kDa), β (37 kDa) and γ (8 kDa). Upon ligand activation, conformational changes are induced that transmit from the receptor to G-protein and make the α subunit release GDP and bind GTP. This action permits a conformational change between the G_{α} subunit and the complex $G_{\beta\gamma}$ separating them. Both G_{α} and $G_{\beta\gamma}$ complex acting with different effector molecules can activate or inhibit a big variety of second messengers. The signal terminates when the intrinsic GTPase activity of G_{α} hydrolyzes GTP to GDP and phosphate (Bourne et al., 1991). Four big families of G_{α} subunits exist in mammals, characteristic by their primary structure and a signaling cascade that they activate (Milligan and Kostenis, 2006). $G_{\alpha s}$ family stimulates adenylate cyclase, $G_{\alpha i/o}$ inhibits adenylate cyclase, $G_{\alpha q/11}$ activates phospholipase C_{β} (PLC_{β}) and $G_{\alpha 12/13}$ regulates Rho proteins.

Two typical examples of signaling cascades initiated by GPCR are those that lead to formation of inositol-1, 4, 5-triphosphate (IP_3/DAG) and cAMP as second messengers. The effector protein target of $G_{\alpha q}$ subunit is PLC, an enzyme that hydrolyses membrane phosphoinositols and generates IP_3 and DAG as second messengers. IP_3 increases intracellular concentration of calcium depleting its intracellular deposits meanwhile DAG activates PKC. The effector molecule of $G_{\alpha s}$ and $G_{\alpha i}$ subunits is adenylate cyclase (AC), an enzyme catalyzing conversion of ATP to cAMP, meanwhile $G_{\alpha s}$ stimulates it and $G_{\alpha i}$ inhibits it. cAMP activates PKA that as PKC, phosphorylates multitude of diverse proteins (receptors, ion channels, enzymes or transcription factors) regulating thus cell functions.

Many responses mediated by GPCRs do not consist simply of stimulation of conventional second messenger, but are a result of integration of different signaling networks among which MAPK and JNK can be included. Activation of MAPK via a GPCR was poorly studied up until the last decade. It was known that this mechanism involved a *Bordetella pertussis* toxin sensible G-protein ($G_{\alpha i/o}$) and strongly dependent of the $G_{\beta\gamma}$ complex

and of not identified tyrosine kinases (van Corven et al., 1993; Faure et al., 1994; Koch et al., 1994). Thus it was deduced that in the absence of ligands with tyrosine kinase receptor (TRK) activity the activation of GPCR could induce the stimulation of TRK generating mitogenic signals. This phenomenon was called transactivation. Once transactivated, TRK initiates a signaling cascade identical to the one generated by its proper ligand, this means MAPK activation via Ras, Raf, MEK and ERK1/2 pathway (Figure 3).

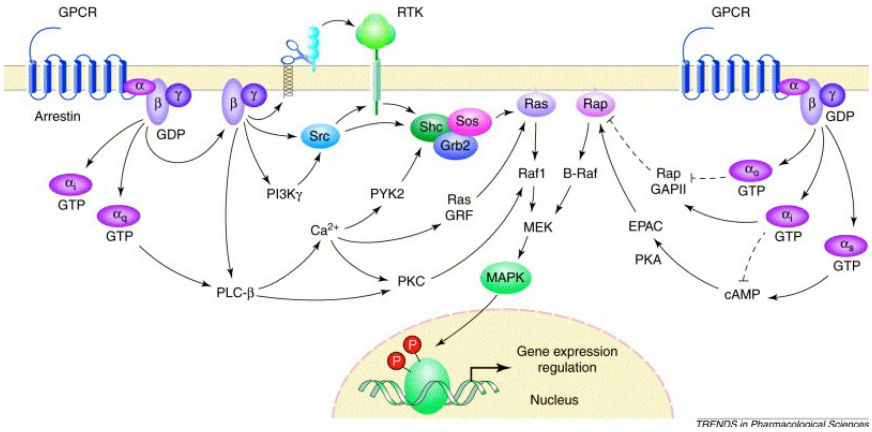

Figure 3. Scheme of multiple pathways linking GPCR to mitogen-activated protein kinase (MAPK). Abbreviations: EPAC: exchange protein activated by cAMP, GAP: GTPase-activating protein, GRF: guanine-nucleotide releasing factor, MEK: MAPK kinase, PI3K: phosphoinositide 3-kinase, PKA: protein kinase A, PLC: phospholipase C, RTK: receptor tyrosine kinase (Marinissen and Gutkind, 2001).

The process is initiated by the $G_{\beta\gamma}$ subunit resulting in recruitment of Sos towards the membrane. This activates the GDP/GTP exchange in Ras protein, acting as a mediator connecting signaling cascades generated by TRK transactivation and ERK1/2 phosphorylation (Marinissen and Gutkind, 2001). Other pathways independent of transactivation exist that can lead to Ras activation, for example, pathways dependent on intracellular calcium concentration induced by GPCR coupled to $G_{\alpha q}$ (Figure 3).

Activation of ERK1/2 requires a phosphorylation of two residues, serine and threonine, separated by only one amino acid and can only be performed by a highly specialized enzyme. This enzyme, MEK, is considered a rate-limiting step of ERK1/2

activation. Finally, $G_{\alpha s}$ subunit activation can lead to ERK1/2 activation via cAMP-PKA dependent signaling pathway. Activated ERK1/2 is transferred to the nucleus where it regulates via phosphorylation other kinases and transcription factors (Davis et al., 1995). Recently, new data revealed more of the complexity of GPCR signaling showing that GPCR can signal not only dependently of G-protein but also by G-protein independent mechanism which probably implicate direct union of Src and/or β-arrestins to the receptors (Daaka et al., 1998; Lefkowitz, 1998; Luttrell and Lefkowitz, 2002).

1.4. GPCR interacting proteins.

Many GPCRs contain sequence motifs that are known to direct protein-protein interactions and, therefore, have the theoretical capacity to interact with a wide range of other proteins. Such interactions might determine receptor properties, like cellular compartmentalization or signaling, and can promote complexes that integrate their functions through protein scaffolding (Bockaert et al., 2004).

GPCR topology offers several potential interaction regions. Their extracellular loops are relatively short causing extracellular interactions to take place in the N-terminus tail. It looks like these extracellular interactions play a key role in GPCR pharmacology, as an example we have adenosine deaminase (ADA), a multifunctional protein that can be present in the cellular surface as an ecto-enzyme, forming heteromeric complexes with adenosine receptors A_1, A_{2A} and A_{2B}. These interactions seem to be essential so the receptors can bind its physiological ligands with a high affinity state (Gracia et al., 2008, 2011; Herrera et al., 2001; Saura et al., 1996).

However, on the intracellular site of GPCR, both the C-terminus tail and the third intracellular loop can be of a considerable size. Thus, these regions are more likely to interact with signaling and other intracellular proteins like cytoskeletal proteins or trafficking-related proteins. The length of these interactions varies from transitory (i.e. signaling purposes) to

more stable interactions. Either way, these complexes are considered dynamic (Canals et al., 2003; Franco et al., 2003). One classical example of GPCR interacting proteins is cytoskeletal-anchoring polypeptides. This is the case of α-actinin and adenosine $A_{2A}R$ (Burgueño et al., 2003b), α-filamin and dopamine D_2R (Lin et al., 2001) and the Shank family of proteins and several other GPCR including type I metabotropic glutamate receptor ($mGluR_1$) (Sheng and Kim, 2000).

Protein-protein interactions can also take place in the plasma membrane. Since the nineties, a great number of studies have shown GPCR oligomerization (George et al., 2002). Nowadays it is accepted that the formation of homodimers, heterodimers and higher order oligomers are a common biological characteristic of these receptors (Agnati et al., 2003, 2010; Bouvier, 2001; Carriba et al., 2008; Devi, 2001; Ferré et al., 2009a, 2010a; Ferre and Franco, 2010; Franco et al., 2003; Prinster et al., 2005; Tadagaki et al., 2012). It is also assumed that when a GPCR participates in an oligomer, its functional properties can be modified, conferring new properties to the receptor and therefore establishing new functional mechanisms that lead to a more complex control over signaling and regulation of these proteins (Figure 4).

2. GPCR oligomerization.

2.1. GPCR oligomerization evidence.

Traditionally GPCR ligand-binding and signal-transduction mechanisms were based on the presumption that these receptors where monomers or independent proteins that acted with a 1:1 stoichiometry with G-protein. Certain indirect pharmacological evidence made the scientific community think that maybe GPCRs acted as dimers. Complex binding competition results, both agonists and antagonists, were interpreted as evidences of a cooperativity that can be explained as receptor interactions forming dimer or oligomer complexes (Franco et al., 1996; Wreggett and Wells, 1995).

In 1993, Maggio and collaborators suggested heterodimer formation using α_2-adrenergic receptors and M_3 muscarinic receptors chimeras, cloning the first five transmembrane domains of one receptor and the two last of the other one and *vice versa*. With these chimeras, complementation and co-immunoprecipitation studies were performed. When chimeras were expressed independently no ligand binding or signaling was observed, otherwise, when they were transfected together, binding and signaling either for adrenergic and muscarinic ligands were reestablished (Maggio et al., 1993). Hence, GPCR oligomerization is not limited to homomerization (physical association between two identical proteins), it is also possible the association of different types of receptors (heteromerization) forming dimers or higher order oligomers. However, oligomers are frequently treated as dimers as the simplest functional unit.

The different cross talk observed between neurotransmitter receptors can not be explained without the possibility of direct GPCR interactions. It has been described higher levels of organization in which GPCRs not only constitute homomers and heteromers but supramolecular complexes constituted by more than one receptor-oligomer type and a group of receptor activity modifying proteins (RAMP). These complexes interact at the plasma membrane and when activated by hormones or neurotransmitters are redistributed in clusters

that can be regulated by other receptors and molecules even though there is no direct physical interaction (Franco et al., 2003).

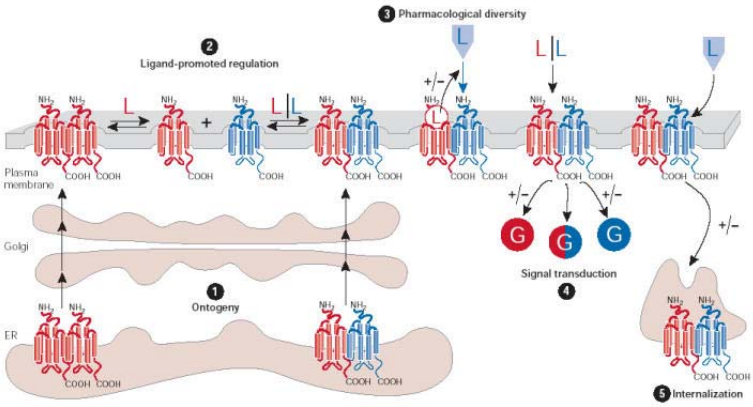

Figure 4. Receptor heteromerization properties. The fact that a receptor heteromerizes can lead to an alteration of its properties in the cell involving changes in the cellular location (1), ligand modulation (2), pharmacological diversity (3), signal transduction (4) or internalization (5) (Terrillon and Bouvier, 2004a).

The number and the increasing complexity of the publications in this field made it necessary to establish new definitions and assign a proper nomenclature to receptor oligomers and its associated phenomena, as Ferré and colleagues published (Ferré et al., 2009a).

2.2. Architecture of the heteromers.

To explain GPCR heteromerization we need to consider two possibilities: a direct interaction where there is physical contact between receptors, or an indirect interaction where some bridge-proteins are necessary like cytoskeletal proteins.

The case of direct interactions are believed to be formed at the plasma reticulum, due to this, they are not affected by ligands, meaning that does not affect to the formation or destruction of the heteromer. With the great structural complexity of the GPCR superfamily

is not recommendable to think of a single direct interaction mechanism (Bouvier, 2001). This interaction can be covalent, through disulfide bonds or non-covalent (electrostatic and hydrophobic forces) between transmembrane domains or intracellular receptors (Figure 5).

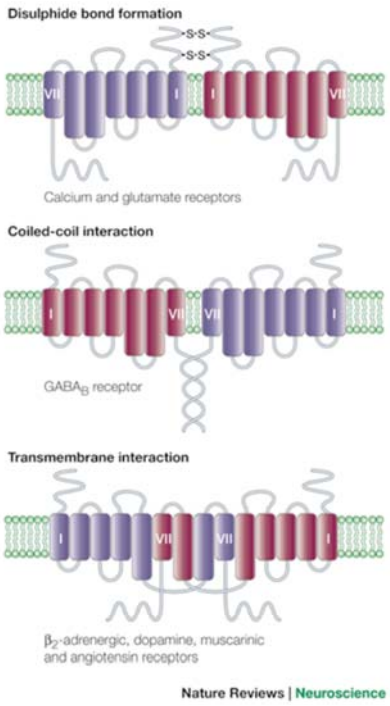

Figure 5. Schematic representation of the different GPCR interactions (Bouvier, 2001).

In family C GPCR, the large extracellular N-terminus domain has some cysteine residues that can contribute to dimerization through disulfide bonds. This is the case of calcium-sensing receptors and metabotropic glutamate receptor (Robbins et al., 1999; Romano et al., 2001) and the case of some family A GPCR like κ - and δ -opioid receptors or dopamine D_1 receptors (Cvejic and Devi, 1997; Jordan and Devi, 1999). It has also been described interactions where C-terminus domain is essential, like δ -opioid receptor dimerization (Cvejic and Devi, 1997) or coiled-coil interactions between carboxyl tails in the formation of $GABA_{B1}$ and $GABA_{B2}$ receptor heteromer (Margeta-Mitrovic et al., 2000; White et al., 1998).

Finally, direct interactions can be established by electrostatic or hydrophobic interactions between extracellular or intracellular domains or transmembrane receptors. It has been demonstrated that ionic interactions take place between peptides in the intracellular domains containing two or more positive adjacent charges and two or more negative charges (Woods and Huestis, 2001). One example of this kind of interactions is adenosine $A_{2A}R$ or dopamine D_2R dimerization (Ciruela et al., 2004) or the interactions between the heterotrimer formed by adenosine A_{2A}, dopamine D_2 and cannabinoid CB_1 receptors (Navarro et al., 2010). Hydrophobic interactions could have a key role in β_2-adrenergic dimer receptor formation, more precisely because of certain glycine and leucine residues of the sixth transmembrane domain (Hebert et al., 1996). It has also been proposed the same type of interactions for the dimerization of some dopamine receptors (Ng et al., 1996). All these interaction mechanisms proposed indicate multiple interaction sites involved in the heteromer assembly and stability.

Computational studies proposed two alternative 3D models that could describe the GPCR dimer assembly (Figure 6). The first model is a "swapping-domain model", in which each functional unit within the dimer is composed by the first five transmembrane domains of one polypeptide chain and the last two of the second. This model would rationalize the functional complementation observed when mutant or chimeric receptors were studied (Maggio et al., 1993; Scarselli et al., 2000). The second model is the "contact model", in which each polypeptide forms a receptor unit that is in contact to the other through interactions involving transmembrane domains five and six (Gouldson et al., 2000).

Validation of these models awaits additional studies, the most direct of which would come from the resolution of the structure of a GPCR receptor dimer. Oligomeric assembly of proteins, allowing expanded diversity with a limited number of modular elements, is the rule rather that the exception in biology. When considering the nervous system, the existence of homo- and heterodimers of neurotransmitter GPCR raises the hypothesis that could

underlie the high degree of diversity and plasticity that is characteristic of such highly organized and complex system.

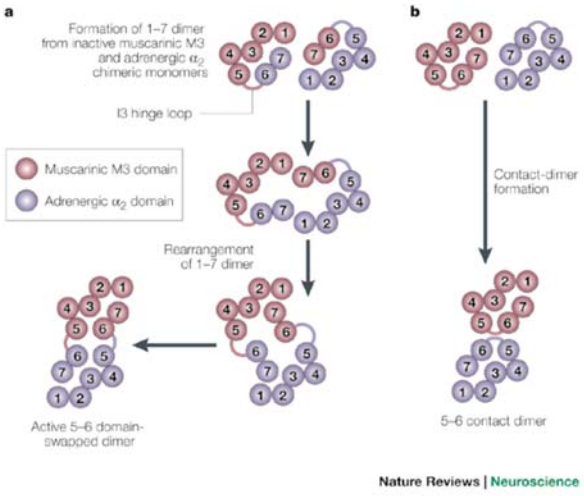

Figure 6. Alternative 3D models showing GPCR dimers. "Swapped-domain model" (a) and "contact model" (b) (Bouvier, 2001).

2.3. Techniques used to identify GPCR dimers.

The first indirect evidence of the existence of GPCR dimers was provided by pharmacological studies. Complex radioligand binding data demonstrating either positive or negative cooperativity, hinted at the possibility of physical interactions between receptors (Mattera et al., 1985). Radioligand binding assays remain to be a very important experimental tool to identify the presence of heteromers in native tissues after the so-called "molecular fingerprints" have been discovered from the studies with membrane preparations of transfected cells.

To demonstrate the formation of heteromers, experiments with chimeric (Maggio et al., 1993) or dominant-negative receptor mutants were performed. Chimeric α_2-adrenergic / M_3 muscarinic receptors were developed composed by the first five transmembrane domains of one receptor and the last two transmembrane domains of the other receptor. When each chimera was expressed alone, no binding or signaling could be detected, but coexpression of

the two different chimeras restores binding and signaling to both muscarinic and adrenergic ligands. Such functional transcomplementations were interpreted as intermolecular interactions between inactive receptors in a way that restored both ligand binding and signaling domains within a heterodimeric complex (Maggio et al., 1993). Also, consistent with this idea, several receptor mutants behaved as dominant-negative mutants when expressed together with their cognate wild type receptors (Benkirane et al., 1997; Zhu and Wess, 1998). In these cases, the observed blunted response was explained by invoking dimerization between wild type and the inactive receptor. Similar experiment was recently performed *in vivo* using a binding deficient and signaling-deficient luteinizing hormone receptor in $KO^{-/-}$ mice model background where these receptors could reestablish normal luteinizing hormonal function through intermolecular functional complementation (Rivero-Müller et al., 2010).

To the first commonly used biochemical technique to investigate GPCR dimerization belongs the coimmunoprecipitation of differentially epitope-tagged receptors. The first study of this kind was performed in 1996 and demonstrated the specific interactions between α_2-adrenergic receptors (Hebert et al., 1996). Since then, similar strategies have been used to document the homodimerization of the dopamine D_2 (Ng et al., 1996) and D_1 receptors (George et al., 1998), $mGlu_5$ receptors (Romano et al., 1996) and CB_1 receptors (De Jesús et al., 2006) among others. Coimmunoprecipitation experiments also were able to demonstrate the existence of heterodimers between closely related receptor subtypes, such as $GABA_BR1$ and $GABA_BR2$ (Jones et al., 1998; Kaupmann et al., 1998; White et al., 1998) or δ- and κ-opioid receptors (Jordan and Devi, 1999), as well as more distantly related receptors including the adenosine A_1 and dopamine D_1 receptors (Ginés et al., 2000), the adenosine A_1 and $mGlu_1$ receptors (Ciruela et al., 2001), the adenosine A_{2A} and $mGlu_5$ receptors (Ferré et al., 2002), or the CB_1 and D_2 receptors (Kearn et al., 2005).

Although coimmunoprecipitation is commonly used to study protein-protein interactions, it requires their solubilization using detergents, which might be problematic when studying highly hydrophobic proteins such as GPCR that could form artifactual aggregates upon incomplete solubilization. So, the general acceptance of these complexes awaited a direct confirmation of GPCR dimerization and utilization of biophysical methods based on light resonance energy transfer.

Theodor Förster formulated the theory of resonance energy transfer in 1948. This phenomenon is based on non-radiative energy transfer from a chromophore in excited state (donor) to a close molecule that absorbs it (acceptor). Techniques based on resonance energy transfer are applicable on living cells using a pair of fusion fluorescent or luminescent proteins cloned, most commonly, to the intracellular C-terminus of GPCR, which are transiently expressed in the cell of interest.

In FRET (Förster Resonance Energy Transfer) both donor and acceptor are fluorescent molecules meanwhile in BRET (Bioluminescence Resonance Energy Transfer) the donor is bioluminescent and the acceptor fluorescent.

Luminescence is a phenomenon occurring naturally in several marine animals such as jellyfishes like *Aequorea victoria* or sea pansy *Renilla reniformis*, from which *Rluc* (Renilla luciferase) was isolated. So that resonance energy transfer can take place, two requisites have to be fulfilled. The first is that the emission spectrum of the donor and excitation spectrum of the acceptor overlay in a manner that the emission energy of the donor can transfer directly to the acceptor fluorophore that emits light as if it was excited directly. The second requisite is the close proximity of donor and acceptor in space (equal or less than 100 Å or 10 nm). The efficiency of energy transfer decreases with the sixth potency of distance. It has to be noted that the major part of multiprotein complexes in the cell are constituted between 10 and 100 Å (Stryer, 1978).

Importantly, resonance energy transfer techniques can detect protein dimerization in living cells without disturbing the cellular environment by this phenomenon. BRET technique exists in two variants, $BRET_1$ and $BRET_2$. In $BRET_1$ the substrate of luciferase *Rluc* is coelenterazine H, which when catalytically oxidized emits light at 480 nm what allows excitation of YFP that emits at 530 nm. In $BRET_2$ DeepBlueC oxidizes the light donor *Rluc* emitting at 400 nm, which excites the acceptor GFP that emitts at 510 nm.

Thanks to RET techniques the existence of different homodimers was discovered, for example β_2-adrenergic homodimer (Angers et al., 2000), δ-opioids (McVey et al., 2001), adenosine A_{2A} receptors (Canals et al., 2004), and heterodimers, for example somatostatin $SSTR_{2A}$ and $SSTR_{1B}$ (Rocheville et al., 2000), adenosine A_{2A} and dopamine D_2 receptors (Canals et al., 2003), adenosine A_1 and A_{2A} receptors (Ciruela et al., 2006a), A_{2A} and cannabinoid CB_1 receptors (Carriba et al., 2007), D_1 and H_3 histamine receptors and D_2 and H_3 receptors (Ferrada et al., 2008, 2009) or dopamine D_1 and D_3 receptors (Marcellino et al., 2008) among others.

It has been developed in the past years a combined resonance energy transfer method called SRET (sequential resonance energy transfer), which permits identification of heterotrimers in living cells. In SRET, the oxidation of a Renilla luciferase (*Rluc*) substrate by an *Rluc*-fusion protein triggers acceptor excitation of the second fusion protein by BRET and subsequent FRET with the third fusion protein. Applying $BRET_1$ or $BRET_2$ gives rise to $SRET_1$ or $SRET_2$. Briefly, in $BRET_1$ using coelenterazine H (485 nm) or $BRET_2$ using DeepBlueC (400 nm) the emission from *Rluc* allows energy transfer to a nearby YFP or GFP^2 acceptor respectively. These acceptors emit at 530 nm (YFP) or 510 nm (GFP^2) light, which can result in a second energy transfer to DsRed or YFP, respectively, and concomitant emission of light at 590 nm or 530 nm. SRET will only occur between these fusion proteins if the two coupling pairs, *Rluc*/GFP^2 and GFP^2/YFP or *Rluc*/YFP and YFP/DsRed, are at a

distance less than 10 nm (Navarro et al., 2008). SRET technique allowed for the first time to identify the existence of $A_{2A}R$-D_2R-CB_1R heterotrimer in transiently transfected HEK cells.

Lately more variants of FRET have been developed, like photobleaching FRET and time-resolved FRET (Pfleger and Eidne, 2005) as well as a series of complementation resonance energy transfer methods like bimolecular fluorescence complementation (BiFC) using two fragments of YFP (nYFP, N-terminal fragment and cYFP, C-terminal fragment) that upon its spontaneous reconstitution when located in proximity (6 nm) becomes fluorescent (Hu et al., 2002). Similarly, fragments of *Rluc* that can reconstitute the enzymatic activity were generated (Paulmurugan and Gambhir, 2003). Finally also a combined complementation of two fluorescent proteins can be used (Gehl et al., 2009) or combination of complementation of *Rluc* and YFP (Gandia et al., 2008). In 2009, Chu and colleagues designed a red fluorescent protein complentation. It was a more stable mutant of mKate (far-red fluorescent protein) called mLumin (Chu et al., 2009). The combination of mLumin with Cerulean- and Venus-based BiFC systems would allow for simultaneous visualization of three pairs of protein-protein interaction in the same cell (Dai et al., 2012).

The main limitation of these assays is that they are performed in heterologous expression systems and consequently can produce artifacts. A structural study performed by Palczewski using atomic force microscopy demonstrated for the first time that rhodopsin exists as an array of dimers in the native retina, revealing an oligomeric organization of GPCR *in vivo* (Fotiadis et al., 2003).

Once proved the possibility of oligomer formation among some GPCR more techniques are needed in order to prove its existence in native tissues or at least be able to detect some of its specific characteristics that could be used as oligomerization fingerprints *in vivo*.

2.3.1. Ligand binding in oligomeric receptors.

Even though it has been proved that the great part of GPCR are found in the membrane as dimers or oligomers, most of the models used do not take into account this factor and keep considering them as monomers. Colquhoun (1973) and Thron (1973) started a series of studies that led to the formulation of different models to explain the behavior of hormone and neurotransmitter receptors (Colquhoun et al., 1973; Costa and Herz, 1989; Franco et al., 1996; Hall, 2000; De Lean et al., 1980; Leff, 1995; Lefkowitz et al., 1993; Lorenzen et al., 2002; Onaran et al., 1993; Samama et al., 1994, 1993; Thron, 1973; Tucek and Proska, 1995; Weiss et al., 1996). All these models have in common that the basic signaling unit is the receptor in its monomeric state and most of them are based in the proposed mechanism on 1957 by Del Castillo and Katz for nicotinic receptors, which are ionic receptors, not GPCR. These authors postulated that the channel was closed in the absence of acetylcholine and when the ligand was bound to the receptor it became in an intermediate state but still closed and later on there was a conformational change that opened the receptor forming the active state of it (Figure 7A).

Later on, a two-state model of receptor activation was proposed where is stated that receptors have two conformational states and they are in equilibrium, being one of them the active molecule capable of signaling. In this model there would be an orthosteric site where agonists would bind to and balance the equilibrium to the active state. This model was able to explain the constitutive activity of some receptors and introduced the concept of inverse agonists (Leff, 1995) (Figure 7B). Other complex models stated the existence of allosteric union sites to explain the existing modulation that some receptors suffer by non-agonist molecules. The ternary complex model proposed by De Lean et al., 1980 considers the G-protein as a non-competitive modulator, but it can also be generalized and consider any allosteric modulator (Figure 7C). Samama et al., 1993 expanded that model adding two activation states where G-protein only binds to the active state and was named Extended

ternary complex model (Figure 7D). Finally, Cubic ternary complex model combines ternary complex models and two-state activation model (Hall, 2000; Weiss et al., 1996) (Figure 7E).

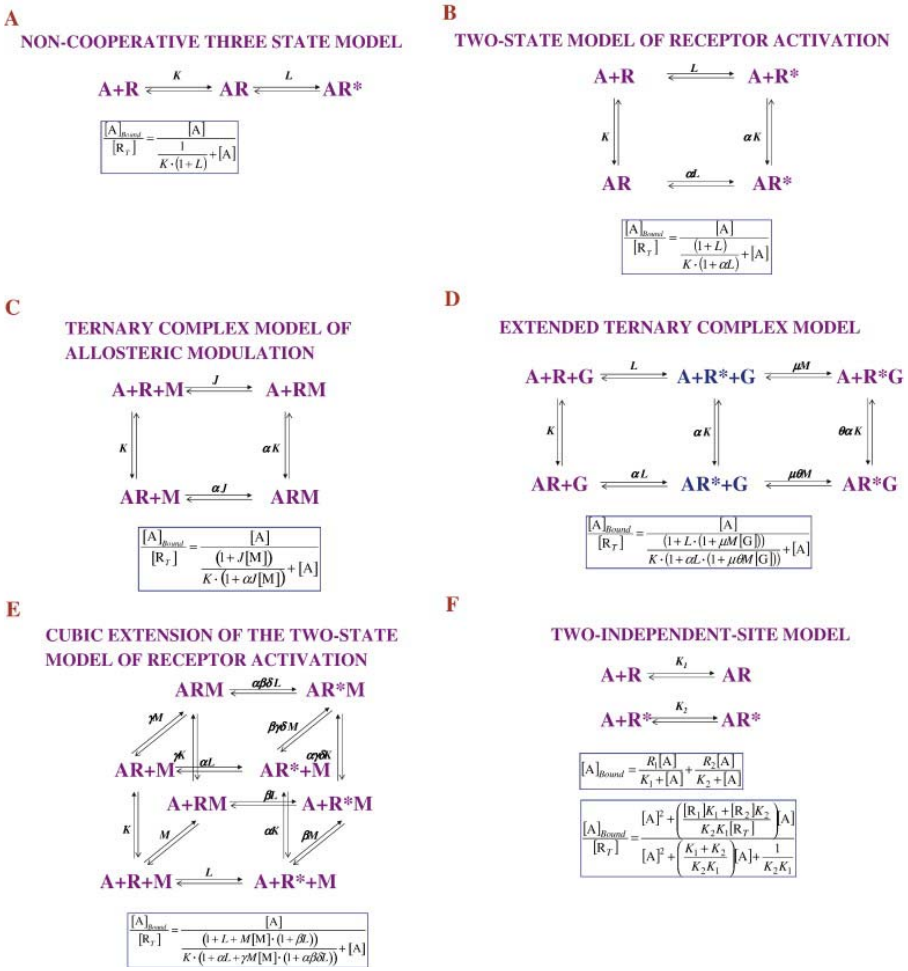

Figure 7. Different models that consider receptors as monomeric units. R and R* are receptor and activated receptor (for example coupled to signaling mechanisms), respectively. A is agonist or antagonist, G is G-protein and M is allosteric modulator that can also be a G-protein (Casadó et al., 2007).

None of these models is capable to explain the biphasic fitting resulting of some experimental binding data. In order to solve this problem, the most common approach is fitting to equations derived from two independent site models considering the existence of two independent states of receptor (non interconvertible states): a high affinity state (or G-protein coupled) and a low affinity state (or G-protein uncoupled) (Casadó et al., 1990) (Figure 7F). Data fitting according to this method allows a calculation of two K_D values: one

for the high affinity state and other for the low affinity state. Nevertheless, it was observed that the agonist could induce changes in the proportion of high affinity and low affinity states, which indicated that these two states cannot exist separately but are interconnected (Wong et al., 1986). This model could only explain negative-cooperativity phenomena but not positive-cooperativity, which despite not being so common has been previously described in muscarinic receptors (Mattera et al., 1985) and opioid receptors (Jordan et al., 2003; Tomassini et al., 2003) among others. Mattera et al., 1985, when GPCR oligomerization was not so evident, proposed the existence of a multivalent receptor with more than one agonist-binding site, which allowed explaining these cooperativity phenomena.

Given that nowadays it is known that GPCR are in the membrane forming dimers (Angers et al., 2000; George et al., 2002; Terrillon and Bouvier, 2004a) all the previous models should be reviewed to take this fact into account. In fact, receptors could be found in the membrane as higher order oligomers whose stoichiometry is not well studied. However, trimer- or tetramer-based models would be mathematically very complex and would not improve significantly in terms of error and experimental data accuracy compared to a dimer-model. For this reason, taking into account all these facts it was developed a model that considers the dimeric receptor binding in two states (two-state dimer receptor model) in which cooperativity is explained in a natural way assuming that the first ligand binding to a monomer can modify the binding equilibrium parameters of a second ligand in the second monomer of the dimer (Franco et al., 2005a, 2006) (Figure 8). Two-state dimer model is based on the possibility that conformational changes from one subunit of the dimer can affect somehow the second subunit, which implies some sort of communication between them (cross-talk). Hence, this model is considering cooperativity phenomena (positive or negative), constitutive activity and inverse agonists. Moreover, the model also explains the duality of some compounds, which could be of interest for the development of new therapeutic strategies.

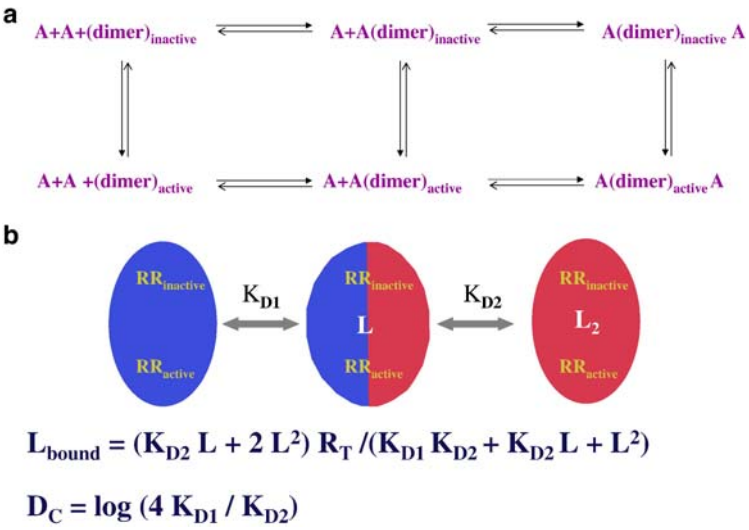

Figure 8. Two-state dimer receptor model scheme and equations. Dimer can be active or inactive and be empty or occupied by one or two ligand molecules (A). a) Macroscopic model. b) Simplified model including macroscopic dissociation constants at the equilibrium (K_{D1} and K_{D2}) that define the first and the second ligand molecule binding to the dimer respectively. It is shown the equations used for the fitting of the radioligand binding data (L) to the receptors forming the dimer and the equation used to calculate the cooperativity index (D_C) (Franco et al., 2008).

It is important to point out that the two-state dimer receptor model besides the agonist and antagonist macroscopic affinity constants (K_{D1} and K_{D2}) for the receptors, allows you to calculate new parameters like the cooperativity index (D_C) that evaluates the cooperativity degree produced when the second ligand molecule binds the dimer already occupied by the first ligand molecule. Essentially, D_C is the induced modification by the first ligand molecule in the macroscopic equilibrium binding parameters of the second ligand molecule in the dimeric receptor (Casadó et al., 2007). Additionally, in competition experiments where there is more than one ligand capable to bind the receptor, the hybrid equilibrium constant appears (K_{DAB}), which is the dissociation constant that measures the ligand (B) affinity for a dimeric receptor that is semi-occupied by a different ligand (A). This parameter becomes important when it comes to cooperativity detection (also known as cross-talk when we are talking about signaling) in competition experiments.

2.4. GPCR heteromerization: functional consequences.

The availability of a wide variety of techniques to study GPCR dimers has facilitated the examination of the functional role of dimerization in these receptors. Dimerization has been found to play a key role in regulation at different levels, from receptor expression modulation on the cell surface to acquisition of new pharmacological properties at a ligand binding level and signaling. This provides a new perspective for future development of drugs acting through GPCR oligomers.

Even if in many cases the physiological relevance is not completely understood, several studies performed in heterologous expression systems suggested distinct functional roles of GPCR oligomerization (Figure 9).

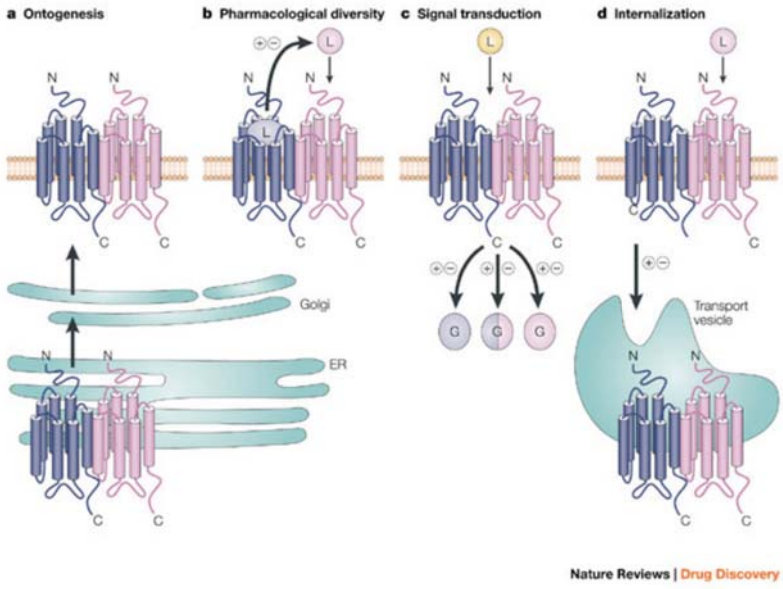

Figure 9. Proposed functional roles of GPCR oligomerization. ER, endoplasmic reticulum and L, ligand. Taken from Ellis et al., 2004.

Firstly, oligomerization can be implicated in GPCR ontogenesis, which means in the protein folding control and membrane targeting of the newly synthetized receptors as well as their internalization (Breit et al., 2004; Bulenger et al., 2005; Law et al., 2005). Similarly, in some cases, it was observed that oligomer formation in the plasma membrane could be regulated by ligand activation. Concerning ligand binding, oligomerization confers new pharmacological properties to the receptor owing to the phenomena of cooperativity and cross talk, as stated previously when binding of a ligand can modify the binding properties of the second receptor of the homo- heterodimer (Ferré et al., 2007a; Franco et al., 2008). When we focus on signaling via interaction with G-protein, oligomerization can modify signaling properties of a receptor leading to signaling potentiation, attenuation or even inverted signaling due to induction of coupling to other G-protein type. Finally, endocytic pattern was seen to be affected by oligomerization (Terrillon and Bouvier, 2004b).

One of the most significant observations to indicate that GPCR dimerization might be important in receptor folding and transport to the cell surface came from the studies of metabotropic $GABA_BR$. Three studies published simultaneously in 1998 (Jones et al., 1998; Kaupmann et al., 1998; White et al., 1998) demonstrated that coexpression of two isoforms of $GABA_BR$, $GABA_BR1$ and $GABA_BR2$ was a prerequisite for a functional $GABA_BR$ formation at the cell surface. The analysis of this phenomenon showed that the isoform $GABA_BR1$ is retained in intracellular compartments as an immature glycoprotein and that, by contrast, $GABA_BR2$ served as a chaperone that is essential for the proper folding and cell surface transport of $GABA_BR1$. $GABA_BR1$/$GABA_BR2$ dimerization masks the ER-retention signal, thereby allowing ER transport and plasma membrane targeting of the dimer (Margeta-Mitrovic et al., 2000). These evidences suggested that the functional unit of the receptor should be the heterodimer (Margeta-Mitrovic et al., 2000). Moreover, taking into account recent receptor definitions that define the receptor as a macromolecule or group of macromolecules capable to induce some sort of signaling, and considering that receptors can

have a quaternary structure we should consider the functional unit of $GABA_BR1/GABA_BR2$ as a single heteromeric receptor. In fact, as a single receptor with a certain quaternary structure and not as a heteromer of GABA receptors (Ferré et al., 2009a).

The paradigm that some GPCR need to form heterodimers to reach the cell surface stems from the fact that dimers might correspond to the functional GPCR signaling unit, at least for signaling events involving G-protein activation. Increasing evidence indicates that class A GPCRS dimer/oligomer biogenesis occurs at an early time point during receptor biosynthesis and processing in the ER and Golgi, where this could have an important role in the quality control of newly synthesized receptors (Herrick-Davis et al., 2006). Once receptor oligomers are trafficked to the plasma membrane, both experimental and theoretical considerations suggest that dimeric GPCR represent the basic functional receptor unit that engages heterotrimeric G-proteins. In addition, it is becoming increasingly clear that "non-obligatory" heterodimers that display pharmacological and functional characteristics that differ from those of their constituent monomers can also exist (Bulenger et al., 2005).

Receptors within heterodimers may have different internalization mechanisms; heteromerization may also modulate agonist-induced trafficking properties of GPCR. For example, somatostatin receptor $SSTR_1$-$SSTR_5$ heterodimer is internalized despite the internalization-resistance of $SSTR_1$ monomer (Rocheville et al., 2000). Most family A GPCR respond to agonist challenge by rapidly becoming internalized away from the cell surface and studies have indicated that the receptor internalizes as a dimer or oligomer (Yesilaltay and Jenness, 2000).

Radioligand-binding studies have provided some insight into the physiological relevance of GPCR homodimers and heterodimers, since they can result in the generation of sites with novel ligand-binding properties. The first report about a heterodimer with distinct properties from their constituent receptors was the discovery of κ-δ-opioid receptors heterodimer (Jordan and Devi, 1999). κ-δ-receptor heterodimers show high affinity for

either κ- or δ-opioid receptor-selective ligands but, on the other hand, these heterodimers show high affinity for partially selective ligands. GPCR heteromerization not only results in changes in the affinity of receptors for several ligands, but binding of one ligand can be able to modify the efficacy or potency of another ligand binding to the neighboring receptor. For instance, in A_1-D_1 receptor heteromer, A_1R agonists induced the disappearance of the high affinity binding sites of D_1R (Ginés et al., 2000). In A_{2A}R-D_2R heteromer, binding of A_{2A}R agonist was seen to reduce the efficiency of D_2R ligands binding by a negative cross talk (Ferré et al., 2001), similarly as in A_{2A}R-A_1R heteromer, where A_1R agonist binding led to reduction of efficiency of A_{2A}R agonist binding (Ciruela et al., 2006a).

One of the first evidence that dimers formed a complex signaling unit demonstrated that the disruption of the dimer by a peptide fragment from the sixth transmembrane domain inhibited the agonist-induced cAMP production. This was seen in the β_2-adrenergic receptor homodimers (Hebert et al., 1996). In addition, heteromerization of two receptors may enhance the signaling of the first and inhibit the signaling of the second, as happened with angiotensin AT_1 and bradykinin B_2 receptor heterodimer (AbdAlla et al., 2000). Taking this into consideration, one of the main issues in elucidating the functional role of GPCR homodimers is to know whether agonist binding to a single subunit of the homodimer is sufficient for G-protein activation or whether both subunits in a ligand-loaded state are required. It has been described that agonist occupation of a single subunit in a dimer is sufficient for G-protein activation, results that are consistent with a number of studies demonstrating trans-complementation between a receptor defective in ligand binding and a receptor defective in G-protein activation (Carrillo et al., 2003; Milligan and Bouvier, 2005). Some current views of the physical organization of GPCR and associated G-proteins favor the model in which GPCR dimers provide for the proper binding of a single heterotrimeric G-protein (Banères and Parello, 2003; Fotiadis et al., 2004). Functional studies using the glutamate receptor demonstrated that only one receptor subunit per

receptor dimer could reach a fully active state at a time (Goudet et al., 2005; Hlavackova et al., 2005).

3. Dopamine receptors.

Dopamine (3,4-dihydroxyphenethylamine, Figure 10) constitutes approximately 80% of the catecholamine present in the brain. Similar to other neurotransmitters, dopamine is unable to cross the blood brain barrier; however, its precursors, both phenylalanine and tyrosine readily cross this barrier allowing its subsequent biosynthesis within neurons.

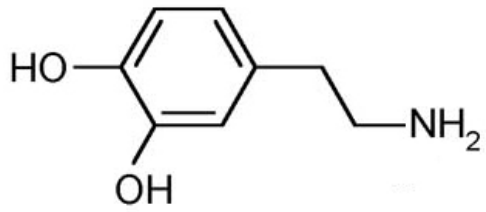

Figure 10. Dopamine. Chemical structure.

Dopamine biosynthesis occurs within the cytosol of the nerve terminal after which the release of synthesized dopamine into the synaptic cleft leads to the subsequent sequence of events (Fuxe and Owman, 1965; Levitt et al., 1965). Calcium ion influx, via voltage-dependent calcium channels, triggers the fusion of the dopamine filled vesicles with the presynaptic membrane. A pore is formed and dopamine is then released into the synaptic cleft. Through diffusion it crosses the synapse and binds to dopamine receptors located pre- and postsynaptically. Upon binding, a conformation change in the receptor is induced and triggers a complex chain of intracellular events. The final outcome of dopamine release is either the activation or inhibition of the postsynaptically located neuron. Finally, the dopaminergic signaling is terminated through the re-uptake of dopamine by specific dopamine transporters (DAT) from the synaptic cleft to the presynaptic terminal where dopamine can be stored and subsequently reused (Amara and Kuhar, 1993; Cooper et al., 1996).

Although the number of neurons that use dopamine as a neurotransmitter is rather small, this system of neurotransmission plays a very important role in many functions. Dopamine interacting with its central receptors in mammals influences a wide range of

functions including movement, motivation, attention, cognition, affect, and control of pituitary hormone secretion (Missale et al., 1998). The most prominent dopamine mediated function is motor behavior regulation . In the absence of dopaminergic tone, mammals are akinetic, or do not move. Increasing dopaminergic stimulation above the basal tone results in increased locomotion, and further increases the appearance of species-typical stereotyped motor patterns. In rats, stereotyped patterns take the form of focused sniffing, licking, or gnawing, and are used to determine overstimulation of dopaminergic signaling pathways. In recent years the dopaminergic system has become of great interest because of the relationship between deregulation of this system and several diseases such as Parkinson's disease, schizophrenia, Tourette syndrome, hyperprolactinemia and drug addiction (Albin, 2006; Bankowski and Zacur, 2003; Blum et al., 2012; Fuxe et al., 2001; Missale et al., 1998; Perreault et al., 2011; Steeves and Fox, 2008; Vallone et al., 2000).

3.1. Dopamine receptor characteristics.

Dopamine exerts its function via interaction with dopamine receptors, which belongs to GPCR family A: D_1R, D_2R, D_3R, D_4R and D_5R (Table 1). In 1978 dopamine receptors were first classified according to their activation or inhibition of adenylate cyclase (Spano et al., 1978). They were later classified in two subfamilies, D_1-like, which comprises D_1R and D_5R, and D_2-like, including D_2R, D_3R and D_4R (Figure 11). D_1-like receptors produce an increase of cAMP levels via G_s which stimulates AC and their localization is mostly postsynaptic in synaptic terminals (Civelli et al., 1993). D_2-like receptors inhibit AC via G_i coupling, in addition activate potassium channels and reduce calcium entry through voltage-gated channels (Nicola et al., 2000). D_2-like receptors can be located on both presynaptic and postsynaptic terminals (Sunahara et al., 1993). D_1-like receptors contain a carboxyterminal domain about seven times longer than D_2-like receptors, while the latter

have a very long third intracellular loop, a common feature in many G_i-coupled receptors (Missale et al., 1998).

Family	**D_1-like**		**D_2-like**		
Subtype	**D_1R**	**D_5R**	**D_2R**	**D_3R**	**D_4R**
G-protein	G_s	G_s	G_i	G_i	G_i
Mechanism of signal transduction	+ AC + PLC	+ AC	- AC + PLC - Ca^{2+} channels + K^+ channels	- AC + PLC - Ca^{2+} channels + K^+ channels	- AC + PLC
Effector molecules	↑ cAMP ↑ PKA ↑ IP_3	↑ cAMP	↓ cAMP ↑ IP_3 ↓ Ca^{2+} ↑ K^+	↓ cAMP ↑ IP_3 ↓ Ca^{2+} ↑ K^+ ↑ Na^+/K^+ exchange	↓ cAMP ↑ arachidonic acid ↑ Na^+/K^+ exchange
Affinity for dopamine K_D (nM)	2340	261	2.8 - 274	4 - 27	28 - 450
Agonist K_D (nM)	SKF-38393 1 - 150	NPA 187	Quinpirole 4.8 - 474	Bromocriptine 5 – 7.4	Apomorfine 4
Antagonist K_D (nM)	SCH-23390 0.11 – 0.35	SCH-23390 0.11 – 0.54	Raclopride 1 - 5	UH-232 2.9 – 9.2	Clozapine 9 - 42

Table 1. Dopamine receptor characteristics.

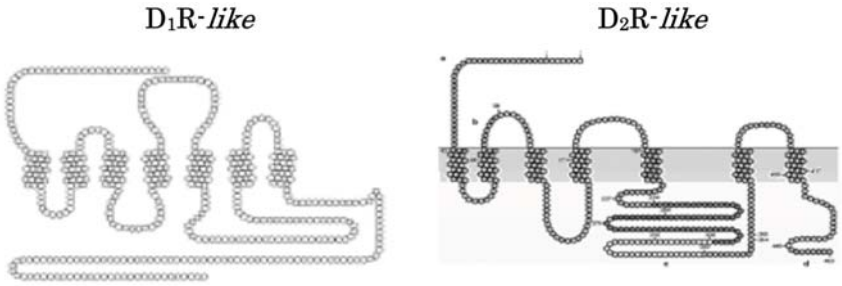

Figure 11. Schematic representation of the structures of D_1-like and D_2-like dopamine receptors.

The carboxyterminal, in both families, contains phosphorylation and palmitoylation sites that are believed to play an important role in receptor desensitization and formation of a fourth intracellular loop, respectively. All of the dopamine receptors subtypes share several conserved residues within their transmembrane domains, which are believed to be the minimal requirements for catecholamine binding. The two serine residues in the fifth transmembrane domain are thought to be involved in recognition of the two hydroxyl groups of catecholamines, and the aspartic acid residue located within the third transmembrane domain is thought to act as a counter ion for the amine group in biogenic amines (Hibert et al., 1991). D_1-like receptors contain two glycosylation sites at the amino terminal and the second extracellular loop, while D_2R and D_3R may have multiple (at least 4) glycosylation sites in their extracellular domains. To study the pharmacological properties of dopamine receptor, ligands that easily discriminate between D_1-like and D_2-like receptors are available, however, they are not selective for members of each subfamily. A remarkable difference inside the D_1-like receptors subfamily is the affinity for dopamine since the D_5R is ten times more affine than the D_1R (Missale et al., 1998). Within the D_2-like subfamily, the D_3R is the one with the highest affinity for dopamine (about 20 times higher compared to the D_2R).

3.2. Dopamine D_2 receptor.

Dopamine D_2 receptor (D_2R) is primarily found in brain tissue, including the caudate-putamen, olfactory tubercle and nucleus accumbens, where it is expressed by GABAergic neurons coexpressing enkephalins. In addition, the mRNA of this receptor is also found in the substantia nigra (SNr) and in the ventral tegmental area (VTA), the nuclei that gives rise to the major dopaminergic pathways of the brain, indicating the role of D_2R as one of the main dopamine receptors to directly control the activity of dopamine containing neurons. However, the D_2R is also found outside the central nervous system, in the anterior and intermediate lobes of the pituitary gland, which indicates that it is also a primary dopamine receptor for regulating hormone release (Vallone et al., 2000).

The alternative splicing of the sixth exon generates the D_{2L} and D_{2S} isoforms (Figure 12). Studies performed using dopamine $D_{2L}R$ knock-out mice indicate a preferential involvement of $D_{2L}R$ in postsynaptic responses while the $D_{2S}R$ appears to be preferentially expressed by midbrain dopaminergic neurons acting as an inhibitory autoreceptor (Lindgren et al., 2003; Mercuri et al., 1997; Rouge-Pont et al., 2002). Previous studies have shown that $D_{2L}R$ and $D_{2S}R$ bind to distinct G-protein, most likely due to their structural differences. However, both isoforms function by binding to the pertussis toxin-sensitive G-protein G_i or G_z, both of which have an inhibitory effect on adenylate cyclase that seems to be the predominant signaling pathway used by D_2R in the central nervous system (Enjalbert and Bockaert, 1983; Kebabian and Greengard, 1971; Leck et al., 2006).

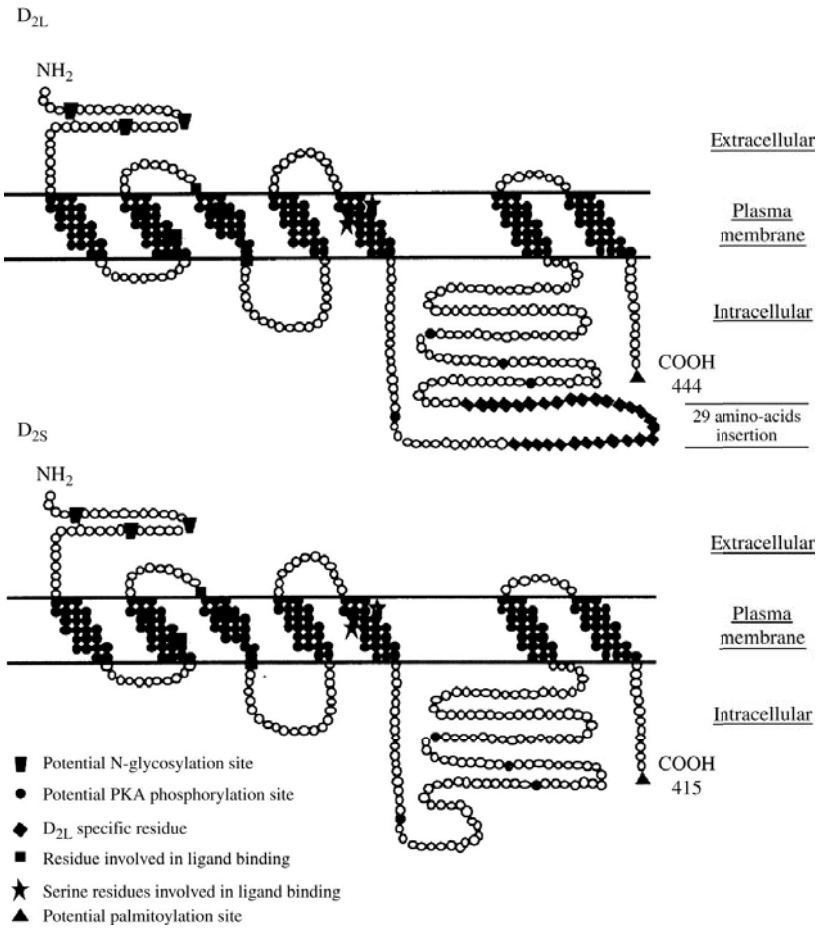

Figure 12. Schematic secondary structure of dopamine $D_{2L}R$ and $D_{2S}R$ isoforms (Pivonello et al., 2007).

Baik et al. generated the D_2R knock-out mice in 1995 (Baik et al., 1995). These mice showed a striking impairment of motor behavior (parkinsonian-like phenotype) supporting an essential role for these receptors in the dopaminergic control of movement. An increase in the density of postsynaptic D_2R was observed in schizophrenia (Joyce et al., 1988) and in Parkinson's disease patients not treated with L-DOPA (Seeman and Niznik, 1990). In mouse models of Parkinson's disease, dopamine depletion caused a loss of endocannabinoid-dependent long-term depression at excitatory synapses onto indirect pathway medium spiny neurons (Kreitzer and Malenka, 2007; Shen et al., 2008).

3.3. Basal ganglia and dopaminergic circuitry.

Basal ganglia are located in the telencephalon and consist of several interconnected nuclei: the striatum, globus pallidus external segment (Gpe), globus pallidus internal segment (Gpi), substantia nigra (SN) and the subthalamic nucleus (STN) (Figure 13).

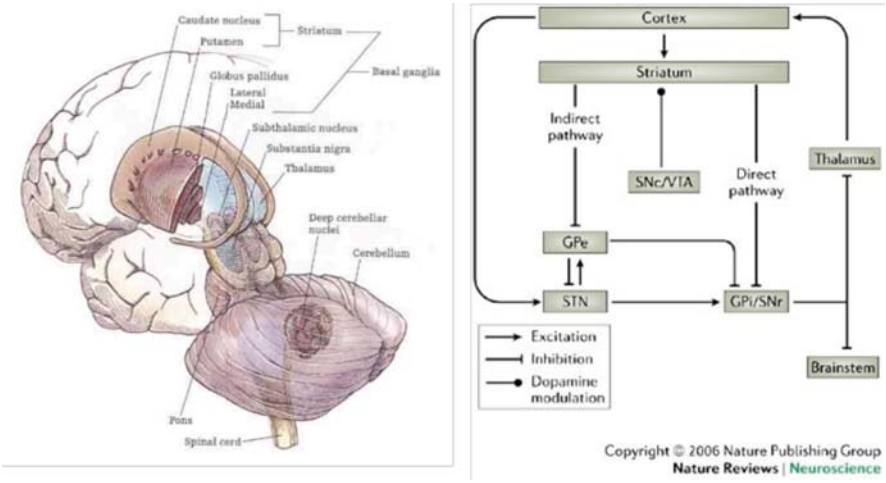

Figure 13. Basal ganglia. Left, anatomy of the human basal ganglia structures and their localization in the brain. Right, motor circuit of the basal ganglia, direct and indirect pathway (Yin and Knowlton, 2006).

Striatum is a major component of basal ganglia (Kase, 2001). It can be divided in dorsal and lateral part. In primates, the dorsal striatum is divided by the internal capsule into the medially located caudate nucleus and the laterally positioned putamen. The putamen (the dorso-medial striatum) receives inputs from sensorimotor cortex (Künzle, 1975; Liles and Updyke, 1985). The ventral striatum, or nucleus accumbens, represents a third subdivision of the striatum (Nicola, 2007). The ventral striatum, like the patches of the dorsal striatum, receives glutamatergic inputs from frontal cortex and limbic regions (Brog et al., 1993). However, the dopaminergic innervation of the ventral striatum derives from the ventral tegmental area, a separate midbrain nucleus adjacent to the substantia nigra pars compacta, SNc (Fields et al., 2007). Dorsal striatum (caudate nucleus and putamen) is implicated in learning or complex motor behavior, ventral striatum (nucleus accumbens) participates in conversion of motivation to action. Neurotransmitter receptors can be expressed differently

in distinct anatomical parts of striatum: for instance, cannabinoid CB_1R are highly expressed in nucleus accumbens and caudate nucleus, but not in putamen (Herkenham et al., 1991).

Medium spiny projection neurons (MSN) are the most numerous in the dorsal striatum, with at least 75% of neurons belonging to this type in primates (Graveland and DiFiglia, 1985; Tepper et al., 2010), and up to 95% in rodents and cats (Graveland and DiFiglia, 1985; Kemp and Powell, 1971). The second class of neurons present in the dorsal striatum are interneurons (GABAergic or cholinergic), that are typically spiny, and unlike the medium spiny neurons, do not send projections outside the striatum (Cowan et al., 1990; Kawaguchi, 1993; Kawaguchi et al., 1995; Phelps et al., 1985; Tepper et al., 2010; Wu et al., 2000). Finally, the striatum also contains a small amount of dopaminergic neurons. Although the amount of these neurons is almost vestigial in normal rodent striatum, it is more prevalent in primates (Dubach et al., 1987; Ikemoto et al., 1996).

Medium spiny neurons form dendritic spines that make synaptic connections (Kreitzer, 2009), they are inhibitory as they use GABA as neurotransmitter, express DARPP-32, are innervated by glutamatergic connections from cortex and dopaminergic innervations from substantia nigra and have a unique firing pattern (Kreitzer, 2009).

Medium spiny neurons can be divided into two types according to expression of different peptides and neurotransmitter receptors. Direct pathway MSN express dynorphin and substance P and dopamine D_1R coupling stimulatory G_s. They are also called striatonigral MSN. They project directly to GPi and SNr. Stimulation of the direct pathway results in motor activation (Figure 13, right). Cortical glutamatergic synapses connecting to striatonigral neurons express adenosine $A_{2A}R$ forming, at least in part, heteromers with adenosine A_1R. Indirect pathway MSN express enkephalin and dopamine D_2R coupling inhibitory G_i. They are also called striatopallidal MSN and project to GPe. Stimulation of indirect pathway MSN results in motor inhibition (Figure 13, right).

In Huntington's disease striatopallidal neurons degenerate first and their dysfunction or degeneration leads to hyperkinetic movements. In striatopallidal MSN dopamine D_2R is coexpressed with adenosine $A_{2A}R$ (Schiffmann and Vanderhaeghen, 1991; Schiffmann et al., 2003, 2007; Svenningsson et al., 1999) in the postsynaptic site of corticostriatal synapses. The excitability of both neuronal types is slightly different: D_2R-containing MSN are more excitable and contain more tree branching (Day, 2008).

Direct and indirect pathways converge in GPi/SNr, the main output of basal ganglia motor circuitry. GPi/SNr neurons are inhibitory, GABAergic and project to the thalamus. The thalamus projects back to cortex with glutamatergic efferents. According to both inputs from direct and indirect pathway the final outcome is transmitted back to cortex. Direct pathway tends to activate voluntary movements and indirect pathway inhibits involuntary components of movement. An adequate equilibrium between both pathways produces normal movements. Dopamine, produced by neurons from substantia nigra pars compacta, is the key regulator for the correct functioning of basal ganglia, it induces motor activation via activation of dopamine D_1R in striatopallidal neurons of direct pathway and inhibition of dopamine D_2R in striatonigral neurons of indirect pathway, which means potentiating the stimulatory direct pathway and depressing the inhibitory indirect pathway. Dopamine thus stimulates movement acting upon both pathways. In Parkinson's disease, due to depletion of dopamine because of the degeneration of nigrostriatal neurons, movement depression or hyperkinesia is experienced. Excess of dopaminergic stimulation would lead to hyperkinesia. In Huntington's disease, hyperkinetic choreic movements are due to a gradual disappearance of the contribution of the indirect inhibitory pathway, but at the end, the subsequent degeneration of the direct pathway and the nigrostriatal neurons finally leads to disappearance of movement (Glass et al., 2000).

The classification of MSN projection in direct and indirect pathways belongs to the classical vision of basal ganglia motor circuitry, as it was defined in mid 80s (Albin et al.,

1989; DeLong, 1990; Penney and Young, 1986). Recently the vision of basal ganglia circuitry is tending to change an is not seen as simple go through structure where the connectivity and functional interactions occur unidirectionally, microcircuits appear and more extensive reciprocal innervation is observed and the issue becomes more complex (Obeso and Lanciego, 2011).

4. Adenosine receptors.

There are four known adenosine receptor subtypes, A_1R, $A_{2A}R$, $A_{2B}R$ and A_3R (Figure 14), each of which has an unique pharmacological profile, tissue distribution and effector coupling (Table 2).

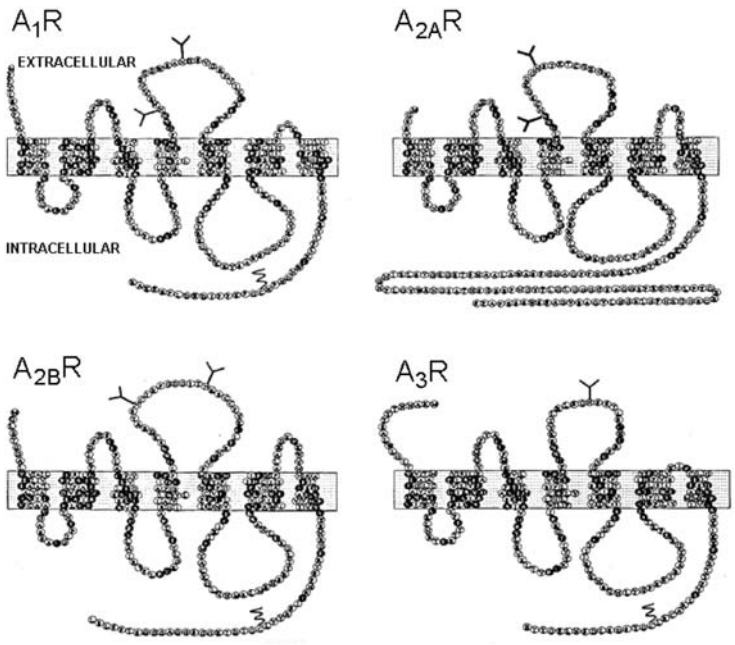

Figure 14. Adenosine receptor scheme. Very long C-terminal tail of the $A_{2A}R$ lacking palmitoylation site. Glycosylation sites in the second extracellular loop of all adenosine receptors. Taken from Dr. F. Ciruela PhD thesis.

Subtype	A_1R	$A_{2A}R$	$A_{2B}R$	A_3R
G-protein	G_i	G_i	G_s	G
Mechanism of signal transduction	- AC + PLC - Ca^{2+} channels + K^+ channels	+ AC - Ca^{2+}channels	+ AC + PLC	- AC + PLC
Effector molecules	↓ cAMP ↑ IP_3 ↓ Ca^{2+} ↑ K^+	↑ cAMP ↑ IP_3 ↑ Ca^{2+}	↑ cAMP ↑ IP_3 ↑ Ca^{2+}	↑ cAMP ↑ IP_3 ↑ Ca^{2+}
Affinity for adenosine K_D (nM)	70	150	5100	6500
Selective agonist	R-PIA	CGS-21680	-	IB-MECA
Selective antagonist	DPCPX	ZM-241385	MRS 1706	L-268605
Physiologic action	Inhibition of synaptic transmission and motor activity. Hyperpolarization. Ischemic preconditioning.	Facilitates neurotransmitter release. Motosensorial integration.	Calcium channels modulation.	Ischemic preconditioning.

Table 2. Adenosine receptors characteristics. Taken from Dr. J. Bakešová PhD thesis.

All of the adenosine receptors have glycosylation sites and all but $A_{2A}R$ a palmitoylation site near the carboxyl terminus, that would allow another insertion in the membrane generating a fourth intracellular loop that has been suggested to participate in the coupling of the receptor to the G-protein (Bouvier et al., 1995). A_1R, $A_{2A}R$ and A_3R have a molecular weight of 36.7, 36.4 and 36.6 kDa respectively, whereas, due to its long C-terminal tail, $A_{2A}R$ has a molecular weight of 45 kDa (Palmer and Stiles, 1995). Originally only two adenosine receptors were known and were classified on their effect on cAMP levels

in different tissues; these were A_1R (inhibitory) and $A_{2A}R$ (stimulatory). A_1R and $A_{2A}R$ show high affinity for their natural agonist adenosine and with major expression profiles in the central nervous system and periphery. Later, $A_{2B}R$ and A_3R were discovered. Their activation becomes more relevant in states of notoriously incremented adenosine levels, at micromolar adenosine concentration (Fredholm et al., 2001) according to their lower affinity for agonists. A_1R and A_3R couple to G_i and $A_{2A}R$ and $A_{2B}R$ couple G_s.

Experiments with chimeric A_1/A_{2A} receptors indicate that structural elements in both the third intracellular loop and the carboxyl terminus influence coupling of A_1R to G_i, whereas elements in the third intracellular loop but not the carboxyl terminus contribute to $A_{2A}R$ coupling to G_s (Tucker et al., 2000). The homology between receptor subtypes is quite low, about 45% (Stehle et al., 1992) with areas of high homology located within the transmembrane regions. These regions, together with the second extracellular loop, were proposed to be mainly involved in ligand binding (Rivkees et al., 1999), while interaction with G-proteins occurs within the third intracellular loop. Moreover, adenosine receptors contain several features common to all G-protein coupled receptors: cysteine residues on the extracellular loop that may be involved on disulfide bond formation and confer a conformational stability to receptors after insertion to the plasma membrane (Dohlman et al., 1990). All the cloned adenosine receptors present a "DRY" motif that has been suggested to mediate G-protein activation. Each of the adenosine receptors possesses consensus sites for N-linked glycosylation on their second extracellular loops that is involved in membrane targeting (Klotz and Lohse, 1986). Intracellular domain phosphorylation sequences consensus are present and phosphorylation is implicated in receptors desensitization (Palmer et al., 1994; Saura et al., 1998).

4.1. Adenosine.

Adenosine is an endogenous nucleoside formed by a purinic base adenine bound to a ribose by a β-N-glycosilic bond (Figure 15). Adenosine and its derivatives are an essential constituent for all living cells. It plays a structural role as a building block of nucleic acids, in cellular metabolism (energy storage: ATP), as intracellular regulators (cofactors: NAD^+, $NADP^+$, FAD; second messenger in cellular neuromodulator: cAMP) (Arch and Newsholme, 1978; Pull and McIlwain, 1972) and as neuromodulator in the control of synaptic transmission acting on adenosine receptors (Cobbin et al., 1974).

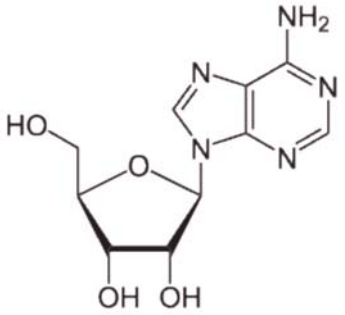

Figure 15. Adenosine molecule. Chemical structure

Under normal conditions, adenosine is continuously formed intracellularly as well as extracellularly. A basal concentration of this nucleoside reflects an equilibrium between synthesis and degradation (Fredholm et al., 2001). The intracellular production is mediated by intracellular 5'-nucleotidase, which dephosphorylates AMP (Schubert et al., 1979; Zimmermann et al., 1998) and by hydrolysis of S-adenosyl-homocysteine (Broch and Ueland, 1980). Intracellular-generated adenosine is transported to the extracellular space mainly via equilibrated transporters. Extracellular AMP dephosphorylation to adenosine, mediated by ecto-5'-nucleotidase, is the last step in the breakdown of extracellular adenine nucleotides, such as ATP to adenosine (Dunwiddie et al., 1997; Zimmermann et al., 1998). Adenosine can also be released to the extracellular space after neuronal activation with specific neurotransmitter ligands. Glutamatergic agonists, such as NMDA or kainate, dose-

dependently increase adenosine levels (Carswell et al., 1997; Delaney et al., 1998). Dopamine D_1R enhance adenosine release via an NMDA receptor-dependent increase in extracellular adenosine levels (Harvey and Lacey, 1997). Extracellular levels of adenosine are decreased by specific adenosine transporters and by extracellular adenosine deaminase (Fredholm et al., 1994; Lloyd and Fredholm, 1995). Under physiological conditions, extracellular adenosine concentrations remain very low (20 to 300 nmol/L) (Delaney and Geiger, 1996), whereas traumatic or hypoxic events, stressful situations and increased neurotransmitter release lead to a several 100-fold increase of extracellular adenosine levels (Latini and Pedata, 2001).

In the brain, which expresses high levels of adenosine receptors, adenosine is secreted by the majority of cells, including neurons and glia, and neuromodulates the activity of the central nervous system in both normal and pathophysiological processes, acting on pre-, post- and/or extra-synaptic sites. Accordingly, adenosine was seen to play a role in the inhibition of excitatory neurotransmitters release (Ciruela et al., 2006b; Phillis et al., 1979), inhibition of spontaneous motor activity, neuronal differentiation and migration (Canals et al., 2005; Rivkees, 1995), memory and learning (Wei et al., 2011), regulation of sleep (Antle et al., 2001; Carús-Cadavieco and de Andrés, 2012), anxiety (Johansson et al., 2001) and excitation, and neuroprotection during hypoxia/ischemia (Pedata et al., 2005). It was related to Alzheimer's disease (Maia and de Mendonça, 2002), Parkinson's disease (Schwarzschild et al., 2002), schizophrenia (Ferré et al., 1997; Shen et al., 2012), epilepsy (Rebola et al., 2005a), drug addiction (Brown and Short, 2008) and finally Huntington's disease (Huang et al., 2011; Reggio et al., 1999) as will be further discussed.

Caffeine is a weak, virtually non-selective adenosine receptor antagonist. It served as a structural model in organic synthesis of more potent and selective antagonists. So the first adenosine receptor antagonists were xanthine (caffeine and theophylline) derivatives (to this group belongs MSX-2 and KW-6002), followed by second class of complex nitric

heterocycles (pyrazolo-thiazolo-pyrimidin-like: ZM-241385, SCH-58261 and SCH-442416, Figure 16), and more recently by structurally unrelated compounds found by library compound screening (Cristalli et al., 2007; Jacobson and Gao, 2006).

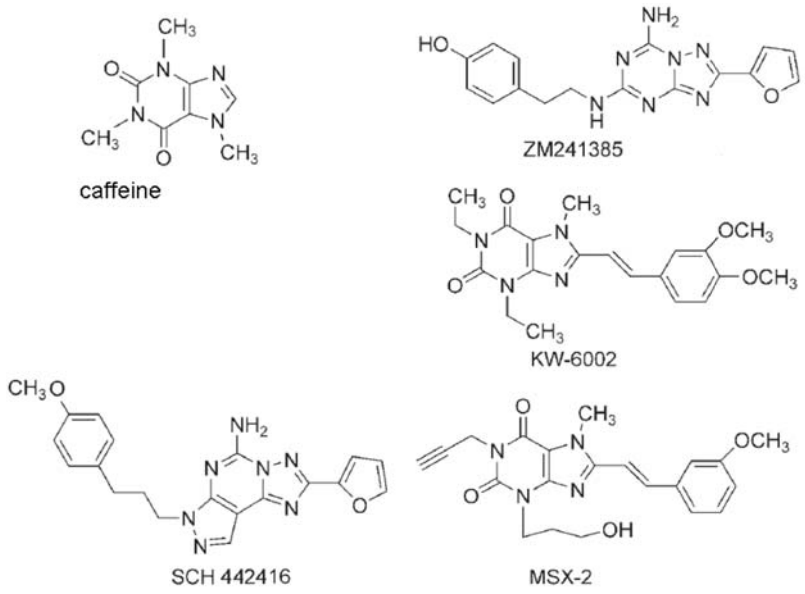

Figure 16. $A_{2A}R$ antagonists. Formula of natural $A_{2A}R$ antagonist caffeine and some selected synthetic compounds. Taken from Dr. J. Bakešová PhD thesis.

The pharmacology of caffeine is still being investigated (Chen et al., 2013; Chrościńska-Krawczyk et al., 2011; Marques et al., 2011; Snel and Lorist, 2011). Studies of caffeine affinity for adenosine receptors in brain tissue brought variable results: showing no difference, a preferential affinity for $A_{2A}R$, or a preferential affinity for A_1R. In the studies using cloned transfected receptors, caffeine displays higher affinity for $A_{2A}R$ that for A_1R (Ciruela et al., 2006a). Interestingly, it was found that the affinity of caffeine for the $A_{2A}R$ depends on the presence of cotransfected receptors. In HEK cells expressing $A_{2A}R$-D_2R heteromer the affinity of caffeine for $A_{2A}R$ was the same as in the cells expressing only $A_{2A}R$ but considerably decreased in cells expressing A_1R-$A_{2A}R$ heteromers (of about twelve-fold less). In A_1R-$A_{2A}R$ heteromer the affinity of caffeine was the same for both adenosine receptors (Ciruela et al., 2006a). This discovery supports the fact that the heteromerization changes receptors' pharmacology.

4.2. Adenosine A_{2A} receptors.

From the first $A_{2A}R$ distribution studies performed with autoradiography using [^{3}H]-CGS-21680 high levels of staining were seen in the striatum, both in dorsal (caudate-putamen) and ventral striatum (nucleus accumbens), in addition in olfactory tubercle and globus pallidus externum in rat (Jarvis et al., 1989; Wan et al., 1990) and human brain (Glass et al., 2000; Martinez-Mir et al., 1991). From northern blot (Fink et al., 1992; Peterfreund et al., 1996) and *in situ* hybridization studies (Fink et al., 1992; Schiffmann and Vanderhaeghen, 1991; Svenningsson et al., 1998, 1999) it was further evident that striatal $A_{2A}R$ was almost exclusively expressed in the medium spiny neurons of the indirect pathway expressing enkephalin and co-expressing dopamine D_2R and not (or at best only to a limited extend) in medium spiny neurons of the direct pathway. By means of more sensible techniques, like immunohistochemistry or radioligand binding assays, lower levels of $A_{2A}R$ were also detected in other brain regions, as amygdala, hippocampus, hypothalamus, thalamus and cerebellum (Rebola et al., 2005b; Rosin et al., 1998). It is not only expressed on neurons, but also on the vessel walls where they mediate vasodilatation (Coney and Marshall, 1998) and on glial cells. In the peripheral tissues, the $A_{2A}R$ can be found in spleen, thymus, heart, lung, kidney, leucocytes and blood platelets (Moreau and Huber, 1999).

In 2008 crystal structure of the human adenosine $A_{2A}R$ was determined in complex with its high-selective antagonist ZM-241385. Not containing the canonical palmitoylation site found in the majority of GPCR, a small helix that does not cross the cell membrane is located at the membrane cytoplasm interface (helix VIII) stabilizes the structure by interacting with helix I. The extracellular surface properties of the $A_{2A}R$ are largely dictated by its second extracellular loop, which in $A_{2A}R$ lacks the prominent secondary structural elements, such as β-sheet and α-helix, as in the rhodopsin and β-adrenergic receptors, respectively. Instead, the second extracellular loop of the $A_{2A}R$ is mainly a spatially constrained random coil having three disulfide linkages with the first extracellular loop. Two

of the three disulfide bonds (Cys71-Cys159 and Cys74-Cys146) are unique to the $A_{2A}R$; the third (Cys77-Cys166) is conserved among a lot of class A GPCR. In addition, a fourth intraloop disulfide bond is formed in the third extracellular loop between Cys259 and Cys262 with the sequence Cys-Pro-Asp-Cys (CPDC), which creates a link in the loop that constrains the position of the third extracellular loop and orient His264 at the top of the ligand-binding site. The extensive disulfide bond network forms a rigid, open structure exposing the ligand-binding cavity to solvent, possibly allowing free access for small molecule ligands. Four amino acid residues are crucial for the ligand binding and their mutation was reported to disrupt antagonist and/or agonist binding, i.e. Glu169 in the second extracellular loop, His250 and Asn253 in helix VI and Ile274 in helix VII (Jaakola et al., 2008).

In 2011 a crystal structure of $A_{2A}R$ bound to agonist (UK-432097, "conformational selective ligand") was obtained. When compared to the inactive antagonist-bound $A_{2A}R$, the agonist-bound structure displays an outward tilt and rotation of the cytoplasmic half of helix VI, a movement of helix V and an axial shift of helix III, resembling the changes associated with the active-state rhodopsin structure. Additionally, a seesaw movement of helix VII and a shift of the third extracellular loop are likely specific to $A_{2A}R$ and its ligand. The availability of both agonist- and antagonist-bound $A_{2A}R$ structures now provide the opportunity to solve the basic question of how ligand binding at the extracellular site of the receptor triggers conformational changes at the intracellular side, where G-protein and other effectors bind and initiate the cascade of downstream signaling pathways (Xu et al., 2011).

Adenosine $A_{2A}R$ can be found both pre- and postsynaptically: presynaptically on the corticostriatal glutamatergic projections (Hettinger et al., 2001), postsynaptically on the GABAergic striatopallidal neurons projecting to the globus pallidus, containing the peptide enkephalin, and enriched with dopamine D_2R (Schiffmann and Vanderhaeghen, 1991). According to a study of Rebola et al., in the striatum, $A_{2A}R$ are more abundantly located

outside the active zone and $A_{2A}R$ present in nerve terminals were most densely located in the postsynaptic density fraction, although they could also be identified in the presynaptic active zone fraction (Rebola et al., 2005b). In addition there is evidence that presynaptic $A_{2A}R$ are preferentially localized in cortical glutamatergic terminals that contact striatal neurons of the direct pathway rather that of indirect pathway (Quiroz et al., 2009), so that there is a segregation of $A_{2A}R$ in the corticostriatal synapses, being presynaptic $A_{2A}R$ expressed in projections of cortical neurons to the medium spiny neurons of the direct pathway and postsynaptic $A_{2A}R$ expressed in striatopallidal medium spiny neurons of the indirect pathway. As we will see later, $A_{2A}R$ plays a different role in each location.

The major signal transduction pathway used by $A_{2A}R$ (Figure 17) includes the activation of adenylate cyclase by means of G_s in general or G_{olf} in the striatum (Kull et al., 1999, 2000). G_{olf} activates adenylate cyclase generating cAMP, which activates the AMP-dependent protein kinase (PKA). PKA regulates the state of phosphorylation of various proteins, importantly GARPP-32 (dopamine and cAMP regulated phosphoprotein, 32 kDa), which is expressed in very high concentration in the GABAergic efferent neurons (Kull et al., 1999, 2000). Under basal conditions, DARPP-32 is phosphorylated at Thr75 and inhibits PKA (Nishi et al., 2000). This inhibition can be rescued by dephosphorylation promoted by protein phosphatase-2A (Nishi et al., 2000). By PKA activation, DARPP-32 is activated by phosphorylation at Thr34 and it becomes a potent selective inhibitor of protein phosphatase-1 (PP-1) (Kull et al., 2000). PP-1 inhibits the activation of CREB in the nucleus. CREB is an important point of convergence of the $A_{2A}R$ signaling and it can be activated through pathways activated by G_{α} or $G_{\beta\gamma}$ subunits, that means by cAMP dependent or independent pathway and involving ERK signaling or not. In cells expressing B-Raf (CHO cells or striatum), the cAMP dependent activation of CREB occurs through PKA-Src-Rap1-B-Raf-MEK-MAPK pathway. Here CREB is only one of many targets of MAPK. This activation can also occur via activation of Ras-Raf1-MEK-MAPK (Vossler et

al., 1997). In cells not expressing B-Raf, i.e. HEK cells, activation of MAPK happens via Ras (Seidel et al., 1999). This signaling pathway is also induced by PLCβ activation (Wirkner et al., 2000) or PI3K-Akt signaling (Lee et al., 2001).

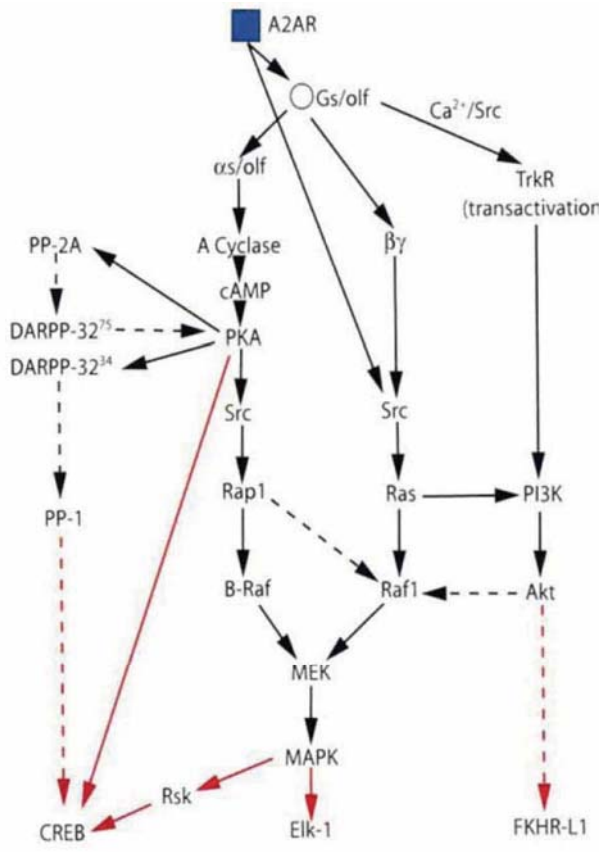

Figure 17. $A_{2A}R$ signal transduction. Full lines represent stimulatory effects and dashed line inhibitory effects. Red lines indicate signaling taking place in nucleus (Fredholm et al., 2007).

ERK1/2 activation in the dorsal striatum is necessary for action-outcome learning and performance of goal-directed actions. In the ventral striatum, ERK1/2 is necessary for the motivating effects of reward-associated stimuli on instrumental performance. Deregulation of ERK1/2 signaling in the striatum by repeated drug exposure contributes to the development of addictive behavior (Shiflett and Balleine, 2011). ERK1/2 influences gene expression through its interaction with transcriptional regulators, such as ribosomal s6 kinase (RSK), mitogen- and stress-activated protein kinase-1 (MSK1) as well as the transcription

factor Elk-1 (Kelleher et al., 2004). Furthermore, treatments that interfere with ERK signaling such as the MEK/ERK inhibitors, i.e. U0126, impaired long-term memory retention (Shiflett and Balleine, 2011). ERK1/2 likely enables corticostriatal plasticity, in part, through regulation of transcription factors such as cAMP response element binding (CREB) protein, as disruption of CREB signaling in the striatum prevents striatal LTP and LTD induction (Pittenger et al., 2006).

Upon agonist stimulation, the $A_{2A}R$ response "quickly" desensitizes within a time frame of less than an hour. Desensitization (attenuation of adenylate cyclase stimulation) has been described in various cellular systems expressing both endogenous and recombinant $A_{2A}R$ (Franco et al., 2005b; Mundell and Kelly, 2011; Palmer et al., 1994; Ramkumar et al., 1991). This rapid desensitization involves $A_{2A}R$ phosphorylation mostly by GRK in the proximal portion of the C-terminus (Thr298) of $A_{2A}R$ (Palmer et al., 1994). Selective activation of G-protein by stimulation of the $A_{2A}R$ is predominantly dictated by its third intracellular loop (in its N-terminal portion) (Olah, 1997). The C-terminal segment seems to be required for the transition of the $A_{2A}R$ to the activated state, since its truncation blunts constitutive activity (Klinger et al., 2002). Finally, the C-terminal segment of the $A_{2A}R$ seems to be involved in the formation of $A_{2A}R$-D_2R heteromeric complexes and to the interaction of $A_{2A}R$ with the actin cytoskeleton. A longer agonist exposure induces receptor internalization, which has been shown to be a necessary step for either resensitization or down-regulation of $A_{2A}R$ through clathrin-coated vesicles (Mundell and Kelly, 2011; Palmer et al., 1994).

$A_{2A}R$-deficient mice were viable with normal development, suggesting that $A_{2A}R$ function may not be critical during neurogenesis. However, they displayed behaviors reflecting increased anxiety and aggression in males (Ledent et al., 1997). Interestingly, $A_{2A}R^{-/-}$ mice were more susceptible than wild type mice to striatal degeneration and weight

loss caused by a low dosage of 3-nitropropionic acid (3NP) which did not induce glutamate-related excitotoxicity (Blum et al., 2003).

4.3. A_{2A} receptor heteromer

4.3.1. Postsynaptic A_{2A} receptor heteromers

Postsynaptic $A_{2A}R$ is found in enkephalin medium spiny neurons of the indirect pathway. It is mainly found perisynaptically to the postsynaptic density in the neck of dendritic spines, adjacent to dopaminergic synapses (Ferré et al., 2007b) where it can be found in different populations of heteromers (Figure 18). It can be expressed as $A_{2A}R$-$A_{2A}R$ homodimer, as $A_{2A}R$-D_2R heterodimer (Ciruela et al., 2006b; Hillion et al., 2002), as $A_{2A}R$-D_2R-$mGlu_5R$ heterotrimer (Cabello et al., 2009) and as $A_{2A}R$-CB_1R-D_2R heterotrimer (Navarro et al., 2008).

The antagonistic interactions between the $A_{2A}R$ and D_2R were demonstrated at the biochemical, functional and behavioral level. The first indication about an antagonist relationship was obtained from behavioral analysis of Parkinson's disease animal models (Fuxe et al., 1974). The use of naturally present $A_{2A}R$ antagonists like caffeine and theophylline in combination with L-DOPA and dopamine agonists led to an increase of motor activity produced by dopaminergic compounds. The first direct clue about the interaction of $A_{2A}R$ with D_2R was brought by experiments in membrane preparations from rat striatum, where stimulation of $A_{2A}R$ produced a decrease in the affinity of D_2R for agonists due to conformational modification in the D_2R binding site (Ferre et al., 1991). This interaction pointed towards the possible existence of $A_{2A}R$-D_2R heteromer. Similar results were seen in different cotransfected cell lines (Dasgupta et al., 1996; Kull et al., 1999; Salim et al., 2000). This was eventually confirmed in 2001 by coimmunoprecipitation and colocalization experiments in transfected cells and primary neuronal cultures and it was observed that a prolonged exposition of $A_{2A}R$ and D_2R agonists led to co-aggregation, co-

internalization and co-desensitization of both receptors (Hillion et al., 2002). Finally, in living co-transfected cells by BRET and FRET experiments it was proved that $A_{2A}R$ and D_2R indeed heteromerized (Canals et al., 2003). From the $A_{2A}R$ and D_2R negative cross talk, the use of $A_{2A}R$ antagonists in Parkinson's disease was proposed.

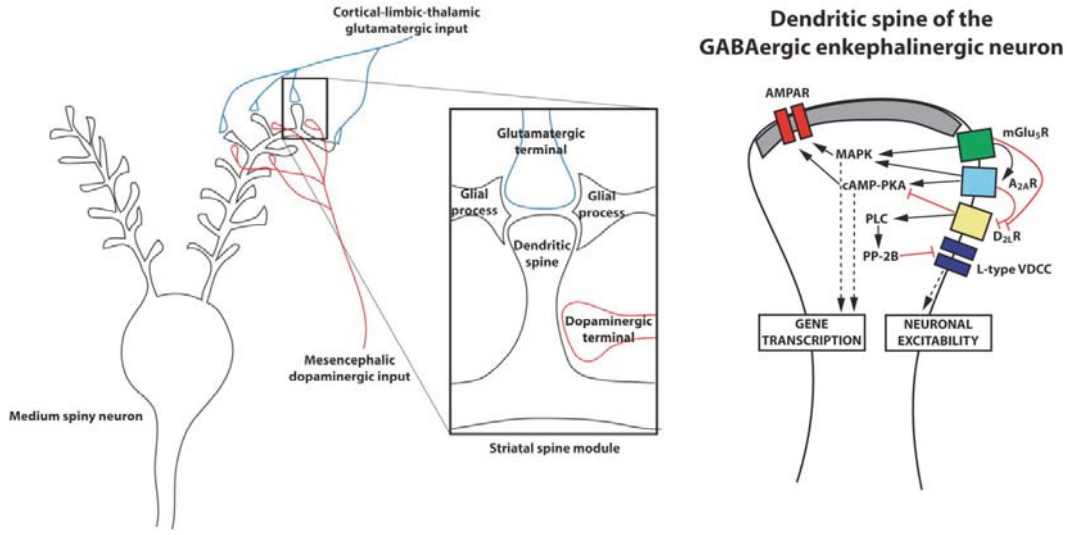

Figure 18. Striatal spine module. Left: Connectivity of dendritic spines with glutamatergic projections on the head and dopaminergic projections on the neck of the spines. Right: $A_{2A}R$ in the postsynaptic terminal. $A_{2A}R$ forming heteromers with D_2R and $mGlu_5R$ and consequences of these interactions (Muller and Ferre, 2007).

From all the selective $A_{2A}R$ antagonists, KW-6002 was the most interesting compound. It already underwent full clinical evaluation with hopeful results, by the time this thesis was written Kyowa Pharmaceutical Inc., the patent owner of KW-6002 under the name of Istradefylline, has not yet received the marketing approval neither for USA nor for Japan. After first positive results obtained from animal models, rodents and monkeys (Fenu et al., 1997; Kanda et al., 1998, 2000), it was started to be taken by patients on clinical trials. The first, proof of concept trial, with KW-6002 was performed in 2003 (Bara-Jimenez et al., 2003). Results from first smaller clinical tests (Bara-Jimenez et al., 2003; Guttman et al., 2007; Hauser et al., 2003) showed certain positive results. KW-6002 alone provided no antiparkinsonian response in moderately advances Parkinson's disease patients, in contrast to

the normalization of locomotor function that had been observed in primates. However, consistent with primate studies was the observation that the antiparkinsonian response could be maintained with less dyskinesia by using Istradefylline in combination with lower L-DOPA doses. In addition, the prolongation of the efficacy half-time following discontinuation of a L-DOPA infusion suggested that Istradefylline might reduce "off-time" in patients with motor fluctuations on L-DOPA. "Off-time" refers to periods of the day when the medication is not working properly, causing worsening of parkinsonian symptoms, these periods become more frequent as the Parkinson's disease progresses.

Larger clinical trials brought similar results (Fernández et al., 2008; LeWitt et al., 2008). To resume it, KW-6002 reduced the "off-time" in moderate to advanced Parkinson's disease patients already receiving dopaminergic therapy, with an increase in non-troublesome dyskinesia. However, the effect on motor function has not been statistically significant in all studies and other side effects were present in some patients (Jenner et al., 2009). Despite the positive findings, in 2008 Kyowa Pharmaceuticals received a "Not approvable" letter from the US Food and Drug Administration (FDA), suspended its development in US, but later on decided to perform further studies in Japan. Importantly, in Parkinson's disease patients KW-6002 has yet to be tested under similar circumstances to those that revealed positive effects in rodent and primate studies. For example, KW-6002 may be co-administrated with a sub-optimal dose of dopamine agonists or L-DOPA, instead of with the optimal doses used so far in clinical trials and to be proven in patients with less advanced Parkinson's disease. Besides KW-6002, other $A_{2A}R$ antagonists are in clinical trials, for example SCH-420814 (Merck-Schering), SYN-115 (Roche), vipadenant, ST-1535 (Armentero et al., 2011).

Similar approaches were used to demonstrate the $A_{2A}R$ interaction with metabotropic glutamate receptor type 5 ($mGlu_5R$). $A_{2A}R$ co-immunoprecipitates with $mGlu_5R$ in co-transfected cells and colocalized in striatal tissue (Ferré et al., 2002).

Radioligand binding assays in rat striatum membranes showed that stimulation of $mGlu_5R$ also produced a decrease in the affinity of D_2R for its agonists. Moreover, when $A_{2A}R$ and $mGlu_5R$ were simultaneously stimulated the inhibitory effect on D_2R was stronger that the reduction induced by stimulation of either receptor alone (Popoli et al., 2001), indicating a possible existence of $A_{2A}R$-D_2R-$mGlu_5R$ heteromer.

In addition to the cross talk at the level of ligand binding, there is a strong antagonistic interaction between $A_{2A}R$ and D_2R at the second messenger level, which may not depend on the heteromerization. Stimulation of D_2R, which are coupled to inhibitory $G_{i/o}$, counteracts adenylate cyclase activation induced by stimulatory G_{olf}-coupled $A_{2A}R$ (Hillion et al., 2002; Kull et al., 1999). Stimulation of $A_{2A}R$ activates adenylate cyclase with consequent activation of the protein kinase A (PKA) signaling pathway and induction of the expression of different genes, such as c-fos and preproenkephalin, by the constitutive transcription factor CREB (Ferré et al., 1997, 2005). In AMPA receptor phosphorylation (Håkansson et al., 2006), which is important for the development of plastic changes at glutamatergic synapses, including recruitment of AMPA receptors to the postsynaptic density (Song et al., 2002). However, under basal conditions, stimulation of $A_{2A}R$ poorly activates cAMP-PKA signaling or increases gene expression owing to strong tonic inhibition of adenylate cyclase by D_2R stimulation with endogenous dopamine (Ferré et al., 1997, 2005; Lee et al., 2002). In accordance, systemic administration of selective $A_{2A}R$ agonists did not lead to an increase of striatal c-fos expression in rats (Karcz-Kubicha et al., 2006). Nevertheless, stimulation of $mGlu_5R$ agonists did induce an increase in striatal expression of c-fos (Ferré et al., 2002). $mGlu_5R$ also activated MAPK in transfected cells and striatal slices (Ferré et al., 2002) and potentiated $A_{2A}R$ signaling in a MAPK-dependent manner (Nishi et al., 2003), so $A_{2A}R$-$mGlu_5R$ and possibly $A_{2A}R$-D_2R-$mGlu_5R$ heteromers are able to modulate plastic changes in the striatum. Indeed, pharmacological or genetic inactivation of

$A_{2A}R$ or $mGlu_5R$ impaired corticostriatal LTP (d' Alcantara et al., 2001; Gubellini et al., 2003).

Even if the signaling of $A_{2A}R$ under normal conditions is depressed by endogenous dopamine levels, it can have an effect upon D_2R ligand binding as described previously in this thesis and consequently upon its signaling via PLC implicated in the activation of L-type voltage dependent L-VDCC channels (Nicola et al., 2000). This in fact is the main role of $A_{2A}R$ inhibitory regulation of D_2R stimulation in the striatum and is independent of cAMP-PKA signaling (Dasgupta et al., 1996; Ferré et al., 2008). According to Azdad et al. the D_2R-mediated suppression of NMDA-induced depolarized plateau is mediated by the suppression of LVDCC calcium channels (type Cav1-3a) current through the D_2R activation of PLC signaling cascade involving the activation of calcineurin and dephosphorylation of these channels. The $A_{2A}R$ is able to counteract this D_2R-mediated suppression of NMDA-induced depolarized plateau via a direct $A_{2A}R$-D_2R interaction at the membrane level through heteromerization (Azdad et al., 2009). This consequently leads to firing of the indirect pathway's medium spiny neurons, that is, to motor inhibition. Thus, central or local administration of $A_{2A}R$ agonists produced a pronounced decrease in motor activity (Ferré et al., 1997). Furthermore, $A_{2A}R$ agonists and antagonists selectively counteract and potentiate, respectively, the motor activation and decrease in neuronal firing and neurotransmitter release that are induced by dopamine D_2R agonists (Ferré et al., 1993, 1997; Strömberg et al., 2000). In different behavioral models, $mGlu_5R$ agonists and antagonists produced similar effects as $A_{2A}R$ agonists and antagonists, respectively, upon the D_2R motor control. So a selective $mGlu_5R$ agonist preferentially inhibited motor activation induced by D_2R agonists (Popoli et al., 2001), whereas $mGlu_5R$ antagonists counteracted the effects of D_2R antagonists (Ossowska et al., 2001). Furthermore, $A_{2A}R$ and $mGlu_5R$ agonists and $A_{2A}R$ and $mGlu_5R$ receptor antagonists also showed synergistic effects at the behavioral level (Ferré et al., 2002; Kachroo et al., 2005; Popoli et al., 2001). $A_{2A}R$-D_2R-$mGlu_5R$

receptor interactions provide the rationale for the possible application of $mGlu_5R$ antagonists or combined $A_{2A}R$ and $mGlu_5R$ antagonists in Parkinson's disease (Ferré et al., 1992, 1997; Jenner, 2005; Kachroo et al., 2005; Ossowska et al., 2001).

4.3.2. Presynaptic A_{2A} receptor heteromers.

At presynaptic level $A_{2A}R$ is found in glutamatergic terminals innervating dynorphinergic medium spiny neurons of the direct pathway (Quiroz et al., 2009; Rosin et al., 2003). Here it forms heteromers with other presynaptically located receptors, like A_1R (Ciruela et al., 2006a) (Figure 19). It was surprising at first to consider a heterodimer controlled by the same neurotransmitter, adenosine, formed by a stimulatory and an inhibitory receptor. As A_1R and $A_{2A}R$ are coupled to $G_{i/o}$ and $G_{s/olf}$-proteins, respectively (Fredholm et al., 2001; Kull et al., 1999), stimulation of presynaptic A_1R decreases the probability of neurotransmitter release, whereas activation of presynaptic $A_{2A}R$ enhances neurotransmitter release (Lopes et al., 2002; O'Kane and Stone, 1998; Quarta et al., 2004; Wu et al., 1997; Yawo and Chuhma, 1993).

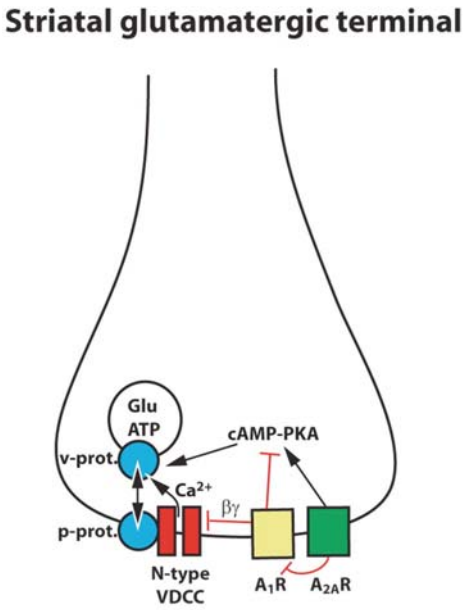

Figure 19. $A_{2A}R$ in the presynaptic terminal. $A_{2A}R$ forming heteromers with A_1R and regulating glutamate release in the cortical synapse (Ferré et al., 2007c).

The evidence for functional antagonistic interactions between A_1R and $A_{2A}R$ modulating glutamate release in the striatum and hippocampus was provided earlier by many studies (Lopes et al., 2002; O'Kane and Stone, 1998; Quarta et al., 2004). The physical interaction was demonstrated by BRET, TR-FRET and co-immunoprecipitation in 2006 (Ciruela et al., 2006a) and it was elucidated that the A_1R-$A_{2A}R$ heteromer indeed played a very important role in the glutamate release control in the striatum and that it was the concentration of extracellular adenosine that decided about the outcome. Because of that, the role of A_1R-$A_{2A}R$ heteromer is also called a concentration dependent switch. As mentioned before, the affinity of A_1R to adenosine is better (K_D=70 nM) than its affinity to $A_{2A}R$ (K_D=150 nM) (Fredholm et al., 2001). The physiological concentration of adenosine lies between this range (Delaney and Geiger, 1996) and is sufficient to activate both receptors, if they are abundantly expressed (Fredholm et al., 2007). The extracellular levels of adenosine increase locally as a function of neuronal firing and synaptic activity (Schiffmann et al., 2007). So, under basal conditions, the relatively low extracellular levels of adenosine preferentially bind to and stimulate A_1R and this preferential stimulation in the A_1R-$A_{2A}R$ heteromer inhibits glutamatergic neurotransmission. Under conditions of dramatic adenosine release, $A_{2A}R$ activation in the A_1R-$A_{2A}R$ heteromer would block A_1R-mediated function, with the overall result of a facilitation of the evoked release of glutamate (Ciruela et al., 2006a).

The inhibitory effect of A_1R on striatal glutamate release probably involves inhibition of N- and P/Q-type VDCC by $G_{\beta\gamma}$-protein subunits; this is the most commonly reported mechanism for inhibition of neurotransmitter release by $G_{i/o}$-coupled receptors, including A_1R (Jarvis et al., 2001; Yawo and Chuhma, 1993). The stimulatory effect of $A_{2A}R$ on striatal glutamate release is probably related to their ability to activate cAMP-PKA signaling as this mechanism has been shown for $A_{2A}R$ induced acetylcholine release in the striatum, GABA release in the globus pallidus and serotonin release in the hippocampus

(Gubitz et al., 1996; Okada et al., 2001; Shindou et al., 2002). This effect is related to the ability of PKA to phosphorylate different elements of the machinery that is involved in vesicular fusion (Leenders and Sheng, 2005).

The postsynaptic $A_{2A}R$ can also control the glutamate release indirectly, and that happens in the indirect pathway. In enkephalinergic medium spiny neurons, the postsynaptic $A_{2A}R$ can control the endocannabinoids production acting on presynaptic CB_1R, which coupling to G_i controls glutamate release in different brain areas (Freund et al., 2003; Piomelli, 2003). Using targeted whole-cell recordings from direct- and indirect-pathway medium spiny neurons, Lerner et al. demonstrated that $A_{2A}R$ antagonists potentiated 2-AG (2-Arachidonoylglycerol) release and induced LTD in indirect-pathway medium spiny neurons, but not the ones from the direct pathway. This suggested that $A_{2A}R$ antagonists can produce locomotor activation by disinhibiting a tonic $A_{2A}R$-mediated inhibition of D_2R-mediated endocannabinoid release in the enkephalinergic medium spiny neurons (Lerner et al., 2010).

4.4. Adenosine receptor in Huntington's disease.

4.4.1. Huntington's disease and huntingtin.

Huntington's disease (HD) is an autosomally dominant inherited progressive neurodegenerative disorder characterized by motor, cognitive and psychiatric impairments. It was named after Dr. George Huntington who first described it in 1872. Patients typically present motor disturbances as chorea (jerky, random and uncontrollable dance-like movements), which explains the middle age name for HD, the St. Vitus' dance (Walker, 2007).

HD affects about 5 individuals per 100.000 and the primary cause is a mutation of the huntingtin gene that leads to an aberrant amplification of CAG (cytosine, adenine and guanine) repeats resulting in a longer polyQ (poliglutamine) in the N-terminus of the

huntingtin protein, a fact that leads to serious pathological consequences. Normal alleles at this site contain up to 35 CAG repeats, but when they reach 41 or more, the disease manifests. With 36 to 40 repeats the disease may or may not manifest. The huntingtin gene (denominated IT15) is located in the short arm of chromosome 4 (4p16.3) and was found in 1993. HD generally starts to manifest in the fourth life decade, but a juvenile form (onset before 20 but as early as 1 year of age) also exists and occurs with a very high number of CAG repeats.

In the prediagnostic phase individuals might become irritable, multitasking becomes difficult and forgetfulness and anxiety appears. In the diagnostic phase the affected individuals show distinct chorea, incoordination and motor impersistence. Patients with early-onset Huntington's disease might not develop chorea, or it might arise only transiently during their illness. Most individuals have chorea that initially progresses but then, with later onset of dystonia and rigidity, it becomes less prominent (Walker, 2007). Cognitive dysfunction in HD often spares long-term memory but impairs executive functions, such as organizing, planning, checking or adapting alternatives, and delays the acquisition of new motor skills. These features worsen over time; speech deteriorates faster than comprehension. As motor and cognitive deficits become severe, patients eventually die, usually from complications of falls, inanition, dysphagia or aspiration. Typical latency from diagnosis to death is 20 years (Walker, 2007). In spite of a unique and known origin of the HD, a monogenic disease, no effective treatment to influence the onset or the progression is presently available.

In 1976 the first induced excitotoxic mouse model (Coyle and Schwarcz, 1976) and in 1996 the first transgenic mouse model (Mangiarini et al., 1996) were developed and several drugs passed to clinical trials with a large investigation going on. At the laboratory level HD is usually studied in cell cultures (Lunkes and Mandel, 1998) and in animal models such as *Caenorhabditis elegans* (Faber et al., 1999), *Drosophila melanogaster* (Marsh et al.,

2003) and rat (von Hörsten et al., 2003). The fly and mouse models consistently show neuronal polyglutamine inclusions and indicate that this pathology is dependent on polyglutamine length, it has a late onset, is progressive and degenerative and with neuronal dysfunction followed by neuronal death. The most studied and best-characterized transgenic mice models up to date are the R6/1 and R6/2 models. R6/1 mice express one copy of N-terminal fragment of human huntingtin with 115 CAG repeats and R6/2 express three copies with about 150 CAG repeats. R6/1 are sometimes compared with the adult and R6/2 with the juvenile form of HD (Mangiarini et al., 1996). The last years a simian model (Yang et al., 2008) and a sheep model were developed (Jacobsen et al., 2010).

Huntingtin is a large completely soluble protein of about 3,144 amino acids and 348 kDa. It is ubiquitously expressed, with the highest levels in the central nervous system neurons and the testes (Ferrante et al., 1997; Fusco et al., 1999). It is found mostly in the cytoplasm, although in lesser amounts also in the nucleus (Kegel et al., 2002). In cytoplasm it is associated with various organelles, endoplasmic reticulum, Golgi complex, both clathrin-coated and non-coated endocytic and autophagic vesicles, endosomal compartments, plasma membrane, microtubules and mitochondria (DiFiglia et al., 1995; Kegel et al., 2002). In neurons is found in soma, dendrites, axons and in nerve terminals (Li et al., 2003b).

The crystal structure of huntingtin is still not known and there are only some identified motifs in the primary amino acid sequence with a defined function. At the very N-terminus beginning at the 18th amino acid it is found the critical polyQ region. In unaffected individuals, contains from 7 to 35 glutamine residues. Perutz et al. showed that this portion forms a polar zipper structure, and suggested that its physiological function is to bind transcription factors that contain a polyQ region (Perutz et al., 1994). It has now been shown that wild-type huntingtin interacts with several partners and that the polyQ tract is a key regulator of such binding (Harjes and Wanker, 2003; Li and Li, 2004).

PolyQ region is followed by a number of prolines, polyQ stretch, which might help with solubility (Steffan et al., 2004). Downstream of these regions there are several so-called HEAT repeats, of about 40 amino acids, which are involved in interactions with other proteins (Neuwald and Hirano, 2000). There are two targeting sequences: nuclear export signal and nuclear localization signal (Xia et al., 2003). Both wild type and mutated huntingtin can be proteolytically cleaved by caspases and calpains (Gafni and Ellerby, 2002; Wellington et al., 1998) in different sites, not all well defined yet, and it is known that some cleavages occur preferentially in striatum and other in cortex (Mende-Mueller et al., 2001). The contribution of huntingtin proteolysis to cell function is not clear. However, modification in the activity of caspase and calpain reduce the proteolysis and toxicity of the mutant protein, and delay disease progression (Wellington et al., 2000).

It is not well known if HD is caused by the absence of the normal functions of huntingtin or by acquired pathological functions of the mutated protein (Cattaneo et al., 2001). Huntingtin protein is essential for normal embryonic development (Nasir et al., 1995; Wexler et al., 1987), it is also important for neuronal survival (Dragatsis et al., 2000) and neuroprotection (Cattaneo et al., 2001; Gervais et al., 2002; Humbert et al., 2002; Leavitt et al., 2006; Rigamonti et al., 2000; Zeron et al., 2002). At synaptic terminals, huntingtin is involved in the control of synaptic transmission (Smith et al., 2005; Sun et al., 2001; Zeron et al., 2002). Many of these functions are lost or affected when the mutation is present. In addition, the mutated huntingtin brings toxicity that cannot be explained by the loss of the physiological function. The late-onset of the disease reminds Alzheimer's disease since there is a production of toxic protein fragments (Temussi et al., 2003). Aggregates of cleaved or entire mutated protein accumulate in different conformations, together with bound proteases in the cytoplasm and also in the nucleus (Wellington et al., 1998) of all the cells in the brain and body. It is not known if these aggregates are toxic (Cooper et al., 1998; Hackam et al., 1998; Yang et al., 2002), are not harmful (Kuemmerle et al., 1999) or are even

neuroprotective (Arrasate et al., 2004; Truant et al., 2008), or if the fragments are more or less toxic than the entire mutated protein. Possibly the smaller fragments but not the larger aggregates are toxic and have negative effects on synaptic transmission (Li et al., 2003a).

Huntingtin's mutation leads to neurodegeneration of specific brain areas, as it is clearly visible in postmortem HD individuals' brains. These regions comprise the striatum and, in a lesser extent, cortex, hippocampus and cerebellum (Vonsattel and DiFiglia, 1998). Interestingly, the first and most affected neurons are the medium spiny neurons (MSN) that are selectively or preferentially vulnerable in HD (Graveland et al., 1985). It is interestingly to note that the enkephalinergic MSN are more vulnerable than the dynorphinergic ones (Albin et al., 1992; Reiner et al., 1988; Richfield et al., 1995) (Figure 20). The primary dysfunction and latter degeneration of enkephalinergic neurons lead to the manifestation of typical hyperkinetic symptoms of HD, chorea and dyskinetic movements as it is logically attributed to the gradual diminution of the inhibitory output of the indirect pathway. Later, when dynorphinergic MSN and nigrostriatal neurons also degenerate, chorea is replaced by a lack of movements due to the total dysfunction of basal ganglia circuitry (Glass et al., 2000). It is important to note that it is not fully elucidated why MSN are the most affected neurons in HD.

The degenerative process of MSN was described by Ferrante et al. (Ferrante et al., 1991). Degenerative changes were characterized by truncated dendritic arbors, spine loss and irregular focal swellings along dendrites. Dendritic arbors are highly dynamic structures, exhibiting frequent branch additions and retractions and maintenance of synaptic input is critical for dendritic stability (Coleman and Riesen, 1968; Jones et al., 1962; Sfakianos et al., 2007). Inversely, lack of synaptic input leads to dendritic loss. Nevertheless, the dendritic loss can also be caused by an excessive synaptic stimulation. This phenomenon is called excitotoxicity. Striatal MSN receive a strong glutamatergic input from cortex, and glutamate receptor agonists reproduced HD symptoms in excitotoxic HD animal models (Beal et al.,

1986; Popoli et al., 1994). Glutamate sensitivity depends in part on the NMDA receptors. NMDA receptors from MSN contain higher amounts of NR2B in their subunit composition than do neurons in other brain regions. This isoform is more susceptible to glutamate activation. Enkephalin neurons interestingly express even higher amounts of NR2B than the dynorphin neurons (Cepeda et al., 2001; Jarabek et al., 2004), which could also contribute to their higher excitotoxicity vulnerability.

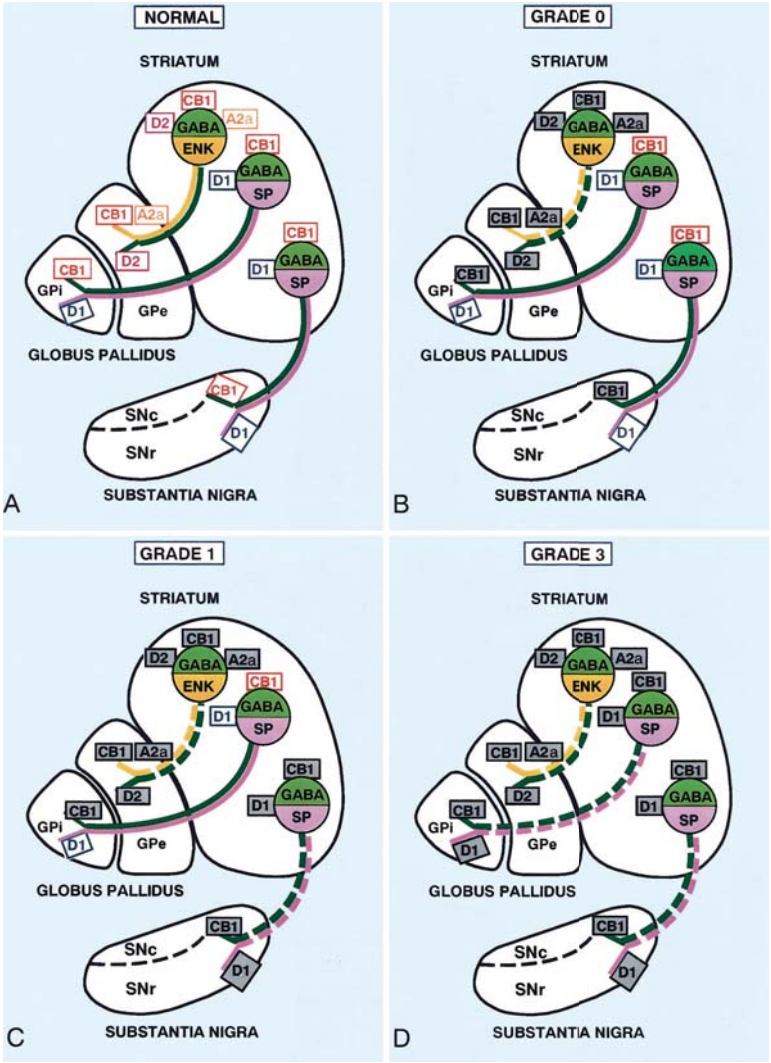

Figure 20. Degeneration of striatal neurons in HD. Gradual degeneration of striatal neurons in the first (grade 0) and late grades (3) of the HD compared with a healthy state (normal). Disappearance of the nervous projection in a dashed line. Disappearance of the $A_{2A}R$, D_1R, D_2R, CB_1R receptors staining: (grey boxes). ENK: enkephalin, SP: substance P, SNc and SNr: Substantia nigra pars compacta and reticulata, respectively (Glass et al., 2000).

4.4.2. Adenosine A_{2A} receptors in HD.

A comparative study of cannabinoid CB_1, dopamine D_1 and D_2, adenosine A_{2A} and $GABA_A$ receptor expression in the basal ganglia of graded HD revealed a complex pattern of degeneration. While loss in dopamine receptors appears to correlate with cell death progression, $A_{2A}R$ and CB_1R exhibit a much more pronounced reduction in all regions suggesting that their dysfunction is occurring prior to cell death (Glass et al., 2000).

From an autoradiography experiment using the $A_{2A}R$ agonist [^{3}H] CGS-21680 performed in post mortem brain slices of patients in early (grade 0), intermediate (grade 1 and 2) and late (grade 3) neuropathological grades of HD, it was demonstrated that the expression of $A_{2A}R$ gradually decreases in the basal ganglia of HD patients (Figure 21). In control brains $A_{2A}R$ binding was fairly homogeneous within the caudate nucleus and putamen. A dramatic loss of $A_{2A}R$ binding was observed in grade 0 (35% of controls), it was a further dramatic decrease in $A_{2A}R$ binding in grade 1 (12% of controls) and more advanced cases showed no detectable $A_{2A}R$ binding. As for the dopamine receptors, the binding appeared to decline in a heterogeneous fashion, with irregular shaped patches of receptors declining slightly more rapidly that the receptors in the surrounding regions. In the globus pallidus, $A_{2A}R$ were present only within the globus pallidus externum where a dramatic and total loss occurred in the very earliest stages of HD (Glass et al., 2000).

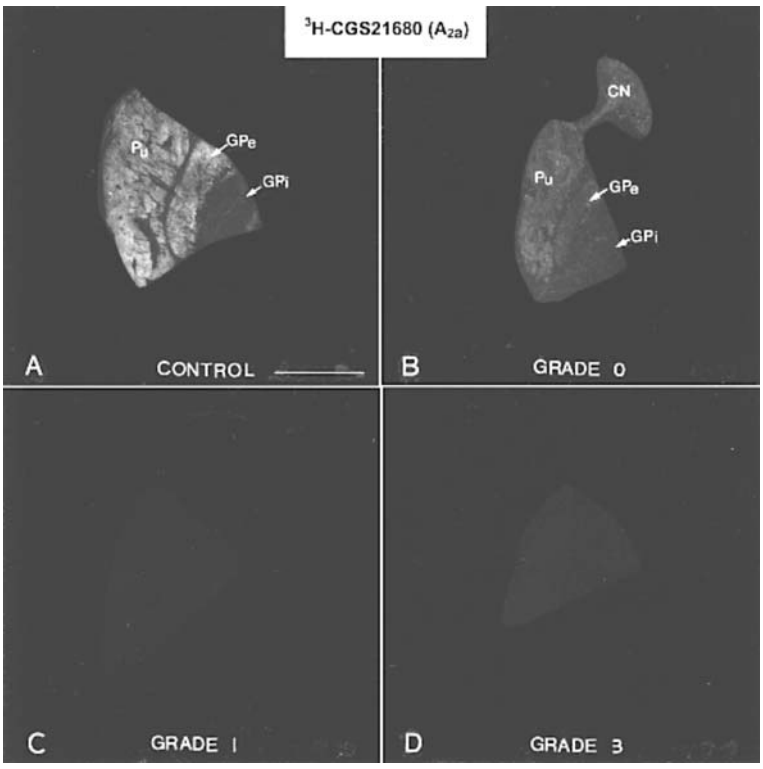

Figure 21. A_{2A} receptors in HD. Gradual disappearance of the $A_{2A}R$, stained by [^{3}H] cgs-21680 binding, in the slices of human striatum in gradual states of the progression of the disease; Pu: putamen, GPe and GPi: globus pallidus externum and internum, CN: caudate nucleus (Glass et al., 2000).

Similar experiments were performed in transgenic HD mouse model by Cha et al. (Cha et al., 1999) in brain slices of R6/2 mice in different disease stages (at 2, 4, 8 and 12 postnatal weeks). Compared to the wild type mice, $A_{2A}R$ levels were normal at two weeks of age, but significantly decreased by four week and they were only about 10% of the control at 12 week, when R6/2 develop neurological symptoms but without evidence of neuronal loss (Mangiarini et al., 1996). Similar results were also seen with R6/1 transgenic mice. D_2R and $A_{2A}R$ binding was decreased as early as three months age, that means before the R6/1 animals became symptomatic (between 15 to 21 weeks of age) (Cha et al., 1999). From the above mentioned autoradiography experiments it is not possible to discriminate between loss of agonist binding and loss in agonist affinity. When the $A_{2A}R$ expression was determined using the $A_{2A}R$ antagonist [^{3}H] ZM-241385 in saturation binding experiments in R6/2 mouse striatal membrane, an initial increase in B_{max} at the postnatal day 9-14, was followed by a decrease before the postnatal day 21 without differences in the antagonist ZM-241385 binding affinity (Tarditi et al., 2006). Giving more complexity, B_{max} and ZM-241385 binding affinity was increased in human peripheral blood cells from both symptomatic and presymptomatic HD patients (Varani et al., 2003). Similar results were observed using the $A_{2A}R$ antagonist SCH-58261 and striatal cell line expressing a mutant huntingtin (Varani et al., 2001).

The role of $A_{2A}R$ in HD is being recently investigated. It was demonstrated that total $A_{2A}R$ knock-out mice were more susceptible than wild type mice to striatal degeneration and weight loss caused by a low dosage of 3NP intoxication that did not induce glutamate-related excitotoxicity (Blum et al., 2003). Very recently, the pathophysiological consequences of genetic deletion of $A_{2A}R$ in HD have been studied by crossing $A_{2A}R$ knockout mice with the N171-82Q HD transgenic model of HD. Knockout of $A_{2A}R$ worsen moderately but significantly motor performances and survival of N171-82Q mice and leaded to a decrease in striatal enkephalin expression. These results supported that early and chronic

blockade of $A_{2A}R$ might not be beneficial in HD (Mievis et al., 2011) but, with this model, it cannot be discarded additional alterations in other protein or receptor expression due to genetic manipulation that can influence the results.

4.4.3. A_{2A} receptor antagonists in HD treatment.

In recent years several works have been published studying the effects of $A_{2A}R$ antagonists in HD animal models but they did not bring clear results. It was observed that $A_{2A}R$ agonists (CGS-21680) as well as antagonists (SCH-58261, ZM-241385) were able to improve the HD pathology. It was observed that the benefit of the effect depended on the dose used, including absolutely opposing outcome. Heteromers specificity was not considered in any of the cases and it was concluded that the mixture of pre- and postsynaptic effects is always present and cannot be eliminated (Chou et al., 2005; Cipriani et al., 2008; Domenici et al., 2007, 2007; Gianfriddo et al., 2004; Minghetti et al., 2007; Popoli et al., 2002; Scattoni et al., 2007).

First experiments were made in excitotoxic animal models. $A_{2A}R$ antagonist SCH-58261 showed neuroprotective effects in an excitotoxic HD rat model. The main mechanism of its effect was the inhibition of quinolinic acid (QA)-evoked increase in extracellular glutamate. SCH-58261 administered at low doses, but not at high doses, before the striatal injection of QA reduced the effects of QA on motor activity, electroencephalographic changes and striatal gliosis (Popoli et al., 2002). This result was confirmed in transgenic R6/2 mice, where SCH-58261 administered through microdialysis into the striatum significantly decreased the glutamate outflow (Gianfriddo et al., 2004). The beneficial effect of this antagonist was also evaluated in the same mice model but in the presymptomatic phase. One week treatment with SCH-58261 before the appearance of symptomatic phenotype prevented emotional/anxious behavior and electrophysiological alterations but tended to exacerbate the motor coordination impairment in R6/2 mice (Domenici et al.,

2007). The authors speculate that SCH-58261 administration between the fifth and sixth week of life might interfere with the modulatory role of $A_{2A}R$ on the activity of other systems and/or receptors. When the effect of SCH-58261 in R6/2 animal model was studied in symptomatic phases, after the administration of SCH-58261 for two weeks, R6/2 mice did not alleviate motor coordination alteration and only led to modest motor improvement in the inclined plane test (Cipriani et al., 2008).

The $A_{2A}R$ agonist CGS-21680 five-week treatment (starting from the seventh week) in R6/2 mice improved motor coordination, reduced the loss of brain weight and the size of neuronal intranuclear inclusions in R6/2 mice (Chou et al., 2005), suggesting that in the frankly symptomatic phase of the disease the treatment with the $A_{2A}R$ agonist, rather than the antagonist, could be beneficial. In agreement with these results, Martire et al. have shown beneficial effects of CGS-21680 but only in symptomatic phases of HD in R6/2 mice. Interestingly, upon the activation of $A_{2A}R$ opposite modulation of NMDA-induced toxicity occurred in wild type versus HD mice. In 12 to 13 weeks old animals CGS-21680 treatment helped the recovery from the NMDA-induced toxicity (measuring the recovery of extracellular field potentials) in the striatum in HD but worsened the recovery in wild type mice. In early symptomatic (7 to 8 weeks) mice, no differences were observed between wild type and HD animals in terms of basal synaptic transmission and response to NMDA (Martire et al., 2007).

5. Cannabinoid receptors.

5.1. CB_1 receptors.

Cannabis, or marijuana, has been used for centuries, but its major psychoactive constituent, Δ^9-tetrahydrocannabinol (Δ^9-THC), was not identified until 1960s (Gaoni and Mechoulam, 1971). In 1990 the first cannabinoid receptor was identified and named CB_1R (Matsuda et al., 1990) and was followed three years later by CB_2R (Munro et al., 1993). CB_2R was initially thought to be expressed mainly in the immune system (Pertwee, 1997) nevertheless, its presence was later described in glial cells (Núñez et al., 2004; Sánchez et al., 2001; Walter et al., 2003). More recently several works reporting its expression in neuronal cells appeared (Ashton et al., 2006; Brusco et al., 2008a, 2008b; Gong et al., 2006; Steindel et al., 2013; Winters et al., 2012).

The endogenous agonists of cannabinoid receptors are endocannabinoids. The first identified endocannabinoid was anandamide, making reference to the Sanskrit name for bliss or happiness, ananda (Devane et al., 1992). Later described, 2-arachidonoylglycerol (2-AG) was found to be 200 times more abundant than anandamide (Stella et al., 1997; Sugiura et al., 1995). Apart from anandamide and 2-AG, other endocannabinoids were identified, as noladin ether (Hanus et al., 2001), virodhamin (Porter et al., 2002) and N-arachinodoyldopamine (Huang et al., 2002).

All the endogenous ligands are lipidic and are biosynthesized from distinct phospholipidic precursors present in cell membranes by Ca^{2+}-dependent synthetizing enzymes also located at the plasma membrane (Bisogno et al., 2003; Okamoto et al., 2004). The enzymes necessary for the anandamide biosynthesis are the Ca^{2+}-dependent N-acyltransferase and N-acylphosphatidylethanolaminephospholipase D. For the 2-AG biosynthesis, the main enzymes involved are the Ca^{2+}-dependent and G_{q-11}-coupled receptor-activated phospholipase C and diacylglycerol lipase (DGL). The fact that the biosynthesis comes from membrane phospholipids indicates that these compounds are not stored in

vesicles like other neurotransmitters but upon demand are synthetized, released to the extracellular space and cross the membrane due to their lipidic nature although there are several pieces of evidence that both releasing and recapturing transporters exist (Beltramo et al., 1997; Hillard et al., 1997), but up to now it was not possible to identify them (Ligresti et al., 2004). Interestingly, activation of D_2R in the striatum increases anandamide but not 2-AG production (Ferrer et al., 2003; Giuffrida et al., 1999). Similarly, activation of NMDA receptors in cortical neurons was shown to increase 2-AG release whereas only simultaneous activation of NMDA and α-7 nicotinic receptors led to anandamide release (Stella and Piomelli, 2001). Endocannabinoids are degradated by presynaptically located monoacylglycerol lipase (Dinh et al., 2002) and by postsynaptically located fatty acid amide hydrolase (FAAH) (Egertová et al., 2003).

Cannabinoid effects include euphoria, relaxation, hypolocomotion or even catalepsy, tachycardia, vasodilatation, hypothermia, immunosuppression and increase of appetite (Ameri, 1999; Di Marzo et al., 2004; Piomelli, 2003). The generalized effect of cannabinoid application in the brain leads to motor suppression.

CB_1R belongs to GPRC family A (Figure 22). CB_1R is an exception of this receptor family, as it does not have a disulfide bond in the second extracellular loop, but it does contain one in the third extracellular loop and it does not have a Pro residue in the fifth transmembrane domain. It can be glycosylated in three loci and its molecular weight can differ up to 10 kDa (Nie and Lewis, 2001). Cannabinoid CB_1R is the most abundant GPCR in the brain (Katona and Freund, 2008). Within the central nervous system, CB_1R are densely distributed in the basal ganglia, hippocampus, cerebral cortex and cerebellum, with low to moderate expression in the diencephalon, brainstem and spinal cord (Glass et al., 1997; Herkenham et al., 1990).

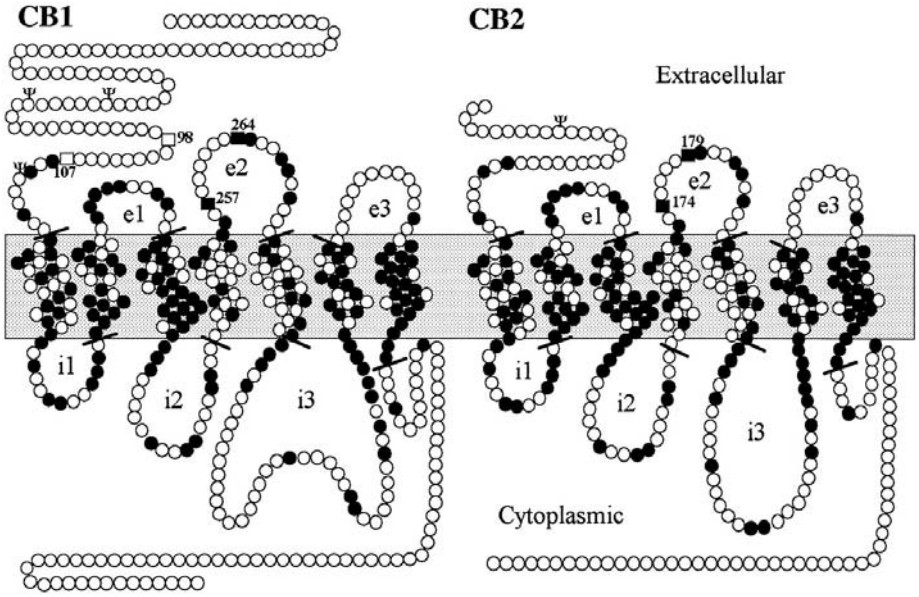

Figure 22. Human CB_1 and CB_2 receptors' structure. In black are represented conserved amino acids in both CB_1R and CB_2R. Glicosylation sites are marked with ψ (Shire et al., 1996).

The main CB_1R signaling pathway is mediated by coupling to inhibitory $G_{i/o}$ proteins, thus inhibiting adenylate cyclase (Howlett et al., 1986). Interestingly, under some conditions, CB_1R can also couple to stimulatory G_s proteins, being a promiscuous G-protein coupling receptor. This occurs, for example upon pretreatment with PTx (Bonhaus et al., 1998) or in CB_1R-D_2R heteromer (Bonhaus et al., 1998; Glass and Felder, 1997; Jarrahian et al., 2004; Kearn et al., 2005). D_2R normally couples to G_i as well as CB_1R but when they form heteromers, the receptor pair couples to only one G-protein that is G_i (Jarrahian et al., 2004). This was seen to happen constitutively (Jarrahian et al., 2004) but some works reported that $G_{s/olf}$ protein-dependent adenylate cyclase activation needs co-stimulation of both receptors (Glass and Felder, 1997; Kearn et al., 2005). CB_1R stimulation leads to activation of ERK1/2 via both PKA dependent ($G_{\alpha s}$) and independent pathways (via $G_{\beta\gamma}$ or independently of G-protein via β-arrestin). In PC12 cells, upon PTx pretreatment, CB_1R signaling was via ERK1/2 even when signaling via G_i was blocked. It is interesting to note that this signaling pattern only occurs with the addition of the agonist HU210 (Scotter et al.,

2010). Recent work showed that a single amino acid in the second intracellular loop is responsible for the preferential G_i or G_s coupling (Chen et al., 2010).

The CB_1R-mediated $G_{i/o}$-dependent signaling via ERK1/2 seemed neuroprotective in a HD cellular model. Conversely, G_s-mediated signaling induced by a promiscuous agonist, i.e. HU210 upon PTx pretreatment or by increasing cAMP levels led to an increase of huntingtin aggregates associated with cellular death (Scotter et al., 2010). The CB_1R-mediated activation of the ERK1/2 pathway, c-Fos and Krox-24 was seen strongly implicated in the protection against glutamate toxicity (Marsicano et al., 2003). Several in vivo studies have shown a robust up-regulation of c-Fos and Krox-24 in specific neuronal populations within the striatum (Glass and Dragunow, 1995; Valjent et al., 2001) and hippocampus (Derkinderen et al., 2003; Marsicano et al., 2003; Valjent et al., 2001) following cannabinoid treatment. Krox-24 and c-Fos are physiologically regulated by CB_1R in specific neuronal cells and are likely involved in neuronal long-term changes induced by cannabinoids. Krox-24 has been associated with important biological functions such as the stabilization of long lasting long-term potentiation (Dragunow, 1996; Hughes et al., 1998), cell differentiation (Krishnaraju et al., 1995; Pignatelli et al., 1999; Sukhatme et al., 1988), as well as cell survival or death signal in neuronal cells (Pignatelli et al., 1999, 2003). CB_1R also activate PKB/Akt and phosphoinositols-3-kinase signaling pathways (Bouaboula et al., 1995; Gómez del Pulgar et al., 2000; Pertwee, 1997). CB_1R inhibit voltage dependent calcium channels of both type N and P/Q and stimulate rectifying potassium channels (McAllister and Glass, 2002).

In the striatum, CB_1R are mainly localized at synapses established between glutamatergic terminals and GABAergic (both enkephalinergic and dynorphinergic) neurons (Martín et al., 2008) and play a pivotal role in the inhibitory control of motor behavior (Katona and Freund, 2008; Pazos et al., 2008). In the corticostriatal synapse CB_1R are mainly localized presynaptically but in lesser amounts also postsynaptically (Köfalvi et al.,

2005; Mátyás et al., 2006; Pickel et al., 2004, 2006; Rodriguez et al., 2001; Uchigashima et al., 2007). The main physiological function of cannabinoids at these synapses is to regulate the neurotransmitters release (Freund et al., 2003; Katona et al., 2006; Marsicano et al., 2003).

One of the best-studied functions of endocannabinoids is their retrograde signaling with stimulation of presynaptic CB_1R and the consequent inhibition of neurotransmitter release. In both hippocampus and cerebellum it was shown that activation of postsynaptic neurons resulted in the release of endocannabinoids from these neurons (Kreitzer and Regehr, 2001; Ohno-Shosaku et al., 2001; Wilson and Nicoll, 2001). Then, the endogenous ligands act as retrograde signaling molecules to inhibit presynaptic calcium influx in axonal terminals and, subsequently, reduce the neurotransmitter release. 2-AG, rather that anandamide, seems to be mainly responsible for endocannabinoid-mediated retrograde signaling in the striatum and, probably in other brain areas (Hashimotodani et al., 2007).

Synthetic cannabinoid receptor agonists were classified into four families according to their chemical structure. The classical agonists, including HU210, show similar structure to THC. The non-classical agonists, i.e. CP-55,940, are similar to the classical ligands but they do not contain the anillopyran ring. The aminoalquilindol family agonists, i.e. WIN-55,212-2, present a different chemical structure and, as it was described, bound to the receptor in a different binding site compared to the other agonists. The last family of eicosanoids, i.e. ACEA, bears a very similar structure to endocannabinoids (Lambert and Fowler, 2005).

5.2. CB_1 receptor heteromers.

In the striatal MSN, CB_1R can be found in different heteromers at the pre- and postsynaptic level in the corticostriatal synapse. These heteromers are different in the direct and the indirect pathway according to the differential distribution of the partner receptors,

namely $A_{2A}R$ and D_2R. To the described CB_1R heteromers belong the CB_1R-CB_1R homodimers (Wager-Miller et al., 2002), $A_{2A}R$-CB_1R (Carriba et al., 2007), CB_1R-D_2R heterodimers (Marcellino et al., 2008) and $A_{2A}R$-CB_1R-D_2R heterotrimers (Navarro et al., 2008).

The exact distribution of these receptor heteromers and their contribution to the control of motor function is being investigated and is not yet fully elucidated, although many pieces of partial knowledge are available. As previously mentioned, at the presynaptic level CB_1R activation leads to inhibition of glutamate release via inhibition of calcium channels thus suppressing the neurotransmission in these synapses. This can theoretically lead to motor inhibition when suppressing the glutamate release in the direct pathway but could also lead to motor activation when suppressing the glutamate release in the indirect pathways. The final motor outcome is a combination of these effects and depends on the neurotransmitter concentration, i.e. the concentration of endocannabinoids, adenosine and dopamine, activation receptor levels by these neurotransmitters and importantly on the heteromerization between receptors that can induce changes in the neurotransmitters affinity. Importantly, not only presynaptic but also postsynaptic CB_1R participate on the motor control. At the presynaptic level in the direct pathway, CB_1R can heteromerize with $A_{2A}R$ and form CB_1R-$A_{2A}R$ heterodimer (Ferré et al., 2010b). Recent work shoed that presynaptic $A_{2A}R$ inhibits the CB_1R-mediated synaptic effects and that this occurs probably via cAMP/PKA pathway (Martire et al., 2011) and may or not be dependent on the formation of CB_1R-$A_{2A}R$ heterodimer, as it could also occur at a signaling level.

On the other hand, in neuroblastoma cells endogenously expressing CB_1R and $A_{2A}R$, CB_1R signaling via $G_{\alpha i}$ is dependent on the $A_{2A}R$ activation (Carriba et al., 2007). The $A_{2A}R$ antagonist ZM-241385 inhibited the CB_1R agonist-induced decrease of forskolin-stimulated cAMP levels and antagonized the motor depressant effect of CB_1R activation, which seems contradictory to the $A_{2A}R$-CB_1R relationship at the presynaptic level. Another

recent work described that $A_{2A}R$ activation, most probably the postsynaptic $A_{2A}R$, potentiated the synaptic effects of CB_1R (Tebano et al., 2009), and that CB_1R-induced depression of synaptic transmission was prevented by pharmacological or genetic inactivation of $A_{2A}R$ (Soria et al., 2004; Yao et al., 2006). According to Tebano et al., in this case, the postsynaptic mechanism would depend on the interaction between $A_{2A}R$ and CB_1R in the enkephalinergic MSN and probably also on the interaction with D_2R as some of the effects of CB_1R-$A_{2A}R$ interactions seem to depend on D_2R function (Andersson et al., 2005). CB_1R-D_2R-$A_{2A}R$ heterotrimers have been detected in HEK cells (Navarro et al., 2008), and they are likely to occur in the striatum (Ferré et al., 2009b). Thus it seems that distinct CB_1R-containing heteromers differentially located at presynaptic or postsynaptic membranes can account for the described diverse relationship between adenosine and cannabinoids.

5.3. CB_1 receptors in Huntington's disease.

In the autoradiographic studies performed by Glass et al. (2000), caudate nucleus and putamen showed low levels of cannabinoid CB_1R binding in the normal brain. The HD grade 0 patients exhibited a moderate decrease in CB_1R binding (50% of control) as compared to controls (Figure 23).

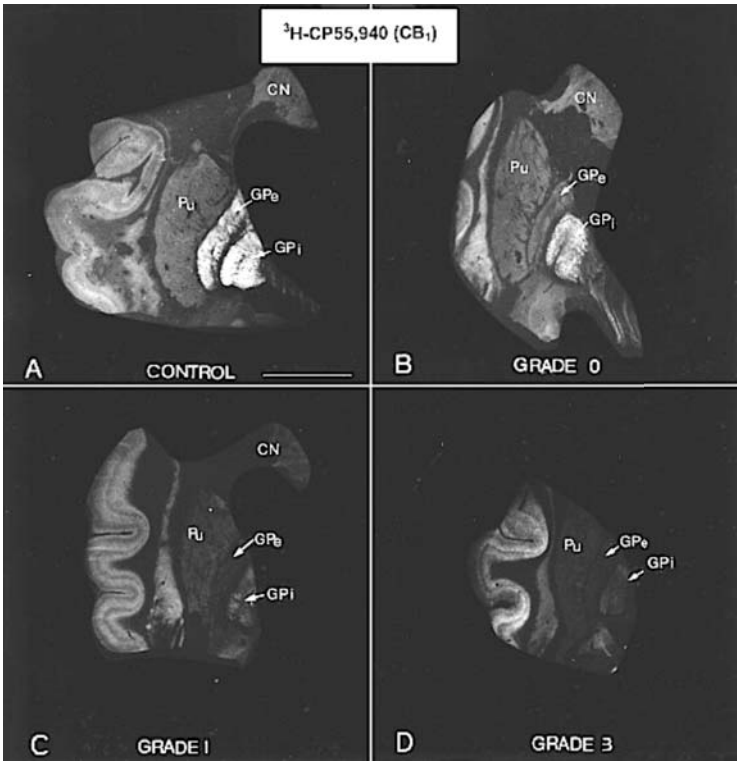

Figure 23. CB$_1$ receptor in Huntington's disease. Gradual disappearance of CB$_1$R, stained with [^{3}H] CGS-21680 binding, in the slices of human striatum in gradual states of the progression of the disease. Pu: putamen, GPe, GPi: globus pallidus externum and internum, SNc, SNr: substantia nigra pars compacta and pars reticulate, CN: caudate nucleus (Glass et al., 2000).

CB$_1$R binding decreased dramatically in all HD patients with more advanced pathology, reaching binding values similar to background levels in grade 2 and 3. Very high densities of CB$_1$R binding sites were seen in globus pallidus from control brains. The highest desities were present in GPi and moderate densities throughout the rostrocaudal extent of the GPe. Cannabinoid receptor binding was decreased in both pallidal segments in all cases of HD (Figure 23). Within the very early stages of HD (grade 0), the loss of CP-55,940 binding was pronounced, being 9% of control level. In contrast, the density of CB$_1$R binding in GPi was reduced to 19% of control. However, in more advanced cases of HD, CB$_1$R binding in both segments was decreased to an average from 3% to 7% of control level. CB$_1$R labeling within substantia nigra was very dense and discreetly localized in the pars compacta. CB$_1$R binding levels showed a marked decrease in grade 0 (19% of control), and even greater

decreases in grade 1 (10% of control). In grade 2 patients, binding was undetectable (Glass et al., 2000).

CB_1R expression down-regulation observed in HD patients and animal models seems to occur at early stages and prior to clinical symptoms appearance, neurodegeneration and changes in other neurochemical parameters (Maccarrone et al., 2007; Pazos et al., 2008). The loss of CB_1R in mutant huntingtin transgenic mice is brain region-specific, as it occurs in the lateral striatum and, to a lesser extent, in the medial striatum, but not in the cortex (Denovan-Wright and Robertson, 2000; McCaw et al., 2004). This early progressive loss subsequently contributes to the hyperkinesia observed in the initial phases of the disease (Denovan-Wright and Robertson, 2000). A significant down-regulation of CB_1R binding and messenger RNA levels has been documented in HD basal ganglia patients (Glass et al., 2000) and animal models (Denovan-Wright and Robertson, 2000; Lastres-Becker et al., 2002; McCaw et al., 2004).

CB_1R activation was protective against mutant huntingtin-induced death via $G_{i/o}$-mediated inhibition of cAMP and phosphorylation of ERK1/2 in an undifferentiated PC12 cell model of HD transfected with CB_1R. Nevertheless, CB_1R activation wit some ligands (HU210, but not WIN-55,212-2 or BAY-59-3074) was in some conditions (upon PTx pretreatment) also capable of G_s-coupling and cAMP stimulation, and resulted in enhanced aggregate formation associated with cell death in this system (Scotter et al., 2010).

In 2011 a double-mutant mouse model expressing human mutant huntingtin exon 1 in a CB_1R-null background was developed, so it was possible to study the role of CB_1R in HD (Blázquez et al., 2011). CB_1R deletion aggravated the symptoms in R6/2 mouse model. Administration of THC to R6/2 mice exerted a therapeutic effect and ameliorated neuropathology and molecular pathology. *In vitro* and *in vivo* evidence supported the CB_1R control of BDNF expression and the decrease in BDNF levels concomitant with CB_1R loss, which may contribute significantly to striatal damage in HD.

The impact of CB_1R down-regulation on HD pathology is associated, at least in part, to a loss of wilt type huntingtin function process, and that the huntingtin-mediated control of CB_1R gene expression relies on REST, a transcriptional repressor that regulates the expression of a large network of neuronal proteins (Johnson and Buckley, 2009). In addition, several reports support that CB_1R confer neuroprotection by enhancing BDNF expression, although the molecular basis of this connection remains unknown (Galve-Roperh et al., 2008). It is thus, conceivable that the decrease of BDNF levels concomitant with CB_1R loss contributes significantly to striatal damage in HD (Zuccato et al., 2008) and CB_1R-evoked neuroprotection (Galve-Roperh et al., 2008).

These results support the notion that CB_1R down-regulation sensitizes striatal cells to excitotoxic damage, while enhanced CB_1R expression renders striatal cells more resistant to excitotoxic damage. Besides this pivotal role of CB_1R, the participation of other endocannabinoid system elements in HD pathology might also be considered. Specifically, the striatal expression of the anandamide degrading enzyme FAAH is upregulated in symptomatic disease HD-like mice as well as in HD human patients, most likely reflecting a process of astroglial activation (Benito et al., 2003, 2007). Accordingly, the levels of anandamide and palmitoylethanolamide (another FAAH substrate) have been shown to decline in the striatum of symptomatic, but not presymptomatic R6/2 mice (Bisogno et al., 2008). This decrease in endocannabinoid and endocannabinoid-like messengers might contribute to the aggravation of HD symptomatology at late stages of the disease.

Pharmacological activation of CB_1R in patients with early-stage HD might be beneficial in attenuating disease progression. The first controlled trial conducted with cannabis component (cannabidiol) reported no effect on chorea severity in 15 HD patients (Consroe et al., 1991). However, cannabidiol, although structurally similar to THC, is not a cannabinoid receptor agonist. The only double-blind, placebo-controlled, cross-over study of CB_1R agonist (nabilone) in HD was reported in 2009 (Curtis et al., 2009). This 44-patient

trial showed improvements in total motor score, chorea, cognition, behavior and neuropsychiatric inventory upon cannabinoid treatment, which was safe and well tolerated.

II. AIMS

G protein coupled receptors were classically considered as individual units capable to produce an intracellular signal. Nowadays is accepted that these receptors can interact with each other forming dimers, trimers or oligomers of higher order. These interactions have to be considered as new entities because they produce important changes in the pharmacology and functionality of these receptors, which is necessary to take into account to understand processes like neuronal transmission or in the research for new pharmaceutical compounds. In this frame, the general aim of this thesis is to investigate the pharmacological and functional consequences of adenosine A_{2A} receptor interaction with other receptors. To reach this overall goal, five particular aims were formulated.

Because of the role of astrocytes in overall GABA transport, a first partial aim was to clarify whether A_1R-$A_{2A}R$ heteromers modulate GAT-1 and/or GAT-3-mediated GABA transport into astrocytes. However, the molecular stoichiometry and dynamics of the formations of these heteromers and the number of bound G proteins (G_i and/or G_s) remain unknown, that is why part of the second aim was to analyze the behavior of the steady-state population of adenosine A_1R-$A_{2A}R$ heteromers at the plasma membrane in the absence of ligands. In order to shine light on these questions this first aim was:

Aim 1. The involvement of A_1R-$A_{2A}R$ heteromer in glial cells and its study at a molecular level.

From the moment when dopamine receptor D_2R and adenosine receptor $A_{2A}R$ heteromer formation was described, these complexes have been of high interest in the development of new therapies for different pathologies. In the latest years new drugs have been developed with different affinities for these receptors and have been used for therapy and

scientific research. These therapies are based on the negative modulation that adenosine $A_{2A}R$ agonists produce on the dopamine D_2R agonists binding, but it is unknown how does this modulation occur and if the A_{2A} ligand binding modifies the D_2R antagonist binding. Considering that, the second aim of the Thesis was:

Aim 2. To find evidence for allosteric interactions between partner receptors in the $A_{2A}R$-D_2R receptor heteromer which confer specific pharmacological characteristics to the heteromer.

The adenosine $A_{2A}R$ has emerged as an attractive non-dopaminergic target in the pursuit of improved therapy for Parkinson's disease, based in part on its unique distribution in the central nervous system. It is enriched in striatopallidal neurons and can form functional heteromeric complexes with other GPCR. Blockade of the adenosine $A_{2A}R$ in striatopallidal neuron reduces postsynaptic effects of dopamine depletion, and in turn lessens the motor deficits of Parkinson's disease (Schwarzschild et al., 2006). In the other hand, adenosine $A_{2A}R$ located presynaptically is believed to be the responsible of neuronal death in Huntington's disease since in the presence of endogenous adenosine provokes a dramatic release of glutamate leading the medium spiny neurons in the striatum to die due to its excitotoxicity. With these hypothesis the third aim was:

Aim 3. Search for selective antagonists of $A_{2A}R$ for presynaptic A_1R-$A_{2A}R$ heteromers versus postsynaptic $A_{2A}R$-D_2R heteromers that can be useful for treatment of neurological disorder's treatment, particularly Huntington's disease.

In addition to forming heteromers with adenosine A_1R and D_2R, $A_{2A}R$ also interacts with cannabinoid receptors CB_1. CB_1R are found pre- and postsynaptically in both the direct and indirect pathways and might modulate the A_{2A} receptor function in the striatum. The $A_{2A}CB_1$ heteromers were previously described in our research group and, although it was known

that activation of $A_{2A}R$ was necessary for CB_1R signaling in neuroblastoma transfected cell line, the pharmacological and functional characteristics of the heteromer are not known. With this background the fourth aim was:

Aim 4. Investigate the pharmacological and functional properties of $A_{2A}R$ in the $A_{2A}CB_1$ heteromer.

Once it was demonstrated that antagonists can show different preferences for a given receptor depending on the partner entity present in the heteromer, we were interested to screen a battery of $A_{2A}R$ antagonists in the different stable cell lines expressing $A_{2A}R$ in hopes of identifying a heteromer specific compound. This would be of great interest due to the involvement of $A_{2A}R$ heteromers in neurodegenerative diseases, addictions, and other disorders. With this the fifth aim was:

Aim 5. Compound screening of different $A_{2A}R$ antagonists in stable CHO cell lines expressing $A_{2A}R$, A_1R-$A_{2A}R$, $A_{2A}R$-D_2R or $A_{2A}R$-CB_1R heteromers.

III. METHODS

First aim methods'

Glial cells study.

Ethics statement.

All animal procedures were carried out according to the European Community Guidelines for Animal Care (European Communities Council Directive – 86/609/EEC). Throughout the underlying experimental work, care was taken to minimize the number of animals used.

Drugs.

Adenosine deaminase [ADA; E.C. 3.5.4.4.; 200 U/mg in 50% glycerol (v/v), 10mM potassium phosphate] was acquired from Roche. GABA was obtained from Sigma, and the [^{3}H]GABA-specific activity 87.00 Ci/mmol was from PerkinElmer Life and Analytical Sciences. [^{3}H]R-PIA, 30.5 Ci/mmol was from Moravek Biochemicals. CGS 21680, SCH 58261, CPA, DPCPX, SKF 89976A, SNAP 5114 and U73122 were obtained from Tocris Bioscience. CADO, PTx, ChTx, forskolin, Rp-cAMPs, and R-PIA were obtained from Sigma.

Cell lines and primary astrocytic cultures.

The astrocytes were prepared from the cortex of newborn (P1-P2) Wistar rats of either sex, according to the European guidelines (86/609/EEC). Rat brains were dissected out of pups, cortex was isolated, and the meninges and white matter were removed. Cortex was dissociated gently by grinding in DMEM, filtered through a cell strainer, and centrifuged at 200 X *g*, 10 min. The pellet was resuspended in DMEM and filtered. The cells were then seeded and kept for 4 weeks in DMEM containing 10% (v/v) fetal bovine serum with antibiotic (Sigma) in a humidified atmosphere (5% CO_2) at 37^{o}C. CHO cell

clones expressing A_1R, $A_{2A}R$, or both were obtained and cultures as indicated previously (Orru et al., 2011). HEK-293T cells were grown in DMEM (Invitrogen) supplemented with 2mM L-glutamine, 100 U/ml penicillin/streptomycin, and 5% (v/v) heat inactivated fetal bovine serum (all supplements were from Invitrogen). Cells were maintained at 37°C in an atmosphere of 5% CO_2 and were passaged when they were 80-90% confluent (i.e., approximately twice a week).

[^{3}H]GABA uptake.

Assays were performed in a non-supplemented low-glucose DMEM. The astrocytes were incubated with ADA for 15 min before the addition of the test drugs; test drugs were added and incubation continued for an additional 20 min. GABA uptake was initiated by the addition of 30 μM [^{3}H]GABA (except otherwise specified). The transport was stopped after 40 seconds with 2 ml of ice-cold PBS. The amount of [^{3}H]GABA taken up by astrocytes was quantified by liquid scintillation counting. The GAT-1 and GAT-3 mediated transports were calculated through the subtraction of the amount of GABA taken up in the presence of the specific blocker of GAT-3, SNAP 5114 (40 μM), respectively, to the total transport.

Expression vectors and cell transfections.

Sequences encoding amino acids residues 1-155 and 155-238 of yellow fluorescent protein (YFP) Venus protein and amino acids residues 1-229 and 230-311 of Rluc8 protein were cloned in pcDNA3.1 vector to obtain the YFP Venus and Rluc8 hemi-truncated proteins. The human cDNAs for $A_{2A}R$ and A_1R, cloned into pcDNA3.1, were amplified without their stop codons using sense and antisense primers harboring unique EcoRI and BamHI sites to clone $A_{2A}R$ in Rluc vector and EcoRI and KpnI to clone A_1R in enhanced YFP (EYFP) vector. The amplified fragments were cloned to be in-frame into restriction

sites of pcDNA3.1Rluc (pRluc-N1; PerkinElmer Life and Analytical Sciences) and pEYPF-N1 (enhanced yellow variant of GFP; Clontech) to give the plasmids that express A_1R or $A_{2A}R$ fused to Rluc or YFP on the C-terminal end of the receptor ($A_{2A}R$-Rluc and A_1R-YFP). The cDNA encoding the serotonin 5-HT_{2B}-YFP fusion protein was kindly provided by Dr. Irma Nardi (University of Pisa, Pisa, Italy). Human cDNA for A_1R was cloned in pcDNA3.1-nRluc8 or pcDNA3.1-nVenus to give the plasmids that express A_1R fused to either nRluc8 or nYFP Venus on the C-terminal end of the receptor (A_1R-nRluc8 and A_1R-nVenus). Expression of constructs was tested by confocal microscopy and the receptor functionality by second messengers, $ERK_{1/2}$ phosphorylation, and cAMP production as described previously (Sarrió et al., 2000; Canals et al., 2003). HEK-293T cells or 2-week cultured primary astrocytes growing in six-well dishes were transiently transfected with the corresponding fusion protein cDNA by the polyethylenimine (PEI; Sigma) method. Cells were incubated (4 h) with the corresponding cDNA together with PEI (5.47nM in nitrogen residues) and 150mM NaCl in a serum-starved medium. After 4 h, the medium was changed to a fresh complete culture medium. Forty-eight hours after transfection, cells were washed twice in quick succession in HBSS with 10mM glucose, detached, and resuspended in the same buffer containing 1mM EDTA. To control the cell number, sample protein concentration was determined using a Bradford assay kit (Bio-Rad) using bovine serum albumin dilutions as standards. Cell suspension (20μg of protein) was distributed into 96-well microplates; black plates with a transparent bottom were used for fluorescence determinations, whereas white plates were used for BRET experiments.

Immunocytochemistry.

For immunocytochemistry with primary cultures of astrocytes, cell were incubated with ADA (1 U/ml) for 15 min, fixed in 4% paraformaldehyde for 20 min, and washed with PBS containing 20mM glycine to quench the aldehyde groups. Then, after permeabilization

wit 10% normal goat serum containing 0.3% Triton X-100 for 5 min, cells were treated with PBS containing 1% bovine serum albumin. After 1 h at room temperature, astrocytes were incubated with antibodies rabbit anti-GAT-1 (1:100; kindly provided by N. Brecha, University of California, Los Angeles, Los Angeles, CA) and mouse anti-GFAP (1:800; Sigma) or rabbit anti-GAT-3 (1:200; kindly provided by N. Brecha) and mouse anti-GFAP (1:800; Sigma) antibodies for 3 h at room temperature. After washes, astrocytes were stained with the secondary antibodies for 1.5 h at room temperature FITC-conjugated anti-rabbit IgG (FI-1000) and TRITC-conjugated anti-mouse IgG (T-2762); Vector Laboratories]. Dishes were then mounted, air dried, and coverslipped using Vectashield mounting medium (H-1000; Vector Laboratories). For immunocytochemistry with transiently transfected HEK-293T cells, cells treated as indicated in figure legends were fixed and permeabilized as indicated above. Cells expressing A_{2A}R-Rluc were labeled with the primary mouse monoclonal anti-Rluc antibody (1:100; Millipore Bioscience Research Reagents) for 1 h, washed, and stained with the secondary antibody Cy3 donkey anti-mouse (1:100; Jackson ImmunoResearch). A_1R-YFP was detected by its fluorescent properties. Samples were rinsed and observed in a Leica SP2 confocal microscope (Leica Microsystems).

Western blot.

For A_1R and A_{2A}R detection, primary astrocytes were rinsed with ice-cold PBS and lysed in 8 M urea, 2% SDS, 100 mM DTT, 375 mM Tris, pH 6.8, by heating to 37°C for 2 h and resolved by SDS-PAGE. Proteins were transferred to plyvinylidene difluoride membranes using a semidry transfer system and immunoblotted with the primary antibodies mouse anti-A_{2A} antibody (1:1000; Millipore) or rabbit anti-A_1 antibody (1:1000; ABR05). The blots were then incubated with a secondary horseradish peroxidase-conjugated rabbit anti-mouse IgG antibody (1:2500) or goat anti-rabbit IgG antibody (1:60,000). The immunoreactive bands were developed using a chemiluminescent detection kit. For GAT-1

and GAT-3 detection, the primary cultures of astrocytes were mechanically lysed with sucrose-containing buffer (0.32 M sucrose, 1 mM EDTA, 10 mM HEPES, 1 mg/ml bovine serum albumin, pH 7.4). To clarify, the homogenate was centrifuged (13,000 X *g*, 10 min), and the supernatant was collected. After denaturation (by Laemli's buffer heated at 95°C for 5 min), the extracts were run on a 10% acrylamide gel. Protein was transferred to a nitrocellulose membrane by electroblotting. Western blotting was performed using the anti-GAT-1 (1:100) and anti-GAT-3 (1:200) (kindly provided by N. Brecha). After exposure to secondary antibody (peroxidase anti-rabbit at 1:250; Vector Laboratories), bands were visualized by Bio-Rad Chemidoc and Quantity One software.

BRET and BRET with bimolecular fluorescence complementation assays.

Primary astrocytes or HEK-293T cells were transiently cotransfected with a constant amount of the cDNA encoding for receptors fused to Rluc, nRluc8, or cRluc8 and with increasingly amounts of the cDNA corresponding to receptors fused to YFP, nYFP Venus, or cYFP Venus. To quantify receptor-YFP expression or receptor-reconstituted YFP Venus expression, cells (20 μg protein) were distributed in 96-well microplates (black plates with a transparent bottom), and fluorescence was read in a Fluo Star Optima Fluorimeter (BMG, Lab Technologies) equipped with a high-energy xenon flash lamp, using a 10nm bandwidth excitation filter at 400nm reading. Receptor-fluorescence expression was determined as fluorescence of the sample minus the fluorescence of cells expressing the BRET donor alone. For BRET or BRET with bimolecular fluorescence complementation (BiLFC) measurements, the equivalent of 20 μg of cell suspension was distributed in 96-well microplates (Corning 3600, white plates; Sigma), and 5 (Corning 3600, white plates; Sigma), and 5μM coelenterazine H (Invitrogen) was added. After 1 min for BRET or after 5 min for BRET with BiLFC of adding coelenterazine H, the readings were collected using a Mithras LB 940 that allows the integration of the signals detected in the short-wavelength

filter at 485 nm (440-500nm) and the long-wavelength filter at 530nm (510.590nm). To quantify receptor-Rluc or receptor-reconstituted Rluc8 expression, luminescence readings were also performed after 10 min of adding 5 μM coelenterazine H. The net BRET is defined as [(long-wavelength emission)/(short-wavelength emission)] for the donor construct expressed alone in the same experiment. BRET is expressed as milli-BRET units (mBU = net BRET X 1000).

Radioligand binding experiments.

Four-week cultured primary astrocytes were disrupted with a Polytron homogenizer (PTA 20 TS rotor, setting 3; Kinematica) for three 5-s periods in 10 ml volume of 50 mM Tris-HCl buffer, pH 7.4, containing a proteinase inhibitor cocktail (Sigma). Cell debris were eliminated by centrifugation at 1000 X *g*, and membranes were obtained by centrifugation at 105,000 X *g* (40 min, 4ºC). Pellet was resuspended and centrifuged under the same conditions. Membranes were stored at -80ºC and were washed once more as described above and resuspended in 50 mM Tris-HCl buffer for immediate use. Competition experiments were performed by incubating (120 min) membranes (0.18 mg protein/ml) at 25ºC in 50 mM Tris-HCl buffer, pH 7.4, containing 10 mM $MgCl_2$ and 0.2 U/ml adenosine deaminase with 0.8 nM [^{3}H]R-PIA in the absence or presence of increasing concentrations of CGS 21680 or SCH 58261. Nonspecific binding was determined in the presence of 10 μM R-PIA. Free and membrane-bound ligand were separated by rapid filtration of 500 μl aliquots in a cell harvester (Brandel) through Whatman GF/C filters embedded in 0.3% polyethylenimine that were subsequently washed for 5 s with 5 ml of ice-cold Tris-HCl buffer. The filters were incubated with 10 ml of Ecoscint H scintillation cocktail (National Diagnosis) overnight at room temperature, and radioactivity counts were determined using a Tri-Carb 1600 scintillation counter (PerkinElmer Life and Analytical Sciences) with an efficiency of 62% (Ciruela et al., 2004). Radioligand displacement curves

were analyzed by nonlinear regression using commercial program GRAFIT (Erithacus Software) as indicated previously (Ciruela et al., 2006).

[^{35}S]GTP- γ -S assay.

For quantification of GTP activity, GDP (10 μM) was added to the primary astrocytic membranes and incubated on ice for 10 min. Membranes were incubated at 37ºC for 10 min with ADA (1 U/ml) before adding the antagonists. After 10 min, the [^{35}S]GTP- γ -S (1 nM) and the agonists were added and incubated for 30 min at 37 ºC. Membranes were collected and solubilized, and the antibodies were added: 5 μg of anti-$G_{\alpha i\text{-}3}$ (sc-262), 10 μg of anti-$G_{\alpha S}$ (sc-6766), or 10 μg of anti-$G_{\alpha q/11}$ (sc-392) for G_i, G_s, and G_q studies, respectively. After an overnight incubation at 4ºC, protein G-Sepharose was added an incubated for 90 min at 4ºC. The Sepharose was washed five times with the solubilization buffer, and the incorporation of [^{35}S]GTP- γ -S was measured by scintillation liquid.

Biotinylation assays.

Astrocytes were incubated for 30 min without (control) or with the agonists or antagonists of A_1R or A_{2A}R or both. When antagonist and agonist were tested together, the antagonist was added 15 min before. Afterward, they were incubated for 1 h with 1 mg/ml Sulfo-NHS-LC-biotin (Pierce) in PBS-Ca-Mg with gentle shaking. The biotin reaction was quenched with 100 mM glycine. The astrocytes were mechanically lysed with sucrose-containing buffer and centrifuged at 14,000 X *g*, 4ºC, 10 min. Biotinylated surface proteins were immunoprecipitated with avidin beads (Pierce) overnight at 4ºC and centrifuged at 14,000 X *g*, 4ºC, 10 min. The pellet (biotinylated fraction) was separated from the supernatant (intracellular fraction). Then, 150 μl of Laemli's buffer (70 mM Tris-HCl, pH 6.8, 6% glycerol, 2% SDS, 120 mM DTT, 0.0024% bromophenol blue) was added to the

pellet and heated to 37°C for 30 min. The avidin beads were removed by filtration. Equal volumes of each sample were loaded on gel and resolved by SDS-PAGE.

CellKey label-free assays.

The CellKey system provides a universal, label-free, cell-based assay platform that uses cellular dielectric spectroscopy (CDS) to measure endogenous and transfected receptor activation in teal time in live cells (Schröder et al., 2010). Changes in the complex impedance (ΔZ or dZ) of a cell monolayer in response to receptor stimulation were measured. Impedance (Z) is defined by the ratio of voltage/current as described by Ohm's law ($Z=V/I$). CHO cell clones stably expressing A_1R, $A_{2A}R$, or both were grown to confluence in a CellKey Standard 96-well microplate that contains electrodes at the bottom of each well. For untreated cells or for cells preincubated (overnight at 37°C) with PTx (10 ng/ml) or ChTx (100 ng/ml), medium was replaced by HBSS buffer (Invitrogen) supplemented with 20 mM HEPES for 30 min before running the cell equilibration protocol. A baseline was recorded for 5 min, and then cells were treated with the A_1R agonist CPA (10 nM) or with the $A_{2A}R$ agonist CGS 21680 (10 nM), and data were acquired for the following 10 min. To calculate the impedance, small voltages at 24 different measurement frequencies were applied to treated or non-treated cells. At low frequencies, extracellular currents that pass around individual cells in the layer were induced. At high frequencies, transcellular currents that penetrate the cellular membrane were induced, and the ratio of the applied voltage/measured current for each well is the impedance. The data shown refer to the maximum complex impedance induced extracellular currents response to the ligand addition.

Data analyses and statistics.

From the indicated number of experiments/ replicates, data are given as mean ± SEM. To test for statistical significance, the data were analyzed by one-way ANOVA, followed by Bonferroni's correction for multiple comparisons or by Student's *t* test (when only two means are analyzed). Values of $p<0.05$ were considered to represent statistical significance.

Molecular study.

Total internal reflection single-molecule microscopy and single particle data analysis.

Single-molecule imaging and tracking were performed on a Nikon Total Internal Reflection Fluorescence (TIRF) system. Typically 500 readouts of a 512 x 512 pixels region, the full array of CCD chip were acquired.

Data processing was performed using Matlab (MathWorks, Natick, MA, USA). By correlation analysis between consecutive images the two dimensional trajectories of individual molecules in the plane of focus were reconstructed by determining the probability and setting a high-confidence threshold that each step in a trajectory was from the same particle (or particle complex) and not interrupted by a photobleaching event or if another particle were not entering in the area. The average length of a trajectory for measured fluorophores was 10 to >100 steps. Multiple data sets were produced for every receptor type and for the existing complexes of the receptors separately. In brief, trajectories were then analyzed as described previously (Lommerse et al., 2004). For the analysis of the (r_i^2, t_{lag}) plots, a positional accuracy of each molecule 14 ± 3 nm in our measurements was considered (Thompson et al., 2002).

The lateral diffusion of Brownian particles in a medium characterized by a diffusion constant *D* is described by the cumulative probability distribution function for the square displacements, r^2 (Schütz et al., 1997):

[Eq.1] $P(r^2, t_{lag}) = 1 - \exp(-r^2/r_0^2)$

$P(r^2, t_{lag})$ presents the probability that the Brownian particle starting at the origin will be found within a circle or radius r at time t_{lag}. Provided that the system under study segregates into two components, characterized by mean-square displacements r_1^2 and r_2^2, and relative fractions α and (1- α), respectively, Equation 1 becomes (Schütz et al., 1997; Lommerse et al., 2004):

[Eq.2] $P(r^2, t_{lag}) = 1 - [\ \alpha \exp(- r^2/r_1^2) + (1- \alpha) \exp(-r^2/r_2^2)]$

The cumulative probability distributions $P(r_i^2, t_{lag})$ were constructed for each time lag from the single-molecule trajectories by counting the number of square displacements with values $<r^2$, and subsequent normalization by the total number of data points (Schütz et al., 1997). Probability distributions with n >1000 data points were least-square fitted to Equation 2, resulting in a parameter set $\{r_1^2(t_{lag}), r_2^2(t_{lag}), \alpha\}$, for each time lag, t_{lag}. This approach of fitting leads to a robust estimation of the mean-square displacements r_i^2 even when the mobility is not purely random (Lommerse et al., 2004).

For mobility analysis, the diffusional behavior of the respective populations of molecules was revealed by plotting the mean square displacement (r_i^2) versus t_{lag}. The (r_i^2, t_{lag}) data sets were fitted by a free diffusion model,

[Eq.3] $r^2(t_{lag}) = 4D_i t_{lag}$

where r_i^2 is proportional to time t_{lag}. When diffusion is hindered by obstruction or trapping in such a way that the mean square displacement is proportional to some power of time <1 ($r_i^2 \sim t^{\alpha}$, $\alpha < 1$), it is called anomalous subdiffusion, and the diffusion constant becomes (Lommerse et al., 2004):

[Eq.4] $D = \Gamma t_{lag}^{1-\alpha}$

If $\alpha = 1$, then $r_i^2 \sim 1$, $D = \Gamma$ is constant, and diffusion is normal. When the MSD does increase with time but leves of to a constant value for longer time lags, this was described with a confined diffusion model. The confined diffusion model assumes that

diffusion is free within a square of side length L, surrounded by an impermeable, reflecting barrier. Then the mean-square displacement depends on L and the initial diffusion coefficient D_0, and varies with t_{lag} as (Lommerse et al., 2004; Kusumi et al., 2005):

[Eq.5] $r_i^2(t_{lag}) = L^2/3\ [1-exp(-12D_0t_{lag}/L^2)]$

In stoichiometry analysis, achievements of single molecule sensitivity by fluorescence permit a detailed analysis of local stoichiometries directly on the surface of the live cells. Fluorescence distribution can predict and assay higher fluorescence levels of molecular clusters to determine local stoichiometry (Schmidt et al., 1996; Harms et al., 2001). The fluorescence image of small fluorophores clusters does not vary from an image of single fluorophores, apart that it shows higher intensity. However, fluorophore photobleaching or blinking has a significant impact on an average intensity of a fluorophore cluster, reducing it and this way making a direct fluorescence intensity count more complicated. The probability density function of the fluorescence intensity displays a discrete structure and could be fitted with a sum of multiple Gaussians to indicate the stoichiometry of many clusters. In the analysis it was calculated the stoichiometry of A_1R and $A_{2A}R$ within the receptor complex combined of mixture of A_1R and $A_{2A}R$.

Computational model of the A_1R-$A_{2A}R$ tetramer in complex with G_i and G_s.

The crystal structure of the $A_{2A}R$ (PDB code 4EIY) (Liu et al., 2012) was used for the construction of $A_{2A}R$ and A_1R molecular models. The C-terminus tails of A_1R, formed by 16 amino acids (Pro311-Asp326), and $A_{2A}R$, formed by 102 amino acids (Gln311-Ser412), were considered to follow the same direction as the C-terminal tail of squid rhodopsin (Murakami and Kouyama, 2008). The active conformations of A_1R bound to G_i and $A_{2A}R$ bound to G_s were modeled from the crystal structure of β_2-adrenergic receptor in complex with G_s (Rasmussen et al., 2011). The globular α-helical domain of the α-subunit was modeled in the closed conformation (Chung et al., 2011), using the crystal structure of

[AlF_4] activated G_i (PDB code 1AGR). The structures of Rluc, nRluc, cRluc (PDB code 2PSD) (Loening et al., 2007), Venus, nVenus, cVenus (PDB code 1MYW) (Rekas et al., 2002) and/or YFP (PDB code 2RH7) (Loening et al., 2007) were fused to the C-terminus of A_1R and $A_{2A}R$, and to the N-terminus of the α- and γ-subunits of G_i and G_s. Although the exact conformation of the C-tail of A_1R and $A_{2A}R$ cannot unambiguously be determined, it has been shown that the C-terminal domain of the OXE receptor expands intracellularly toward the N-terminal of both the β- and γ-subunits (Blättermann et al., 2012). Accordingly, YFP fused to the C-terminal tail of the receptor was positioned near the N-terminus of the gamma subunit as described in the OXE receptor. Cysteine cross-linking experiments have suggested that receptor oligomerization involves the surfaces of TM1, TM4 and/or TM5 (Guo et al., 2008). Recently, the crystal structure of the μ-opioid receptor has revealed crystallographic two-fold axis through the TM1 and TM5 interfaces (Maurice et al., 2010), while the crystal structure of the histamine H_1-receptor shows a parallel dimer through TM4 (Shimamura et al., 2011). Thus, the structures of adenosine receptor dimerization, both homo- and hetero-dimerization, were modeled either via TM1, TM4 or TM5 interfaced using the structures of the μ-opioid receptor and histamine H_1R as template. However, it is important to note that in order to accommodate Rluc and YFP fused to the N-terminal α-helix of the α-subunits of G_i and G_s respectively, it is necessary to modify the TM5 interface midway between the interface observed in the μ-opioid receptor (Maurice et al., 2010) and the proposal reported by Cys-crosslinking (Guo et al., 2008). Thus, in the proposed molecular model of the tetrameric A_1R-$A_{2A}R$ heteromer in complex with G_i and G_s, a small shit in the TM5 interface between A_1R and $A_{2A}R$ was performed, which results in a large change in the orientation of G_i and G_s.

Expression vectors.

Sequences encoding YFP Venus, Rluc8, $A_{2A}R$ and A_1R were cloned as explained above. $G_{\alpha s}$ cloned in *SFV1* vector, $G_{\alpha i}$ cloned in the pcDNA3.1 vector or G_γ cloned in

pEYFP-C1 vector, were amplified without their stop codons using sense and antisense primers harboring unique *HindIII* and *BamHI* sites to clone them into the pcDNA3.1-Rluc vector or EcoRI and KpnI to clone $G_{\alpha s}$ into the *pEYFP-N1* vector. The amplified fragments were subcloned to be in-frame with restriction sites of pcDNA3.1Rluc or *pEYFP-N1* vectors to give the plasmids that express proteins fused to Rluc or YFP on the C-terminal end. The human cDNA for A_1R was cloned into pcDNA3.1-nRluc8 or pcDNA3.1-nVenus to give plasmids that express A_1R fused to either nRluc8 or n-YFP Venus on the C-terminal end of the receptor. The human cDNA for $A_{2A}R$ was cloned into pcDNA3.1-cRluc8 or pcDNA3.1-cVenus to give plasmids that express $A_{2A}R$ fused to either cRluc8 or cYFP Venus on the C-terminal end of the receptor. Expression of constructs was tested by confocal microscopy and the receptor-fusion protein functionality by second messengers, $ERK_{1/2}$ phosphorylation and cAMP production as described previously (Navarro et al., 2010).

Cell culture and transient transfection.

HEK-293T cells were grown in DMEM (Gibco) supplemented with 2mM L-glutamine, 100U/ml penicillin/streptomycin, and 5% (v/v) heat inactivated FBS (all supplements were from Invitrogen, Paisley, Scotland, UK). Cells were maintained at 37ºC in an atmosphere of 5% CO_2, and were passaged when they were 80-90% confluent, i.e. approximately twice a week. Cells growing in 6-well dishes were transiently transfected with the PEI method as described above. For single-molecule imaging, cells were seeded into six-well plates containing glass coverslips (No. 1, round, 24 mm; Assistant, Sodheim, Germany) or into Lab-Tek Chambered #1.0 Borosilicate Coverglass System (Nunc, Thermo Fisher Scientific, Scwerte, Germany). Cell transient transfections were performed with Lipofectamine™2000 (Invitrogen, Life Technologies, Darmstadt, Germany) or FuGENE 6 (Roche Applied Science, Indianapolis, IN, USA) and application of 0.1-0.2 μg plasmid

DNA per well (A_1-GFP, A_{2A}R-mCherry). Before each experiment cells were washed three times with 200 μL phenol red-free DMEM. During measurements cells were kept in 200 μL air buffer (Ohrt et al., 2011).

Energy Transfer Assays.

BRET and BRET with BiLFL assays were performed as described above.

Second aim methods'

Mutant A_{2A}R and fusion proteins.

Human cDNAs of the A_{2A}R and D_2R cloned in pcDNA3.1 were used. The Ser_{374} in the C-terminal domain of the human A_{2A}R was mutated to Ala to obtain the A_{2A}^{A374}R cloned in pcDNA3.1. Mutations were performed by site-directed mutagenesis (Cellogenetics, Ijamsville, MD, USA). A_{2A}R, A_{2A}^{A374}R and D_2R cDNA's were amplified without their stop codons using sense and antisense primers harboring unique EcoRI and BamHI sites to clone A_{2A}R and A_{2A}^{A374}R in the Rluc corresponding vector or D_2R in the EYFP corresponding vector. The amplified fragments were cloned to be in-frame into restriction sites of the multiple cloning sites of pcDNA3.1-Rluc or pEYFP-N1 (Clontech, Heidelberg, Germany) to give the plasmids corresponding to A_{2A}-Rluc, A_{2A}^{A374}-Rluc or D_2-YFP receptor fusion proteins. The fusion proteins were expressed at the membrane level, were not highly over-expressed and were quantitatively expressed in similar amounts (Carriba et al., 2008).

Cell culture and transient transfection.

CHO cell lines were maintained in α-MEM medium without nucleosides containing 5% FBS, 50 μg/mL penicillin, 50 μg/mL streptomycin, and 2 mM L-glutamine

(300 μg/mL). Cells were maintained at 37ºC in an atmosphere of 5% CO_2, and were passaged when they were 80-90% confluent, twice a week. For transient transfection, human cDNAs of the $A_{2A}R$, $A_{2A}^{A374}R$ and D_2R cloned in pcDNA3.1 were used. CHO cells growing in 150 cm^2 dishes at 70-80% confluence were transiently transfected with 2 μg of D_2R cDNA or double transfected with 2 μg of D_2R cDNA and 3 μg of $A_{2A}R$ or $A_{2A}^{A374}R$ cDNA with lipofectamine (Invitrogen™, Carlsbad, USA), as described by the supplier. After 4 hours, the medium was changed to a fresh complete culture medium. Forty-eight hours after transfection, cells were washed twice in quick succession in PBS, detached, and resuspended in the same buffer, Sample protein concentration was determined as indicated above to control cell number.

BRET assays.

CHO cells growing in 6-well plates were transiently transfected with the indicated amounts of plasmid cDNAs corresponding to the indicated fusion proteins by the same procedure described above. BRET assays were also performed as described above.

Brain samples.

Sheep brain samples were obtained from the local slaughterhouse 5 to 10 hours after death and striatum were rapidly dissected on ice. Human brain samples were obtained at autopsy in the Basque Institute of Legal Medicine (Bilbao, Spain) from male subjects without a history of neuropathological or psychiatric disorders and who had died suddenly, mainly by car accident. Toxicological screening was negative for all these subjects and brain samples were histologically determined as normal. Samples from caudate nucleus of each subject were dissected at the time of autopsy, stored at -70ºC until assay and encoded in order to identify the subject. The time interval between death and autopsy (postmortem

delay at 4ºC) was 26±4hours. All tissue samples were collected in accordance with protocols approved by the Human Studies Committee of each of the institutions involved.

Membrane preparation and protein determination.

Membrane suspensions from brain samples or CHO cells were disrupted with a Polytron homogenizer (PTA 20 TS rotor, setting 3; Kinematica, Basel, Switzerland) for two periods of 5 second in 10 ml of 50mM Tris-HCl buffer, pH 7.4 containing a proteinase inhibitor cocktail (Sigma, St. Louis, MO, USA). Cell debris was removed by centrifugation at 1,500 *g* for 5 min at 4ºC and membranes were obtained by centrifugation at 105,000 *g* (40 min, 4ºC). Membranes were resuspended and centrifuged under the same conditions. The pellet was stored at -20ºC, washed once more as described above and resuspended in 50 mM Tris-HCl buffer for immediate use. Membrane protein was determined by the bicinchoninic acid method (Pierce Chemical Co., Rockford, IL, USA) using bovine serum albumin dilutions as standard.

Radioligand binding assays.

Membrane suspensions (0.5 mg of protein/ml) were incubated for 2 h at 25ºC in incubation buffer with the indicated free concentration of the dopamine D_2R antagonist [^{3}H]raclopride (GE Healthcare, UK) the dopamine D_2R agonist [^{3}H]quinpirole (NEN PerkinElmer, Wellesley, MA, USA) or the $A_{2A}R$ antagonist [^{3}H]ZM 241385 (American Radiolabelled Chemicals, St. Louis, MO, USA), in the absence or in the presence of increasing concentrations of the adenosine $A_{2A}R$ ligands CGS 21680 (Sigma) or caffeine (Sigma) or increasing concentrations of the adenosine A_1R ligands R-PIA (Sigma), CCPA (Sigma) or DPCPX (Tocris). The incubation buffer was 50 mM Tric-HCl buffer, pH 7.4 supplemented with 10 mM $MgCl_2$, 120 mM NaCl and 5 mM KCl for [^{3}H]raclopride or [^{3}H]ZM 241385 binding. To determine the affinity constants for $A_{2A}R$, competition

experiments were performed with [^{3}H]ZM 241385 (2 nM) and increasing concentrations of CGS 21680, caffeine or DPCPX were added to the incubation medium. To determine affinity constants for D_2R, competition experiments were performed with [^{3}H]raclopride (2 nM) or [^{3}H]quinpirole (6 nM) and increasing concentrations of raclopride or quinpirole in the absence or in the presence of the indicated concentrations of $A_{2A}R$ ligands. Non-specific binding for D_2R was determined in the presence of 50 μM raclopride and non-specific binding for $A_{2A}R$ was determined in the presence of 50 μM CGS 21680. In all cases, free and membrane-bound ligand were separated by rapid filtration of 500 μl aliquots in a cell harvester (Brandel, Gaithersburg, MD, USA) through Whatman GF/C filters embedded in 0.3% polyethylenimine that were subsequently washed for 5 s with 5 ml of ice-cold Tris-HCl buffer. The filters were incubated with 10 ml of Ecoscint H scintillation cocktail (National Diagnostics, Atlanta, GA, USA) overnight at room temperature and radioactivity counts were determined using a Tri-Carb 1600 scintillation counter (PerkinElmer, Boston, MA, USA) with an efficiency of 62% (Sarrió et al., 2000).

Binding data analysis.

Radioligand competition curves were analyzed by non-linear regression using the commercial Grafit curve-fitting software (Erithacus Software, Surrey, UK), by fitting the binding data to the mechanistic two-state dimer receptor model (Franco et al., 2005; Casadó et al., 2009). Since there is now abundant evidence for GPCR oligomerization, including A_1R, $A_{2A}R$ and D_2R (Ciruela et al., 1995; Canals et al., 2004; Guo et al., 2008) and the minimal functional unit of GPCRs in biological tissues seems to imply dimerization (Guo et al., 2008), this model considers a homodimers as the minimal structural unit of the receptor. Here, we also consider the possibility of a homodimers as the minimal structural unit of a receptor forming homomers or forming heteromers with another receptor. To calculate the

macroscopic equilibrium dissociation constants the following equation for a competition experiment deduced previously (Casadó et al., 2007, 2009) was considered:

$$A_{\text{total bound}} = (K_{DA2}A + 2A^2 + K_{DA2}AB / K_{DAB})\, R_T / (K_{DA1}K_{DA2} + K_{DA2}A + A^2 + K_{DA2}AB / K_{DAB} + K_{DA1}K_{DA2}B / K_{DB1} + K_{DA1}K_{DA2}B^2 / (K_{DB1}K_{DB2})) + A_{\text{non-specific bound}}$$

where A represents free radioligand (the adenosine A_1R or A_{2A} ¡R od dopamine D_2R antagonist [^{3}H]DPCPX, [^{3}H]ZM 241385 or [^{3}H]YM 09151-2, respectively or the A_1R agonist [^{3}H]R-PIA) concentration, R_T is the total amount of receptor dimers and K_{DA1} and K_{DA2} are the macroscopic equilibrium dissociation constants describing the binding of the first and the second radioligand molecule (A) to the dimeric receptor; B represents the assayed competing compound concentration, and K_{DB1} and K_{DB2} are, respectively, the macroscopic equilibrium dissociation constants for the binding of the first ligand molecule (B) to a dimer and for the binding of the second ligand molecule (B) to the semi-occupied dimer; K_{DAB} is the hybrid equilibrium radioligand/competitor dissociation constant, which is the dissociation constant of B binding to a receptor dimer semi-occupied by A.

When the radioligand A shows non-cooperative behavior, the previous equation can be simplified to this next equation due to the fact that $K_{DA2} = 4K_{DA1}$ (Casadó et al., 1990, 2007) and, therefore, K_{DA1} is enough to characterize the binding of the radioligand A:

$$A_{\text{total bound}} = (4K_{DA1}A + 2A^2 + 4K_{DA1}AB / K_{DAB})\, R_T / (4K_{DA1}^2 + 4K_{DA1}A + A^2 + 4K_{DA1}AB / K_{DAB} + 4K_{DA1}^2B / K_{DB1} + 4K_{DA1}^2B^2 / (K_{DB1}K_{DB2})) + A_{\text{non-specific bound}}$$

Binding to GPCRs quite often displays negative cooperativity. Under these circumstances $K_{D2}/K_{D1}>4$ and then K_{D1} and K_{D2} represent the high-affinity and the low-affinity binding sites, respectively. On the other hand, for positive cooperativity, $K_{D2}/K_{D1}<4$ and then K_{D2} represents the high-affinity and K_{D1} represents the low-affinity binding sites (Casadó et al., 1990). The two-state dimer model also introduces a cooperativity index (D_{CB}). The dimer cooperativity index for the competing ligand B is calculated as (Casadó et al., 1990, 2007):

$D_{CB} = \log (4K_{DB1} / K_{DB2})$

The way the index is defined is such that its value is "0" for non-cooperative binding, positive values of D_C indicate positive cooperativity, whereas negative values imply negative cooperativity (Ferré et al., 2007; Casadó et al., 2009).

In experimental conditions when both the radioligand A and the competitor B (i.e., most adenosine $A_{2A}R$ antagonists tested in the study) show non-cooperativity, it results that $K_{DA2} = 4K_{DA1}$ and $K_{DB2} = 4K_{DB1}$, and the first equation showed can be simplified to:

$$A_{\text{total bound}} = (4K_{DA1}A + 2A^2 + 4K_{DA1}AB / K_{DAB}) R_T / (4K_{DA1}^2 + 4K_{DA1}A + A^2 + 4K_{DA1}AB / K_{DAB} + 4K_{DA1}^2B / K_{DB1} + K_{DA1}^2B^2 / K_{DB1}^2) + A_{\text{non-specific bound}}$$

When both the radioligand A and the competitor B (DPCPX, ZM 241385, SCH 23390 or YM 09151-2) are the same compound and the binding is non-cooperative, the previous equation simplifies to:

$$A_{\text{total bound}} = (4K_{DA1}A + 2A^2 + AB) R_T / (4K_{DA1}^2 + 4K_{DA1}A + A^2 + AB + 4K_{DA1}B + B^2) + A_{\text{non-specific bound}}$$

Goodness of fit was tested according to reduced χ^2 value given by the non-linear regression program. The test of significance for two different population variances was based upon the F-distribution. Using this *F* test, a probability greater than 95% ($p<0.05$) was considered the criterion to select a more complex equation to fit binding data over the simplest one. In all cases, a probability of less than 70% ($p>0.30$) resulted when one equation to fit binding data was not significantly better than the other. Results are given as parameter values ± S.E.M. of three-four independent experiments.

Third aim methods'

Ethics statement.

All animals used in the study were handled in accordance with the National Institutes of Health Animal care guidelines. The animal research conducted to perform this study was approved by NIDA IRP Animal Care and Use Committee (under the auspices of protocol 09-BNRB-73) on 12/07/2009.

Animals.

Male Sprague-Dawley rats (Charles River Laboratories, Wilmington, MA) weighting between 300-350 g were used in these experiments. Rats were housed 2 per cage and they maintained at a temperature of 22±2°C on a regular 12 h light-dark cycle. Food and water were available *ad libitum*.

Adenosine $A_{2A}R$ antagonists. The following $A_{2A}R$ antagonists were used: SCH 442416, SCH 58261, SCH 420814, ZM 241385, KW 6002, MSX 2, MSX 3. MSX 3 is a water-soluble phosphate pro-drug of MSX 2 (Sauer et al., 2000). For their systemic administration, the compounds were prepared as follows: SCH 442416 and SCH 58261 were suspended in a solution of 5% dimethyl-sulfoxyde (DMSO) (Sigma-Aldrich, St. Louis, MI), 5% TWEN80 (Sigma-Aldrich, St. Louis, MI) and 90% ddH_2O; SCH 420814 was suspended in a solution of 20% PEG400, 40% β-cyclodextrin and 40% Lutrol 1% (in ddH_2O); ZM 241385 was suspended in a solution of 15% DMSO, 10% TWEEN80 and 75% ddH_2O; KW 6002 was suspended in a solution of 8% TWEEN80 and 92% ddH_2O; MSX 3 was dissolved in sterile saline (with 3 µl/ml saline of 1 M NaOH solution, final pH 7.4). All drugs but MSX 3 (Sigma-Aldrich, St. Louis, MI) were provided by CHDI Foundation Inc. (Los Angeles, CA, US). SCH 420814 was administered subcutaneously

(s.c.) at 1 ml/kg and the other drugs were administered via intraperitoneal (i.p.) injection at volume of 2 ml/kg.

Locomotor activity.

Locomotor activity was measured by placing the animals individually in motility soundproof chambers (50 X 50 centimeters; Med Associates Inc., VT). Locomotion was measured by counting the number of breaks in the infrared beams at noon on the day of testing. A lamp inside each chamber remained lit during this period. Following 90 min of habituation, the rats were injected i.p. with different doses of each compound or vehicle and locomotor activity was recorded for 90 min after the drug or vehicle administration. All the animals were tested only once. The effect of different doses of the $A_{2A}R$ antagonists on locomotor activity were analyzed using a one-way analysis of variance (ANOVA), followed by Newman-Keuls' *post-hoc* test.

Surgical procedures.

Rats were anesthetized with 3 ml/kg of Equithesin (4.44 g of chloral hydrate, 0.972 g on Na pentobarbital, 2.124 of $MgSO_4$, 44.4 ml of propylene glycol, 12 ml of ethanol and distilled H_2O up to 100 ml of final solution; NIDA Pharmacy, Baltimore, MD) and implanted unilaterally with bipolar stainless steel electrodes, 0.15 mm in diameter (Plastics One, Roanoke, VA), into the orofacial area of the lateral agranular motor cortex (3 mm anterior, 3 and 4 mm lateral, and 4.2 mm below bregma). The electrodes and a head holder (connected to a swivel during stimulation) were fixed on the skull with stainless steel screws and dental acrylic resin. For the experiments with electromyographic (EMG) recording, electrodes were also implanted in mastication muscles (during the same surgical procedure). Two 5 mm-long incisions were made in the skin on the upper and lower jaw areas to expose the masseter and the lateral pterygoid muscles. Two silicon rubber-coated coiled stainless

steel recording electrodes (Plastics One, Roanoke, VA) were slipped below the skin from the incision in the skull until the tips showed up from the incisions in the jaw. The bare tips of the electrodes were then held in contact with the masseter and the lateral pterygoid muscles and the skin was closed with surgical staples. The other end of the recording electrodes was encased in a model plastic pedestal with a round threaded post, which was attached to an electrical swivel and then to a differential amplifier (Grass LP511, Grass Instruments, Warwick, RI). The pedestal was secured to the skull with dental cement together with the stimulation electrodes. For the *in vivo* microdialysis experiments, concentric microdialysis probes with 2-mm long dialysis membranes (Eicom Corp. Tokio, Japan) were implanted respectively into the striatum ipsilateral to the stimulation electrodes (0.0 mm AP, 4.5 ML and 7.0 mm DV)

EMG recording and power correlation analysis.

Rats were placed in individual bowl chambers. Both stimulation electrodes and recording electrodes were attached using flexible shielded cabling to a four channel electrical swivel. Stimulation electrodes were connected to two-coupled constant current isolation units (PSIU6X, Grass Instruments Wes Warwick, RI) driven by an electrical stimulator (Grass s88X; Grass Instruments). The recording electrodes were connected to a differential amplifier (GrassLP511, West Warwick, RI). This configuration allows the rat to move freely while the stimulation and EMG recordings are taking place. After 60 min of habituation, biphasic current pulse trains (pulse of 0.1 ms at 120-200μA; 100Hz, 160 ms trains repeating once per 2 seconds) were delivered. The current intensity was adjusted to the threshold level, defined as the minimal level of current intensity allowing at least 95% of the stimulation pulses to elicit a positive EMG response. Positive EMG response was defined as at least 100% increase of the peak amplitude respect to the background tonic EMG activity lasting more that 100 ms or at least 70% increase in the power of the EMG signal respect to the

baseline. Positive EMG responses always matched observable small jaw movements. The threshold level was different for each animal but it was very stable and reproducible once established. The threshold level was in the 100 to 150 μA range for most cases and it reached 200 μA in a few (6) animals. Animals that failed to show a positive EMG response with electrical cortical stimulation intensities of 200 μA were discarded from the experimental procedure (less than 10%). Both stimulator monitoring and the amplified and filtered EMG signal (20,000 times gain, bandwidth from 10 to 1,000 Hz with a notch filter set at 60 Hz) were directed to analog-to-digital converter for recording (Lab-Trax-4, World Precision instruments, Sarasota, FL) and backup (NI 9215, National Instruments, Austin, TX) and digitized at a sampling rate of 10,000 samples/second. Recordings of the digitized data were made using the software Data Trax2 software (World Precision Instruments) and LabVIEW SignalExpress (National Instruments). A power correlation analysis was used to quantify the correlation between the stimulation pulses of current delivered into the orofacial motor cortex (input signal; μA) and the elicited EMG response in the jaw muscles (output signal; μV). Decrease in the power correlation coefficient (PCC) between these two signals is meant to describe a decrease in the efficacy of the transmission in the neural circuit. Off-line, both signals were rectified and the root mean square (RMS) over each period of the stimulation pulses was calculated in the recorded signals using Data Trax2 software. The transformed data (RMS) from the stimulator monitor and the EMG were then exported with a time resolution of 100 samples/second to a spreadsheet file. The stimulation signal values were used as a reference to select data in a time window of 320 ms starting at the beginning of each train of pulses. This time window was chosen to ensure the analysis of any EMG response whose occurrence or length was delayed from the onset of the stimulation trains and to maximize the exclusion from the analysis of spontaneous jaw movements not associated with the stimulation. Pearson's correlation between RMS values from the stimulation and EMG signals was then calculated for each experimental subject. PCC was

calculated using the data recorded 40 min after the administration of the dose of any compound or vehicle. The effects of the different doses of $A_{2A}R$ antagonists on PCC were analyzed by a one-way ANOVA, followed by Dunnett's *post-hoc* test.

In vivo microdialysis.

The experiments were performed on freely moving rats 24 h after probe implantation. An artificial cerebrospinal solution of (in mM) 144 NaCl, 4.8 KCl, 1.7 $CaCl_2$, and 1.2 $MgCl_2$ was pumped through the microdialysis probe at a constant rate of 1 μl/min. After a washout period of 90 min, dialysate samples were collected at 20.min intervals. After 60 min of collecting samples for baseline, the rats were injected either with the $A_{2A}R$ antagonists KW 6002 or SCH 442416. Both compounds were compared to vehicle controls (5% DMSO, 5% of TWEEN80 and 90% of ddH_2O). After 20 min from drug or vehicle injection, electrical stimulation pulses were applied through the electrodes implanted in the orofacial motor cortex for 20 min (pulse of 0.1 ms at 50-150 μA; 100 Hz, 160 ms trains repeating once per second) and samples were collected for 2 additional hours. Glutamate content was measured by reverse-phase HPLC coupled to a fluorimetric detector (Shimadzu Inc., Tokio, Japan) (Quarta et al., 2004). Glutamate values were transformed as percentage of the mean of the three values before the drug or vehicle injection and transformed values were statistically analyzed. The effect of KW 6002, SCH 442416 and vehicle were analyzed using a one-way ANOVA for repeated measures followed by a Turkey's *post-hoc* test.

Cell clones.

To obtain CHO cells expressing single receptors or coexpressing $A_{2A}R$ and A_1R or $A_{2A}R$ and D_2R, the human cDNAs for A_1R or D_2R cloned in pcDNA3.1 vector (containing a geneticin resistance gene) were used. The human $A_{2A}R$ was cloned into a pcDNA3.1/Hygro vector with a hygromycin resistance gene. For single transfections, CHO

cells were transfected with the cDNA corresponding to $A_{2A}R$, A_1R or D_2R using lipofectamine (Invitrogen, Carlsbad, USA) method following the instructions of the supplier. 24 h after transfection the selection antibiotic was added at a concentration that was previously determined by a selection antibiotic test. Antibiotic resistant clones were isolated in the presence of the selection antibiotic (1,200 μg/ml geneticin or 1,000 μg/ml hygromycin). After an appropriate number of days/passages, several stable lines were selected and cultured in the presence of the selection antibiotic (600 μg/ml geneticin or 300 μg/ml hygromycin). To obtain clones co-expressing $A_{2A}R$ and A_1R or $A_{2A}R$ and D_2R, CHO cells expressing high affinity $A_{2A}R$ (obtained as above described) were transfected with the human cDNAs for A_1R or D_2R cloned in pcDNA3.1 vector using lipofectamine. After an appropriate number of days/passages stable lines were selected and cultured in the presence of the selection antibiotic. The receptor(s) expression in the cell clones was first detected by dot-blot of cell lysates using commercial available antibodies and wild-type CHO cells lysates as negative basal staining. Positively moderated stained clones were grown to obtain membranes in which the receptor expression was quantified by radioligand-binding experiments.

Bioluminescence Resonance Energy Transfer (BRET) assays.

The fusion proteins $A_{2A}R$-Rluc, A_1R-YFP and D_2R-YFP were prepared and characterized as described elsewhere (Navarro et al., 2009). The cDNA encoding serotonin $5HT_{2B}$-YFP receptor was kindly provided by Dr. Irma Nardi (University of Pisa, Italy). CHO cells were transiently transfected with the corresponding fusion protein cDNA using lipofectamine. Cells were incubated (4 h) with the corresponding cDNA together with lipofectamine and Opti-MEM medium (Invitrogen). After 4 hours, the medium was changed to a fresh complete culture medium. Twenty-four hours after transfection, cells were washed twice in quick succession in HBSS with 10 mM glucose and scraped in 0.5 ml

of the same buffer. To control the cell number, sample protein concentration was determined using a Bradford assay kit (Bio-Rad, Munich, Germany) using bovine serum albumin dilutions as standards. To quantify fluorescence proteins, cells (20 μg protein) were distributed in 96-well microplates (black plates with a transparent bottom) and fluorescence was read at 400 nm in a Fluo Star Optima Fluorimeter (BMG Labtechnologies, Offenburg, Germany) equipped with a high-energy xenon flash lamp, using a 10 nm bandwidth excitation filter. Receptor-fluorescence expression was determined as fluorescence of the sample minus the fluorescence of cells expressing protein-Rluc alone. For BRET measurements, the equivalent of 20 μg of cell protein were distributed in 96-well plates (Corning 3600, white plates; Sigma) and 5 μM coelenterazine H (Molecular Probes, Eugene, OR) was added. After 1 minute of adding coelenterazine H, the readings were ceollected using a Mithras LB 940, which allows the integration of the signals detected in the 485 nm-short- (440-500 nm) and the 530 nm-long- (510-590 nm) wavelength filters. To quantify receptor-Rluc expression luminescence readings were performed after 10 minutes of adding 5 μM coelenterazine H. The net BRET is defined as [(long-wavelength emission)/(short-wavelength emission)]-Cf where Cf corresponds to [(long-wavelength emission)/(short-wavelength emission)] for the Rluc construct expressed alone in the same experiment.

Radioligand binding experiments.

Cell membranes were disrupted and prepared as described above. The competition experiments were also performed as described above.

Fourth aim methods'

Receptor ligands.

The following $A_{2A}R$ antagonists were used: ZM 241385 (Tocris, Bristol, UK), SCH 442416 (Tocris, Bristol, UK), KW 6002 (Axon Medchem, Groningen, Netherlands) and VER 7835 (Kindly provided by Dr. Sergi Ferré). As $A_{2A}R$ agonists CGS 21680 (Sigma, St. Louis, MO, USA) was used. As CB_1R agonist CP 55,940 (Tocris, Bristol, UK) was used.

Cell clones and cell culture.

CHO cell lines were obtained and maintained as described above. To obtain CHO cells co-expressing $A_{2A}R$ and CB_1R, the human cDNA of CB_1R cloned in pcDNA3.1 was amplified without its codon stop using sense and antisense primers harboring unique BamHI and EcoRI. The amplified fragment was subcloned to be in-frame into restriction sites of the multiple cloning sites of *pEYFP-N1* vector, with a geneticin resistance gene (Clontech, Heidelberg, Germany), to give the plasmids corresponding to CB_1-YFP receptor fusion protein. CHO-A_{2A} cells were transfected with the cDNA for CB_1YFP receptor construct using the lipofectamine method. After an appropriate number of days/passes, stable lines were selected and cultured in the presence of the selection antibiotic (300 μg/ml hygromycin, 1200 μg/ml geneticin). Expression of CB_1R was first detected by monitoring its own fluorescence emission at 530 nm in a fluorescent microscope Zeiss Axiovert 25 (Göttingen, Germany) and fluorescent clones were cultured in presence of the selection antibiotic (300 μg/ml hygromycin, 600 μg/ml geneticin). Moderately fluorescent clones (500 – 5,000 fluorescent units in 0.2 mg/ml protein solution), were selected by fluorescence reading in a Fluostar Optima Fluorimeter (BMG Labtechnologies, Offenburg, Germany) equipped with a high-energy xenon flash lamp, using an excitation filter at 485 nm and emission filter at 530 nm. The selected clone (CHO A_{2A}-CB_1 cells) was grown to obtain membranes in which the receptor expression was quantified by radioligand-binding experiments.

$ERK_{1/2}$ phosphorylation assay.

CHO A_{2A} or CHO A_{2A}-CB_1 cells were cultured in serum-free medium containing 0.2 U/ml of ADA for 16 h before the addition of any agent. Cells were stimulated at 37ºC in the same fresh medium for 5 min with the indicated concentrations of A_{2A}R agonist CGS 21680 and/or the CB_1R agonist CP 55,940. Cells were washed with ice-cold PBS and lysed by the addition of 500 μl of ice-cold lysis buffer [50 mM Tris-HCl pH 7.4, 50 mM NaF, 150 mM NaCl, 45 mM 2-glycerolphosphate, 1% Triton X-100, 20 μM phenyl-arsine oxide, 0.4 mM sodium orthovanadate and protease inhibitor cocktail]. Cell debris was removed by centrifugation at 13,000 *g* for 5 min at 4ºC and the protein was quantified using the BCA method using BSA dilutions as standards. To determine the level of $ERK_{1/2}$ phosphorylation, equivalent amounts of protein (15 μg) were separated by electrophoresis on denaturing SDS-PAGE (10% acrylamide gels) and transferred on to PVDF-FL membranes. Odyssey blocking buffer (LI-COR Biosciences) was then added, and membranes were rocked for 60 min. Membranes were then probed with a mixture of a mouse anti-(phosphor-$ERK_{1/2}$) antibody (1:2,500 dilution; Sigma) and rabbit anti-$ERK_{1/2}$ antibody (1:40,000 dilution; Sigma) overnight. Bands were visualized by the addition of a mixture of IRDye 800 (anti-mouse) antibody (1:10,000 dilution; Sigma) and IRDye 680 (anti-rabbit) antibody (1:10,000 dilution; Sigma) for 1 h, washed with PBS and scanned by the Odyssey scanner (LI-COR Biosciences). Bands densities were quantified using the scanner software and exported to Excel (Microsoft). The level of phosphorylated $ERK_{1/2}$ isoforms was normalized for differences in loading using the total $ERK_{1/2}$ protein band intensities.

CellKey label-free assays.

These assays were performed and analyzed as described above.

Radioligand binding experiments.

Cells were disrupted and cell membranes obtained as described above. Competition experiments were performed as described above with the difference that for CB_1R the Tris-HCl buffer contained 1 mg/ml fatty acid free BSA (Sigma, St. Louis, MI, USA), with the indicated free concentration of the $A_{2A}R$ antagonist [^{3}H]ZM 241385, $A_{2A}R$ agonist [^{3}H]CGS 21680 or the CB_1R agonist [^{3}H]CP 55,940 (NEN PerkinElmer, Welleskey, MA, USA) and increasing concentrations of ZM 241385, CGS 21680, SCH 442416, KW 6002 or VER 7835 in the absence or, when indicated , in the presence of a constant concentration of the compound acting as a modulator. Non-specific binding was determined in the presence of 11 μM of the corresponding non-radiolabelled ligand. Free and membrane bound ligand were separated by rapid filtration of 500 μl aliquots in a cell harvester (Brandel, Gaithersburg, MD, USA) through Whatman GF/C filters embedded in 0.3% polyethylenimine containing 1 mg/ml fatty acid free BSA for CB_1R binding, that were subsequently washed (or washed twice for CB_1R binding) for 5 s with 5 ml of ice-cold 50 mM Tris-HCl buffer containing 1 mg/ml fatty acid free BSA for CB_1R binding. The filters were incubated and counted as described above.

Binding data analysis.

Binding data was analyzed as described above.

Fifth aim methods'

Radioligand binding experiments.

Cells were seeded, disrupted and processed as described above.

Binding data analysis.

Binding data was analyzed as described above.

IV. RESULTS AND DISCUSSION

CHAPTER 1

1.1. A_1R-$A_{2A}R$ heteromers coupled to G_s and $G_{i/0}$ proteins modulate GABA transport into astrocytes.

Astrocytes modulate synaptic transmission because they can release and uptake neurotransmitters (Hamilton and Attwell, 2010) and, therefore, fine tune the balance between excitation and inhibition. GABA is the main inhibitory neurotransmitter in the CNS, in which it plays a crucial role in the control of excitability (Schousboe and Waagepetersen, 2007), plasticity (Artola and Singer, 1987), and network synchronization (Blatow et al., 2003). These actions depend on changes in the extracellular concentrations of GABA, which are under control of GABA transporters (GATs) expressed in both neurons and astrocytes (Minelli et al., 1995, 1996). Cortical astrocytes express GAT-1 and GAT-3 subtypes, and it has been estimated that approximately 20% of extracellular GABA may be taken up into astrocytes (Hertz et al., 1992).

Astrocytes release large amounts of ATP, which is then hydrolyzed into adenosine by the action of ecto-nucleotidases (Hamilton and Attwell, 2010). Extracellular adenosine operates through GPCRs. In the case of neural cells, the A_1R and $A_{2A}R$ subtypes are those that are most likely activated by basal levels of extracellular adenosine. The A_1R is often inhibitory and couple $G_{i/o}$ proteins, whereas the $A_{2A}R$ is usually coupled to G_s proteins, enhancing cAMP accumulation and PKA activity (Fredholm et al., 2001). A_1R and $A_{2A}R$ may closely interact in such a way that activation of $A_{2A}R$ can lead to inhibition of A_1R-mediated responses (Correia-de-Sá and Ribeiro, 1994; Cunha et al., 1994; Lopes et al., 1999). Some interactions may occur at the functional and transducing system levels

(Sebastião and Ribeiro, 2000), but energy transfer assays in the form of bioluminescence (BRET) and fluorescent (FRET) resonance energy transfer have identified the presence of A_1R-$A_{2A}R$ heteromers in immortalized transfected cells (Ciruela et al., 2006). Together, these data strongly suggest a putative role of A_1R-$A_{2A}R$ heteromers in neurons. However, direct evidence for A_1R-$A_{2A}R$ heteromerization in neural cells is still lacking.

Due to the role of astrocytes in overall GABA transport, a first aim of the present work was to clarify whether A_1R and $A_{2A}R$ modulate GAT-1 and/or GAT-3-mediated GABA transport into astrocytes. We detected a tight interaction between A_1R and $A_{2A}R$, including evidence of cross-antagonism, a biochemical property often demonstrated for receptor heteromers (Ferré et al., 2001). In addition we found A_1R-$A_{2A}R$ heteromers in astrocytes. We found these heteromers couple to two different G proteins, G_s and $G_{i/0}$, both regulating GABA transport in an opposite way, with the A_1R protomer mediating inhibition of GABA transport and the $A_{2A}R$ protomer mediating facilitation of GABA transport into astrocytes. This A_1R-$A_{2A}R$ functional unit may, therefore, operate as a dual amplifier to control ambient GABA levels at synapses.

1.1.1. Endogenous adenosine tonically modulates GABA uptake.

To assess the role of adenosine during GABA uptake, we first incubated the astrocytes with different concentrations of CADO, an adenosine analog with similar affinity for A_1R and $A_{2A}R$ that is resistant to hydrolysis or uptake by the cells. At a relatively low CADO concentration (0.3 μM), there was an inhibition of total GABA taken up by astrocytes, whereas at higher concentrations (3-10 μM), CADO facilitated total GABA uptake (Fig. 1A). This biphasic influence on GABA transport could be either attributable to activation of different adenosine receptors, namely A_1R and $A_{2A}R$, or a differential influence over the two GATs present in astrocytes, GAT-1 and GAT-3 (Fig. 1F,G). Hence, GAT-1 or GAT-3 activity was independently assayed. The removal of endogenous adenosine with ADA (1 U/ml) led to a decrease in GABA transport, and this decrease was highly significant when transport was mediated by either GAT-1 (Fig. 1B) or GAT-3 (Fig. 1C), suggesting that extracellular adenosine is tonically facilitating GAT-1 and GAT-3 activity. When endogenous adenosine had not been removed by pre-incubation with ADA, CADO at a low conecntration (1 μM) already enhanced GABA transport (33 ± 9%, n=3, p<0.05), most probably because the effect of endogenous and the exogenous agonists is additive; at a higher concentration (10 μM) CADO caused a pronounced decrease in GABA transport (46 ± 3%, n=3, p<0.05), comnpatible with receptor internalization due to receptor overstimulation. To control occupation of adenosine receptors with known agonist concentrations and to avoid variability due to differences in endogenous adonosine in different cultures (Vaz et al., 2011), all subsequent transport assays were performed in cells preincubated with ADA (1 U/ml).

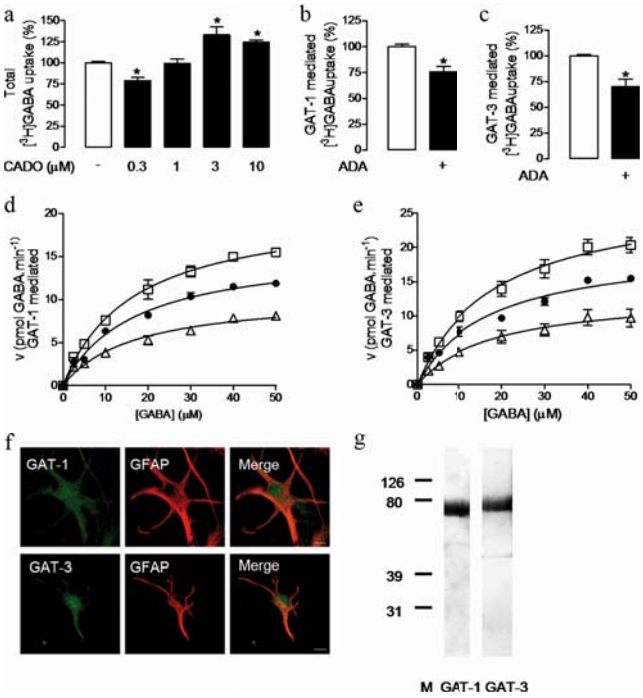

Figure1. Adenosine receptor activation modulates [^{3}H]GABA uptake in astrocytes. Astrocytes were incubated with medium or with increasing CADO concentrations (**a**) or 1 U/ml ADA (**b**,**c**) and the total [^{3}H]GABA uptake (**a**) or GAT-1 –mediated (**b**) or GAT-3-mediated (**c**) uptake was determined. In (**d**) and (**e**), uptake was determined using increasing [^{3}H]GABA concentrations. The A_{2A}R agonist CGS 21680 (30 nM, squares) enhanced and the A_1R agonist CPA (30 nM, triangles) decreased the GAT-1-mediated (**d**) and GAT-3-mediated (**e**) uptake (control uptake: circles) (V_{max} of GAT-1: 25.1 ± 1.7 pmol GABA/min vs 14.9 ± 0.9 pmol GABA/min of control, *p<0.01, n=6; and V_{max} of GAT-3: 30.9 ± 1.6 pmol GABA/min vs 22.5 ± 1.6 pmol GABA/min of control, *p<0.001, n=6). In (**f**), for immunohistochemistry analysis of GAT-1 (green, top row) and GAT-3 (green, bottom row) expression by astrocytes, GFAP (red) was used as astrocyte marker. In (**g**), solubilized astrocytes were analyzed by SDS-PAGE and immunoblotted using rabbit anti-GAT-1 antibody (1:100) or rabbit anti-GAT-3 antibody (1:200) (M: molecular mass markers). Results in a-e are shown as mean ± SEM of four to six independent experiments. Statistical significance was calculated by one-way ANOVA, followed by Bonferroni's multiple comparison test; *p<0.001 compared with control (white bars).

1.1.2. A_1R activation decreased and $A_{2A}R$ activation enhanced GABA uptake.

Selective agonists of A_1R and $A_{2A}R$ were used to assess the influence of the adenosine receptors on GABA transporters. The selective A_1R agonist CPA (30 nM) decreased maximal velocity (V_{max}) of GABA transport mediated by GAT-1 (Fig. 1D) or GAT-3 (Fig. 1E), whereas the selective agonist for $A_{2A}R$, CGS 21680 (30 nM), enhanced V_{max} for GAT-1 (Fig. 1D) and GAT-3 (Fig. 1E), without affecting transport K_M values ($p>0.05$, n = 6). These data indicate that adenosine receptor activation modified maximum transport capacity rather that in the affinity of the transporters for GABA and that inhibition of GAT-1 and GAT-3 is mediated by A_1R, whereas facilitation requires $A_{2A}R$ activation. To further confirm that A_1R and $A_{2A}R$ affect GABA transport in opposite ways, we used combinations of agonists and antagonists selective for either receptor (Table 1).

Table1. Binding affinity of agonists and antagonists of adenosine receptors [KD values with 95% confidence intervals (in parentheses) or ± SEM].

Drug	A_1R	$A_{2A}R$	$A_{2B}R$	A_3R
CPA	2.3[a]	790[a]	34,400[b] 21,000[d]	43[a]
CGS 21680	290[a]	27[a]	361,000[b]	67[a]
DPCPX	3.9[a]	129[a]	50[b] 51[d]	4,000[a]
SCH 58261	290[c]	0.6[c]		>10,000[c]

[a] (Klotz et al., 1998), [b] (Linden et al., 1999), [c] (Ongini et al., 1999) and [d] (Ji and Jacobson, 1999).

Results are summarized in Figure 2. CPA and CGS 21680 effect were measured in the presence of the A_1R-selective antagonist DPCPX (50 nM) or the $A_{2A}R$-selective antagonist SCH 58261 (50 nM). Surprisingly, the effect of the A_1R agonist was fully prevented not only by previous blockade of the A_1R with DPCPX but also by the blockade

of $A_{2A}R$ with SCH 58261. For these experiments, the concentration of each compound was chosen to act in a selective way. Analogously, facilitation of GABA transport by the $A_{2A}R$ agonist CGS 21680 was completely abolished by the blockade of either $A_{2A}R$ or A_1R. These results strongly indicate that A_1R and $A_{2A}R$ are tightly interacting and represent a clear example of cross antagonism between the two receptors. Such antagonism may be attributable to heteromerization (Callén et al., 2012; Ferrada et al., 2009; Moreno et al., 2011); thus, we decided to test whether A_1R and $A_{2A}R$ may form heteromers in astrocytes.

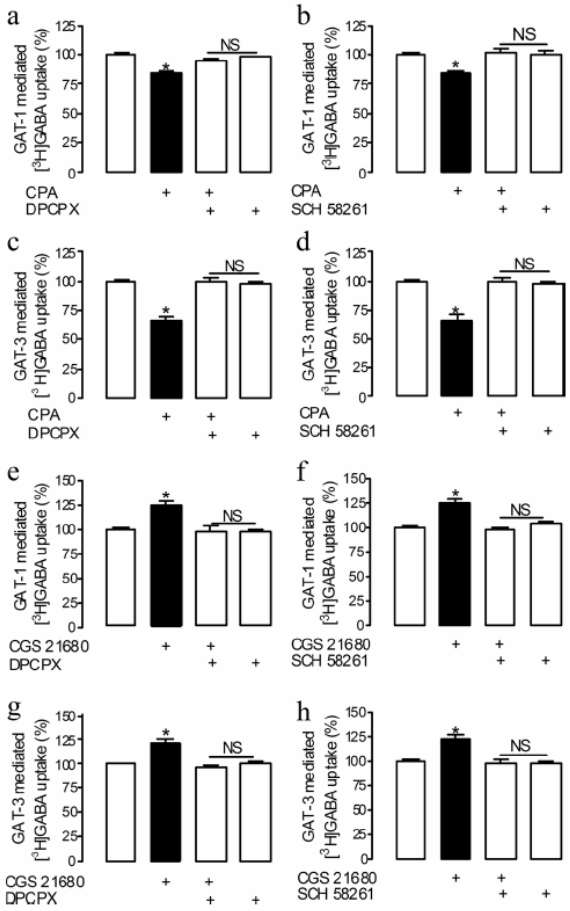

Figure 2. Inhibition of [^{3}H]GABA uptake is promoted by A_1R, whereas facilitation is mediated by $A_{2A}R$. Astrocytes were treated for 15 min with 1 U/ml ADA before the addition of medium, the A_1R antagonist DPCPX (50 nM), or the $A_{2A}R$ antagonist SCH 58261 (50 nM). After 20 min, the A_1R agonist CPA (30 nM) (**a**-**d**) or the $A_{2A}R$ agonist CGS 21680 (30 nM) (**e**-**h**) were added, and the GAT-1 (**a**, **b**, **e**, **f**) or GAT-3 (**c**, **d**, **g**, **h**) mediated [^{3}H]GABA uptake was measured as indicated in Methods. Results are mean ± SEM of six independent experiments. Statistical significance was calculated by one-way ANOVA followed by Bonferroni's multiple comparison test; *p<0.001 compared with control (white bars); NS, p>0.05.

1.1.3. A_1R-$A_{2A}R$ heteromers in astrocytes.

The BRET approach was used to evaluate the ability of A_1R to heteromerize with $A_{2A}R$ in astrocytes. First, the endogenous A_1R and $A_{2A}R$ expression in astrocytes was investigated by Western blot (Fig. 3A, B). A_1R and $A_{2A}R$ expression is relatively low at 2 weeks of cell culture but increases later, BRET measurements were performed using 2-week cultured astrocytes transiently cotransfected with a constant amount of $A_{2A}R$-Rluc (7.5 μg of cDNA) and increasing amounts of A_1R-YFP (4-15 μg of cDNA). Fusion of Rluc to $A_{2A}R$ or YFP to A_1R did not modify receptor function as determined by cAMP assays (Canals et al., 2003). A positive and saturable BRET signal was found for the pairs $A_{2A}R$-Rluc and A_1R-YFP (Fig.3C). From the saturation curve, a $BRET_{max}$ of 94 ± 15 mBU and a $BRET_{50}$ of 16 ± 2 were calculated. As a negative control, the $A_{2A}R$-Rluc and serotonin $5\text{-}HT_{2B}R$-YFP pair was used. As shown in Figure 3C, the negative control gave a linear nonspecific between $A_{2A}R$-Rluc and A_1R-YFP in astrocyte primary cultures.

Ligand binding assays to receptor heteromers in isolated membranes usually reveal a "biochemical fingerprint", which consists of changes in ligand binding characteristics of one receptor when the partner receptor is occupied by agonist (Ferré et al., 2009). No intracellular crosstalk can occur in disrupted membranes, and therefore it can be assumed that the "fingerprint" results from intramembrane receptor-receptor interactions. Although an indirect approach, it is accepted as identifier of receptor heteromers in native tissues or in cells expressing the natural non-heterologous receptors (Ferré et al., 2009). Therefore, binding experiments were performed to identify native A_1R-$A_{2A}R$ heteromers in 4-week cultured astrocytes. As shown in Figure 3D, the displacement of A_1R agonist [^{3}H]R-PIA binding by the $A_{2A}R$ agonist CGS 21680 (but not by the $A_{2A}R$ antagonist SCH 58261) was significantly ($p<0.01$) better represented by a biphasic than by a monophasic curve. It is not expected that the $A_{2A}R$ agonist, at concentrations lower that 500 nM, would significantly bind to A_1R (<1% binding to A_1R, according to the know K_D value). However, 500 nM

CGS 21680 significantly ($p<0.05$) displaced the binding of the selective A_1R agonist [^{3}H]R-PIA, with an IC_{50} value of 90 ± 30 nM. Obviously, higher concentrations of CGS 21680 caused an additional displacement of [^{3}H]R-PIA binding that, according to its IC_{50} value (8 ± 4 μM), reflects the binding of CGS 21680 to the A_1R. As expected, the $A_{2A}R$ antagonist SCH 58261 only displaced A_1R agonist binding (IC_{50} of 500 ± 120 nM) at concentrations known to lose $A_{2A}R$ selectivity and to bind to A_1R (Fig. 3D). Together, these data indicate that the biphasic [^{3}H]R-PIA binding displacement curve observed in the presence of the $A_{2A}R$ agonist constitutes a fingerprint of the A_1R-$A_{2A}R$ heteromer in non-transfected primary cultured astrocytes.

To evaluate whether A_1R-$A_{2A}R$ heteromerization could be influenced by agonist or antagonist binding, a series of experiments were performed in transiently cotransfected HEK-293T cells using a constant amount of $A_{2A}R$-Rluc (1.5 μg of cDNA) and increasing amounts of A_1R-YFP (1-8 μg of cDNA). In agreement with previous results (Ciruela et al., 2006), a positive and saturable BRET signal was found. Stimulation (20 min) with the $A_{2A}R$ agonist (CGS 21680, 30 nM) (Fig. 3E) or with the A_1R agonist (CPA, 30 nM) (Fig. 3F) did not promote any consistent ($p>0.05$) change in $BRET_{max}$ or $BRET_{50}$ values. Similar BRET values were also obtained in the presence or absence of $A_{2A}R$ (Fig. 3G) or A_1R (Fig. 3H) antagonists, indicating that neither agonist nor antagonist binding affected the receptor oligomerization state.

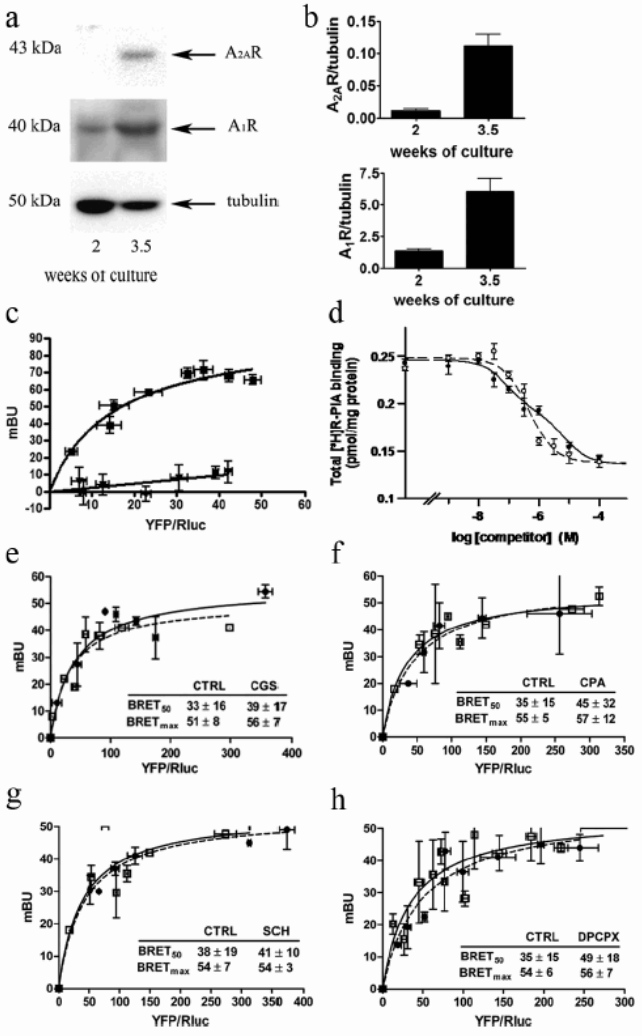

Figure 3. A_1R-$A_{2A}R$ heteromers in astrocytes. In (**a**), the expression of A_1R an $A_{2A}R$ in astrocytes after different weeks of culture was detected by Western blot as indicated in Methods using α-tubulin as loading control. Averaged (n = 3) densitometric analysis of immunoblots is shown in (**b**). In (**c**) and (**e**-**h**), BRET saturation experiments were performed using 2-weeks cultured astrocytes (**c**) or HEK-293 cells (**e**-**h**) cotransfected with 1.5 μg (**c**) or 1 μg (**e**-**h**) cDNA corresponding to $A_{2A}R$-Rluc and increasing amounts of cDNA corresponding to A_1R-YFP (squares) or 5-HT_{2B}-YFP (triangles, as negative control) constructs. In (**e**-**h**), cells were treated for 10 min with medium (squares, solid line) or with 30 nM CGS 21680 (**e**), 30 nM CPA (**f**), 50 nM SCH 58261 (**g**), or 50 nM DPCPX (**h**) (circles, solid line). The $BRET_{max}$ and $BRET_{50}$ values are shown in the insets. Both fluorescence and luminescence for each sample were measured before every experiment to confirm similar donor expressions (~100,000 luminescent units) while monitoring the increase acceptor expression (500-10,000 fluorescent units). Data are means ± SD of three different experiments grouped as a function of the amount of BRET acceptor. In (**d**), competition experiments of 0.8 nM [^{3}H]R-PIA versus increasing concentrations of the $A_{2A}R$ agonist CGS 21680 (solid line) or the $A_{2A}R$ antagonist SCH 58261 (dotted line) were performed using astrocytic membranes (0.18 mg protein/ml). Data are mean ± SEM of a representative experiment (n = 3) performed in triplicate.

1.1.4. A_1R or $A_{2A}R$ activation, but no its blockade, leads to internalization of the heteromers.

Heteromerized receptors are expected to internalize together. To test this possibility, agonist-mediated internalization of A_1R and $A_{2A}R$ was studied in astrocytes. Western blot data clearly showed that A_1R immunoreactivity at the cell surface did not only decrease after the incubation with the $A_{2A}R$ agonist (Fig. 4A). This decrease was accompanied by an increase in A_1R immunoreactivity in the intracellular fraction (Fig. 4B). No significant changes in surface (Fig. 4C) or intracellular (Fig. 4D) A_1R immunoreactivity were detected during incubation with either A_1R or $A_{2A}R$ antagonists. Interestingly, when the A_1R agonist was added after previous blockade of either A_1R or $A_{2A}R$ by the selective antagonists, it was no longer able to modify A_1R immunoreactivity at the cell surface (Fig. 4E) or in the intracellular fraction (Fig. 4F). Similarly, adding the $A_{2A}R$ agonist after a previous blockade of A_1R or $A_{2A}R$ did not promote any modification of A_1R immunoreactivity at the cell surface (Fig. 4E) or in the intracellular fraction (Fig. 4F). It therefore becomes clear that blockade of either A_1R or $A_{2A}R$ prevent A_1R internalization induced by exposure to A_1R or $A_{2A}R$ agonists.

Cointernalization of A_1R and $A_{2A}R$ after incubation with A_1R or $A_{2A}R$ agonists was also assessed by confocal microscopy analysis of HEK-293T cells coexpressing A_1R-YFP and $A_{2A}R$-Rluc. After exposure to either A_1R- or $A_{2A}R$-selective agonists, intracellular A_1R-YFP fluorescence and $A_{2A}R$-Rluc immunoreactivity markedly increased; a similar phenomenon was observed after exposure to an A_1R agonist but not after exposure to A_1R or $A_{2A}R$ antagonists (Fig. 5). Collectively, these results indicate that A_1R and $A_{2A}R$ do internalize together in response to A_1R- or $A_{2A}R$-selective agonists.

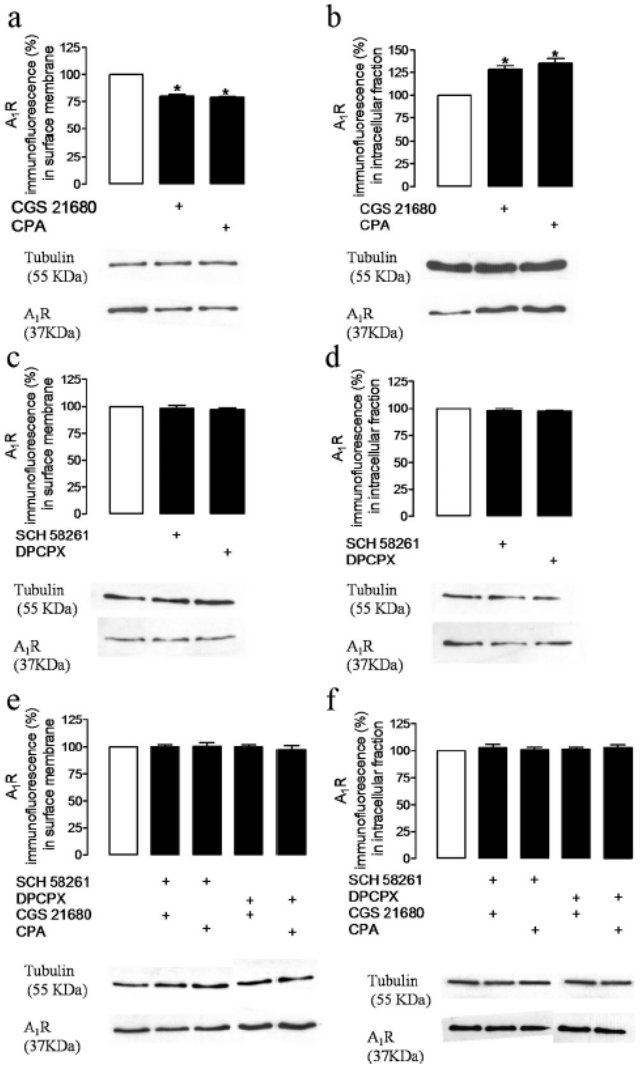

Figure 4. A_1R or $A_{2A}R$ activation (but not its blockade) in astrocytes promotes internalization of A_1R and $A_{2A}R$. Astrocytes were incubated for 30 min with the A_1R agonist CPA (30 nM) or with the $A_{2A}R$ agonist CGS 21680 (30 nM), alone (**a**, **b**) or in the presence of either the A_1R antagonist DPCPX (50 nM) or the $A_{2A}R$ antagonist SCH 58261 (50 nM) (**e**, **f**) or only with DPCPX (50 nM) or SCH 58261 (50 nM) (**c**, **d**), before starting the Biotinylation protocol. When testing the action of agonists in the presence of antagonists, the antagonists were added 15 min before the agonists. A_1R expression at surface membranes (left panels) and intracellular fraction (right panels) was determined as indicated in Methods. Results are mean ± SEM of five independent experiments. Statistical significance was calculated by one-way ANOVA followed by Bonferroni's multiple comparison test; *p<0.001 compared with control (100%, white bar).

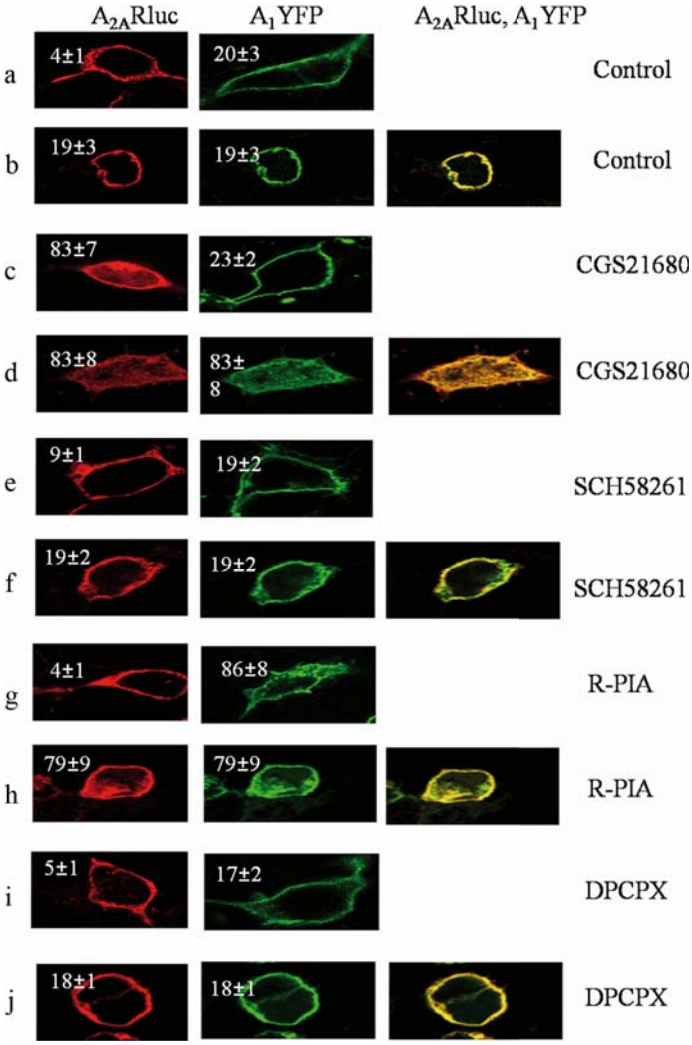

Figure 5. A_1R and $A_{2A}R$ are internalized together during exposure to either A_1R or $A_{2A}R$ agonists. HEK-293 cells were transfected with 1 μg of cDNA corresponding to $A_{2A}R$-Rluc (red) or 1 μg of cDNA corresponding to A_1R-YFP (green) (**a**, **c**, **e**, **g**, **i**) or both (**b**, **d**, **f**, **h**), and 48 h after transfection cells, were treated for 60 min with medium (**a**, **b**), 100 nM $A_{2A}R$ agonist CGS 21680 (**c**, **d**), 1 μM performed as indicated in Methods, and $A_{2A}R$-Rluc was labeled with the anti-Rluc antibody, and A_1R-YFP was detected by its fluorescence properties. Colocalization was shown in yellow. The quantification of receptor internalization after the exposure to ligands was determined by analyzing, for each condition, 40 – 50 cells from different fields in three independent preparations by confocal microscopy. Values are expressed as mean ± SEM.

1.1.5. The A_1R-$A_{2A}R$ heteromer is coupled to $G_{i/o}$ and G_s proteins.

To figure out which G proteins are coupled to the A_1R-$A_{2A}R$ heteromer, assays of [^{35}S]GTP-γ binding followed by immunoprecipitation using antibodies against different G proteins (G_s, $G_{i/o}$, and $G_{q/11}$) were performed (Rashid et al., 2007). As illustrated in Figure 6A (left), the A_1R-selective agonist CPA (30 nM) but not the $A_{2A}R$-selective agonist CGS 21680 (30 nM) significantly increased the $G_{i/o}$ activity, an effect unpredictably prevented by the $A_{2A}R$-selective antagonist. In what concerns G_s activity (Fig. 6A, middle), it was enhanced by the $A_{2A}R$-selective agonist CGS 21680 (30 nM) but not by the A_1R agonist CPA (30 nM); again, and unpredictably, the effect of the $A_{2A}R$ agonist was fully abolished by the A_1R antagonist DPCPX (50 nM). None of the adenosine receptor agonist affected $G_{q/11}$ activity, which was enhanced by acetylcholine (10 μM), used as a positive control in the same batch of astrocytic membranes (Fig. 6C, right). These data suggests that A_1R-$A_{2A}R$ heteromers are coupled to both $G_{i/o}$ and G_s proteins and not to a unique $G_{q/11}$ protein.

G protein activity may be permanently modified by the binding of several toxins, thus these are useful tools to dissect out a differential receptor-G protein coupling in intact cells and to evaluate the functional consequences of G protein-mediated-signaling blockade. GABA uptake assays were therefore performed using ChTx, which uncouples G_s from the receptors as a result of ADP-ribosylation and permanent activation of the α_s subunit (Gill and Meren, 1978), as well as using PTx, which catalyzes the ADP-ribosylation of the $G\alpha_{i/o}$ subunit and locks it in the GDP-bound inactive state, thus preventing $G_{i/o}$ protein activation (Bokoch and Gilman, 1984). Inhibition of either GAT-1- or GAT-3-mediated GABA uptake induced by the A_1R agonist CPA was fully prevented by PTx, but, interestingly, this toxin also prevented $A_{2A}R$-mediated facilitation of GAT-1- and GAT-3-mediated GABA uptake (Fig. 6B). Similar results were obtained in the reciprocal experiment using ChTx. In fact, the toxin prevented not only the facilitation of GAT-1- and GAT-3-mediated transport caused by the $A_{2A}R$ agonist CGS 21680 but also the inhibition of GABA transport

mediated by the A_1R agonist CPA (Fig. 6C). The ChTx and PTx data strongly suggests that the A_1R-$A_{2A}R$ heteromer is coupled to both G_s and G_i proteins. The results also indicate that, if one G protein (G_s or G_i) is blocked or receptor uncoupled, both A_1R and $A_{2A}R$ agonists lose their effect on GABA uptake. It seems that the A_1R-$A_{2A}R$ heteromer is the mediator of both the inhibitory and the excitatory effects triggered by, respectively, CPA and CGS 21680.

As a further approach, $G_{i/o}$, G_s, or G_q activity was also measured by the CellKey label-free assay in intact CHO cells stably transfected with A_1R, $A_{2A}R$, or both. In A_1R-transfected cells, the signaling obtained during A_1R activation with the agonist CPA (10 nM) showed a G_i profile (increases in impedance) that was completely blocked when cells were treated with PTx. Impedance did not significantly change when cells were treated with ChTx (Fig. 6D, left). In $A_{2A}R$-transfected cells, the $A_{2A}R$ agonist CGS 21680 (10 nM) induced a G_s profile (decreases in impedance) that was completely blocked when cells were treated with ChTx but not significantly modified during PTx treatment (Fig. 6D, middle). Interestingly, in cells coexpressing $A_{2A}R$ and A_1Rm the impedance profiles obtained by activation with CPA (G_i profile) or CGS 21680 (G_s profile) were fully blocked by either PTx or ChTx (Fig. 6D, right). These results strongly reinforce the notion that the A_1R-$A_{2A}R$ heteromer is coupled to both G_s and G_i proteins.

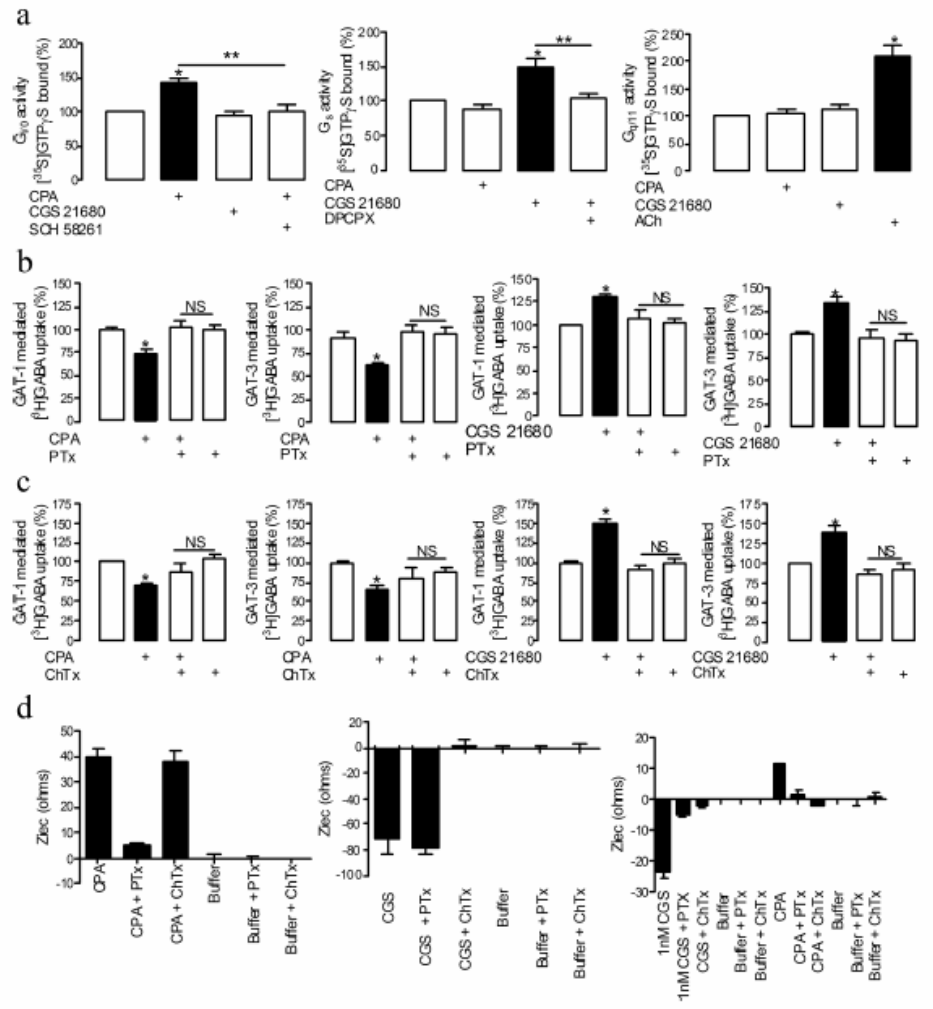

Figure 6. A_1R-$A_{2A}R$ heteromers in astrocytes is coupled to both G_s and $G_{i/o}$. In (**a**), [^{35}S]GTP-γ assays were performed as described in Methods to test $G_{i/o}$ activity (left), G_s activity (middle), or $G_{q/11}$ activity (right) using membranes from astrocytes treated for 10 min with medium, the $A_{2A}R$ antagonist SCH 58261 (50 nM), or the A_1R antagonist DPCPX (50 nM) before the activation with $A_{2A}R$ agonist CGS 21680 (30 nM) or A_1R agonist CPA (30 nM) or Ach (10 μM) as positive control. In (**b**) and (**c**), astrocytes were treated with medium, PTx (**b**, 5 μg/ml), or ChTx (**c**, 5 μg/ml) before stimulation with CPA (30 nM) or CGS 21680 (30 nM), and GAT-1- and GAT-3-mediated [^{3}H]GABA uptake was measured as indicated in Methods. Toxins were preincubated with the astrocytes for 4 h and then removed before uptake assays. (**d**), CellKey label-free assays were performed in CHO cells stably expressing A_1R (left), $A_{2A}R$ (middle), or both (right), treated with medium, PTx (10 ng/ml), or ChTx (100 ng/ml), and stimulated or not with CGS 21680 (10 nM) or CPA (10 nM). Results are as mean ± SEM from four to eight independent experiments. Statistical significance was calculated by one-way ANOVA followed by Bonferroni's multiple comparison test; *p<0.001 compared with control (100%, white bar), **p<0.001 compared with cells treated only with the agonist. NS, p>0.05.

1.1.6. A transducing unit constituted by an A_1R-$A_{2A}R$ heterotetramer.

The above-described data strongly support the notion that the heteromer is, at least, in an A_1R-A_1R-$A_{2A}R$-$A_{2A}R$ tetrameric form and is coupled to $G_{i/o}$ and G_s but not to $G_{q/11}$. This arrangement predicts that the transducing system operated by adenosine receptors to modulate GABA transport into astrocytes is centered in the adenylate cyclase AC/cAMP/PKA cascade. To address the question of whether a single cAMP/PKA-centered transducing unit is able to both inhibit and facilitate GABA transport, we tested the influence of drugs known to interfere with this transducing pathway on the effect of A_1R and $A_{2A}R$ receptor agonists on GABA transport. In addition, we also tested the blocker of phospholipase C (PLC) to evaluate a putative transducing pathway classically associated with $G_{q/11}$.

The inhibitory action of A_1R agonist on GAT-1 (Fig. 7A) and GAT-3 (Fig. 7C) still occurred in the presence of PLC blocker U73122 (3 μM; (Smith et al., 1990)), but it was totally abolished by the blockade of PKA by Rp-cAMPs (100 μM; (Wang et al., 1991)). The activation of AC with a supramaximal concentration of forskolin (10 μM; (Awad et al., 1983)) increased GABA transport and occluded the inhibitory effect of the A_1R agonist (CPA) during GABA transport (Fig. 7A, C). The facilitatory effect of the $A_{2A}R$ agonist CGS 21680 was not affected by the PLC inhibitor U73122 but was totally impaired by the PKA blocker Rp-cAMPs. The AC activator forskolin mimicked the action of the $A_{2A}R$ agonist, and its facilitatory effect was not additive with that of CGS 21680, indicating a common mechanism (Fig. 7B, D).

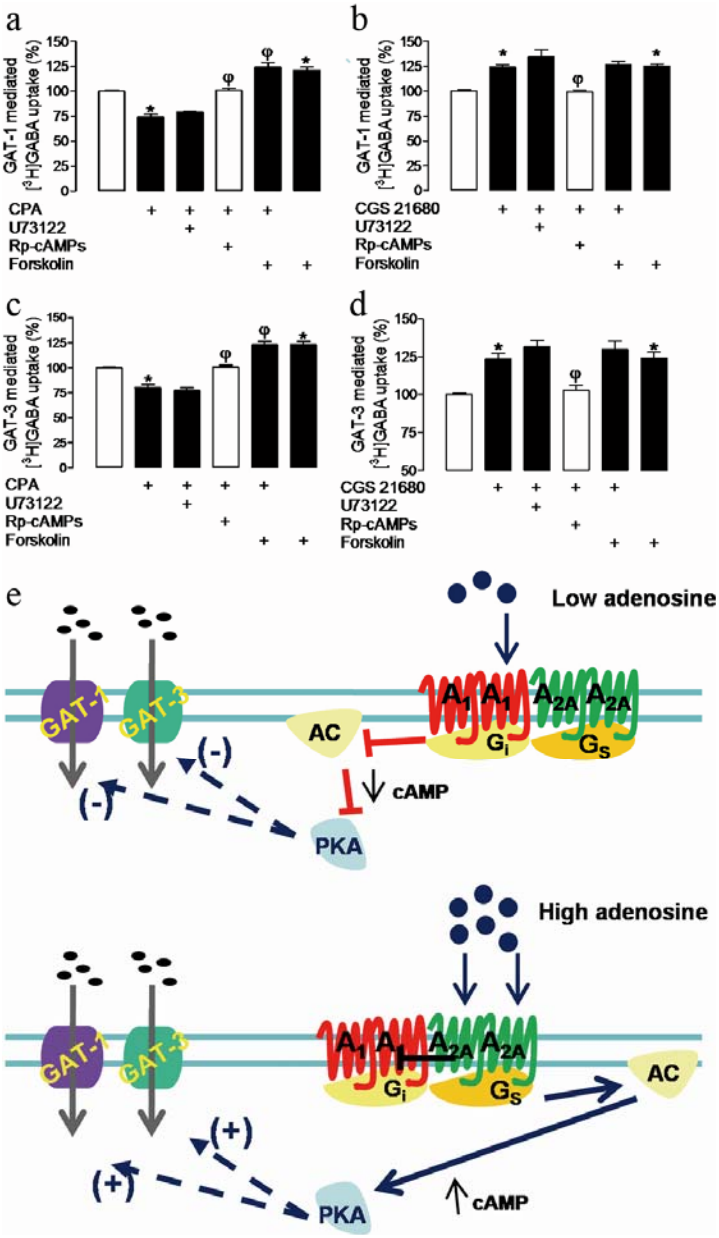

Figure 7. A_1R-$A_{2A}R$ heteromer signaling. Astrocytes were treated for 15 min with 1 U/ml ADA before the addition of medium, the PLC inhibitor U73122 (3 μM), the PKA inhibitor Rp-cAMPs (100 μM), or the AC enhancer forskolin (10 μM). After 20 min, the A_1R agonist CPA (30 nM) (**a**, **c**) or the $A_{2A}R$ agonist CGS 21680 (30 nM) (**b**, **d**) were added, and the GAT-1-mediated (**a**, **b**) or GAT-3-mediated (**c**, **d**) mediated [^{3}H]GABA uptake was measured as indicated in Methods. Results are mean ± SEM from 4 – 10 independent experiments. Statistical significance was calculated by one-way ANOVA followed by Bonferroni's multiple comparison test; *p<0.001 versus control (100%, white columns), ◦p<0.001 versus cells treated with the agonist alone. (**e**), Schematic representation of A_1R-$A_{2A}R$ heteromer function. At low levels, adenosine binds preferentially to the A_1R promoter of the heteromer, which will activate $G_{i/o}$ protein, and through a mechanism that involves AC and PKA activity, leads to a decrease (-) in GABA uptake mediated by GAT-1 and GAT-3. At higher concentrations, adenosine activates the $A_{2A}R$ promoter of the heteromer inhibiting A_1R and, through G_s protein, couples to the AC/cAMP/PKA pathway, leading to an enhancement (+) of GABA uptake.

1.1.8. Discussion.

This work clearly shows that GABA uptake by astrocytes is under modulation by extracellular adenosine, which, by interacting with a functional unit constituted by A_1R-$A_{2A}R$ heteromers coupled to two distinct G-proteins, $G_{i/o}$ and G_s, can either boost or depress the amount of inhibitory neurotransmitter available to neurons.

Using an adenosine analog, CADO, with high structural similarity to adenosine but with the advantage of not being taken up by the cells nor metabolized by ecto-enzymes, we observed that submicromolar concentrations of this agonist inhibit GABA uptake, whereas at low micromolar concentrations, there is an enhancement of GABA transport. Considering that the affinity of adenosine for the A_1R is slightly higher than for the $A_{2A}R$ (Fredholm et al., 2001), it is likely that the inhibition was mediated by A_1R and facilitated by $A_{2A}R$. Accordingly, the A_1R-selective agonist CPA inhibited GABA uptake into astrocytes, whereas the $A_{2A}R$-selective agonist CGS 21680 facilitated it. Unexpectedly, the blockade of either receptor with selective antagonists prevented the effects mediated by either agonist, a strong indication that A_1R and $A_{2A}R$ are interacting at the molecular level in primary cortical astrocytes. Abundant evidence of A_1R-$A_{2A}R$ functional crosstalk has been described, namely, $A_{2A}R$ activation attenuates A_1R-mediated responses in the hippocampus ((Cunha et al., 1994; Lopes et al., 1999), at the neuromuscular junction (Correia-de-Sá and Ribeiro, 1994), and in transfected cells (Ciruela et al., 2006); however, no attempt has been made to unequivocally and directly identify A_1R-$A_{2A}R$ heteromerization in neural cells. Thus, we looked for energy transfer in primary cultures of astrocytes transfected with cDNAs for $A_{2A}R$-Rluc and A_1R-YFP. In these assays, a positive, specific, and saturable BRET signal for the energy transference between $A_{2A}R$-Rluc and A_1R-YFP was detected in living primary astrocytes. Moreover, the heteromer in native astrocytes was detected by looking for a fingerprint that consists of changes in ligand binding characteristics of A_1R

when the $A_{2A}R$ is activated. These results complemented and strengthened the evidence for A_1R-$A_{2A}R$ heteromerization in non-transfected astrocytes. Evidence for A_1R-$A_{2A}R$ heteromers in living tissues awaits further development of the already-available BRET-FRET near-infrared dot technology for in vivo imaging (Xiong et al., 2012), not yet developed for nervous system analysis.

As it is the case from GABA transporters in astrocytes (Vaz et al., 2011), membrane proteins usually recycle, being internalized and sent back to the membrane in a controlled way. Biotinylation assays showed that exposure to either A_1R or $A_{2A}R$ agonists led to similar decreases in surface expression of A_1R, and to similar increases in the A_1R levels in intracellular fractions. It then appears that binding of a single ligand to the heteromer is sufficient to promote internalization of the two receptors. The previous blockade of A_1R or $A_{2A}R$ prevents the heteromer internalization mediated by both A_1R and $A_{2A}R$ agonists, suggesting that internalization of heteromer in response to agonists is a consequence of heteromer activity. Confocal imaging of transfected HEK-293T cells confirmed that exposure to an A_1R agonist led to internalization of not only A_1R but also $A_{2A}R$ and, conversely, exposure to an $A_{2A}R$ agonist led to internalization of not only $A_{2A}R$ but also A_1R. Thus, in this aspect, A_1R-$A_{2A}R$ heteromers behaved as the β2-adrenoreceptor-δ-opioid (Jordan et al., 2001) and μ-opioid-tachykinin NK_1 (Pfeiffer et al., 2003) receptor heteromers but different from other heteromers whose promoters do not co-internalize (Smith and Milligan, 2010). It is technically difficult to know to what extent adenosine receptor internalization affects GABA transport in astrocytes. In fact, GABA transport into astrocytes is itself affected by inhibitors of arrestin-dependent endocytosis (Vaz et al., 2011) that would be required to prevent adenosine receptor internalization.

Agonist exposure did not affect BRET, suggesting that agonist binding does not induce pronounced allosteric modifications in the receptors. It therefore appears that the A_1R-$A_{2A}R$ heteromer in astrocytes mostly works as an integral entity, leaving and probably

also reaching the cell surface as a heteromeric structure. Furthermore, because antagonists did not modify the receptor levels at the membrane or the BRET signal, the loss of effect of one agonist on previous blockade of the other receptor cannot be attributed to heteromer disruption or formation. Cross-antagonism, which is considered a heteromer fingerprint (Ferré et al., 2009), is likely attributable to conformational changes induced by the antagonist and leads to a nonfunctional state of the signaling receptor by uncoupling it from G protein-mediated signaling.

Heteromers may couple to G proteins different from those to which each individual receptor partner usually couple. This is indeed the case of the dopamine D_1-D_2 receptor heteromer, which couples to G_q (Rashid et al., 2007) in a clear shift from the canonical D_1 coupling to G_s and D_2 coupling to $G_{i/o}$. To identify the transducing system operated by the A_1R-$A_{2A}R$ heteromer in astrocytes, we first used an approach similar to that used by Rashid et al. (2007), i.e., [^{35}S]GTP-γ binding followed by differential immunoprecipitation. Data obtained allowed to conclude that the A_1R-$A_{2A}R$ heteromer in astrocytes seems to be coupled to both $G_{i/o}$ and G_s proteins. Interestingly, the crossantagonism was also evident in these assays. Thus, the A_1R agonist, but not the $A_{2A}R$ agonist, increased $G_{i/o}$ activity, but the enhancement was also prevented when the $A_{2A}R$ antagonist was present. Reciprocally, G_s activation, which was restricted to the $A_{2A}R$ agonist, was prevented when the A_1R was blocked with the antagonist. Similar conclusions could be drawn from GABA uptake assays because toxin-induced prevention of coupling of receptors to either G_s or $G_{i/o}$ led to reciprocal impaired function of A_1R or $A_{2A}R$ agonists to modulate GABA transport. The crossinhibition of heteromer function by the toxins was observed in both cultured astrocytes and heterologous cells coexpressing A_1R and $A_{2A}R$ but not in cells expressing only one receptor subtype. Altogether, these data provide strong evidence for a heteromeric functional entity regulating GABA uptake by astrocytes. This functional unit consists of an A_1R-$A_{2A}R$ heteromer/$G_{i/o}$-G_s complex, which signals through G_s when the $A_{2A}R$ protomer is activated

and through G_i when the A_1R protomer is activated. Most importantly, the blockade of a single partner in the complex led to adjustments in the whole unit. Since two GPCR molecules cannot bind to more than a single G protein (Han et al., 2009), A_1R-$A_{2A}R$ heteromers in astrocytes may be expressed as heteromers of homomers with a minimal structure consisting of an A_1R-A_1R-$A_{2A}R$-$A_{2A}R$ complex, making possible to accommodate two different G proteins (Figure 7E). The transducing system operated by the heteromer seems to involve the AC, consistent with the G protein data and the data obtained in the presence of forskolin or the inhibitor of the PKA (Rp-cAMPs), both of which occluded the effects of the A_1R- or $A_{2A}R$-selective agonists during GABA uptake.

A ten-fold rise in concentration of the non-selective ligand CADO was enough to gate $A_{2A}R$ activation and engage a completely opposite modulation of GABA uptake. Assuming a near 10-fold higher potency of CADO compared with adenosine (Ribeiro and Sebastião, 1987), the shift from inhibition to enhancement of GABA uptake might occur at low micromolar concentrations of extracellular adenosine. These concentrations are easily attained at a tripartite synapse, in which astrocytes and neurons release considerable amounts of ATP, which are degradated into ADP, AMP, and adenosine by ecto-5'-nucleotidases. The higher the release of ATP, as at high neuronal firing rated in reciprocal neuron-to-astrocyte communication at the tripartite synapse (Fields and Burnstock, 2006), the higher the expected concentration of extracellular adenosine. It is therefore likely that sustained neuronal firing promotes activation of the $A_{2A}R$ protomer of the A_1R-$A_{2A}R$ heteromer, leading to facilitation of GABA uptake. Activation of GABA uptake by astrocytes will lead to a decrease in ambient GABA and a subsequent depression of tonic GABAergic inhibition, resulting in enhanced excitatory tonus. Conversely, at submicromolar adenosine concentrations, there is a preferential activation of the A_1R protomer of the A_1R-$A_{2A}R$ heteromer, and GABA uptake by astrocytes would be inhibited and tonic inhibition by GABA would be enhanced. Thus, through an adenosine action on A_1R-$A_{2A}R$ heteromers,

astrocytes might behave as dual amplifiers, facilitating excitation at intense astrocytic to neuronal signaling and increasing inhibition at low neuronal firing rates. This switch in neural activity may require a highly efficient control to avoid sudden state transition, and this seems to be the main advantage of heteromerization of A_1R and $A_{2A}R$ in astrocytes. Indeed, overstimulation of just one of the receptor protomers leads to internalization of the whole functional unit, therefore allowing a double brake in the system and avoiding an abrupt inhibitory signaling and a sudden switch from excitation to inhibition as a consequence of desensitization of only the excitatory protomer.

1.2. Adenosine A_1R and $A_{2A}R$ heteromers form dynamic but stable tetrameric complexes with two different G proteins.

The once controversial idea of GPCR dimerization is now heavily supported by recent biochemical and structural data (Guo et al., 2005; Fung et al., 2009; Albizu et al., 2010; Maurice et al., 2010; El Moustaine et al., 2012; Manglik et al., 2012). This debate has now moved to the question of heterocomplexes, where a number of studies point to the presence of heterodimers and higher order heteromers in a broad spectrum of GPCRs (Gurevich and Gurevich, 2008; Sohy et al., 2009; van Rijn et al., 2010; Décaillot et al., 2011; Kamal and Jockers, 2011; Callén et al., 2012). A well-characterized example is the adenosine A_1R-$A_{2A}R$ heteromer, first described as a concentration sensing device in striatal glutamatergic neurons (Ciruela et al., 2006). The A_1R-$A_{2A}R$ heteromer is thought to function as a switching mechanism by which low and high concentrations of adenosine inhibit and stimulate, respectively, glutamate release (Ciruela et al., 2006; Orru et al., 2011). However, the molecular stoichiometry and dynamics of the formation of these A_1R-$A_{2A}R$ heteromers and the number of bound G proteins (G_i and/or G_s) remain unknown.

Numerous biochemical studies have attempted to identify the G protein receptor stoichiometry (Seifert et al., 1999; Nobles et al., 2005; Bayburt et al., 2007; Whorton et al., 2007; Dorsch et al., 2009; Han et al., 2009; El Moustaine et al., 2012; Orban et al., 2012) and the influence of ligand binding to the dynamics of oligomerization (Dorsch et al., 2009; Fung et al., 2009; Birdsall, 2010; Kasai et al., 2011; Scarselli et al., 2012). For instance, single-molecule imaging techniques have shown that the ionotropic kainate receptors, known to oligomerize, can form with a 2:2 stoichiometry (Reiner et al., 2012), while fluorescence recovery after photobleaching (FRAP) techniques have been used to investigate homomeric interactions in living cells (Dorsch et al., 2009; Calebiro et al., 2013). The present study aims to shed light, by a combination of single-molecule microscopy, molecular

modeling and energy transfer assays, on the steady-state population of adenosine A_1R-$A_{2A}R$ heteromers at the plasma membrane (PM) in the absence of ligands. We found that co-expressed A_1R-$A_{2A}R$ organizes mostly into heterotetramers containing two protomers of A_1R and two protomers of $A_{2A}R$ bound simultaneously to G_i and G_s proteins.

1.2.1. Individual adenosine receptors form stable heteromers with restricted diffusion in the plasma membrane of living cells.

To examine how stable A_1R-$A_{2A}R$ heteromers are in the PM of a living cell, we performed a Single Particle Tracking (SPT) analysis of the receptors tagged with fluorescent proteins in HEK 293 cells. eGFP was fused to the C-terminus of A_1R (A_1R-eGFP) and mCherry to the C-terminus of $A_{2A}R$ ($A_{2A}R$-mCherry). Previously, we have shown that fusion to the C-terminus does not affect function of these receptors (Canals et al., 2003). Trajectories and intensities of the individual fluorescent particles over time were recorded by Total Internal Reflection (TIRF) microscopy using an electron multiplying (EMCCD) camera (Fig. 1A, 1B, 1D and 1E). An example of a cell and the individual receptor trajectories tracked in its analysis are shown in Fig. S1. The SPT mobility analysis in cells expressing A_1R-eGFP alone (Fig. 1A) led to a linear relationship between the mean square displacement (MSD) versus time lag in the trajectories of up to 1,600 single molecules (Fig. 1C). These results demonstrate that A_1R-eGFP molecules have no restrictions and, therefore, follow a Brownian motion. Co-expression of $A_{2A}R$-mCherry (Fig. 1B) led to a reduction on lateral mobility, with the diffusion coefficient changing from 0.381 ± 0.002 $\mu m^2/s$ to 0.291 ± 0.003 $\mu m^2/s$, and to a change in the type of diffusion, now confined to regions of 0.461 ± 0.004 μm in diameter (Fig. 1C). Thus, the presence of $A_{2A}R$ dramatically alters the mobility of A_1R, a result that strongly supports the formation of receptor heteromers. Importantly, when the reverse comparison was made, analysis of cells expressing only $A_{2A}R$-mCherry (Fig. 1D) versus the double transfected cells (Fig. 1E), a change in

mobility was also observed (Fig. 1F). $A_{2A}R$ alone had diffusion coefficient of 0.317 ± 0.002 $\mu m^2/s$ and in the presence of A_1R their mobility was reduced to 0.143 ± 0.005 $\mu m^2/s$. $A_{2A}R$ alone displayed confined motion within a circle of 0.941 ± 0.007 μm in diameter that was reduced to 0.360 ± 0.001 μm when both receptor types were co-expressed.

Although comparing the mobility of receptors in the presence or absence of the partner receptor is meaningful, observing the behavior of the heteromers themselves would be more informative. Consequently, only particles where both A_1R and $A_{2A}R$ colocalized (yellow dots in Fig. 1G) were analyzed. More that 70% of the Colocalization cases were stable on the cell membrane for over 1 min of the acquisition time for the individual movies (Fig. 1H). These more stable complexes exhibited movement confined to a square of a side length of 0.291 ± 0.003 μm and with a diffusion coefficient of 0.232 ± 0.001 $\mu m^2/s$ (Fig. 1I and Fig. S2A). We also observed a small subpopulation of transiently colocalized A_1R-$A_{2A}R$ agglomerations (Fig. S2B), which lasted less than 200 ms (Fig. 1H).

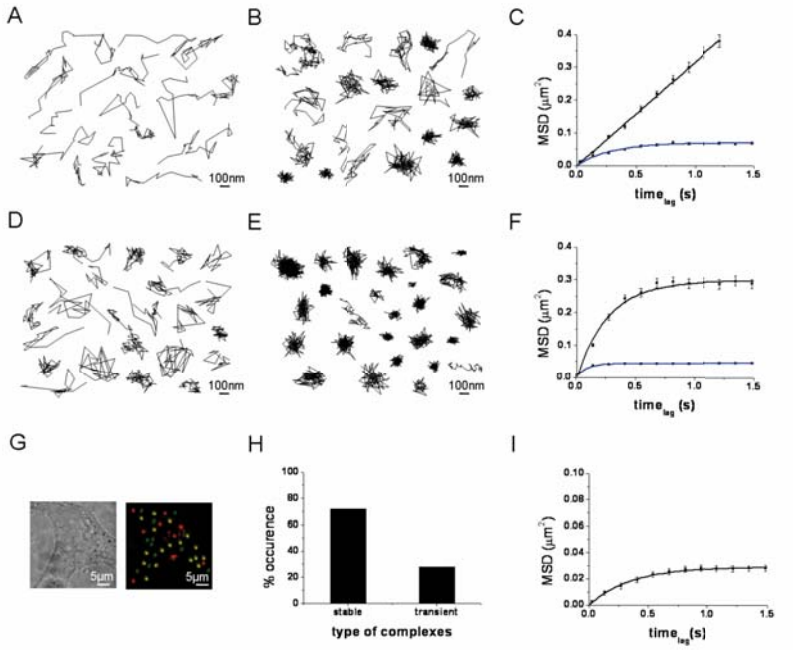

Figure1. Lateral mobilities of A_1R and $A_{2A}R$ change substantially when both receptor subtypes are simultaneously expressed on the cell surface. Examples of individual trajectories for A_1-eGFP (**A** and **B**) or A_{2A}-mCherry (**D** and **E**) were analyzed on HEK 293 cells expressing A_1-eGFP (**A**) or A_{2A}-mCherry (**D**) or both (**B** and **E**). Scale bar: 100 nm. The average motion of receptors was determined by plotting mean square displacement (MSD) of A_1-eGFP (**C**) alone (black line) or in the presence of A_{2A}-mCherry (blue line) or A_{2A}-mCherry (**F**) alone (black line) or in the presence of A_1-eGFP (blue line) versus time lag. Data sets were fitted to mathematical models of free and confined diffusion, for A_1R and $A_{2A}R$ respectively. In (**G**) Colocalization of A_1-eGFP and A_{2A}-mCherry is observed (yellow dots). 70% of the colocalized receptors correspond to the stable complexes on the cell membrane (lasting >1 min) and the rest show transient behavior (lasting <200 ms) (**H**). In (**I**) the MSD versus time lag for stable complexes was examined and more than 1,600 stably colocalized receptors were considered. Error bars, S.E. of each MSD data point for each particular lag time.

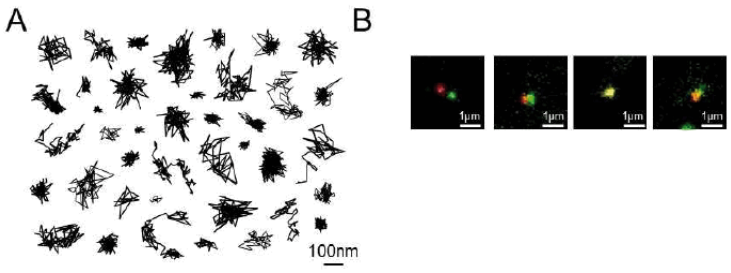

Figure S2. Stable and transient receptor colocalization. In (**A**) individual trajectories of receptors stably colocalized (>1 min) on HEK 293 cell surface expressing A_1-eGFP and A_{2A}-mCherry is shown. Scale bar: 100 nm. In (**B**), four time-lapse images exhibiting colocalization dynamics of two receptors, A_1-eGFP and A_{2A}-mCherry colocalizing transiently.

1.2.2. A_1R-$A_{2A}R$ heteromers organize as tetramers formed by two protomers of A_1R and two protomers of $A_{2A}R$.

The brightness distribution of individual fluorescent particles permits a detailed analysis of local stoichiometry directly on the surface of living cells (Schmidt et al., 1996; Harms et al., 2001). We analyzed the probability density function of the fluorescence intensity first on clusters form cells expressing single $A_{2A}R$-mCherry or A_1R-GFP, we found the majority of clusters to consist of either two (~50%) or four (~30%) receptors, and a small portion of clusters with 1 or 3 receptors (~10% in both cases) (Fig. 2A and B black bars). In cells expressing $A_{2A}R$-mCherry, receptors were mostly expressed as trimers (~45%) with dimers and tetramers the second most common populations (Fig. 2C and D black bars). In cells coexpressing A_1R and $A_{2A}R$, the overall stoichiometry distribution of the receptor particles was indeed affected (Fig. 2B and D blue bars and Fig. S3), which suggests the formation of dynamic but stable complexes. Interestingly, the dimer population significantly increased and became the predominant species.

The molecular composition of the stable heteromers was analyzed by calculating the stoichiometry of A_1R-GFP and A_{2A}-mCherry receptor complexes (Fig. 2E and Fig. S4). Interestingly, in ~1.000 analyzed clusters, a dimer of A_1R and a dimer of $A_{2A}R$ was the most prevalent form (Fig. S4), with 75% of the clusters containing A_1R dimers and 75% of the clusters containing $A_{2A}R$ dimers (Fig. 2E). These results strongly suggest that the most common species is a tetramer consisting of two A_1R and two $A_{2A}R$. There were also significant populations of clusters that contained A_1R monomers (~22%) and $A_{2A}R$ trimers (~19%), suggesting the existence of A_1R:$A_{2A}R$ (1:3) heteromers. It is difficult to estimate their significance, but one possibility is that they are remnants of the $A_{2A}R$ trimers found in the cells expressing this receptor alone. Alternatively, they could indicate the coexistence of minor species formed during the dynamic organization of the heterotetramers, which are expected to exist in reversible equilibrium.

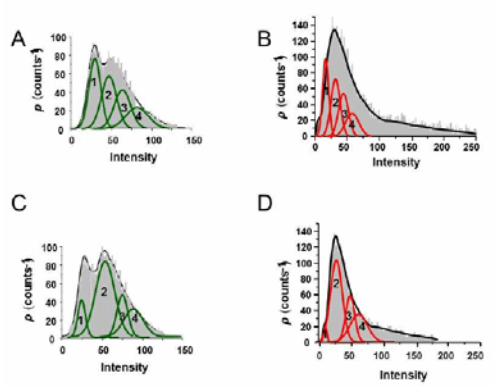

Figure S3. Stoichiometry analysis of the receptor distribution. In (**A** and **B**), the theoretical intensity distribution measured for a population of individual spots over time was modeled as the sum of four Gaussian terms, corresponding to complexes with 4, 3, 2 and 1 molecules for eGFP (**A**) or for mCherry (**B**). In (**C** and **D**), the intensity distribution was measured in HEK 293 cells expressing both A_1-eGFP and A_{2A}.mCherry. The stoichiometry analysis was performed for A_1-eGFP (**C**) and A_{2A}-mCherry (**D**). Curves show approximate amount of monomers, dimers, trimers and tetramers.

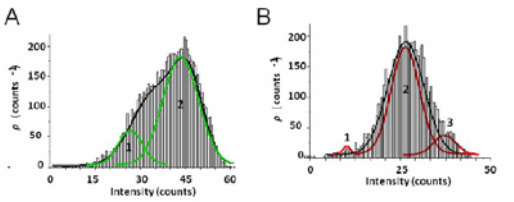

Figure S4. Stoichiometry analysis of the stably colocalized receptors. Distribution of the fluorescence signal and the stoichiometry of A_1 –eGFP (**A**) and A_{2A}-mCherry (**B**) within the stably colocalized receptors in HEK 293 cells expressing both A_1-eGFP and A_{2A}-mCherry. Curves represent approximate amounts of monomers, dimers, or trimers within the colocalized complex.

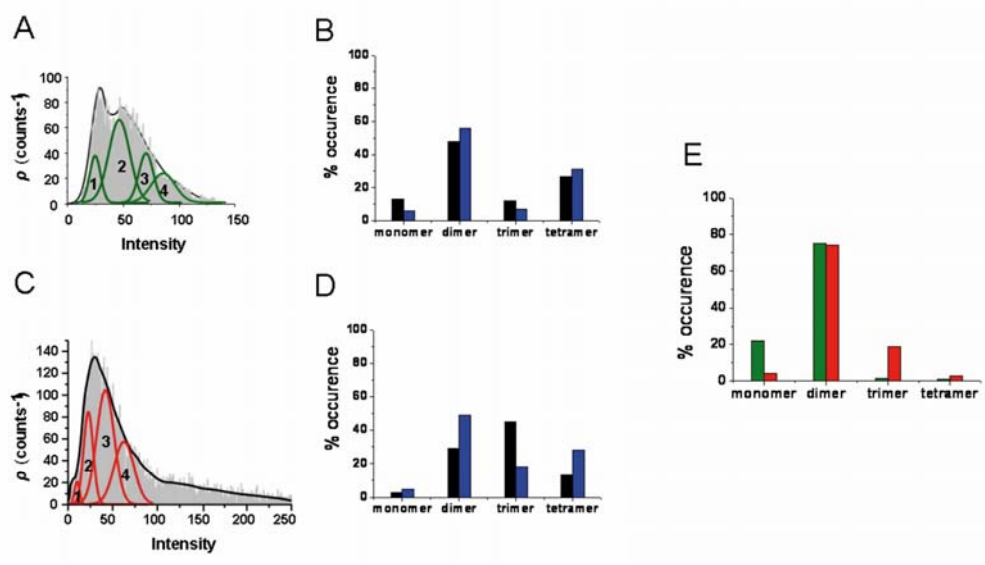

Figure 2. Analysis of the fluorescence signal intensity indicates that A_1R and $A_{2A}R$ exist in a heterotetramer composed of two receptors of each type. In (**A** and **C**), the fluorescence signal intensity distribution (grey area) detected from more than 7,000 independent observations is given for HEK 293 cells expressing A_1R-GFP (**A**) or $A_{2A}R$-mCherry (**C**). Curves showing approximate amounts of monomers, dimers, trimers and tetramers were also displayed in green for A_1R-GFP (**A**) and in red for $A_{2A}R$-mCherry (**C**). The occurrence of monomers, dimers, trimers and tetramers for A_1R-GFP (**B**) expressed alone (black bars) or in the presence of $A_{2A}R$-mCherry (blue bars) or $A_{2A}R$-mCherry (**D**) alone (black bars) or in the presence of A_1R-GFP (blue bars) on the cell surface was calculated by stoichiometry analysis from results shown in (**A**) or (**C**) regarding the single transfection or from Fig. S4 **C-D** for the co-transfection. In (**E**) the stoichiometry analysis was performed for stably colocalized A_1R-GFP and $A_{2A}R$-mCherry receptors co-expressed in HEK 293 cells. Green corresponds to A_1R-GFP and red to $A_{2A}R$-mCherry.

1.2.3. G protein binding can stabilize receptor dimerization.

To date, it is not fully understood whether GPCR dimerization is induced and/or stabilized by scaffolding proteins. Various studies have raised the possibility that non-receptor proteins, like G proteins, could influence receptor dimerization (Whorton et al., 2007; Mary et al., 2012). To gain insight into this issue and taking into account that A_1R selectively couples to G_i and $A_{2A}R$ to G_s (Fredholm et al., 2001), we used BRET assays to monitor receptor homo- and hetero-dimerization, in the presence and absence of pertussis or cholera toxins. BRET experiments in cell expressing A_1R fused to Rluc (A_1R-Rluc) and fused to YFP (A_1R-YFP) led to a saturable curve (Fig. 3A, black line), along with $A_{2A}R$-Rluc and $A_{2A}R$-YFP (Fig. 3B, black line), indicating homodimers formation. Cells treated with the G_i-specific pertussis toxin (Fig. 3A and B, green line), specifically reduced the value of $BRET_{max}$ for $A_{2A}R$-$A_{2A}R$ homodimers by 45%.

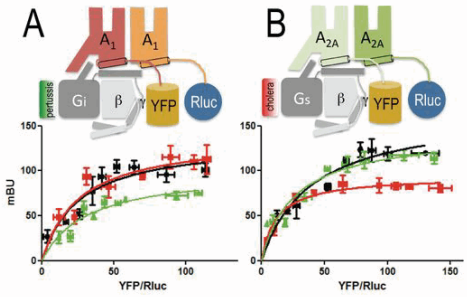

Figure 3. Influence of G protein on A_1R or $A_{2A}R$ homodimerization. BRET saturation experiments were performed in HEK 293 cells transfected with 0.3 μg cDNA corresponding to A_1R-Rluc (**A**) or 0.2 μg of cDNA corresponding to $A_{2A}R$-Rluc (**B**) and increasing amounts of cDNA corresponding to A_1R-YFP (**A**, 0.1 to 1.5 μg cDNA) or $A_{2A}R$-YFP (**B**, 0.1 to 1.0 μg cDNA). Cells were treated for 16 h with medium (black lines) or with 10 ng/ml of pertussis toxin (green lines) or 100 ng/ml cholera toxin (red lines) prior BRET determination. Both fluorescence and luminescence of each sample were measured before every experiment to confirm similar donor expressions (approximately 100,000 bioluminescence units) while monitoring the increase in acceptor expression (1,000 to 40,000 fluorescence units). The relative amount of BRET is given as a function of 100 X the ratio between the fluorescence of the acceptor (YFP) and the luciferase activity of the donor (Rluc). BRET is expressed as mili BRET units (mBU) and is given as the mean ± SEM of four to six different experiments grouped as a function of the amount of BRET acceptor. At the top of each panel, a schematic representation of the components of the complex is shown in which Rluc is fused to the C-terminal domain of one receptor protomer and YFP is fused to the other protomer in the homodimer.

These results indicate that G_i and G_s are bound to their respective receptor homodimers in the absence of ligands. Moreover, since the value of $BRET_{max}$ is a function of the number of homodimers formed, the decrease observed here suggests the binding of the G protein may induce and/or stabilize receptor homodimerization.

1.2.4. G_s and G_i can bind and stabilize adenosine A_1R-$A_{2A}R$ heteromers.

Our single molecule microscopy data supports the hypothesis that A_1R-$A_{2A}R$ heteromers mainly exist as tetrameric complexes formed by two homodimers of A_1R and $A_{2A}R$. To study the role of G proteins on A_1R-$A_{2A}R$ heteromer formation we performed BRET experiments. Cells transfected with A_1R-Rluc and $A_{2A}R$-YFP show a saturable BRET curve indicating that A_1R and $A_{2A}R$ form heteromers (Fig. 4A, black line). Notably, the presence of either pertussis or cholera toxin led to a decrease in $BRET_{max}$ (Fig. 4A, green and red lines), indicating that both G_i and G_s proteins are bound and either induce and/or stabilize A_1R-$A_{2A}R$ heteromerization. Nevertheless, these experiments do not give information on the stoichiometry of the stabilized complexes.

To study the role of G proteins on tetramer formation we combined BiFC with BRET (Kerppola, 2006; Robitaille et al., 2009). For this purpose the N-terminal fragment Rluc8 was fused to A_1R (A_1R-nRluc8) and its C-terminal domain to $A_{2A}R$ ($A_{2A}R$-cRluc8), which only upon complementation can act as BRET donor (Rluc8) (Fig. 4B). The BRET acceptor protein was obtained upon complementation of the N-terminal fragment of YFP Venus protein fused to A_1R (A_1R-nVenus) and its C-terminal domain fused to $A_{2A}R$ ($A_{2A}R$-cVenus) (Fig. 4B). When all four receptor constructs are transfected in the cell we obtain a positive and saturable BRET signal with a $BRET_{max}$ of 35 ± 2 mBU and $BRET_{50}$ of 16 ± 3 (Fig. S5) that shows heterotetramer formation. Remarkably, pre-incubating the cells with either pertussis or cholera toxins decreased the $BRET_{max}$ by 35% (Fig. 4B). These findings reinforce our previous observations and strongly suggest that both G_s and G_i proteins bind to the A_1R-$A_{2A}R$ heterotetramer. This was further explored by analyzing the energy transfer between the α-subunit of G_i protein (G_i-Rluc, Rluc fused to the N-terminal domain of the α-subunit of G_i) and $A_{2A}R$-YFP in cells co-expressing or not A_1R. A BRET saturation curve was observed only in the presence of A_1R (Fig. 4C, black line), but not in its absence (Fig. 4C, blue line) and the $BRET_{max}$ was reduced by cell treatment with pertussis toxin (Fig.

4C, green line). These results indicate that G_i is bound to the A_1R homodimer and in complex with the A_1R-$A_{2A}R$ heterotetramer.

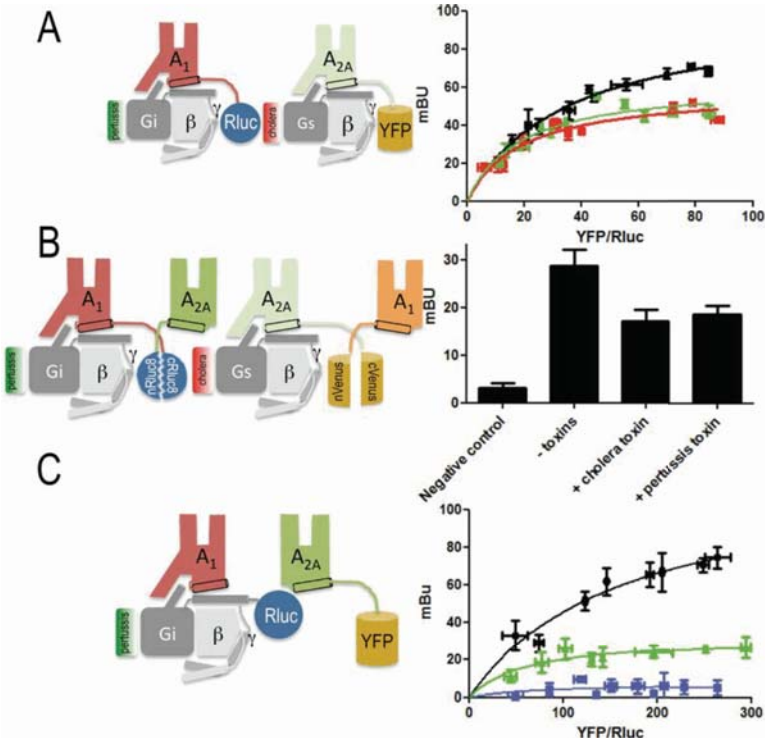

Figure 4. Influence of g protein on A_1R and $A_{2A}R$ heteromerization. Experiments were performed using HEK 293 cells treated for 16 h with medium (black lines in **A** and **C** or – toxin in **B**) or with 10 ng/ml of pertussis toxin (green lines in **A** and **C** or + PTx in **B**) or 100 ng/ml of cholera toxin (red lines in **A** or + ChTx in **B**) prior to BRET determination. In (**A**) BRET saturation curves were performed in cells transfected with 0.3 μg of cDNA corresponding to A_1R-Rluc and increasing amounts of cDNA corresponding to $A_{2A}R$-YFP (0.1 to 1.0 μg cDNA). In (**B**) BiFC with BRET experiments were performed in cells transfected with 1.5 μg of cDNA corresponding to A_1R-cRluc8 and $A_{2A}R$-nRluc8 and 1.5 μg of cDNA corresponding to A_1R-nVenus and $A_{2A}R$-cVenus. Negative control corresponds to cells transfected with 1 μg of cDNA corresponding to nRluc8 and 1.5 μg of cDNA corresponding to $A_{2A}R$-nRluc8, A_1R-nVenus and $A_{2A}R$-cVenus. In (**C**) BRET saturation curves were performed in cells transfected with 2 μg of cDNA corresponding to α-subunit of G_i fused to Rluc, increasing amounts of cDNA corresponding to $A_{2A}R$-YFP (0.1 to 0.5 μg cDNA) and 0.5 μg cDNA corresponding to A_1R. Control BRET curves were performed in the absence of A_1-R expression (blue curve). In BRET curves, both fluorescence and luminescence of each sample were measured before every experiment to confirm similar donor expressions (approximately 50,000 bioluminescence units) while monitoring the increase in acceptor expression (1,000 to 10,000 fluorescence units). The relative amount of BRET is given as a function of 100 X the ratio between the fluorescence of the acceptor (YFP) and the luciferase activity of the donor (Rluc). BRET is expressed as mili BRET units (mBU) and is given as the mean ± SEM of five to eight different experiments grouped as a function of the amount of BRET acceptor. At left, a schematic representation of the components of the complex indicating the protomer to which Rluc and YFP (**A** and **C**) or the hemi luminescent or fluorescence proteins (**B**) were fused is shown.

1.2.5. Molecular model of the $A_{2A}R$ homodimer in complex with G_s.

To identify the orientation of the G protein in the receptor homodimer we analyzed the energy transfer between the α-subunit if the G_s protein (G_s-Rluc, Rluc fused to the N-terminal domain of the α-subunit of G_s) and $A_{2A}R$-YFP (Fig. 5A). A BRET saturation curve was observed (Fig. 5B, black line) and the $BRET_{max}$ was reduced by cell treatment with ChTx (fig. 5B, red line). These results indicate a close proximity between the N-tail of G_s and the C-tail of $A_{2A}R$. Constructing a molecular model of the $A_{2A}R$-G_s complex taking into account the recently described crystal structure of β_2-adrenergic receptor in complex with G_s (Rasmussen et al., 2011), shows that Rluc attached to the N-terminal αN helix of G_s and YFP attached to the C-terminal domain of $A_{2A}R$ point toward distant positions in space (Fig. 5C). Therefore, the observed BRET might occur between G_s-Rluc and a second $A_{2A}R$-YFP protomer in the homodimer that is not bound to G_s. To understand these effects at the molecular level, we constructed hypothetical arrangements of $A_{2A}R$ homodimers using the transmembrane (TM) 1 (Fig. 5E), TM4 (Fig. 5D), and TM5 (Fig. 5F) interfaces taken from crystal structures featuring such contacts. Clearly, the TM4 interface would favor BRET between G_s-Rluc and the second (G_s-unbound) $A_{2A}R$-YFP protomer. We, thus, propose that receptor homodimerization occurs via the TM4 interface.

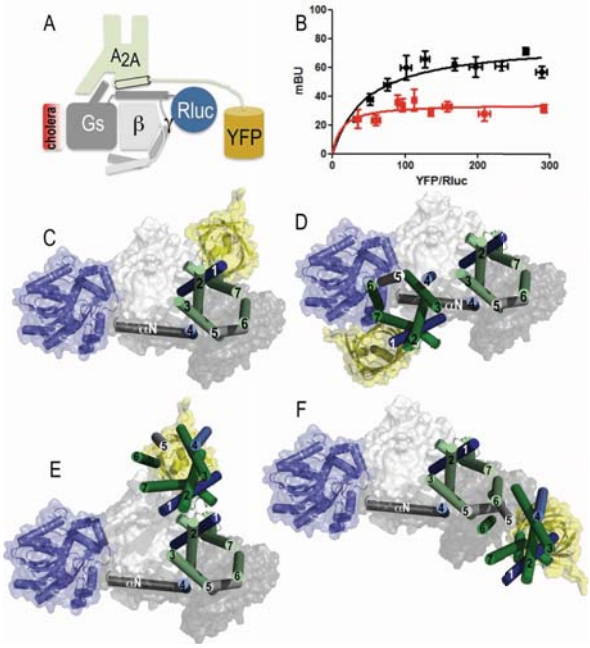

Figure 5. Molecular models of G_s bound to the $A_{2A}R$. In (**A**), schematic of Rluc fused to the N-terminal domain of the α-subunit of G_s and YFP to the N-terminal domain of $A_{2A}R$. In (**B**) BRET saturation experiments were performed in HEK 293 cells transfected with 2 μg of cDNA corresponding to α-subunit of G_s fused to Rluc and increasing amounts of $A_{2A}R$-YFP (0.1 to 0.5 μg) cDNA. Cells were treated for 16 h with medium (black line) or with 100 ng/ml of ChTx (red line) prior BRET measure. Both fluorescence and luminescence of each sample were measured before every experiment to confirm similar donor expressions (approximately 50,000 bioluminescence units) while monitoring the increase in acceptor expression (1,000 to 10,000 fluorescence units). The relative amount of BRET is given as a function of 100 X the ratio between the fluorescence of the acceptor (YFP) and the luciferase activity of the donor (Rluc). BRET is expressed as mili BRET units (mBU) and is given as the mean ± SEM of four to five different experiments grouped as a function of the amount of BRET acceptor. In (**C**), molecular model of the $A_{2A}R$-G_s complex, constructed from the recently described crystal structure of β_2-adrenergic receptor in complex G_s. Rluc (in blue) is attached to the N-terminal αN helix of G_s (in gray) and YFP (in yellow) is attached to the C-terminal domain of $A_{2A}R$ (in light green). Although the exact conformation of the $A_{2A}R$ C-tail cannot unambiguously be determined, the C-tail of $A_{2A}R$ was ambiguously modeled in the direction found in the C-tail of squid rhodopsin and YFP positioned near the N-terminus of the γ-subunit as described in the OXE receptor. In (**D**-**F**), hypothetical arrangements of $A_{2A}R$ homodimers using the experimentally proposed TM1 (**E**), TM4 (**D**), and TM5 (**F**) interfaces. TM helices 1, 4, and 5 involved in receptor dimerization are highlighted in dark blue, and gray, respectively. $A_{2A}R$ protomers bound to G_s are shown in dark green. Only the molecular model depicted in panel **D** would favor the observed high-energy transfer (see panel **B**) between G_s-Rluc and $A_{2A}R$-YFP.

1.2.6. Molecular model of G_s and G_i bound to the A_1R-$A_{2A}R$ heterotetramer.

To model the A_1R-$A_{2A}R$ heterotetramer, A_1R and $A_{2A}R$ homodimers were initially using the TM4 interface for homodimers and the TM5 (Fig. S6A) or the TM1 (Fig. S6B) interface for the heteromer. To discern between these two structures we took advantage of the BiFC experiments (Fig. 4B). From the schemes depicted in Fig. S6A, it is deduced that A_1R-nRluc 8 and $A_{2A}R$-cRluc8, as well as A_1R-nVenus and $A_{2A}R$-cVenus, can only complement if A_1R-$A_{2A}R$ heteromerization occurs via the TM5 interface.

We next evaluated, by computational tools, whether the proposed A_1R-$A_{2A}R$ heterotetramer could simultaneously bind G_i and G_s proteins. Clearly, G_i and G_s binding to the inner protomers of the A_1R-$A_{2A}R$ tetramer is not feasible due to a steric clash between α-subunits (Fig. S6C). In contrast, there is not steric clash between any of the two G proteins when G_i and G_s bind the A_1R-$A_{2A}R$ heterodimer via the external protomers (Fig. S6D and Fig. 6). This binding mode positions the γ-subunits of G_i and G_s facing the inside of the tetrameric complex.

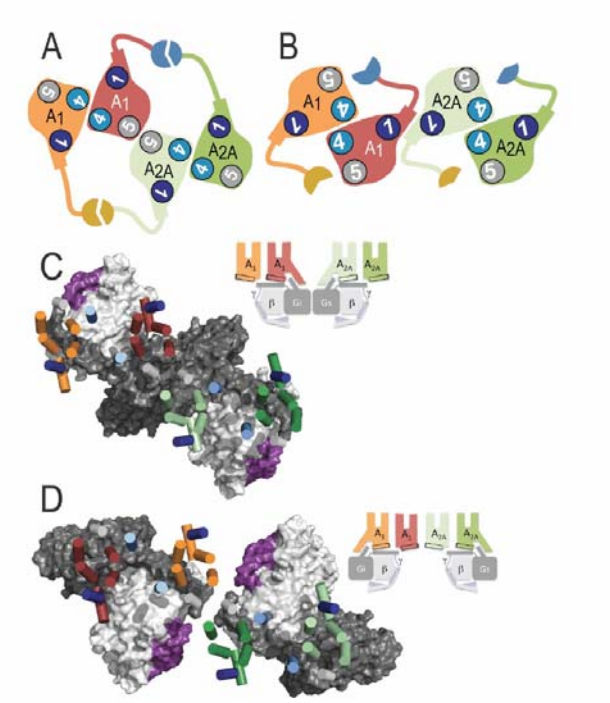

Figure S6. Molecular model of G_s and G_i bound to the adenosine A_1R-$A_{2A}R$ heterotetramer. In (**A** and **B**), schematic representation of the A_1R-$A_{2A}R$ tetramer. A_1R and $A_{2A}R$ homodimerization were modeled via the TM4 interface and A_1R-2aR Heterodimerization was modeled either via TM1 (**B**) or TM5 (**A**) interfaces. nRluc8 and cRluc8 are shown in blue and nVenus and cVenus in dark yellow. In (**C** and **D**), molecular models of the A_1R-$A_{2A}R$ heterotetramer, constructed as in panel **A**, in complex with G_i and G_s proteins. G_i and G_s bind either the inner (**C**) or the outer (**D**) protomers of the A_1R-$A_{2A}R$ tetramer. The color code of the proteins is depicted in the adjacent schematic representations. TM helices 1, 4, and 5 involved in receptor dimerization are highlighted in dark blue, light blue, and gray, respectively.

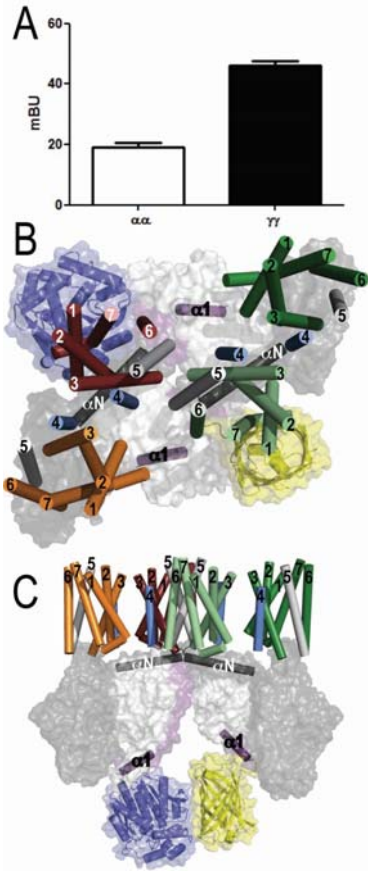

Figure 6. Molecular model of tetrameric A_1R-$A_{2A}R$ heteromer in complex with G_i and G_s proteins. In (**A**), BRET experiments were performed in HEK 293 cells 48 h post-transfection with 0.2 μg of cDNA corresponding to A_1R, 0.15 μg of cDNA corresponding to $A_{2A}R$ and 2 μg of cDNA corresponding to α-subunit of G_i fused to Rluc and increasing amounts of cDNA corresponding to α-subunit of G_s fused to YFP (white column) or 0.3 μg of cDNA corresponding to γ-subunit fused to Rluc and increasing amounts of cDNA corresponding to γ-subunit fused to YFP (black column). Maximum BRET, expressed as mBU, was represented and is given as the mean ± SEM of four different experiments. In (**B – C**), molecular models of the A_1R-$A_{2A}R$ tetramer in complex with G_i and G_s are presented. A_1R and $A_{2A}R$ homodimerization was modeled via the TM4 interface, A_1R-$A_{2A}R$ heteromerization was modeled via the TM5 interface, and G_i and G_s bind to the external protomers of the A_1R-A2aR heterotetramer. The color code of the depicted proteins is: A_1R bound to G_i is shown on orange, G_i-unbound A_1R in red, $A_{2A}R$ bound to G_s is dark green, G_s-unbound $A_{2A}R$ in light green, the α-, β-, and γ-subunits of G_i and G_s in dark grey, light gray and purple, respectively, Rluc in blue, and YFP in yellow. TM helices 4 and 5 involved in receptor dimerization are highlighted in light blue and gray, respectively. B, Rluc and YFP fused to the α-subunit s of G_i and G_s, respectively, point toward different positions in space in agreement with the low energy transfer between them shown in panel **A** white columns. **C**, Rluc and YFP fused to the γ-subunits of G_i and G_s, are close in space in agreement with the high energy transfer between then shown un the panel **A** (black column).

1.2.7. G_s and G_i can bind simultaneously to the external protomers of A_1R-$A_{2A}R$ heterotetramers.

In order to experimentally test whether both G_i and G_s bind simultaneously to the external protomers of the A_1R-$A_{2A}R$ tetramer, two complementary BRET experiments were performed. First, Rluc and YFP were respectively fused to the N-terminal domains of the α-subunit of G_i (α_i-Rluc) and G_s (α_s-YFP). Second, Rluc and YFP were respectively fused to the N-terminal domains of the γ-subunit of G_i (γ-Rluc) and G_s (γ-YFP). The cDNAs of the corresponding pair of constructs were cotransfected with the cDNA of A_1R and $A_{2A}R$ and BRET was measured. The significant energy transfer between γ-Rluc and γ-YFP (Fig. 6A) confirms our hypothesis of simultaneous G_i and G_s binding to the A_1R-$A_{2A}R$ heterotetramer. Comparison of this value of $BRET_{max}$ with the observed low energy transfer between α_i-Rluc and α_s-YFP (Fig. 6A) indicates that the distance between Rluc and YFP is larger when fused to the N-terminal αN helix domains of the α-subunit of both G proteins than when fused to the N-terminal domain of their γ-subunits. This is in agreement with the molecular model of the tetrameric A_1R-$A_{2A}R$ heteromer in complex with G_i and G_s (Fig. 6B and 6C). Finally, the model is also compatible with the large BRET signal between G_i-Rluc and $A_{2A}R$-YFP found in the presence of A_1R (Fig. 4C). Thus, heteromers consists of a non-square displaced tetramer, using the TM4 interface for homodimerization and the TM5 interface for heteromerization (Fig. S6A) and both G_i and G_s bound to the external protomers of the A_1R and $A_{2A}R$ homodimers (Fig. S6D), respectively.

1.2.8. Discussion.

It has become generally accepted that GPCRs can form homomers. Crystallographic studies support this concept including the recent demonstration that μ-opioid receptor crystalizes as a two-fold symmetrical homodimer (Manglik et al., 2012). Although GPCR can also form heteromers, the molecular architecture of heteromers has been poorly studied. One interesting observation from the SPT experiments is that A_1R and $A_{2A}R$ are forming dynamic but stable heteromers at the PM in which the most common complex is a tetramer consisting of two A_1R and two $A_{2A}R$. Due to the penetration limit of the evanescent wave (< 100 nm) used to excite the sample in the TIRF microscopy experiments, it is clear that these complexes are able to occur at or near PM. SPT technology was also used to detect receptor homomer for muscarinic M_1 receptors and for the N-formyl peptide receptor (Hern et al., 2010; Kasai et al., 2011). Recently, the same technique was used to shown that Gluk2 and Gluk5 ionotropic kainate receptors assemble with 2:2 stoichiometry (Reiner et al., 2012). This is in line with our results and supports the general idea that heteromers tend to organize as dimers of dimers. Moreover, these A_1R and $A_{2A}R$ heterotetramers appear to be very stable, most of them remaining associated at least in the order of minutes. To our knowledge, this is the first time that the expression at the PM and the stability of GPCR heteromers has been assessed.

A variety of experiments using different techniques have shown the functional relevance of GPCR asymmetry within dimers in ligand binding, ligand-induced conformational changes and G protein coupling (Han et al., 2009; Maurice et al., 2010; Gomes et al., 2011). Dimers can provide more regulatory and signaling flexibility (Canals et al., 2011; Maurice et al., 2011). Considering A_1R-$A_{2A}R$ heteromers as stable tetramers, as shown by our single molecule tracking experiments, four fundamental questions immediately rise: Is there a role of G proteins in stabilizing the receptor heterotetramer? Can two

different G proteins simultaneously bind this heterotetramer? What is the orientation of the G proteins in the complex that gives rise to the asymmetry in the heterotetramer? What is the molecular architecture of the signaling unit? To answer these questions we took advantage of previous analysis of the interfaces between homomers, showing symmetric interfaces between TMs 1, 4 or 5 depending on the technique used (Guo et al., 2003, 2008; Lopez-Gimenez et al., 2007; Gorinski et al., 2012; Hu et al., 2012). In the case of tetramers, their association requires that there is more than one interaction interface per protomer. BRET assays to monitor receptor homo- and hetero-dimerization, together with molecular models of receptor oligomerization, indicate that the homomerization interface is TM4 whereas the TM5 interface is used for heteromerization. Another interesting aspect reported here is that the heteromer is able to bind G proteins in the absence of extracellular ligands. Thus, the previously described concept of "pre-coupling" of G proteins prior to receptor stimulation (Galés et al., 2005) is supported by the decrease of energy transfer between protomers in both homomers (A_1R-A_1R and $A_{2A}R$-$A_{2A}R$) and heteromers (A_1R-$A_{2A}R$) in the presence of the G_i-specific PTx or the G_s-specific ChTx. Since the maximum energy transfer is a function of the number of protomers formed, our results indicate that G proteins may induce and/or stabilize receptor dimerization. Importantly, BRET assays to monitor G protein binding shows that both G_i and G_s can be recruited simultaneously in the A_1R-$A_{2A}R$ heterotetramer. To avoid the steric clash between both G proteins, G_i and G_s binding to the A_1R-$A_{2A}R$ heterotetramer occurs via the external protomers. This binding mode positions the βγ-subunits of G_i and G_s facing towards the inner portion of the tetrameric complex. Interestingly, the two surfaces for G protein binding constituted by the two homodimers in the displaced tetramer resemble the ones modeled for the μ-opioid receptor bound to two G_i proteins (Manglik et al., 2012), with the exception that the external protomers in the μ-opioid tetramer interact via the TM1 interface.

CHAPTER 2

2. Agonist and antagonist allosteric interactions between receptors in the $A_{2A}R$-D_2R heteromer.

Dopamine is one of the most important neurotransmitters in the brain and exerts its functions by interacting with dopamine receptors that are GPCRs. Signaling through the D_1-like receptor family (D_1 or D_5 receptors) or D_2-like receptor family (D_2, D_3 and D_4 receptors), translates into activation/inhibition of specific neurons and circuitries. D_1-like receptors are known to stimulate adenylate cyclase activity via a G_s mechanism and D_2-like receptors are known to stimulate adenylate cyclase activity via a G_i mechanism (Missale et al., 1998). D_1 and D_2 dopamine receptors are mainly segregated in the two GABAergic striatal efferent neurons that constitute more that 95% of the striatal neuronal population. GABAergic dynorphinergic neurons, in the direct pathway, express the peptide dynorphin and dopamine D_1 receptors and GABAergic enkephalinergic neurons, in the indirect pathway, express the peptide encephalin and dopamine D_2 receptors. Interestingly, adenosine $A_{2A}R$ are also segregated in the striatal efferent neurons and are mainly expressed in the indirect pathway where they colocalize with dopamine D_2R (Rosin et al., 1998; Schiffmann et al., 2007). In fact, D_2R are under the control of adenosine $A_{2A}R$. At least in part, such control is through formation of a receptor heteromer (Bulenger et al., 2005; Ferré et al., 2007; Smith and Milligan, 2010; Terrillon and Bouvier, 2004; Waldhoer et al., 2005). A receptor heteromer is a macromolecular complex composed of at least two functional receptor units with biochemical properties that are demonstrably different from those of its individual receptors (Ferré et al., 2009). Heteromers of adenosine $A_{2A}R$ and D_2R were one of the first GPCR heteromer to be described (Hillion et al., 2002). A close physical interaction between both receptors was shown using co-immunoprecipitation and co-

localization assays (Hillion et al., 2002) and FRET and BRET techniques (Canals et al., 2003; Ciruela et al., 2004; Kamiya et al., 2003). The existence of $A_{2A}R$-D_2R heteromers in lamb striatum has also been recently inferred based on the effects of bivalent ligands (Soriano et al., 2009) and the expression of these heteromers in mouse striatum was based on the proximity ligation assays (Trifilieff et al., 2011). The $A_{2A}R$-D_2R heteromers in the striatum are very relevant for motor activity control since it is generally accepted that stimulation of the direct and indirect pathway results in motor activation and motor inhibition, respectively, and that smooth motor drive results from the counterbalanced influence of the direct and indirect pathways on the neural activity of the output structures (Obeso et al., 2002).

Allosteric interaction is a common biochemical property of receptor heteromers, and it is defined as an intermolecular interaction by binding of a ligand to one of the receptor units in the receptor heteromer changes the binding properties of another receptor unit (Ferré et al., 2009). Understanding how different ligands for the partner receptors regulate a GPCR within a heterodimer through allosteric effects between the two protomers of the dimer is crucial in the development of new therapeutic strategies. Allosteric interactions in the $A_{2A}R$-D_2R heteromer have received a lot of attention but have been restricted to agonist-agonist allosteric interactions. It has been considered as a main mechanism responsible for the antiparkinsonian effect of $A_{2A}R$ antagonists (Ferré et al., 2004, 2008; Muller and Ferré, 2007) and it seems that by means of this phenomenon, $A_{2A}R$ counteracts the D_2 receptor-mediated inhibitory modulation of the effects of NMDA receptor stimulation in the indirect striatal efferent neurons (Azdad et al., 2009; Higley and Sabatini, 2010). Allosteric interactions have also been suggested to be mostly responsible for the locomotor depressant and activating effects of $A_{2A}R$ agonist and antagonists, respectively (Ferré et al., 2008). In all cases, the $A_{2A}R$ antagonists were considered as an agonist displacer. However, the direct effect on the modulation of D_2R pharmacological properties exerted by the antagonist binding to $A_{2A}R$ has never been considered. In this study we demonstrate that not only the

agonist CGS 21680, but also the non-selective $A_{2A}R$ antagonist caffeine decreased the binding of both the D_2R agonist [^{3}H]quinpirole and the D_2R antagonist [^{3}H]raclopride in membrane preparations from transfected cells and from sheep striatum by allosteric interactions between both receptors in the $A_{2A}R$-D_2R heteromer. Using these allosteric interactions as a heteromer fingerprint, we demonstrated the $A_{2A}R$-D_2R heteromer expression in human brain striatum.

2.1. CGS 21680 and caffeine binding to $A_{2A}R$ decrease dopamine D_2R agonist and antagonist binding by an allosteric interaction in the $A_{2A}R$-D_2R heteromer.

To evaluate the modulatory role of $A_{2A}R$ agonists and antagonists on D_2R agonist and antagonist binding, CHO cells expressing $A_{2A}R$-D_2R heteromers were used. First of all, as previously shown in HEK 293 cells (Canals et al., 2003), the ability of $A_{2A}R$ to form heteromers with D_2R was demonstrated by BRET experiments in CHO cells transiently co-expressing $A_{2A}R$-Rluc and D_2R-YFP. A positive BRET signal for the energy transfer was obtained (Fig. 1). The BRET signal increased reaching as a hyperbolic function of the concentration of the YFP-fusion construct added reaching an asymptote. As a negative control the BRET pair formed by $A_{2A}R$-Rluc and $5HT_{2B}R$-YFP was used. As shown in Fig. 1, the negative control was fit in a linear non-specific BRET signal. The hyperbolic BRET signal found for these fusion proteins indicates that the intermolecular interaction between $A_{2A}R$ and D_2R in CHO cells is specific.

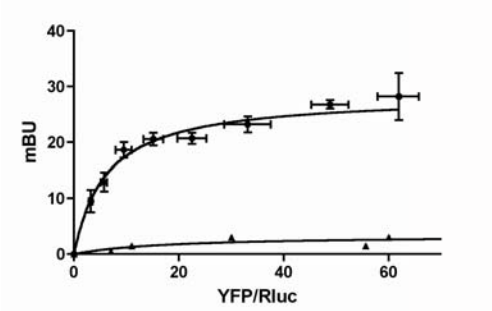

Figure 1. Identification of $A_{2A}R$-D_2R heteromers in CHO cells by BRET experiments. BRET saturation curves were performed with CHO cells co-transfected with increasing amount of cDNA (0.2 to 0.5 μg) corresponding to D_2R-YFP and 0.5 μg of cDNA corresponding to $A_{2A}R$-Rluc (circles). Both fluorescence and luminescence of each sample were measured before every experiment to confirm similar donor expressions (about 100,000 luminescent units) while monitoring the increase acceptor expression (10,000 – 25,000 fluorescent units). As a negative control, linear BRET was obtained in cells expressing equivalent luminescence and fluorescence amounts corresponding to $A_{2A}R$-Rluc (0.5 μg cDNA transfected) and serotonin $5HT_{2B}R$-YFP (0.5 to 8 μg cDNA transfected) receptors (triangles). The relative amount of receptor is given as 100 X the ratio between the fluorescence of the acceptor minus the fluorescence of cells expressing the donor alone (YFP) and the luciferase activity of the donor (Rluc). BRET data are expressed as means ± SD of four to six different experiments grouped as a function of the amount of BRET acceptor.

Using CHO cells transiently transfected with $A_{2A}R$ and D_2R we first tested if the selective $A_{2A}R$ agonist CGS 21680 and the non-selective adenosine receptor caffeine were able to modulate [^{3}H]raclopride (4 nM) binding to D_2R. Both CGS 21680 (Fig. 2A) and caffeine (Fig. 2C) nor caffeine (Fig. 2D) were able to modulate [^{3}H]raclopride (4 nM) binding in membranes from cells only expressing D_2R. Only the highest concentration of caffeine (10 mM) slightly but significantly reduced [^{3}H]raclopride binding, which cannot be attributed to the binding of caffeine to the $A_{2A}R$ (see below the affinity constant of $A_{2A}R$ for caffeine). These results indicated that agonist and antagonist binding to $A_{2A}R$ negatively modulate the antagonist binding to D_2R. Similarly, the D_2R agonist [^{3}H]quinpirole (10 nM) binding to membranes from cells expressing $A_{2A}R$ and D_2R significantly decreased in the presence of increasing concentrations of CGS 21680 (Fig. 2E) or caffeine (Fig. 2F), an effect that was not observed using membranes from cells only expressing D_2R. Interestingly, CGS 21680 and caffeine were more potent at displacing the D_2R agonist [^{3}H]quinpirole that the

D_2R antagonist [^{3}H]raclopride binding. These results indicate that binding of any ligand (agonist or antagonist) to the $A_{2A}R$ decreased the binding of any ligand (agonist or antagonist) to the D_2R.

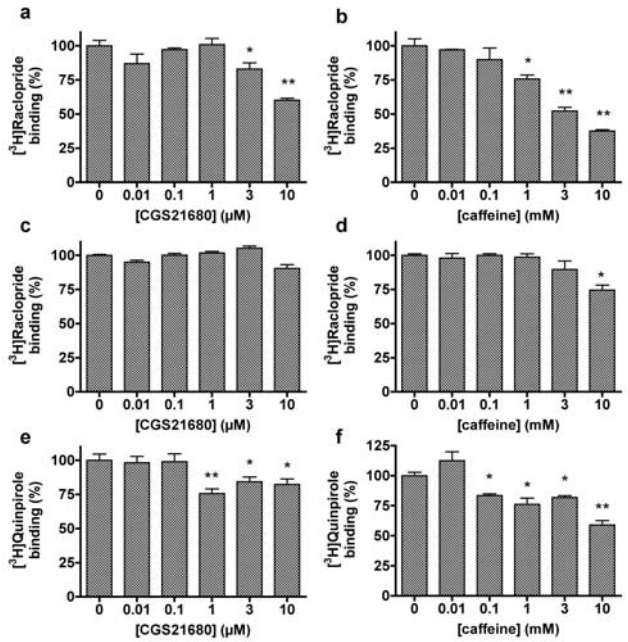

Figure 2. Effect of $A_{2A}R$ ligands on the raclopride and quinpirole binding to cells expressing D_2R or $A_{2A}R$ and D_2R. CHO cells were transfected with 2 μg of the cDNA corresponding to D_2R (**c** and **d**) or co-transfected with 3 μg of the cDNA corresponding to $A_{2A}R$ and 2 μg of the cDNA corresponding to D_2R (**a**, **b**, **e** and **f**). [^{3}H]raclopride (4 nM) binding (**a** to **d**) of [^{3}H]quinpirole (10 nM) binding (**e** and **f**) to cell membranes (0.5 mg of protein/ml) was performed in the absence or in the presence of increasing concentrations of the $A_{2A}R$ agonist CGS 21680 (**a**, **c** and **e**) or the $A_{2A}R$ antagonists caffeine (**b**, **d** and **f**). Specific binding is represented as percentage respect to the sample in absence of $A_{2A}R$ ligands. Data are mean ± SEM of triplicates. Significant differences respect to the samples in absence of $A_{2A}R$ ligands were calculated by Student's t test (* $p<0.05$ and ** $p<0.01$).

To test if these interactions are a consequence of allosteric interactions between both receptors in the $A_{2A}R$-D_2R heteromer and constitute biochemical properties of the heteromer, we analyzed if they can be modified by alterations of the quaternary structure of the heteromers. It has been recently shown that an electrostatic interaction between intracellular domains of the two receptor-units in the $A_{2A}R$-D_2R heteromer is essential for the establishment of its quaternary structure (Navarro et al., 2010). This electrostatic

interaction involves an arginine-rich domain of the third intracellular loop of the D_2R and a phosphorylated serine (Ser-374) in the C-terminus of the $A_{2A}R$. Mutation of this critical phosphorylated serine (substitution to alanine) leads to a significant decrease in BRET values (Navarro et al., 2010). We therefore disrupted the electrostatic interaction (with mutation of Ser-374 of the $A_{2A}R$ to Ala-374; $A_{2A}^{A374}R$) and tested the ability of $A_{2A}^{A374}R$-Rluc to form heteromers with D_2R-YFP. As expected, the BRET between Rluc and YFP was reduced when compared with BRET values obtained with non-mutated receptors (Fig. 3), indicating a change in the quaternary structure that increases the distance between Rluc and YFP, which are placed at the C-terminal part of the receptors.

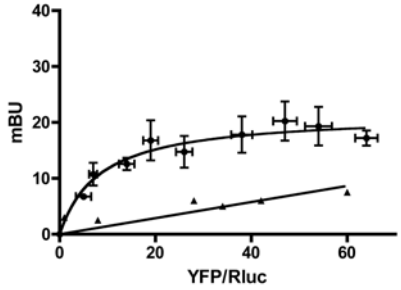

Figure 3. Identification of $A_{2A}^{A374}R$-D_2R heteromers in CHO cells by BRET experiments. BRET saturation curves were performed with CHO cells co-transfected with increasing amounts of cDNA (0.2 to 5 μg) corresponding to D_2R-YFP and 0.5 μg cDNA corresponding to $A_{2A}^{A374}R$-Rluc (solid line). Both fluorescence and luminescence of each sample were measured before every experiment to confirm similar donor expressions (about 100,000 luminescence units) while monitoring the increase acceptor expression (10,000 – 25,000 fluorescent units). The relative amount of acceptor is given as 10 X the ratio between the fluorescence of the acceptor minus the fluorescence of cells expressing the donor alone (YFP) and the luciferase activity of the donor (Rluc). BRET data are expressed as means ± SD of four to six different experiments grouped as a function of the amount of BRET acceptor.

Using membranes from CHO cells expressing this structurally different $A_{2A}^{A374}R$-D_2R heteromer, we tested the effect of $A_{2A}R$ ligands on agonist and antagonist binding to D_2R. Radioligand binding experiments were performed incubating cell membranes with the D_2R antagonist [^{3}H]raclopride (4 nM, Fig. 4A and B) or D_2R agonist [^{3}H]quinpirole (10 nM, Fig. 4C and D) and increasing concentrations of the $A_{2A}R$ agonist CGS 21680 (Fig.

4A and C) of the $A_{2A}R$ antagonist caffeine (Fig. 4B and D). Compared with cells transfected with the wild-type $A_{2A}R$ and D_2R (see Fig. 2), a significantly lower potency in the ability of both CGS 21680 and caffeine to decrease [^{3}H]raclopride and [^{3}H]quinpirole binding was observed. These results therefore strongly suggest that these interactions are a consequence of allosteric interactions between both receptors in the $A_{2A}R$-D_2R heteromer and constitute biochemical properties of the heteromer.

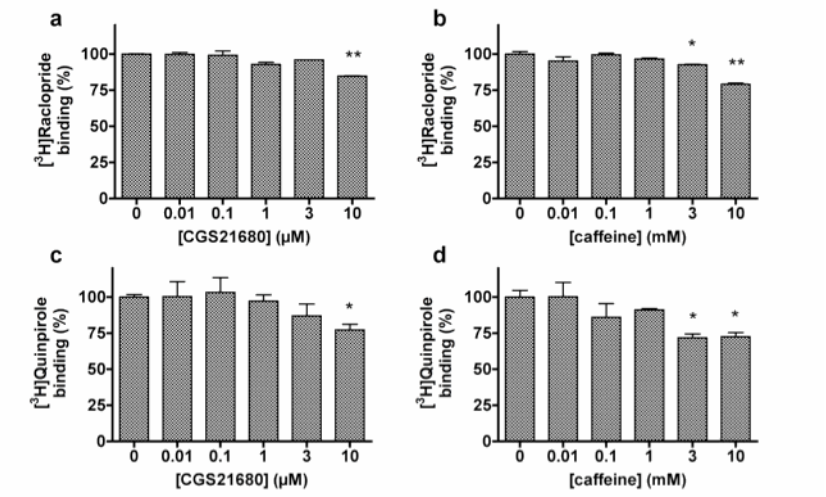

Figure 4. Effect of a serine point mutation in the $A_{2A}R$ C-terminal domain in the $A_{2A}R$ receptor-mediated modulation of ligand binding to D_2R. CHO cells were co-transfected with 3 μg of the cDNA corresponding to $A_{2A}^{A374}R$ and 2 μg of the cDNA corresponding to D_2R. [^{3}H]raclopride (4 nM) binding (**a** and **b**) or [^{3}H]quinpirole (10 nM) binding (**c** and **d**) to cell membranes (0.5 mg of protein/ml) was performed in the absence or in the presence of increasing concentrations of the $A_{2A}R$ agonist CGS 21680 (**a** and **c**) or the $A_{2A}R$ antagonist caffeine (**b** and **d**). Specific binding is represented as percentage respect to the samples in absence of $A_{2A}R$ ligands. Data are mean ± SEM of triplicates. Significant differences respect to the samples in absence of $A_{2A}R$ ligands were calculated by Student's t test (* $p<0.05$ and ** $p<0.01$).

2.2. Allosteric modulations in the $A_{2A}R$-D_2R heteromer in native tissue.

To test the effect of ligand binding to $A_{2A}R$ on the agonist or antagonist binding to D_2R in a native tissue, Radioligand binding experiments were performed using sheep brain striatal membranes were both $A_{2A}R$ and D_2R are highly co-expressed and where they form heteromers (Soriano et al., 2009). We first analyzed the effect of ligand binding to $A_{2A}R$ on the antagonist binding to D_2R in sheep striatal membranes. As shown in Figure 5, both CGS 21680 (Fig. 5A) and caffeine (Fig. 5C) significantly decreased [^{3}H]raclopride (2 nM) binding to D_2R with the same potency that in co-transfected cells. To test if the agonist and antagonists affinity for $A_{2A}R$ correlates with ligand concentration able to significantly decrease the [^{3}H]raclopride binding to D_2R, affinity constants of $A_{2A}R$ for CGS 21680 and caffeine were determined at the same experimental conditions.

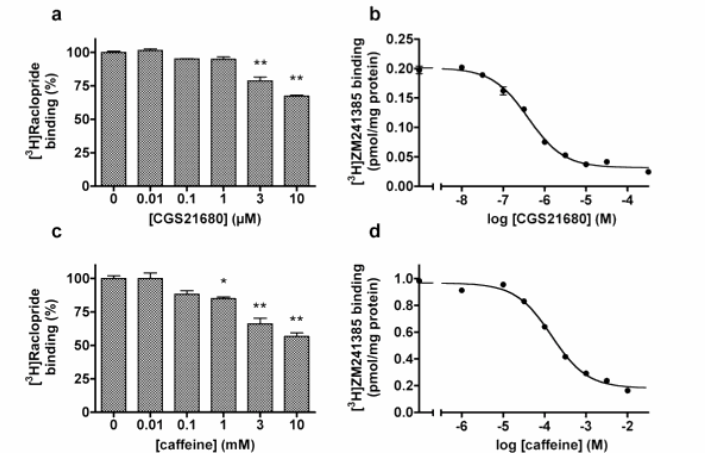

Figure 5. Effect of $A_{2A}R$ agonist and antagonist on the raclopride binding to sheep brain striatum D_2R. In (**a**) and (**c**) 2 nM [^{3}H]raclopride binding to sheep striatal membranes (0.5 mg of protein/ml) was performed in the absence or in the presence of increasing concentrations of the $A_{2A}R$ agonist CGS 21680 (**a**) or the $A_{2A}R$ antagonist caffeine (**c**). Specific binding is represented as percentage respect to the samples in absence of $A_{2A}R$ ligands. Data are mean ± SEM of triplicates. Significant differences respect to the samples in absence of $A_{2A}R$ ligands were calculated by Student's t test (* $p<0.05$ and ** $p<0.01$). In (**b**) and (**d**) competition experiments of 2 nM [^{3}H]ZM 241385 binding versus increasing concentrations of the $A_{2A}R$ agonist CGS 21680 (**b**) or the $A_{2A}R$ antagonist caffeine (**d**) were performed in 50 mM Tris-HCl buffer, pH 7.4 containing 10 mM $MgCl_2$, 120 mM NaCl and 5 mM KCl using sheep striatal membranes (0.5 mg protein/ml). Data are mean ± SEM from a representative experiment (n = 3) performed in triplicate.

As shown in Fig. 5, the competition curve with the antagonist (Fig. 5D) was monophasic (D_C = 0, see Methods) according to a non-cooperative behavior described for the $A_{2A}R$ antagonists, whereas the competition to an antagonist/agonist modulation (K_{DAB} = 32 ± 8 nM, see Methods) (Casadó et al., 2009a). Data fitting to equation 2 did not improve data fitting to equation 3; thus, equilibrium constants were calculated by fitting data to equation 3. The dissociation equilibrium constant (K_{DB1}) value for CGS 21680 and caffeine binding to $A_{2A}R$ were 45 ± 5 nM and 25 ± 2 μM, respectively (mean ± SEM of three different assays). Thus, at these experimental conditions the agonist and antagonist affinity for $A_{2A}R$ correlates with ligand concentration able to significantly decrease the [^{3}H]raclopride binding to D_2R. The $A_{2A}R$ ligand-induced decrease in the [^{3}H]raclopride binding is consistent with an $A_{2A}R$ receptor-mediated increase of D_2R antagonist affinity constant. In fact, competition experiments of [^{3}H]raclopride (4 nM) binding versus raclopride (0.01 nM to 3 μM) performed in the absence or in the presence of 3 μM CGS 21680 or 3 mM caffeine gave monophasic competition curves (D_C = 0, see Methods). The K_{DA1} values obtained by fitting binding data to equation 4 (see Methods) appear in Table 1 and indicate that CGS 21680 and caffeine significantly decrease the affinity of striatal D_2R for [^{3}H]raclopride.

Table 1. Equilibrium dissociation constant (K_{DA1}) for [^{3}H]raclopride or [^{3}H]quinpirole binding to D_2R in the absence (control) or in the presence of $A_{2A}R$ ligands.

Treatment	[^{3}H]raclopride binding K_{DA1} (nM)	[^{3}H]quinpirole binding K_{DA1} (nM)
Control	1.8 ± 0.7	5 ± 2
CGS 21680 (3 μM)	4.2 ± 0.7*	10 ± 2*
Caffeine (3 mM)	3.7 ± 0.7*	14 ± 3*

Data are means ± SEM values of three experiments. * $p < 0.05$ compared to control.

The experiments in co-transfected cells demonstrated that the caffeine-mediated modulation of antagonist and agonist binding to D_2R is dependent on its ability to bind to $A_{2A}R$. However, in the striatum, the non-selective adenosine antagonist caffeine also binds to A_1R. Therefore, we also tested the role of A_1R ligands in D_2R antagonist binding. Competition experiments of [^{3}H]raclopride (2 nM) versus increasing concentrations of the A_1R agonists r-PIA (Fig. 6A) or CCPA (Fig. 6B) showed that A_1R agonists do not modulate D_2R antagonist biding. When the A_1R antagonist DPCPX was used as competitor, concentrations of DPCPX up to 100 nM, able to produce a >99% A_1R saturation, did not affect [^{3}H]raclopride binding (Fig. 6C). Nevertheless, higher concentrations of this ligand significantly decreased [^{3}H]raclopride binding (Fig. 6C), which was due to the ability of high concentrations of DPCPX to bind to $A_{2A}R$. In fact, high concentrations of DPCPX also displace [^{3}H]ZM 241385 (Fig. 6D) and fitting binding data to equation 3 gave a K_{DB1} = 50 ± 4 nM. These demonstrate that ligands (agonist and antagonist) binding to $A_{2A}R$ but not A_1R act as modulators of antagonist binding to D_2R.

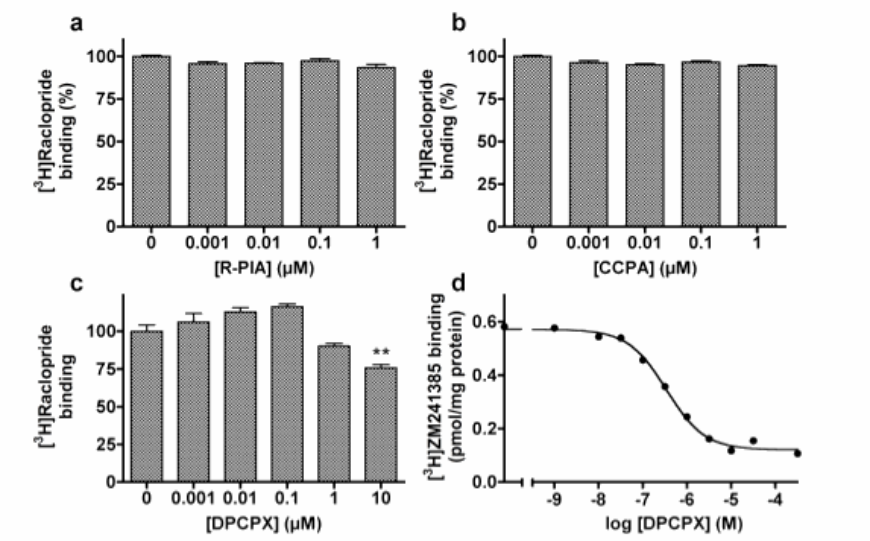

Figure 6. Ligand binding to adenosine A_1R does not affect the raclopride binding to sheep brain striatum D_2R. In (**a**), (**b**) and (**c**) 2 nM [^{3}H]raclopride binding to sheep striatal membranes (0.5 mg of protein/ml) was performed in the absence or in the presence of increasing concentrations of the A_1R agonists R-PIA (**a**) or CCPA (**b**) or the A_1 receptor antagonists DPCPX (**c**). Specific binding is represented as percentage respect to the samples in absence of A_1R ligands. Data are mean ± SEM of triplicates. Significant differences respect to the samples in absence of A_1R ligands were calculated by Student's t test (** $p<0.01$). In (**d**) competition experiments of 2 nM [^{3}H]ZM 241385 binding versus increasing concentrations of DPCPX in sheep brain striatal membranes are shown. Data are mean ± SEM from a representative experiments performed in triplicate.

To test the effect of $A_{2A}R$ ligands on D_2R agonist binding, experiments were performed incubating sheep striatal membranes with the D_2R agonist [^{3}H]quinpirole (6 nM) and increasing concentrations of CGS 21680 (Fig. 7A) or caffeine (Fig. 7B). Both ligands significantly decreased [^{3}H]quinpirole binding to D_2R. Furthermore, as with the experiments in co-transfected cells, CGS 21680 and caffeine were more potent at modulating [^{3}H]quinpirole than [^{3}H]raclopride binding. To test if the decrease in agonist binding is consistent with an $A_{2A}R$ receptor-mediated increase of D_2R agonist affinity constant, competition experiments of [^{3}H]quinpirole (6 nM) binding versus quinpirole (0.01 nM to 3 μM) were performed in the absence or in the presence of CGS 21680 (3 μM) or caffeine (3 mM). At low concentrations of [^{3}H]quinpirole , competition curves were monophasic (D_C = 0) due to the extremely low [^{3}H]quinpirole binding to the second protomer of the

homodimer, so binding data was fitted to equation 4. The K_{DA1} values obtained appear in Table 1 and indicate that CGS 21680 and caffeine significantly decrease the affinity of striatal D_2R for [^{3}H]quinpirole.

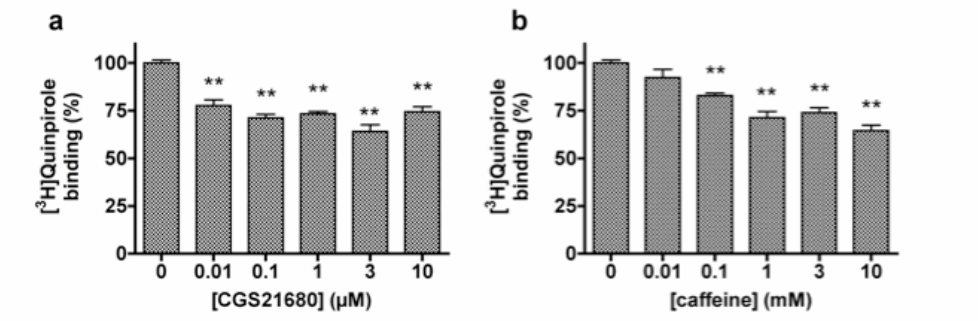

Figure 7. Effect of agonist and antagonist binding to $A_{2A}R$ on the quinpirole binding to sheep brain striatum D_2R. 6 nM [^{3}H]quinpirole binding to sheep striatal membranes (0.5 mg of protein/ml) was performed in the absence or in the presence of increasing concentrations of the $A_{2A}R$ agonist CGS 21680 (**a**) or the $A_{2A}R$ antagonist caffeine (**b**). Specific binding is represented as percentage respect to the samples in absence of $A_{2A}R$ ligands. Data are mean ± SEM of triplicates. Significant differences respect to the samples in absence of $A_{2A}R$ ligands were calculated by Student's t test (** $p<0.01$).

2.3. $A_{2A}R$-D_2R heteromer in human brain caudate nucleus.

As recently established, the identification of a biochemical property of a receptor heteromer can be used as a biochemical fingerprint of their presence in native tissues (Ferré et al., 2009). Since, as described above, the allosteric interactions between $A_{2A}R$ and D_2R in the $A_{2A}R$-D_2R heteromer constitute biochemical properties of the heteromer. We used these allosteric modulations as a biochemical fingerprint to detect $A_{2A}R$-D_2R heteromer in human brain striatum (caudate nucleus). Experiments were performed incubating human caudate nucleus membranes with [^{3}H]raclopride (2 nM) and increasing concentrations of CGS 21680 (Fig. 8A), caffeine (Fig. 8B) or the A_1R agonist CCPA (Fig. 8C). Both the $A_{2A}R$ agonist and caffeine significantly decreased [^{3}H]raclopride binding to D_2R with exactly the same potency than in membranes from sheep striatum and co-transfected cells. As expected, the A_1R agonist did not modulate the antagonist binding to D_2R (Fig. 8C). These results provide the first evidence for the existence of $A_{2A}R$-D_2R heteromers in human striatum.

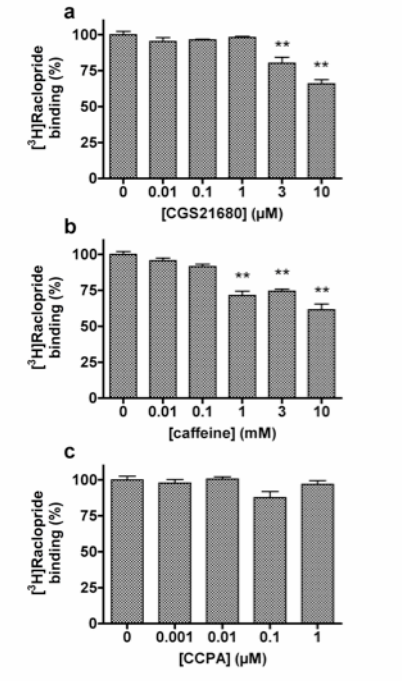

Figure 8. Effect of agonist and antagonist binding to $A_{2A}R$ on the raclopride binding to human caudate nucleus D_2R. [^{3}H]raclopride (2 nM) binding to human caudate nucleus membranes (0.2 mg of protein/ml) was performed in the absence or in the presence of increasing concentrations of the $A_{2A}R$ agonist CGS 21680 (**a**), the $A_{2A}R$ antagonist caffeine (**b**) or the A_1R agonist CCPA (**c**). Specific binding is represented as percentage respect to the samples in absence of adenosine receptor ligands. Data are mean ± SEM of triplicates. Significant differences respect to the samples in absence of $A_{2A}R$ (**a** and **b**) or A_1R (**c**) ligands were calculated by Student's t test (** $p<0.01$).

2.4. Discussion.

One important property of receptors heteromers is the capacity to establish allosteric interactions between partner receptors in the receptor oligomer that confers the specific pharmacological and functional characteristics of the heteromer (Casadó et al., 2007, 2009a). In this work we focused on this property for $A_{2A}R$-D_2R heteromers. We first demonstrated that binding of any ligand (agonist or antagonist) to the $A_{2A}R$ decreases the binding of any ligand (agonist or antagonist) to the D_2R. Second, we established that these interactions are a consequence of allosteric interactions between both receptors in the $A_{2A}R$-D_2R heteromer and constitute biochemical properties of the heteromer. Third, we demonstrated that adenosine $A_{2A}R$ but not A_1R agonist and antagonist decreases both agonist and antagonist affinity for D_2R in sheep brain striatal membranes were $A_{2A}R$-D_2R heteromer have been described (Soriano et al., 2009). Finally, using these allosteric interactions as the heteromer fingerprint, we demonstrated the $A_{2A}R$-D_2R heteromer expression in human brain striatum.

Both the $A_{2A}R$ agonist CGS 21680 or the non-selective adenosine receptor antagonist caffeine, the most consumed psychoactive drug in the world, decreased the affinity of the D_2R for the selective tritiated agonist and antagonist [^{3}H]quinpirole and [^{3}H]raclopride. Here we demonstrated that these interactions between $A_{2A}R$ and D_2R are allosteric interactions between the different receptor units in the $A_{2A}R$-D_2R heteromer that constitute a biochemical property of the heteromer. In fact, it has been described that finding a correlation between significant changes in the quaternary structure of the heteromer with significant changes in receptor pharmacology or function, allows establishing the biochemical properties of the heteromer (Ferré et al., 2009). Following this concept, we have taken profit of the use of an $A_{2A}R$ mutant with a mutation of a key serine residue localized in its C-terminus ($A_{2A}^{A374}R$). We previously demonstrated that such as mutation results in a decrease in BRET values that implies a significant change in the quaternary structure of the

A_{2A}R-D_2R heteromer by disrupting the intracellular intermolecular electrostatic interaction of the heteromer (Borroto-Escuela et al., 2010; Navarro et al., 2010). As expected, here we observed a decrease in BRET for the A_{2A}^{A374}R- Rluc – D_2R-YFP pair compared to A_{2A}R-Rluc – D_2R-YFP pair and this change in the quaternary structure of the heteromer also resulted in the counteraction of allosteric interactions in the heteromer. Therefore, the allosteric interactions in the A_{2A}R-D_2R heteromers here described constitute a biochemical characteristic of the receptor heteromer.

A biochemical property of the receptor heteromer can be used as a heteromer biochemical fingerprint to demonstrate its presence in native tissues (Ferré et al., 2009). As we demonstrated that the allosteric interactions in the A_{2A}R-D_2R heteromer constitute biochemical properties of the receptor heteromer, we used these allosteric interactions to detect and characterize A_{2A}R-D_2R heteromers in sheep brain striatum and, more importantly, in human brain caudate nucleus. In human brain caudate nucleus membranes, CGS 21680 and caffeine decreased the affinity of the D_2R for [^{3}H]raclopride with practically the same dose-response range we found in membrane preparations from CHO cells expressing A_{2A}R-D_2R heteromers. Consequently, we were able to find the heteromer biochemical fingerprint using these membranes that gives, for the first time, a demonstration of the existence of A_{2A}R-D_2R heteromers in the human brain. These findings are relevant considering that both A_{2A}R and D_2R in the striatum are targets for many therapeutic drugs and neurodegenerative disorders and remain a primary focus of many biomedical and pharmaceutical research (Cristalli et al., 2009; V. Lopes et al., 2011; Millan, 2010; Pinna, 2009; Thaker, 2007). In fact, receptor heteromers possess unique biochemical characteristics that are demonstrably different from those of its individual units (Ferré et al., 2009). Those properties, including allosteric modulations between units here described, can be fundamental in drug discovery, since the pharmacological parameters of a drug selected for instance by HTS (High-throughput screening) strategies using receptors expressed alone in a

cell line can be very different from the actual pharmacological parameters in native tissues expressing the receptor forming heteromers with another receptor and in the presence or in the absence of ligands for the partner receptor (Casadó et al., 2009a, 2009b; Ferré et al., 2009). In this frame, one interesting aspect is that an allosteric interaction between protomers in a heteromer must be interpreted as an intermolecular interaction by which binding of a ligand to one of the receptor units in the receptor heteromer changes the binding properties of the other receptor unit (Ferré et al., 2009). Some findings initially demonstrated that the $A_{2A}R$ agonist decreases the agonist binding to D_2R and suggested that this allosteric interaction between $A_{2A}R$ and D_2R was a key mechanism involved in the motor depressant effects of $A_{2A}R$ agonists and the motor stimulant effects of $A_{2A}R$ antagonists including caffeine (Ferré et al., 2008) or in the $A_{2A}R$ agonist-induced depletion of the D_2R receptor-mediated inhibition of NMDA-induced neuronal firing (Schiffmann et al., 2007). Also agonist-agonist allosteric interaction has been considered as a main mechanism responsible for the antiparkinsonian effect of $A_{2A}R$ antagonists (Ferré et al., 2004, 2008; Muller and Ferre, 2007). Since now, $A_{2A}R$ antagonists were not considered to induce direct allosteric interactions in the $A_{2A}R$-D_2R heteromer and were only considered as molecules able to displace the agonist binding and, consequently, block the agonist-agonist allosteric interactions in the $A_{2A}R$-D_2R heteromer. Our results demonstrate than an allosteric interaction in the $A_{2A}R$-D_2R heteromer not also includes agonist-agonist interactions but also agonist-antagonist, antagonist-agonist and antagonist-antagonist interactions in cell and brain tissue membranes including human striatum. Thus, antagonist binding to $A_{2A}R$ unit in the receptor heteromer also decreases the agonist and antagonist binding to the D_2R unit. This behavior must be taken into account when analyzing the functional and pharmacological role of $A_{2A}R$ ligands, in particular $A_{2A}R$ antagonist on D_2R functionality and point out that not only allosteric interactions but also complex cross-talk between receptors in the heteromer at the signaling level must be taken into account to

explain the role of $A_{2A}R$ ligands on D_2R modulation. Another important aspect, our results can also have implications in the field of human PET neuroimaging. In PET, [^{11}C]raclopride is often used as a marker of D_2R, and caffeine intake is usually not controlled when using the ligand. A few studies of the effect of caffeine on [^{11}C]raclopride PET have been performed, and they already indicated a caffeine-induced decrease in the D_2R antagonist binding (Kaasinen et al., 2004a, 2004b). Taking into account the results here described, this decrease in [^{11}C]raclopride binding can be interpreted by caffeine acting on $A_{2A}R$-D_2R heteromers in the human brain. However in PET studies was only evaluated the effect of an oral dose of caffeine on habitual coffee drinkers after 24 hours of caffeine abstinence (Kaasinen et al., 2004a, 2004b) and results are difficult to interpret, as [^{11}C]raclopride binding is only significantly modified in thalamic areas and the effects of caffeine could sometimes be reproduced by placebo (Kaasinen et al., 2004a, 2004b). Nevertheless, the results here described strongly suggest that the $A_{2A}R$-D_2R heteromer-mediated effect of caffeine on raclopride binding have to be taken into account in [^{11}C]raclopride PET experiments and point out that parameters such as tendecy to drink coffee, periods of coffee abstinence or different doses of caffeine must be take into consideration.

3. Striatal pre- and postsynaptic profile of adenosine $A_{2A}R$ antagonists.

The striatum is the major input structure of the basal ganglia (Gerfen, 1992). More than ninety five percent of striatal neurons are γ-aminobutyric-acidergic (GABAergic) medium spiny neurons (MSNs). These neurons receive two main inputs: glutamatergic afferents from cortical, thalamic and limbic areas and dopaminergic afferents from the substantia nigra pars compacta and the ventral tegmental area (Gerfen, 1992). MSNs are efferent neurons that give rise to the two efferent pathways (Gerfen, 1992). It is generally accepted that stimulation of the direct and indirect pathways results in motor activation and motor inhibition, respectively, and that smooth motor drive results from the counterbalanced influence of the direct and indirect pathways on the neural activity of the output structures (DeLong and Wichmann, 2007; Obeso et al., 2002). Direct MSNs express dopamine receptors predominantly of the D_1R subtype, whereas indirect MSNs are known for their high expression of dopamine D_2R and adenosine $A_{2A}R$ (Ferré et al., 2008; Gerfen, 1992; Quiroz et al., 2009).

There is clear evidence for the existence of postsynaptic mechanisms in the control of glutamatergic neurotransmission to the indirect MSN by at least two reciprocal antagonistic interactions between $A_{2A}R$ and D_2R (Ferré et al., 2008). In one type of interaction, $A_{2A}R$ and D_2R are forming heteromers and, by means of an allosteric interaction, $A_{2A}R$ counteracts the D_2R-mediated inhibitory modulation of the effects of NDMA receptor stimulation in the indirect MSN, which includes Ca^{2+} influx, transition to the up-state and neuronal firing in the up-state (Azdad et al., 2009; Higley and Sabatini, 2010). This interaction has been suggested to be mostly responsible for the locomotor depressant and activating effects of $A_{2A}R$ agonist and antagonists, respectively (Ferré et al.,

2008). The second type of interaction involves $A_{2A}R$ and D_2R that do not form heteromers, but most probably homomers (Ferré et al., 2008). In this interaction, which takes place at the level of adenylyl-cyclase (AC), stimulation of G_i-coupled D_2R counteracts the effects of G_s-coupled $A_{2A}R$ (Ferré et al., 2008). Due to a strong tonic effect of endogenous dopamine on striatal D_2R, this interaction keeps $A_{2A}R$ from signaling through AC. However, under conditions of dopamine depletion or with blockade of D_2R, $A_{2A}R$-mediated AC activation is unleashed. This is biochemically associated with a significant increase in the phosphorylation of PKA-dependent substrates, which increases gene expression and the activity of the indirect MSN, producing locomotor depression (Ferré et al., 2008). This interaction seems to be the main mechanism responsible for the locomotor depression induced by D_2R antagonists. Thus the motor depressant and most biochemical effects induced by genetic or pharmacologic blockade of D_2R are counteracted by the genetic or pharmacological blockade of $A_{2A}R$ (Chen et al., 2001; Håkansson et al., 2006; Svenningsson et al., 2000).

Striatal $A_{2A}R$ are not only localized postsynaptically but also presynaptically, in glutamatergic terminals, where they heteromerize with A_1R and where their stimulation facilitates glutamatergic neurotransmission (Ciruela et al., 2006; Quiroz et al., 2009). Interestingly, presynaptic $A_{2A}R$ are preferentially localized in glutamatergic terminals of cortico-striatal afferents to the direct MSN (Quiroz et al., 2009). According to the widely accepted functional basal circuitry model (DeLong and Wichmann, 2007; Obeso et al., 2002), blockade of postsynaptic $A_{2A}R$ localized in the indirect MSN should produce motor activation (by potentiating D_2R mediated effects by means of $A_{2A}R$-D_2R receptor interactions). On the other hand, according to the same model, blockade of presynaptic $A_{2A}R$ localized in the cortico-striatal glutamatergic terminals that make synaptic contact with the direct MSN should decrease motor activity (by inhibiting glutamate release). The preferential locomotor-activating effects of systemically administered $A_{2A}R$ antagonists can be explained by a stronger influence of a tonic adenosine and $A_{2A}R$ receptor-mediated

modulation of the indirect pathway *versus* the direct pathway under basal conditions. In any case, the potency at inducing locomotor activation can be used as an *in vivo* measure of the ability of an $A_{2A}R$ antagonist to block postsynaptic striatal $A_{2A}R$. Recently it was established an *in vivo* model that evaluated the efficacy of cortico-striatal glutamatergic neurotransmission to the direct MSN, by quantifying the correlation between the current delivered into the orofacial premotor cortex and the concomitant electromyographic response elicited in the jaw muscles (Quiroz et al., 2009). In this model, $A_{2A}R$ or D_1R antagonists were able to counteract the motor output induced by cortical electrical stimulation, which can only be explained by blockade of striatal presynaptic $A_{2A}R$ or postsynaptic D_1R, respectively (Quiroz et al., 2009, 2010).

Receptor heteromers are defined as a macromolecular complex composed by at least two (functional) receptor units with biochemical properties that are demonstrably different from those of its individual components (Ferré et al., 2009). Specific ligand binding characteristics are one of those properties (Ferré et al., 2007, 2009). The aim of the present study was as stated in Aims, first, to investigate the possible existence of different pre- and postsynaptic profiles of several $A_{2A}R$ antagonists. The potency at blocking the motor output and striatal glutamate release induced by cortical electrical stimulation and the potency at inducing locomotor activation were used as *in vivo* measures of pre- and postsynaptic activities, respectively. Second, we wanted to evaluate if the different pre- and postsynaptic profiles could be related to different affinities that $A_{2A}R$ could have for those compounds when forming heteromers with either A_1R or D_2R. In fact, the results strongly suggest that heteromerization plays a key role in the pre- and postsynaptic profile of $A_{2A}R$ antagonists.

3.1. Striatal pre- *versus* postsynaptic profile of $A_{2A}R$ antagonists.

Dose-response experiments with the six $A_{2A}R$ antagonists indicated that four compounds (SCH 420814, SCH 58261, MSX 3 and ZM 241385) had similar potency (similar minimal significant effective doses) at inducing locomotor activation (Fig. 1) and at reducing the power correlation coefficient (PCC) (Fig. 2). The other two compounds had a very different profile: KW 6002 produced a strong locomotor activation already at the dose of 0.3 mg/kg i.p., while it did not reduce PCC at the highest tested dose (10 mg/kg i.p.). On the other hand, SCH 442416 produced a very weak locomotor activation, only significant at doses higher that 3 mg/kg i.p., while it significantly decreased PCC already at the dose of 0.1 mg/kg i.p.

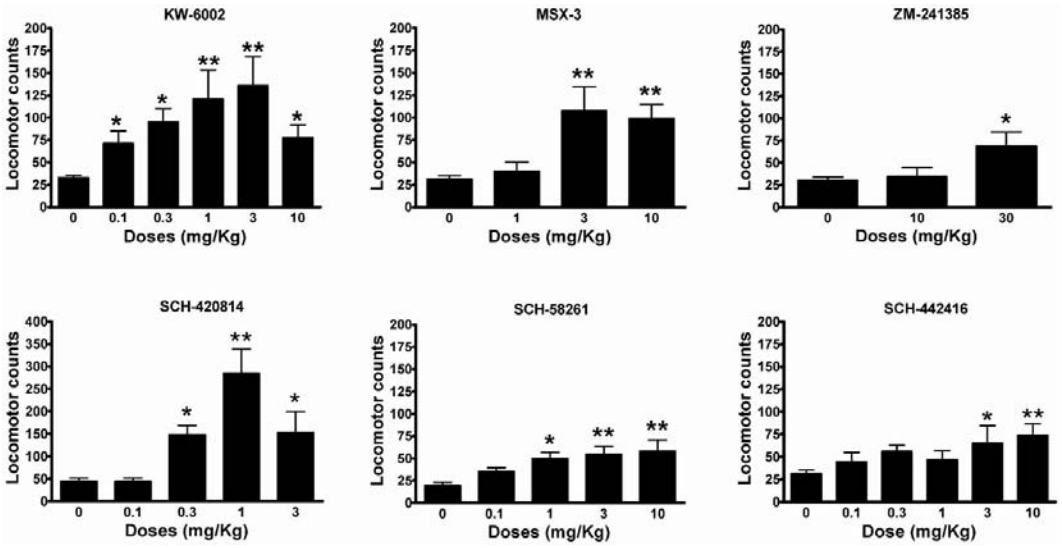

Figure 1. Locomotor activation in rats induced by $A_{2A}R$ antagonists. Data represent means ± SEM of the locomotor activity (distance traveled, in cm, of total accumulated counts) in habituated rats (90 min) during 90 min following the drug administration (n = 6 – 8 per froup). * and **: $p<0.05$ and $p<0.01$, respectively in comparison to vehicle-treated animals (0 mg/kg); ANOVA with *post-hoc* Newman-Keul's comparisons, $p<0.5$ and $p<0.01$, respectively.

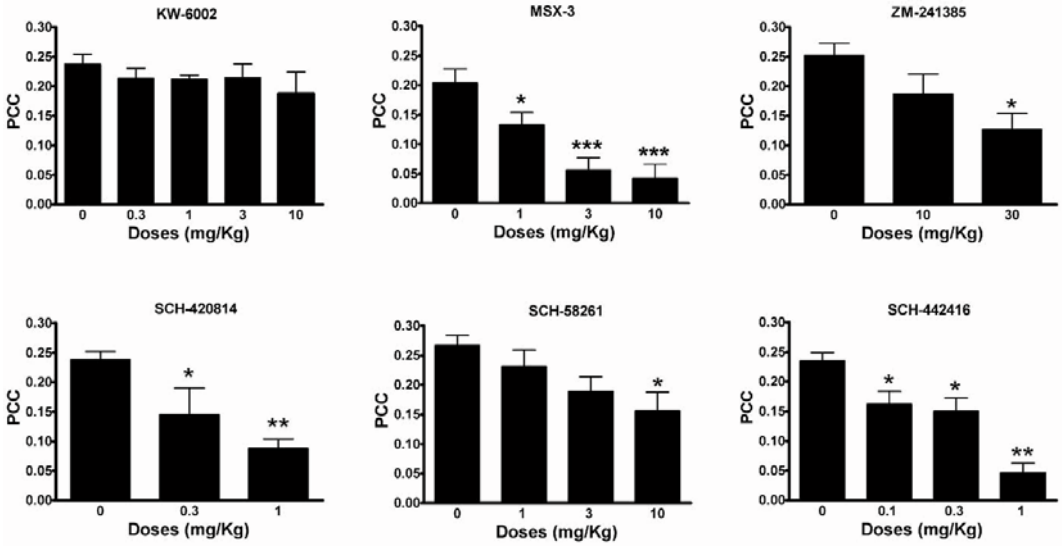

Figure 2. Blockade by $A_{2A}R$ antagonists of the motor output induced by cortical electrical stimulation. Dose-dependent decrease in the power correlation coefficient (PCC) induced by the administration of different $A_{2A}R$ antagonists. Results represent means ± SEM (n = 5 – 6 per group). * and **: p<0.05 and p<0.01, respectively in comparison to vehicle-treated animals (0 mg/kg); ANOVA with *post-hoc* Dunnett's comparisons, p<0.5 and p<0.01, respectively.

In vivo microdialysis with cortical electrical stimulation was used as an additional *in vivo* evaluation of the preferential pre- and postsynaptic activity of SCH 442416 and KW 6002, respectively. SCH 442416 significantly counteracted striatal glutamate release induced by cortical stimulation at a dose that strongly reduced PCC but did not induce locomotor activation (1 mg/kg i.p.; Fig. 3). On the other hand, KW 6002 did not modify striatal glutamate release induced by cortical stimulation at a dose that produced a pronounced locomotor activation but did not reduce PCC (1 mg/kg i.p.; Fig.3).

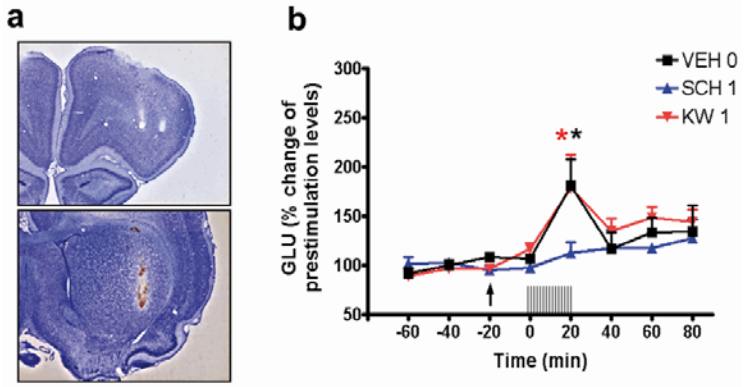

Figure 3. Blockade by $A_{2A}R$ antagonists of striatal glutamate release induced by cortical electrical stimulation. (**a**) Representative coronal sections of a rat brain, stained with crystal violet, showing the tracks left by the bipolar stimulation electrode in the orofacial area of the lateral agranular motor cortex (top) and by the microdialysis probe in the lateral striatum (bottom). (**b**) Effect of systemic administration of the $A_{2A}R$ antagonists SCH 442416 and KW 6002 (1 mg/kg i.p., in both cases) on the increase in glutamate extracellular levels in the lateral striatum induced by cortical electrical stimulation. Results are expressed as means ± SEM of percentage of the average of the three values before the stimulation (n = 5 – 7 per group). Time '0' represents the values of the samples previous to the stimulation. The arrow indicates the time of systemic administration. The train of vertical lines represents the period of cortical stimulation. *: $p<0.05$ compared to value of the last sample before the stimulation (repeated-measures ANOVA followed by Tukey's test).

3.2. Development of CHO cell-lines expressing A_1R-$A_{2A}R$ or $A_{2A}R$-D_2R heteromers.

Cell clones expressing $A_{2A}R$, A_1R-$A_{2A}R$ heteromers or $A_{2A}R$-D_2R heteromers and control clones expressing A_1R or D_2R were generated (See Methods). First of all, the ability of $A_{2A}R$ to form heteromers with A_1R or D_2R in CHO cells was demonstrated by BRET experiments in cells transiently co-expressing $A_{2A}R$-Rluc and A_1R-YFP or $A_{2A}R$-Rluc and D_2R-YFP. A positive BRET signal for energy transfer was obtained (Fig. 4). The BRET signal increased as a hyperbolic function of the concentration of the YFP-fusion construct added reaching an asymptote. As a negative control the BRET pair formed by $A_{2A}R$-Rluc and 5-$HT_{2B}R$-YFP was used. As shown in Figure 4, the negative control gave a linear non-specific BRET signal. The significant and hyperbolic BRET signal found for these fusion proteins indicates that the intermolecular interaction between $A_{2A}R$ and A_1R or $A_{2A}R$ and D_2R in CHO cells is specific.

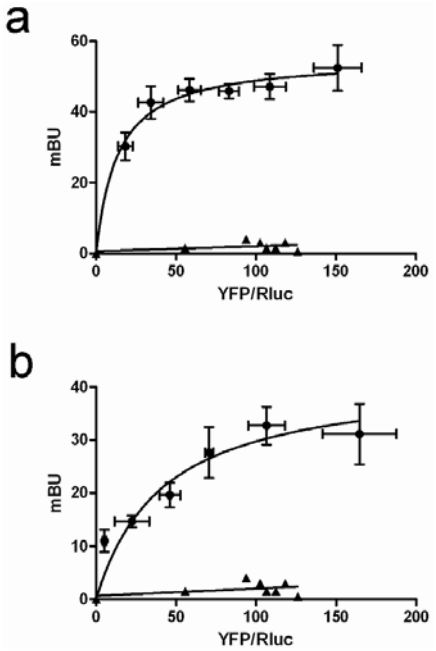

Figure 4. Identification of receptor heteromers in CHO cells by BRET saturation curve. BRET experiments were performed with CHO cells co-expressing $A_{2A}R$-Rluc and A_1R-YFP (**a**) or $A_{2A}R$-Rluc and D_2R-YFP (**b**). Co-transfections were performed with increasing amounts of plasmid-YFP (0.25 to 4 μg cDNA corresponding to A_1R-YFP and 0.5 to 8 μg corresponding to D_2R-YFP) whereas the $A_{2A}R$-Rluc construct was maintained constant (0.5 μg cDNA). Both fluorescence and luminescence were measured before every experiment to confirm similar donor expressions (about 100,000 luminescent units) while monitoring the increase acceptor expression (10,000 – 25,000 fluorescent units). As a negative control, linear BRET was obtained in cells expressing equivalent luminescence and fluorescence amounts corresponding to $A_{2A}R$-Rluc, (0.5 μg transfected cDNA) and serotonin 5-$HT_{2B}R$-YFP (0.5 to 8 μg transfected cDNA). The relative amount of acceptor is given as the ratio between the fluorescence of the acceptor minus the fluorescence value of cells expressing the donor expressed as means ± SD of four to 6 different experiments grouped as a function of the amount of BRET acceptor.

$A_{2A}R$-D_2R and A_1R-$A_{2A}R$ heteromerization in stably transfected CHO cells was shown by ligand binding experiments. This is an indirect approach for the identification of a receptor heteromer in native tissues or cells (Ferré et al., 2009). In the $A_{2A}R$-D_2R heteromer, an allosteric interaction between both receptors in the heteromer has been described, in which the dopamine D_2R agonist affinity decreases in the presence of an $A_{2A}R$ agonist (Ferré et al., 2007). In CHO cells stably expressing $A_{2A}R$ and D_2R, the affinity of the D_2R for the dopamine was determined by competition experiments of the D_2R antagonist [^{3}H]YM 09151-2 *versus* dopamine in the presence (Fig. 5A) or in the absence (Fig. 5B) of the $A_{2A}R$ agonist CGS 21680 (200 nM). By fitting data obtained in the absence of CGS 21680 to equation 3 (see Methods; considering K_{DA1} = 2.9 nM see below) the calculated K_{DB1} was 9 ± 2 μM. In the presence of CGS 21680, 5 μM of dopamine was unable to decrease the Radioligand bound and more than 50% of radioligand bound was found in the presence of 100 μM of dopamine (Fig. 5B). A K_{DB1} > 30 μM was estimated and it was shown that CGS 21680 induced a decrease in the dopamine affinity for D_2R.

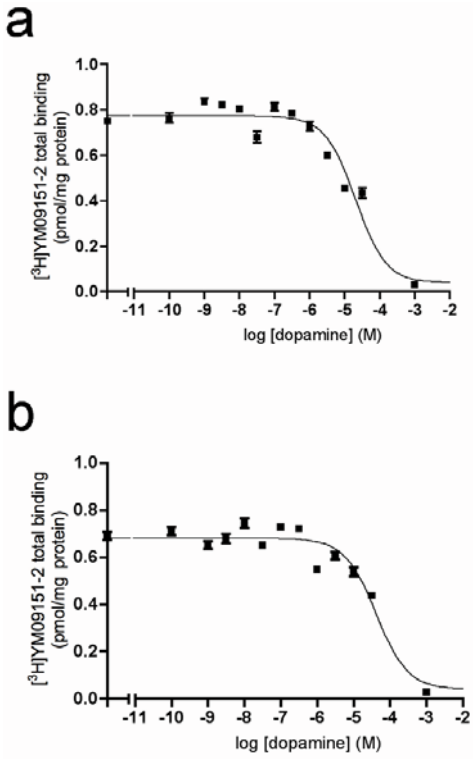

Figure 5. Allosteric interaction between $A_{2A}R$ and D_2R in $A_{2A}R$-D_2R CHO cells. Competition experiments were performed in membrane preparations from CHO cells expressing $A_{2A}R$ and D_2R with 0.5 nM [^{3}H]YM 09151-2 and increasing concentrations of dopamine (from 0.1 nM to 30 μM) in the absence (**a**) or in the presence (**b**) of 200 nM CGS 21680 as indicated in Methods. Data represent means ± SEM of a representative experiment performed with triplicates.

An allosteric interaction in the A_1R-$A_{2A}R$ heteromer has also been described, in which the A_1R agonist affinity decreases in the presence of an $A_{2A}R$ agonist (Ciruela et al., 2006). As shown in Figure 6A, the displacement of the A_1R agonist [^{3}H]R-PIA by CGS 21680 was significantly ($p<0.001$) better fitted by a biphasic that by a monophasic curve. At low CGS 21680 concentrations, when it binds preferentially to $A_{2A}R$ (at concentrations of CGS 21680 <500 nM, the direct binding of CGS 21680 to A_1R is <1%, according to the calculated affinity of A_1R for CGS 21680), CGS 21680 decreased the binding of [^{3}H]R-PIA to the A_1R with an IC_{50} value of 386 ± 35 nM (n = 3). At high concentrations (>10 μM), the [^{3}H]R-PIA binding displacement reflects the binding of CGS 21680 directly to the A_1R and the competition between CGS 21680 and R-PIA for the binding to the A_1R. In fact, in the control clone expressing only A_1R, the displacement by CGS 21680 of [^{3}H]R-PIA only occurred at CGS 21680 concentrations higher that 10 μM (Fig. 6B).

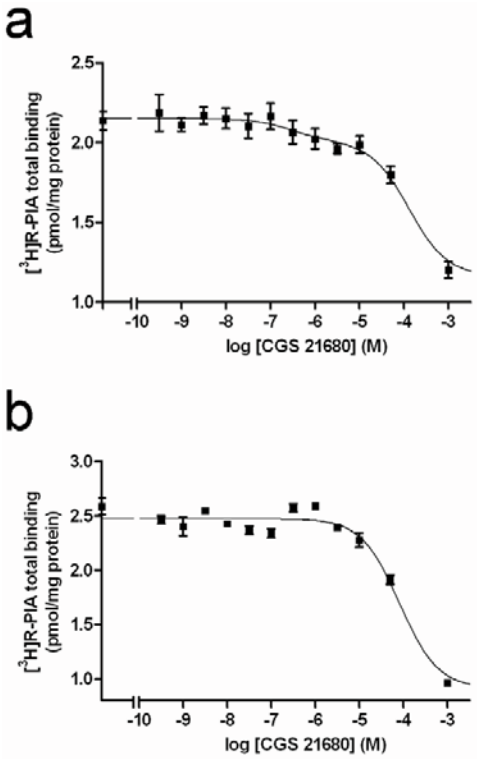

Figure 6. Allosteric interaction between A_1R and $A_{2A}R$ in A_1R-$A_{2A}R$ CHO cells. Competition experiments were performed in membrane preparations from CHO cells expressing A_1R or A_1R and $A_{2A}R$ with 12 nM [^{3}H]R-PIA *versus* increasing concentrations of the $A_{2A}R$ agonist CGS 21680 as indicated in Methods. Data represent means ± SEM of a representative experiment performed with triplicates.

A pharmacological characterization of selected cell clones was performed with competition experiments of radiolabeled antagonists of A_1R, $A_{2A}R$ and D_2R *versus* selective agonists or antagonists. In all cases, the competition curves of the $A_{2A}R$ antagonist [^{3}H]ZM 241385 (2 nM) *versus* ZM 241385 (0.1 nM to 11 μM), the D_2R antagonist [^{3}H]YM 09151-2 (0.2 nM) *versus* YM 09151-2 (0.01 nM to 11 μM) or the A_1R antagonist [^{3}H]DPCPX (2 nM) *versus* DPCPX (0.1 nM to 11 μM), were monophasic, indicating the absence of cooperativity (see Methods). By fitting the data to equation 4 (see Methods), the K_D (K_{D1}) values obtained for the antagonists ZM 241385 or YM 09151-2 were 8 ± 3 nM and 2.9 ± 0.3 nM, respectively, for the chosen $A_{2A}R$-D_2R clone. The K_D value obtained for A_1R and $A_{2A}R$ antagonists were 8 ± 2 nM (DPCPX) and 1.8 ± 0.4 nM (ZM 241385), respectively, for the chosen A_1R-$A_{2A}R$ cell clone and the K_D value obtained for $A_{2A}R$ antagonist (ZM 241385) was 0.9 ± 0.3 nM for the chosen $A_{2A}R$ cell clone. Also by fitting the binding data to equation 4, the K_D value obtained for the A_1R antagonist (DPCPX) was 8.6 ± 0.9 nM for the A_1R cell clone and the K_D value obtained for the D_2R antagonist (YM 09151-2) was

0.23 ± 0.08 nM for the D_2R cell clone. These values were then used to determine the affinity constants showed in Tables 1 and 2. The agonists affinity in each selected clone was determined by competition experiments using the $A_{2A}R$ antagonist [^{3}H]ZM 241385 (2 nM) *versus* the agonist CGS 21680 (1 nM to 50 μM), the D_2R antagonist [^{3}H]YM 09151-2 (0.2 nM) *versus* the agonist quinpirole (0.1 nM to 30 μM), or the A_1R antagonist [^{3}H]DPCPX (2 nM), *versus* the agonist R-PIA (1 nM to 50 μM). As it is shown in Tables 1 and 2, the agonist affinity for $A_{2A}R$ in $A_{2A}R$, $A_{2A}R$-D_2R or in $A_{2A}R$-A_1R cells is in the same range as that reported for brain striatum or for cells expressing human $A_{2A}R$ (between 30 and 250 nM) (Higley and Sabatini, 2010). Nevertheless, the affinity of the $A_{2A}R$ for the selective agonist CGS 21680 was slightly but significantly lower when co-expressed with D_2R (see Table 2). A_1R (but not $A_{2A}R$ or D_2R) agonist binding showed negative cooperativity (negative D_{CB} values, see Methods), both in cells expressing A_1R and in cells co-expressing A_1R and $A_{2A}R$ (Tables 1 and 2)

Parameters	$A_{2A}R$ cells	A_1R cells	D_2R cells
K_{DB1}	90 ± 30 nM	13 ± 3 nM	120 ± 60 nM
K_{DB2}	360 ± 120 nM	1 ± 0.3 mM	480 ± 240 nM
D_{CB}	0	- 1.3	0
B_{50}	180 ± 60 nM	110 ± 30 nM	240 ± 120 nM

Table 1. Pharmacological parameters for agonist binding to A_1R, $A_{2A}R$ and D_2R in A_1R, $A_{2A}R$ and D_2R CHO cells.

Binding data from competition experiments were fitted assuming that receptors from homodimers, and cooperativity ($D_{CB} \neq 0$, fitting to equation 2; Methods) or non-cooperativity ($D_{CB} = 0$, fitting to equation 3; Methods) in competitor ligand binding were statistically tested (F test). K_{DB1} and K_{DB2} are, respectively, the equilibrium dissociation constants of the first and second binding of the ligand B, and B_{50} is the concentration providing half saturation for B. Data are mean ± SEM values of three experiments.

Parameters	$A_{2A}R$-D_2R cells		$A_{2A}R$-A_1R cells	
	$A_{2A}R$	D_2R	$A_{2A}R$	A_1R
K_{DB1}	200 ± 40 nM	1.2 ± 0.6 μM	70 ± 10 nM	0.7 ± 0.3 nM
K_{DB2}	0.8 ± 0.4 μM	4.8 ± 2.4 μM	280 ± 40 nM	1.1 ± 0.5 μM
D_{CB}	0	0	0	- 2.6
B_{50}	0.4 ± 0.008 μM	2.4 ± 1.2 μM	140 ± 20 nM	30 ± 10 nM

Table 2. Pharmacological parameters for agonist binding to A_1R-$A_{2A}R$ and $A_{2A}R$-D_2R CHO cells.

Binding data from competition experiments were fitted assuming that receptors (also when heteromerizing) from homomers, and cooperativity ($D_{CB} \neq 0$, fitting to equation 2; Methods) or non-cooperativity ($D_{CB} = 0$, fitting to equation 3; Methods) in competitor ligand binding was statistically tested (F test). K_{DB1} and K_{DB2} are, respectively, the equilibrium dissociation constants of the first and second binding of B (the A_1R, $A_{2A}R$, or D_2R agonists: R-PIA, CGS 21680 or quinpirole, respectively) to the dimer. D_{CB} is the "dimer cooperativity" index for the binding of the ligand B, and B_{50} is the concentration providing half saturation for B. Data are mean ± SEM values of three experiments.

*: $p<0.05$ compared to K_{DB1} values in A_1R-$A_{2A}R$ and $A_{2A}R$ cells (Table 1); one-way ANOVA, followed by Newman-Keuls test.

3.3. Screening of $A_{2A}R$ antagonists on cells expressing A_1R-$A_{2A}R$ or $A_{2A}R$-D_2R heteromers.

To test of selected $A_{2A}R$ antagonists display different selectivity for A_1R-$A_{2A}R$ or $A_{2A}R$-D_2R heteromers, competition experiments with these ligands were performed using CHO cells expressing $A_{2A}R$, A_1R-$A_{2A}R$ or $A_{2A}R$-D_2R. We found that none of the six $A_{2A}R$ antagonists first tested in the *in vivo* models were able to bind with moderate affinity to A_1R or to D_2R in CHO cells expressing A_1R or D_2R (data not shown), indicating that these compounds are specific ligands for $A_{2A}R$. Competition experiments of [^{3}H]ZM 241385 (2 nM) binding *versus* increasing concentrations of each $A_{2A}R$ antagonist (1 nM to 100 μM) were performed as indicated in Methods and binding data from competition experiments were fitted assuming that receptors are dimers and statistically (F test, see Methods) testing whether the competitor ($A_{2A}R$ antagonists) binding was cooperative (biphasic competition curves; fitting to equation 2) or non-cooperative (monophasic competition curves; fitting to equation 3). Since the screened compounds are $A_{2A}R$ antagonists, competition curves were expected to be monophasic, assuming that antagonist binding is not cooperative. In fact, in all cell clones, MSX 2, KW 6002, SCH 420814, ZM 241385 and SCH 58261 gave monophasic competition curves (fitting binding data to equation 2 was not better that fitting to equation 3; see Methods and Fig. 7 A-C as an example). Accordingly, the pharmacological characterization for these compounds gave $D_{CB} = 0$ and $K_{DB2} = 4K_{DB1}$ (see Table 3). For all compounds, co-transfection with A_1R did not significantly modify their affinity for $A_{2A}R$. On the other hand, co-transfection with D_2R significantly reduced the affinity of $A_{2A}R$ for MSX 2, SCH 420814, SCH 58261 and ZM 241385, from two to about nine times, and did not significantly modify the affinity of $A_{2A}R$ for KW 6002 (Table 3).

K_{D1} (nM)	$A_{2A}R$ cells	A_1R-$A_{2A}R$ cells	$A_{2A}R$-D_2R cells
ZM 241385	0.9 ± 0.3	1.8 ± 0.4	8 ± 3*
SCH 58261	3.3 ± 0.3	4.7 ± 0.6	23 ± 8*
MSX 2	3.2 ± 0.2	4.2 ± 0.3	7 ± 2*
KW 6002	100 ± 10	100 ± 20	160 ± 70
SCH 420814	0.5 ± 0.1	1.1 ± 0.1	2.7 ± 0.8*

Table 3. Pharmacological parameters for $A_{2A}R$ antagonist binding to $A_{2A}R$, A_1R-$A_{2A}R$ and $A_{2A}R$-D_2R CHO cells.

Competition experiments of [^{3}H]ZM 241385 (2 nM) binding *versus* increasing concentrations of $A_{2A}R$ antagonists were performed as indicated in Methods in membrane preparations from CHO cells expressing $A_{2A}R$ or A_1R and $A_{2A}R$ or $A_{2A}R$ and D_2R. Binding data were fitted assuming that receptors (also when heteromerizing) form homodimers, and cooperativity ($D_{CB} \neq 0$, fitting to equation 2; Methods) or non-cooperativity ($D_{CB} = 0$, fitting to equation 3; Methods) for competitor ligand binding was statistically tested (F test). Only K_{DB1} values (equilibrium dissociation constant of the first binding of B: ZM 241385, MSX 2, SCH 58261, SCH 420814 or KW 6002) are shown, since the analysis demonstrated non-cooperativity for the five $A_{2A}R$ antagonists. Data are means ± SEM values of three experiments.

*: $p<0.05$ compared to K_{DB1} values in $A_{2A}R$ cells; one-way ANOVA, followed by Newman-Keuls test.

For SCH 442416, a careful statistically-based analysis of the monophasic or biphasic nature of the competition curves led to an unexpected finding: in A_{2A}-D_2R cells, competitions curves of [^{3}H]ZM 241385 (2 nM) binding *versus* SCH 442416 in cells expressing $A_{2A}R$, A_1R-$A_{2A}R$ and $A_{2A}R$-D_2R. In $A_{2A}R$ and A_1R-$A_{2A}R$ cells the curves were monophasic. Accordingly, the pharmacological characterization gave a D_{CB} values of 0 and $K_{DB2} = 4K_{DB1}$. In contrast, as mentioned above, in cells expressing $A_{2A}R$-D_2R, competition curves were biphasic, and binding data were obtained (Table 4). Thus, in a $A_{2A}R$-D_2R cells, SCH 442416 binding showed a strong negative cooperativity and, consequently, with a marked loss of affinity (an increase of 600 times in K_{DB2}) respect to cells expressing $A_{2A}R$. This is reflected by the B_{50} value (concentration competing 50% of radioligand binding), which was more than 40 times higher in $A_{2A}R$-D_2R cells than A_1R-$A_{2A}R$ cells or $A_{2A}R$ cells.

Parameters	$A_{2A}R$ cells	A_1R-$A_{2A}R$ cells	$A_{2A}R$-D_2R cells
K_{DB1}	2.0 ± 0.3 nM	2.4 ± 0.4 nM	7 ± 4 nM
K_{DB2}	8 ± 2 nM	10 ± 2 nM	5 ± 2 μM**
D_{CB}	0	0	- 2.3
B_{50}	4.0 ± 0.6 nM	4.8 ± 0.8 nM	190 ± 80 nM**

Table 4. Pharmacological parameters for SCH 442416 binding to $A_{2A}R$, A_1R-$A_{2A}R$ and $A_{2A}R$-D_2R CHO cells. Competition experiments of [^{3}H]ZM 241385 (2 nM) binding *versus* increasing concentrations of SCH 442416 were performed as indicated in Methods in membrane preparations from CHO cells expressing $A_{2A}R$ or A_1R and $A_{2A}R$ or $A_{2A}R$ and D_2R. Results were fitted assuming that receptors (also when heteromerizing) form homodimers, an cooperativity ($D_{CB} \neq 0$, fitting to equation 2; Methods) or non-cooperativity ($D_{CB} = 0$, fitting to equation 3; Methods) of SCH 442416 binding was statistically tested (F test). K_{DB1} and K_{DB2} are, respectively, the equilibrium dissociation constants of the first and second binding of B (SCH 442416) to the dimer. D_{CB} is the "dimer cooperativity" index for the binding of the ligand B, and B_{50} is the concentration providing half saturation for B. Data are means ± SEM values of three experiments.

**: $p<0.01$, respectively compared to the K_{DB2} and B_{50} values in $A_{2A}R$ and A_1R-$A_{2A}R$ cells; Kruskal-Wallis, follored by Dunn's test.

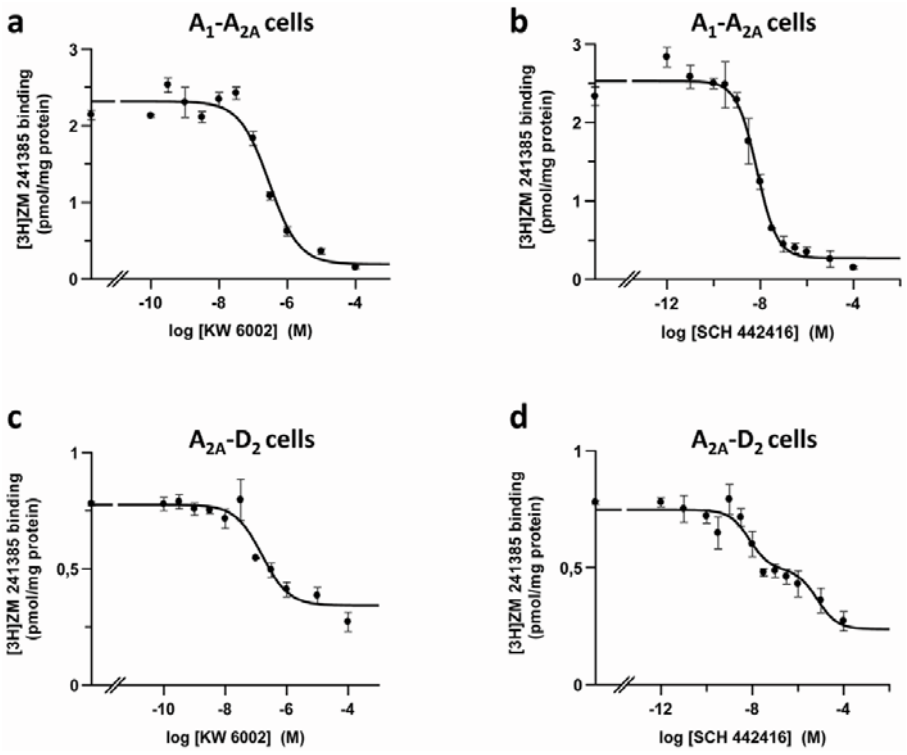

Figure 7. Binding of the $A_{2A}R$ antagonists KW 6002 and SCH 442416 to A_1R-$A_{2A}R$ and $A_{2A}R$-D_2R CHO cells. Competition experiments of [^{3}H]ZM 241385 (2 nM) *versus* increasing concentrations of KW 6002 (**a** and **c**) or SCH 442416 (**b** and **d**) were performed as indicated in Methods in membrane preparations from CHO cells expressing A_1R and $A_{2A}R$ (**a** and **b**) or $A_{2A}R$ and D_2R (**c** and **d**). Data are means ± SEM of a representative experiment performed with triplicates.

3.4. Pharmacological characterization of adenosine A_1R, $A_{2A}R$ and dopamine D_2R on striatum tissue from rats with Huntington's disease.

In order to contrast all the previous results observed in cellular and animal models, a pharmacological characterization in rat striatum tissue of all the involving receptors was performed. The rat brains were provided by Dr. S. Ferré's laboratory. Six different types of rat brain were sent; wild type rats, Huntington's disease rat models genetically heterozygotes and Huntington's disease rat models genetically homozygotes. From each type six months old and twelve months old rats were provided. Ten brains of each type were available. All the brains were dissected and the striatum was isolated and processed as detailed in Methods.

The first step was determining the pharmacological parameters of adenosine A_1R, $A_{2A}R$ and dopamine D_2R (Table 5). It was characterized both agonist and antagonist dissociation constants as well as the B_{max}. These first tests did not reveal big differences among the different samples. The only changes worth mentioning were observed in D_2R were the constant affinity of the agonist quinpirole slightly worsened (increased) in 12 months old homozygotes. When focusing on the constants of the agonist dopamine we firstly observed that the parameters were better fitted to a two center binding equation than one center. The high affinity dissociation constant decreased 2-fold in 6 months old heterozygotes and homozygotes when compared to wild types. However the low affinity dissociation constant increased 3-fold in the same brain samples. The antagonist YM 09151-2 dissociation constant seemed to have a slight tendency to increase.

			WT		HETEROZIGOTS		HOMOZIGOTS	
			6months	12months	6months	12months	6months	12months
A_1	R-PIA	K_d	3.6 ± 0.4 nM	4.7 ± 0.5 nM	3.7 ± 0.5 nM	4.6 ± 0.15 nM	5.2 ± 0.6 nM	5.4 ± 0.5 nM
		B_{max}	1.5 pmol	1.3 pmol	1.1 pmol	1.2 pmol	1.8 pmol	1.3 pmol
	DPCPX	K_d	2.9 ± 0.5 nM	2.1 ± 0.2 nM	1.2 ± 0.1 nM	2.3 ± 0.1 nM	1 ± 0.1 nM	2.3 ± 0.2 nM
		B_{max}	2.5 pmol	1.6 pmol	1.4 pmol	2.1 pmol	1 pmol	1.6 pmol
A_{2A}	CGS	K_d	22 ± 11 nM	N.A.	47 ± 14 nM	N.A.	6.6 ± 6 nM	N.A.
		B_{max}	1.2 pmol	N.A.	2.2 pmol	N.A.	0.8 pmol	N.A.
	ZM	K_d	1.3 ± 0.15 nM	3.1 ± 0.3 nM	2.5 ± 0.4 nM	3 ± 0.3 nM	2.1 ± 0.3 nM	4.8 ± 0.9 nM
		B_{max}	1.7 pmol	1.1 pmol	2.2 pmol	1 pmol	1.8 pmol	0.8 pmol
D_2	Quinpirole	K_d	N.A.	8.3 ± 1.2 μM	N.A.	8.4 ± 0.8 μM	N.A.	14 ± 2 μM
	Dopamina	K_{d1}	36.5 ± 7 nM	N.A.	13.3 ± 3.5 nM	N.A.	14.8 ± 3.9 nM	N.A.
		K_{d2}	36 ± 10 μM	N.A.	90 ± 32 μM	N.A.	98 ± 28 μM	N.A.
	YM	K_d	N.A.	1.3 ± 0.1 nM	N.A.	2.1 ± 0.2 nM	N.A.	2.5 ± 0.4 nM
		B_{max}	N.A.	0.8 pmol	N.A.	1 pmol	N.A.	0.7 pmol

Table 5. Pharmacological parameters of the typical agonists and antagonists of the adenosine A_1R, $A_{2A}R$ and dopamine D_2R. R-PIA, CGS, Quinpirole and Dopamine are agonists and DPCPX, ZM and YM are antagonists. N.A.: not analyzed.

When comparing the allosteric interaction observed in the heteromer A_1R-$A_{2A}R$ we observed that this interaction was increased 8-fold in heterozygotes and homozygotes compared to wild type samples in 6 months old rats and about 6-fold in 12 months old rats (Table 6).

	WT	
	6 months	12 months
EC_{50}	67 ± 32 nM	88 ± 25 nM
K_D	3 ± 1 μM	3.8 ± 1.5 μM

	Heterozygotes	
	6 months	12 months
EC_{50}	9 ± 4 nM	23 ± 12 nM
K_D	0.9 ± 0.2 μM	1.3 ± 0.3 μM

	Homozygotes	
	6 months	12 months
EC_{50}	7 ± 3 nM	11.6 ± 0.6 nM
K_D	0.9 ± 0.1 μM	1.4 ± 0.4 μM

Table 6. Allosteric interactions between A_1R and $A_{2A}R$ in the A_1R-$A_{2A}R$ heteromer. EC_{50} is the effect due to the presence of CGS. K_D is the dissociation constant of CGS when it is in competition with [^{3}H] R-PIA.

Interestingly, when comparing the cross talk of $A_{2A}R$-D_2R heteromer in the different brain samples we observed a clear negative cross talk in wild type 6 months old rats, a positive cross talk in heterozygotes and no cross talk in homozygotes. In 12 months old rats the tendency is the same as well. These differences could be due to the different severity of the disease in heterozygotes and homozygotes. The constitutive way of acting of the $A_{2A}R$-D_2R heteromer is by a negative cross talk of the D_2R over $A_{2A}R$. In heterozygotes rats suffering from not so severe Huntington's disease, the heteromer is somehow affected shifting its cross talk from negative to positive. In the other hand, in homozygotes rats suffering form severe Huntington's disease, the heteromer could be disrupted, thus, no cross talk can be observed (Table 7).

	WT			
	6 months		12 months	
Quinpirole	-	+	-	+
K_{D1}	6.6 ± 3 nM	25 ± 7 nM	0.6 ± 0.2 µM	1 ± 0.2 µM
K_{D2}	0.3 ± 0.1 µM	1.2 ± 0.7 µM	∅	∅

	Heterozygotes			
	6 months		12 months	
Quinpirole	-	+	-	+
K_{D1}	11.8 ± 6 nM	1.8 ± 0.9 nM	3 ± 1 µM	1.6 ± 0.6 µM
K_{D2}	240 ± 90 nM	121 ± 25 nM	∅	∅

	Homozygotes			
	6 months		12 months	
Quinpirole	-	+	-	+
K_{D1}	9.8 ± 3 nM	7.8 ± 2.5 nM	0.25 ± 0.1 µM	0.73 ± 0.45 µM
K_{D2}	348 ± 120 nM	360 ± 150 nM	∅	∅

Table 7. Cross talk $A_{2A}R$-D_2R. Competition experiment using the $A_{2A}R$ antagonist [^{3}H] ZM 241385 and the $A_{2A}R$ agonist CGS 21680 in the presence or absence of the dopamine D_2R agonist quinpirole. The changes observed with or without quinpirole correspond to a positive (in the case of a decrease in the K_{D1}) or negative (when the K_{D1} increases) cross talk between receptors. ∅: Better fit with a one-center equation.

3.5. Discussion.

An important finding of this study is that several $A_{2A}R$ antagonists previously thought as being pharmacologically similar present different striatal pre- and postsynaptic profiles. Six compounds already known as selective $A_{2A}R$ antagonists were first screened for their ability to block striatal pre- and postsynaptic $A_{2A}Rs$ with *in vivo* models. Locomotor activation was used to evaluate postsynaptic activity while PCC reduction was used to evaluate presynaptic activity. Two compounds, SCH 442416 and KW 6002, showed preferential pre- and postsynaptic profiles, respectively, and four compounds, MSX 3, SCH 420814, SCH 58261 and ZM 241385, showed mixed pre-postsynaptic profiles. Combining *in vivo* microdialysis with cortical electrical stimulation was used as an additional *in vivo* evaluation of presynaptic activity of SCH 442416 and KW 6002. In agreement with its preferential presynaptic profile, SCH 442416 significantly counteracted striatal glutamate release induced by cortical stimulation at a dose (1 mg/kg i.p.) that strongly reduced PCC but did no induce locomotor activation. On the other hand, according to its preferential postsynaptic profile, KW 6002 did not modify striatal glutamate release induced by cortical stimulation at a dose (1 mg/kg i.p.) that produced a pronounced locomotor activation but did not counteract PCC. In a previous study, we reported that intrastriatal perfusion of MSX 3 almost completely counteracted striatal glutamate release induced by cortical electrical stimulation (Quiroz et al., 2009), which agrees with its very effective reduction of PCC shown in this study.

Another important finding of this study is that at least part of these pharmacological differences between $A_{2A}R$ antagonists can be explained by the ability of pre- and postsynaptic $A_{2A}R$ to form different receptor heteromers, with A_1R and D_2R, respectively (Azdad et al., 2009; Ciruela et al., 2006; Ferré et al., 2007, 2008; Quiroz et al., 2009). Radioligand-binding experiments were performed in CHO cells stably expressing $A_{2A}R$,

$A_{2A}R$-D_2R heteromers or A_1R-$A_{2A}R$ heteromers to determine possible differences in the affinity of these compounds for different $A_{2A}R$ heteromers. Co-expression with A_1R did not significantly modify the affinity of $A_{2A}R$ for the different ligands, but co-expression with D_2R decreased the affinity of all compounds, with the exception of KW 6002. The structural changes in the $A_{2A}R$ induced by heteromerization with the D_2R could be detected not only by antagonists but also by agonists. Indeed, the affinity of the selective $A_{2A}R$ agonist CGS 21680 was reduced in cells co-transfected with D_2R. When trying to explain the differential action of SCH 442416 observed *in vivo*, it is interesting to note that SCH 442416 showed a much higher affinity for the $A_{2A}R$ in a presynaptic-like than in a postsynaptic-like context. The binding of SCH 442416 to the $A_{2A}R$-D_2R heteromer displayed a strong negative cooperativity, phenomenon that was not observed for the binding of SCH 442416 to the A_1R-$A_{2A}R$ heteromer. This negative cooperativity explains the pronounced decrease in affinity of $A_{2A}R$ in cells expressing $A_{2A}R$-D_2R heteromers (B_{50} values 40 times higher in cells expressing $A_{2A}R$-D_2R than $A_{2A}R$-D_2R heteromers).

The loss of affinity of $A_{2A}R$ upon co-expression of D_2R was much less pronounced for ZM 241385, SCH 58261, MSX 2 or SCH 420814, for which the affinity was reduced from two to about nine fold. Taking into account that these $A_{2A}R$ antagonists behave similarly than the $A_{2A}R$ agonist CGS 21680 in terms of binding to A_1R-$A_{2A}R$ and $A_{2A}R$-D_2R heteromers, it is expected that these four compounds compete equally for the binding of the endogenous agonist at pre- and at postsynaptic sites. This would fit with the *in vivo* data, which shows that these compounds have a non-preferred pre-postsynaptic profile. Yet, KW 6002 was the only antagonist whose affinity was not significantly different in cells expressing $A_{2A}R$, A_1R-$A_{2A}R$ heteromers or $A_{2A}R$-D_2R heteromers. Thus, KW 6002 showed the best relative affinity for $A_{2A}R$-D_2R heteromers of all compounds, which can at least partially explain its preferential postsynaptic profile.

The present results support the notion that receptor heteromers may be used as selective targets for drug development. The main reasons are the specific neuronal localization of receptor heteromers (even more specific that for receptor subtypes), and a differential ligand affinity of a receptor depending on its partner (or partners) in the receptor heteromer. In the striatum, $A_{2A}R$ provides a particularly interesting target, eventually useful for a variety of neuropsychiatric disorders. $A_{2A}R$-D_2R and A_1R-$A_{2A}R$ heteromers are segregated in different striatal neuronal elements. While $A_{2A}R$-D_2R heteromers are located postsynaptically in the dendritic spines of the indirect MSNs (Azdad et al., 2009; Ferré et al., 2007, 2008; Quiroz et al., 2009), A_1R-$A_{2A}R$ heteromers are located presynaptically in glutamatergic terminals contacting the MSNs of the direct pathway (Ciruela et al., 2006; Ferré et al., 2007; Quiroz et al., 2009). Blocking postsynaptic $A_{2A}R$ in the indirect MSN should potentiate D_2R-mediated motor activation, which is a strategy already used in the development of anti-parkinsonian drugs (Jenner, 2003; Schwarzschild et al., 2006; Stacy et al., 2008). However, blocking $A_{2A}R$ in glutamatergic terminals to the direct MSN could potentially be useful in dyskinetic disorders such as Huntington's disease and maybe in obsessive-compulsive disorders and drug addiction (Quiroz et al., 2009). This results give a mechanistic explanation to the already reported anti-parkinsonian activity of KW 6002 (Jenner, 2003; Mizuno et al., 2010; Pourcher et al., 2012; Stacy et al., 2008) and suggest that SCH 442416 could be useful in dyskinetic disorders, obsessive-compulsive disorders and in drug addiction. Medicinal chemistry and computerized modeling should help understanding the molecular properties that determine the particular pharmacological profile of SCH 442416 and KW 6002, which may be used as lead compounds to obtain more effective anti-dyskinetic and anti-parkinsonian compounds, respectively. It will also be of importance to take into account potential changes in the expression of pre- and postsynaptic $A_{2A}R$s and in their respective heteromers that can occur in those mentioned neuropsychiatric disorders. For instance, dopamine denervation seems to differentially modify the expression of striatal

$A_{2A}R$-A_1R and D_2R (Kaasinen et al., 2000; Pinna et al., 2002; Stacy et al., 2008; Varani et al., 2010). This could be addressed by applying the *in vivo* methodology here described to animal models.

Besides these conclusions, we found evidence that the heteromer $A_{2A}R$-D_2R is affected in rat models of Huntington's disease. There is a direct correlation between the severity of the disease and the affection in this heteromer, as the heterozygotes models have a shifted cross talk between the $A_{2A}R$ and the D_2R meanwhile the homozygotes apparently did not express the heteromer itself.

This results point out that those neurons expressing this heteromer might be more vulnerable to the disease.

Supplemental results.

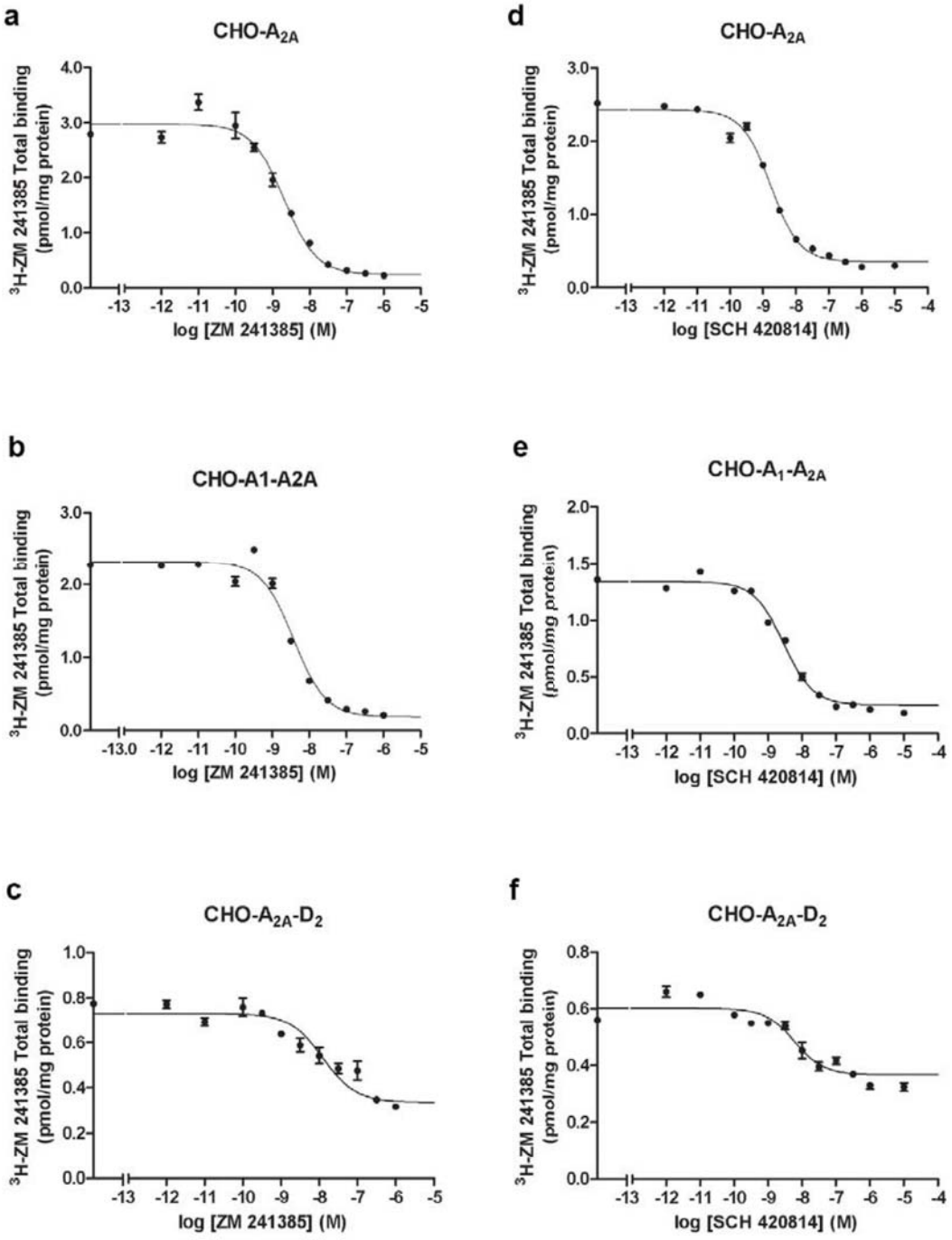

Figure S1. Competition curves corresponding to the values of displacement of [^{3}H]ZM 241385 with ZM 241385 and SCH 420814 stated in Table 3.

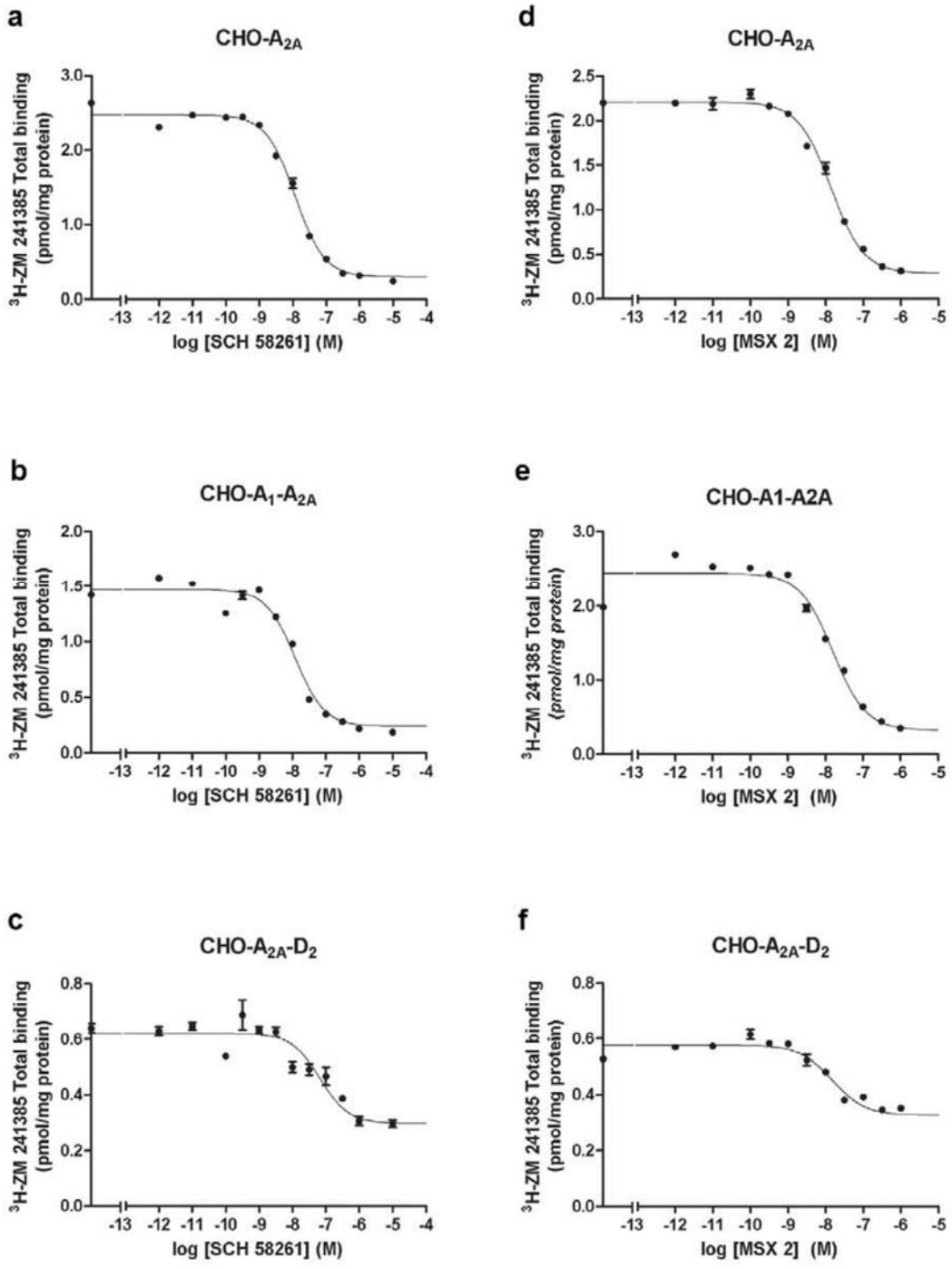

Figure S2. Competition curves corresponding to the values of displacement of [^{3}H]ZM 241385 with SCH 58261 and MSX 2 stated in Table 3.

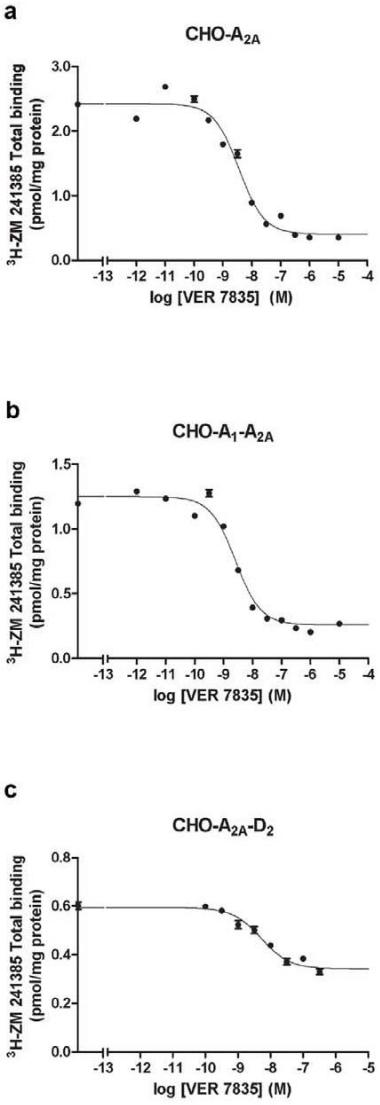

Figure 3. Competition curves corresponding to the values of displacement of [^{3}H]ZM 241385 with VER 7835 stated in Supplementary Table 1.

K_{D1} (nM)	$A_{2A}R$ cells	A_1R-$A_{2A}R$ cells	$A_{2A}R$-D_2R cells
VER 7835	1.1 ± 0.15 nM	1.5 ± 0.22 nM	2.7 ± 0.10 nM

Supplementary Table 1. Binding of $A_{2A}R$ antagonist VER 7835 to $A_{2A}R$, A_1R-$A_{2A}R$ and $A_{2A}R$-D_2R CHO cells. Competition experiments oh [^{3}H]ZM 241385 (2 nM) binding *versus* increasing concentrations of $A_{2A}R$ antagonists were performed as indicated in Methods in membrane preparations from CHO cells expressing $A_{2A}R$ or A_1R and $A_{2A}R$ or $A_{2A}R$ and D_2R. Binding data were fitted assuming that receptors (also when heteromerizing) form homodimers, and cooperativity ($D_{CB} \neq 0$, fitting to equation 2; Methods) or non-cooperativity ($D_{CB} = 0$, fitting to equation 3; Methods) for competitor ligand binding was statistically tested (F test). Only K_{DB1} values (equilibrium dissociation constant of the first binding of B: VER 7835) are shown, since the analysis demonstrated non-cooperativity for the five $A_{2A}R$ antagonists. Data are mean ± SEM values of three experiments. One-way ANOVA, followed by Newman-Keuls test.

4. Pharmacological and functional characterization of $A_{2A}R$-CB_1R heteromer.

Adenosine $A_{2A}R$ are the most abundant subtype of adenosine receptors present in the striatum (Albin et al., 1989; Svenningsson et al., 1999) where they influence dopaminergic and glutamatergic neurotransmission, regulate motor activity and modulate excitotoxic mechanisms (Cunha, 2005; Fredholm et al., 2005; Popoli et al., 2004, 2007a, 2007b; Schiffmann et al., 2007; Svenningsson et al., 1999). $A_{2A}R$ can be found both post- and presynaptically. Postsynaptically, $A_{2A}R$ are found in the striatal efferent GABAergic neurons, also called the medium spiny neurons (MSN). These neurons constitute more that 95% of the striatal neuron population (Gerfen, 1992) and are classified in two main subtypes, the encephalin MSNs projecting to the globus pallidus (the indirect pathway), expressing adenosine $A_{2A}R$ and the dynorphin MSNs (the direct pathway) expressing adenosine receptors of the A_1R but no $A_{2A}R$ subtype (Agnati et al., 2003; Ferré et al., 1997). Presynaptically, $A_{2A}R$ are found on the corticostriatal glutamatergic projections (Hettinger et al., 2001). There is recent evidence that presynaptic $A_{2A}R$ are preferentially localized in cortical glutamatergic terminal that contact striatal neurons of the direct pathway rather then that of the indirect pathway (Quiroz et al., 2009). At the postsynaptic level in the indirect pathway, the activation of $A_{2A}R$ leads to counteraction of D_2R-mediated suppression of NMDA-induced depolarization increasing the action of the indirect pathway leading to motor depression (Azdad et al., 2009). This phenomenon was demonstrated to occur through $A_{2A}R$-D_2R heteromer formation where via the heteromer $A_{2A}R$ agonists decreased the affinity of D_2R for dopamine (Azdad et al., 2009). At the presynaptic level in the direct pathway, the activation of $A_{2A}R$ increases glutamate release enhancing the glutamatergic

neurotransmission and inducing motor activation (Ciruela et al., 2006). This phenomenon was demonstrated to occur through A_1R-$A_{2A}R$ heteromers (Ciruela et al., 2006).

Cannabinoid CB_1R are the most abundant G protein in the brain (Katona et al., 2006) and are densely distributed in the striatum (Glass and Felder, 1997; Herkenham et al., 1990). In the striatum CB_1R are localized in both types of MSNs, in enkephalinergic and dynorphinergic neurons of indirect and direct pathways respectively (Fusco et al., 2004; Herkenham et al., 1990). At this postsynaptic localization, CB_1R negatively modulate locomotion (Ferré et al., 2010; Monory et al., 2007). Furthermore, striatal CB_1R are localized in parvalbumin-expressing GABAergic interneurons (Fusco et al., 2004; Hohmann and Herkenham, 2000) and presynaptically are found in glutamatergic and GABAergic terminals (Köfalvi et al., 2005; Mátyás et al., 2006; Pickel et al., 2004, 2006; Rodriguez et al., 2001). The major physiological function of presynaptic CB_1R is to regulate the release of various neurotransmitters (Freund et al., 2003; Katona et al., 2006; Marsicano et al., 2003). High expression of $A_{2A}R$ and CB_1R in the striatum suggests that direct or indirect interactions between $A_{2A}R$ and CB_1R are involved in the modulation of motor activity and goal-directed behaviors. It is known that $A_{2A}R$ regulate CB_1R action on both pre- and postsynaptic levels (Andersson et al., 2005; Martire et al., 2011; Tebano et al., 2009). A recent work showed that presynaptic $A_{2A}R$ inhibit the CB_1R-mediated synaptic effects and that this occurs probably via the cAMP-PKA pathway (Martire et al., 2011), and may be or not dependent on a physical interaction between both receptors, as it could also occur at the level of signaling. It seems that interactions between $A_{2A}R$ and CB_1R localized in glutamatergic terminals that contact dynorphinergic MSNs are primarily involved in the hypolocomotor and rewarding effects of THC. However, it has been also suggested that postsynaptic mechanisms are involved in striatal $A_{2A}R$-dependent CB_1R function (Andersson et al., 2005; Tebano et al., 2009). In fact, we have previously demonstrated that $A_{2A}R$ and CB_1R form heteromers in HEK cells and in human neuroblastoma (Carriba et al., 2008) and

CB_1R co-localize and co-immunoprecipitate with $A_{2A}R$ in the rat striatum (Carriba et al., 2007). In a human neuroblastoma cell line, CB_1R signaling was found to be completely dependent on $A_{2A}R$ activation. Accordingly, blockade of $A_{2A}R$ counteracted the motor depressant effects produced by the intrastriatal administration of a cannabinoid CB_1R agonist (Carriba et al., 2007). Although the effect of $A_{2A}R$ activation on CB_1R function was studied, the effect of CB_1R on $A_{2A}R$ function is not known. As heteromerization with CB_1R can exert a fine tuned modulation of the $A_{2A}R$ pre- and postsynaptic behavior, in this work we wanted to characterize the $A_{2A}R$-CB_1R heteromers in order to know whether CB_1R modulated the pharmacological and functional characteristics of the $A_{2A}R$.

4.1. Pharmacological characterization of cells expressing $A_{2A}R$ or $A_{2A}R$-CB_1R.

Using energy transfer experiments and co-immunoprecipitation, it was previously described that $A_{2A}R$ and CB_1R form heteromers when expressed in cells or in the brain striatum (Carriba et al., 2007, 2008). To compare the functional characteristics of $A_{2A}R$ when expressed alone or forming heteromers with CB_1R, we first generated CHO cell clones expressing $A_{2A}R$ (CHO $A_{2A}R$) or $A_{2A}R$-CB_1R (CHO $A_{2A}R$-CB_1R) as indicated in Methods. The pharmacological characterization of $A_{2A}R$ in these cells was performed by radioligand binding experiments. Competition experiments of the $A_{2A}R$ antagonist [^{3}H]ZM 241385 (1.5 nM) *versus* ZM 241385 (0.01 nM to 11 mM) or the $A_{2A}R$ agonist [^{3}H]CGS 21680 (19 nM) *versus* CGS 21680 (0.1 nM 100 μM) using CHO $A_{2A}R$ cell membranes gave the competition curves shown in Figure 1. Binding data were fitted assuming that receptors are dimers and statistically (F test, see Methods) testes whether the competitor ($A_{2A}R$ antagonist or agonist binding was cooperative (biphasic competition curves; fitting to equation 2) or non-cooperative (monophasic competition curves; fitting to equation 5). Fitting data from Figure 1 A or B to equation 2 was not better that fitting data to equation 5 according to the

monophasic nature of both competition curves and indicating that agonist and antagonist binding to $A_{2A}R$ in non-cooperative.

Ligand	CHO $A_{2A}R$	CHO $A_{2A}R$-CB_1R
CGS 21680	90 ± 20 nM	60 ± 20 nM 100 ± 40 nM (treated with CP 55,940)
ZM 241385	2.8 ± 0.6 nM	4 ± 1 nM
CP 55,940		2 ± 1 nM 2.3 ± 0.7 nM (treated with CGS 21680)

Table 1. Equilibrium dissociation constant (K_{DA1}) of ligand binding to CHO $A_{2A}R$ or CHO $A_{2A}R$-CB_1R cell membranes. Data are means ± SEM (n = 3-5).

The equilibrium dissociation constant (K_{DA1}) values for the antagonist ZM 241385 and the agonist CGS 21680 appears in Table 1. The $A_{2A}R$ ligand binding parameters were also determined as described above using CHO $A_{2A}R$-CB_1R cell membranes. Competition curves of [^{3}H]ZM 241385 (1.6 nM) *versus* ZM 241385 (0.01 nM to 11 mM) or [^{3}H]CGS 21680 (19 nM) *versus* CGS 21680 (0.1 nM to 100 μM) are shown in Figure 2. Using CHO $A_{2A}R$-CB_1R cell membranes competition curves were also monophasic and K_{DA1} values (Table 1) were obtained by fitting data to non-cooperative binding equation 5. The agonist and antagonist dissociation constants were very similar in both cell lines and are comparable with the data obtained from analogous experiments performed using native tissues (Cristalli et al., 2007).

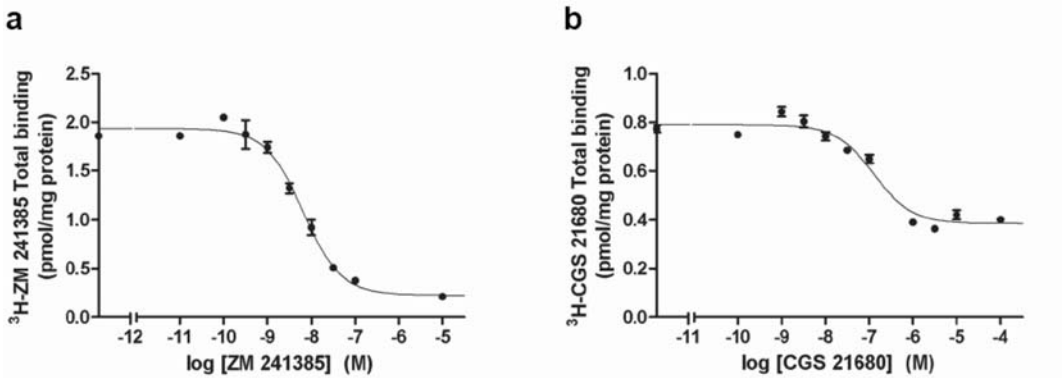

Figure 1. A_{2A}R agonist and antagonist binding to CHO A_{2A}R cell membranes. Competition experiments were performed in membranes preparations (0.2 mg protein/ml) from CHO A_{2A}R cells using 1.5 nM of the A_{2A}R antagonist [^{3}H]ZM 241385 and increasing concentrations (0.01 nM to 10 μM) of non-radiolabeled ZM 241385 (**a**) or 19 nM of the A_{2A}R agonist [^{3}H]CGS 21680 and increasing concentrations (0.1 nM to 100 μM) of non-radiolabeled CGS 21680 (**b**) as described in Methods. Data are means ± SEM of a representative experiment performed with triplicates.

The pharmacological characterization of CB_1R was performed by competition experiments using CHO A_{2A}R-CB_1 R cell membranes. The competition curve of 0.7 nM [^{3}H]CP 55,940 *versus* CP 55,940 (0.001 nM to 10 μM) appears in Figure 2C. Data fitting to equation 2 (cooperative binding) was not better than fitting data to equation 5 (non-cooperative binding) according to the monophasic nature of the curve and indicating that agonist binding to CB_1R is non-cooperative. The equilibrium dissociation constant (K_{DA1}) value for the CP 55,940 binding obtained by fitting data to equation 5 appears in Table 1. The dissociation constant is comparable to the data obtained form native tissues (Pertwee, 1997).

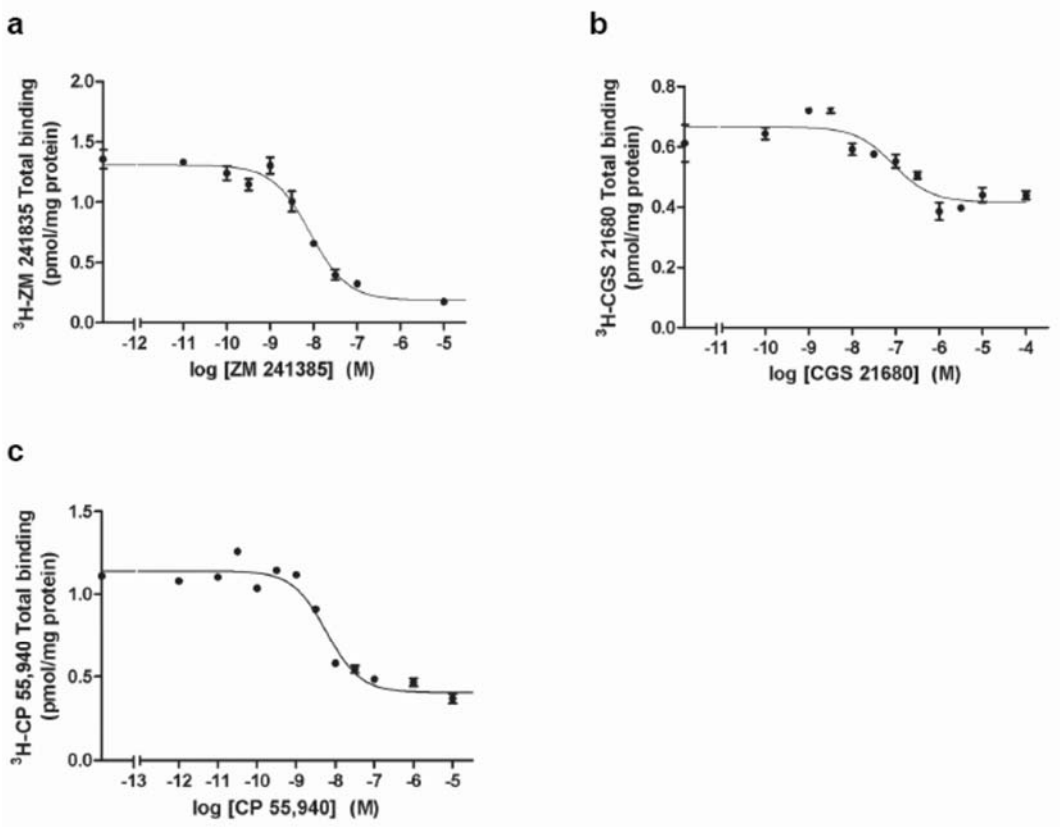

Figure 2. $A_{2A}R$ and CB_1R ligand binding to CHO $A_{2A}R$-CB_1R cell membranes. Competition experiments were performed in membrane preparations (0.2 mg protein/ml) from CHO $A_{2A}R$-CB_1R cells using 1.6 nM of $A_{2A}R$ antagonist [^{3}H]ZM 241385 and increasing concentrations (0.01 nM to 10 μM) of non-radiolabeled ZM 241385 (**a**), 19 nM of $A_{2A}R$ agonist [^{3}H]CGS 21680 and increasing concentrations (0.1 nM to 100 μM) of non-radiolabeled CGS 21680 (**b**) or 0.7 nM of CB_1R agonist [^{3}H]CP 55,940 and increasing concentrations (0.001 nM to 10 μM) of non-radiolabeled CP 55,940 (**c**), as described in Methods. Data are means ± SEM of a representative experiment performed with triplicates.

4.2. Functional characteristics of $A_{2A}R$-CB_1R heteromers.

One of the reported specific characteristics of $A_{2A}R$-CB_1R heteromers is that CB_1R signaling via cAMP pathway is dependent on $A_{2A}R$ activation (Carriba et al., 2007). We used this characteristic as a fingerprint to check the $A_{2A}R$-CB_1R heteromerization in CHO $A_{2A}R$-CB_1R cells and to further characterize the heteromer signaling. Since cAMP is a signal pathway under G protein activation, we looked for the heteromer fingerprint measuring the cross-talk between $A_{2A}R$ and CB_1R on G protein activation by the CellKey label free assay (see Methods) induced a G_s profile (decreases in impedance) that was completely blocked

when cells were treated with cholera toxin (ChTx) but not significantly modified upon pertussis toxin (PTx) treatment (Figure 3A) according to $A_{2A}R$ coupling to a G_s protein (Fredholm et al., 2001; Kull et al., 1999, 2000). Surprisingly, in CHO $A_{2A}R$-CB_1R cells the $A_{2A}R$ agonist CGS 21680 (10 nM to 1 μM) produced a moderate increase in impedance corresponding to a G_i profile only at high CGS 21680 concentrations, but did not produce decreases in impedance. According to a G_i profile, the impedance increase was reverted by PTx treatment (Figure 3B). These results indicate that $A_{2A}Rs$ are poorly coupled to G_i protein in these cells. As expected for a receptor coupled to a G_i protein, like CB_1R, activation of CHO $A_{2A}R$-CB_1R cells with the CB_1R agonist CP 55,940 (10 nM to 1 μM) showed increases in impedance corresponding to a G_i profile that were completely blocked when cells were treated with PTx (Figure 3B). Interestingly, in CHO $A_{2A}R$-CB_1R cells co-activated with a suboptimal concentration of CGS 21680 (100 nM) and a suboptimal concentration of CP 55,940 (100 nM), a synergistic increase in impedance was observed and was blocked by PTx. On one hand, the synergistic cross-talk between both receptors indicates that $A_{2A}R$ and CB_1R form heteromers in CHO $A_{2A}R$-CB_1R cells and on the other hand, the G protein profile and moreover its blockade by PTx indicates that both receptors are coupled to G_i protein in the heteromer.

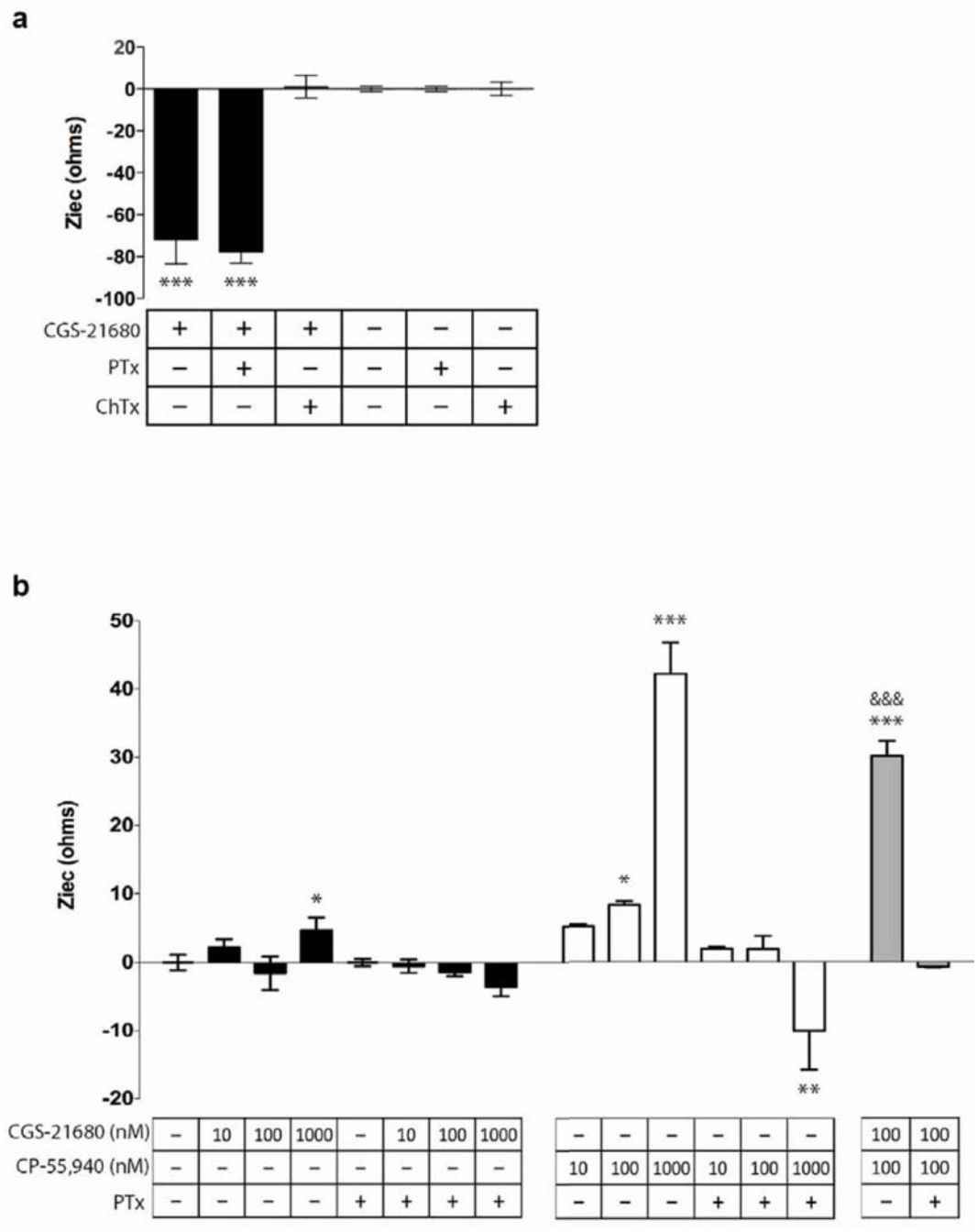

Figure 3. G_i-dependent signaling of $A_{2A}R$-CB_1R heteromers. CellKey label-free assays were performed in CHO $A_{2A}R$ cells (**a**) or in CHO $A_{2A}R$-CB_1R cells (**b**) as indicated in Methods. Cells were treated with medium (Buffer), PTx (10 ng/ml) or ChTx (100 ng/ml) and were stimulated or not with 10 nM (**a**) or increasing concentrations (**b**) of $A_{2A}R$ agonist CGS 21680, increasing concentrations of CB_1R agonist CP 55,940 or both (**b**). Results are mean ± SEM from 3 to 4 independent experiments. Statistical significance was calculated by one way ANOVA followed by Dunnett multiple comparison test; $^{*}p<0.05$, $^{**}p<0.01$, $^{***}p<0.005$ compared with the respective control (buffer or buffer plus toxin), $^{\&\&\&}p<0.005$ compared with cells treated only with one agonist.

Apart from G protein-mediated signaling, many GPCRs are able to signal in a G protein-independent way (Beaulieu et al., 2005; DeWire et al., 2007; Shenoy and Lefkowitz, 2003; Shenoy et al., 2006; Valjent et al., 2000). ERK1/2 phosphorylation is one of the MAPK pathways that has been described to be activated in a G protein-independent and arrestin-dependent mechanism (DeWire et al., 2007). In this context, we sought to study if heteromer formation might also influence $A_{2A}R$- or CB_1R-mediated ERK1/2 signaling. CHO $A_{2A}R$ or CHO $A_{2A}R$-CB_1R cells were activated for 5 minutes with 200 nM of $A_{2A}R$ agonist CGS 21680, 100 nM of CB_1R agonist CP 55,940 or both and ERK1/2 phosphorylation was determined as indicated in Methods. As it can be seen in Figure 4 and as expected, CP 55,940 only induced ERK1/2 phosphorylation in CHO $A_{2A}R$-CB_1R cells. Activation with CGS 21680 induced ERK1/2 phosphorylation in CHO $A_{2A}R$ cells and only a moderate effect in CHO $A_{2A}R$-CB_1R cells. Interestingly, when CHO $A_{2A}R$-CB_1R cells were co-activated with both agonists, ERK1/2 phosphorylation was not significantly different from the signaling induced by CP 55,940 alone, indicating that CB_1R is controlling ERK1/2 signaling under the heteromer.

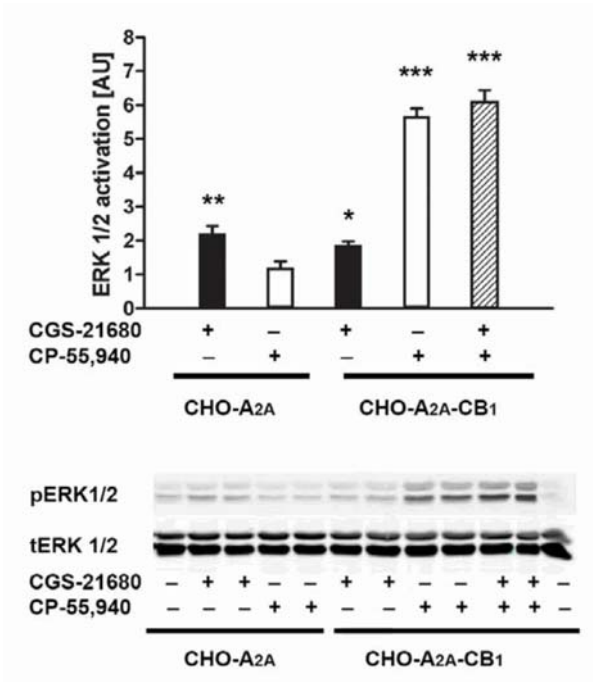

Figure 4. $A_{2A}R$-CB_1R heteromer-mediated $ERK_{1/2}$ phosphorylation. CHO $A_{2A}R$ or CHO $A_{2A}R$-CB_1R cells were stimulated with the $A_{2A}R$ agonist CGS 21680 (200 nM, black columns) or the CB_1R agonist CP 55,940 (100 nM, white columns) alone or in combination (dashed column) and ERK1/2 phosphorylation was determined as indicated in Methods. Values are represented in-fold respect to basal levels in absence of agonist and are means ± SEM of three independent experiments. On the bottom a representative Western blot is shown for samples in duplicates. Statistical significance was calculated by one way ANOVA followed by Dunnett multiple comparison test; *p<0.05, **p<0.01, ***p<0.005 compared with the respective basal.

4.3. Pharmacological characteristics of $A_{2A}R$-CB_1R heteromers.

A receptor heteromer is defined as a macromolecular complex composed by at least two receptor units with biochemical properties that are demonstrably different from those of its individual components (Ferré et al., 2009). Often times a property of a heteromer can be seen in specific ligand binding characteristics or in functional properties , as described above, (Ferré et al., 2007, 2009). For a receptor heteromer, the ligand binding to one protomer can induce changes in the ligand binding to the other protomer through an allosteric phenomenon driven by a molecular interaction between protomers in the heteromer (Ferré et al., 2009). To this end, we investigated the effect of agonist binding to CB_1R on the agonist affinity for $A_{2A}R$ and *vice versa* (the effect of agonist binding to $A_{2A}R$ on agonist affinity for CB_1R) in CHO $A_{2A}R$-CB_1R cell membranes. Competition experiments of the $A_{2A}R$ agonist [^{3}H]CGS 21680 (19 nM) *versus* CGS 21680 (0.1 nM to 100 μM) were performed in the presence of the CB_1R agonist CP 55,940 (300 nM) and competition experiments of the CB_1R agonist [^{3}H]CP 55,940 (0.7 nM) *versus* CP 55,940 (0.001 nM to 10 μM) were performed in the presence of CGS 21680 (100 nM). In both cases, competition curves (Figure 5) were monophasic and K_{DA1} values (Table 1) were obtained by fitting data to non-cooperative binding equation 5. Since no significant changes were observed in K_{DA1} values in the presence or in the absence of the agonist for the partner receptor we can conclude that there is not an allosteric effect on ligand binding for $A_{2A}R$-CB_1R heteromers.

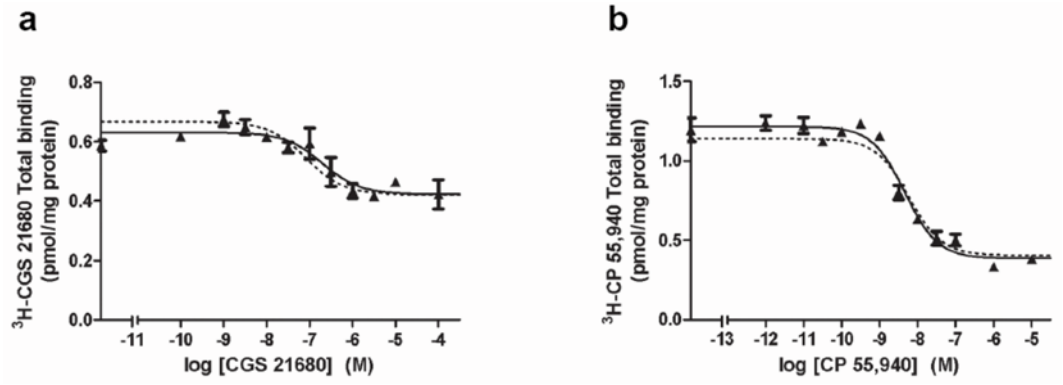

Figure 5. Lack of allosteric interaction between $A_{2A}R$ and CB_1R in $A_{2A}R$-CB_1R heteromers. Competition experiments were performed in membranes preparations (0.2 mg protein/ml) from CHO $A_{2A}R$-CB_1R cells using 19 nM of $A_{2A}R$ agonist [^{3}H]CGS 21680 and increasing concentrations (0.1 nM to 100μM) of non-radiolabeled CGS 21680 in the presence (triangles, solid line) or in the absence (dotted line) of CB_1R agonist CP 55,940 (300 nM) (**a**) or using 0.7 nM [^{3}H]CP 55,940 and increasing concentrations (0.001 nM to 10 μM) of non-radiolabeled CP 55,940 in the presence (triangles, solid line) or in the absence (dotted line) of 100 nM CGS 21680 (**b**), as described in Methods. Data are means ± SEM of a representative experiment performed with triplicates.

4.4. Discussion.

G protein-coupled receptors cannot only be considered as single functional units, but as forming part of multi-molecular aggregates localized in the plane of the plasma membranes (Bouvier, 2001; Ferré et al., 2009; Marshall, 2001; Pin et al., 2007). In fact, it seems that most members of this family can exist as homomers or heteromers (Albizu et al., 2010; Birdsall, 2010; Fuxe et al., 2010). A receptor heteromer is a macromolecular complex composed of at least two functional receptor units with biochemical properties that are demonstrably different from those of its individual receptors (Ferré et al., 2009). We reported that cannabinoid CB_1 and adenosine A_{2A}receptors form heteromers in co-transfected cells and rat striatum where they co-localize in fibrilar structures (Carriba et al., 2007). Although it was known that activation of $A_{2A}R$ was necessary for CB_1R signaling in a human neuroblastoma cell line where the heteromers were expressed (Carriba et al., 2007), the pharmacological and functional characteristics of these heteromers are far from being completely studied. Here we report several major conclusions on the biochemical characteristics of $A_{2A}R$-CB_1R heteromers. First, by measuring G protein activation by the CellKey label-free assay, we demonstrated that $A_{2A}R$ and CB_1R are coupled to G_i protein in the heteromer. Second, we observed a synergistic cross-talk in G protein activation when both receptors are co-activated it is mainly the CB_1R controlling the ERK1/2 signaling under the heteromer. Third, we demonstrated that there is not an allosteric effect on ligand binding for $A_{2A}R$-CB_1R heteromers.

A receptor unit in the heteromer can display several biochemical properties that can be dependent on the presence of the other unit or on co-stimulation of the two receptors in the heteromer. Changes in G protein coupling only by the presence of the partner receptor are a common characteristic of neurotransmitter receptor heteromers. In opioid receptors δOR-μOR heteromer, the receptor units in the heteromer couple to other G proteins than

those usually associated with the individually expressed receptors. Thus, signaling by stimulating the receptor units in the δOR-μOR heteromer (which causes inhibition of adenylate cyclase) is not sensitive to PTx, suggesting a G protein switch from G_i to G_z (George et al., 2000; Levac et al., 2002). There are examples of changes in G protein coupling that are dependent on co-activation of the receptor units in the receptor heteromer. Dopamine D_2R normally couples to $G_{i/o}$ proteins, but in the dopamine D_1R-D_2R heteromer it switches to $G_{q/11}$ when D_1R is co-activated. In this way, the D_1R-D_2R heteromer provides a selective mechanism by which dopamine activates phospholipase C-mediated calcium signaling (Rashid et al., 2007). Here we demonstrated that adenosine $A_{2A}R$, coupled to G_s protein when expressed alone, switch to G_i protein in $A_{2A}R$-CB_1R heteromers in the absence or in the presence of CB_1R agonists. Thus $A_{2A}R$-CB_1R heteromer provides a selective mechanism by which cannabinoid receptor blocks the $A_{2A}R$-mediated cAMP production.

Frequently, activation of one receptor unit in the heteromer implies intermolecular cross-talk involving conformational changes sensed by the other receptor unit in the heteromer. These conformational changes lead to modulation of ligand binding and/or signaling of the partner receptor. In some cases, stimulation of one receptor unit decreases the affinity and signaling of the other receptor unit as it has been described for adenosine A_1R-$A_{2A}R$ and $A_{2A}R$-D_2R heteromers, that show antagonistic allosteric interactions and a negative cross-talk (Canals et al., 2003; Ciruela et al., 2006; Ferre et al., 1991; Hillion et al., 2002). In other cases stimulation of one receptor unit increases the signaling and the affinity of the other receptor unit for endogenous or exogenous ligands as occurs for dopamine D_2-somatostatine SST5 receptor heteromer in which stimulation of D_2R significantly increases the affinity of SST5 receptors for agonists (Rocheville et al., 2000). For the $A_{2A}R$-CB_1R heteromers, ligand binding to CB_1R did not modify the ligand binding to $A_{2A}R$ and vice versa, indicating a lack of allosteric interactions for this heteromer. However, a synergistic increase in G_i protein activation was observed when both receptors were co-activated. This is

in accordance with the fact that activation of $A_{2A}R$ was necessary for CB_1R signaling in neuroblastoma cell line previously described (Carriba et al., 2007). Our results imply a processing of information, at the membrane level, of the signals impinging on the $A_{2A}R$-CB_1R heteromers. In this case, the neurotransmitter receptor heteromer functions as a processor of computations that modulates G protein-mediated signaling because quantitative or qualitative aspects of the signaling generated by stimulation of either receptor unit in the heteromer are different from those obtained during co-activation. Apart from G protein-mediated signaling, many GPCRs are able to signal in a G protein-independent way (Beaulieu et al., 2005; DeWire et al., 2007; Shenoy and Lefkowitz, 2003; Shenoy et al., 2006; Valjent et al., 2000). ERK1/2 phosphorylation is one of the MAPK pathways that has been described to be activated on a G protein-independent and arrestin-dependent mechanism (DeWire et al., 2007). Looking at the ERK1/2 phosphorylation when both receptors in the $A_{2A}R$-CB_1R heteromers are co-activated it seems that is mainly the CB_1R controlling the ERK1/2 signaling under the heteromer. Since ERK1/2 phosphorylation is related to plasticity (Shiflett and Balleine, 2011) it seems that cannabinoids are controlling changes in ERK1/2 -mediated plasticity in cells where the heteromers are present.

Striatal adenosine $A_{2A}R$ are highly expressed in MSNs of the indirect efferent pathway and are also localized presynaptically in cortico-striatal glutamatergic terminals contacting MSNs of the direct efferent pathway and in both localizations $A_{2A}R$ co-distributed with CB_1R. It has been hypothesized that postsynaptic $A_{2A}R$ antagonists might be useful in Parkinson's disease, while presynaptic $A_{2A}R$ antagonists could be beneficial in dyskinetic disorders, such as Huntington's disease, obsessive-compulsive disorders and drug addiction (Armentero et al., 2011; Blum et al., 2003; Orru et al., 2011). Thus, in the near future it would be of interest to look for an $A_{2A}R$ antagonist selectively targeting $A_{2A}R$ or $A_{2A}R$-CB_1R heteromers due to its relevancy for therapeutic purpose.

5. Compound screening of different $A_{2A}R$ antagonists in stable CHO cell lines expressing $A_{2A}R$, A_1R-$A_{2A}R$, $A_{2A}R$-D_2R or $A_{2A}R$-CB_1R heteromers.

It has been widely proven the importance of adenosine receptor in different diseases such as epilepsy, Parkinson's disease, Huntington's disease and other diseases and dysfunctions (Boison, 2012; Hickey and Stacy, 2012; Kumar et al., 2010; Stone et al., 2009). Additionally, when considering the possibility of heteromer formation as we have discussed in the previous chapters, it is particularly interesting the possibility of having characterized a battery of antagonists that are differentially selective for the adenosine $A_{2A}R$ depending on the partner that is present in the heteromer. Because of the different involvement of the different $A_{2A}R$ heteromers in these diseases and dysfunctions these antagonists would be perfect candidates for the treatment.

To test the compounds the stable cell lines used in the previous chapters were analyzed, these are CHO-$A_{2A}R$, CHO A_1R-$A_{2A}R$, CHO $A_{2A}R$-D_2R and CHO $A_{2A}R$-CB_1R. Competition experiments were performed using [^{3}H] ZM 241385 and the compounds tested. We compared the dissociation constants between the different cell membranes. Fourteen compounds were tested until the writing of this thesis (Table 1).

	$A_{2A}R$	A_1R-$A_{2A}R$	$A_{2A}R$-D_2R	$A_{2A}R$-CB_1R	Selectivity
Compound 1	4.8 μM	2.8 μM	6.6 μM	2.3 μM	No
Compound 2	62 nM	42 nM	219 nM	79 nM	No
Compound 3	321 nM	524 nM	>10 μM	7 μM	$A_{2A}=A_1A_{2A}>A_{2A}CB_1=A_{2A}D_2$
Compound 4	16 nM	366 nM	>10 μM	232 nM	$A_{2A}>A_1A_{2A}=A_{2A}CB_1>A_{2A}D_2$
Compound 5	1.6 nM (K_{D1})	>10 μM	>10 μM	1.8 nM (K_{D1})	
Compound 6	>10 μM	>10 μM	>10 μM	>10 μM	No
Compound 7	2.5 μM	2.3 μM	3 μM	2 μM	No
Compound 8	200 nM	118 nM	5.5 μM	135 nM	$A_{2A}=A_1A_{2A}=A_{2A}CB_1>A_{2A}D_2$
Compound 9	962 nM	1.2 μM	473 nM	1.8 μM	$A_{2A}D_2\geq A_{2A}=A_1A_{2A}\geq A_{2A}CB_1$
Compound 10	134 nM	157 nM	1.1 μM	98 nM	$A_{2A}=A_1A_{2A}=A_{2A}CB_1>A_{2A}D_2$
Compound 11	14.7 μM	1.3 μM	15 μM	7.5 μM	No
Compound 12	300 nM	301 nM	3.2 μM	253 nM	$A_{2A}=A_1A_{2A}=A_{2A}CB_1>A_{2A}D_2$
Compound 13	1.35 μM	870 nM	3 μM	651 nM	No
Compound 14	58 nM	63 nM	245 nM	62 nM	No
ZM 241385	8 nM	5 nM	80 – 200 nM	8 nM	-

Table 1. Dissociation constants of the compounds for $A_{2A}R$. [^{3}H] ZM 241385 was used as radioligand. In grey background all the K_D values higher that 1 μM.

5.1. Discussion

When comparing all the K_D values, two compounds showed interesting results among the others. The first one, compound number 4, showed about 20-fold better affinity for $A_{2A}R$ when compared with A_1R-$A_{2A}R$ or $A_{2A}R$-CB_1R and more than 1000-fold than $A_{2A}R$-D_2R. The second interesting compound was number 9. Adenosine $A_{2A}R$ forming $A_{2A}R$-D_2R heteromer had a surprising value of dissociation constant 3 to 4-fold lower when compared to A_1R-$A_{2A}R$ and $A_{2A}R$-CB_1R. This is remarkable because when comparing these differences with other compounds, the $A_{2A}R$ involved in the $A_{2A}R$-D_2R heteromer always showed higher affinities that the rest of the heteromers.

V. CONCLUSIONS

Conclusions derived from the **first** aim: **The involvement of A_1R-$A_{2A}R$ heteromer in glial cells and its study at a molecular level.**

- Upon GABA uptake, adenosine has a biphasic effect, which is mediated by A_1R-$A_{2A}R$ heteromers coupled to both $G_{i/0}$ and G_s proteins. Extracellular adenosine acting on these A_1R-$A_{2A}R$ functional units operates in a concerted way to balance a PKA-dependent action on GABA uptake. The neural output would thus be inhibitory at low firing rates and facilitatory at high firing rates.

- Adenosine by acting on adenosine receptors in astrocytes may significantly contribute to neurotransmission in a dual manner, which depends on the concentration of the nucleoside that is in turn dependent on neuronal firing activity.

- BRET and single molecule tracking with TIRF microscope show that the minimal GPCR heteromer unit may consist of four protomers and two G proteins. The strong similarity between GPCRs suggests that the molecular model proposed could apply to other receptors.

- These heteromers can be formed in the plasma membrane and are stable on the order of minutes. Such stability suggests that designing ways to target these heteromers may indeed be a viable strategy.

- ❖ The orientation of the α-subunits of the G proteins is on the distal receptors, suggesting that G proteins cross-talk could occur via receptors across the heteromer complex.

- ❖ The heteromeric unit described, with its dynamic and structural limitations, provides the molecular framework to understand why heteromers are functionally distinct units and not merely the aggregation of two entities with independent functions.

Conclusions derived from the **second** aim: **To find an evidence for allosteric interactions between partner receptors in the A_{2A}R-D_2R receptor heteromer which confer specific pharmacological characteristics to the heteromer.**

- ❖ In cell culture, the agonist and antagonist binding to the adenosine A_{2A}R diminish the affinity of dopamine D_2R agonists and antagonists.

- ❖ Those negative interactions between ligands are consequence of allosteric interactions between both receptors conforming the A_{2A}R-D_2R heteromer and constitute a unique biochemical property of this heteromer.

- ❖ In *ex vivo* tissue, using these allosteric interactions as a heteromer fingerprint, it has been demonstrated the expression of A_{2A}R-D_2R heteromer in human striatum.

- The fact that the $A_{2A}R$ antagonists are able to modulate dopamine D_2R pharmacology has to be taken into account to understand pathologies such as Parkinson's disease or for human PET neuroimaging.

Conclusions derived from the **third** aim: **Search for selective antagonists of $A_{2A}R$ for presynaptic A_1R-$A_{2A}R$ heteromers versus postsynaptic $A_{2A}R$-D_2R heteromers that can be useful for neurological disorder's treatment, particularly Huntington's disease.**

- The physical presence of dopamine D_2R in the $A_{2A}R$-D_2R heteromer induced a strong negative cooperativity in the $A_{2A}R$ that was detected by SCH-442416. This cooperativity indicates that $A_{2A}R$-$A_{2A}R$ homodimers are present in the $A_{2A}R$-D_2R heteromer.

- Based on *in vitro* and *in vivo* approaches, the compound SCH-442416 was classified as a preferential presynaptic $A_{2A}R$ antagonist, and the compound KW-6002 was classified as a preferential postsynaptic $A_{2A}R$ antagonist. Considering this, SCH-442416 can be used as a lead compound in the development of antidyskinetic drugs in Huntington's disease; meanwhile KW-6002 can be beneficial in Parkinson's disease.

Conclusions derived from the **fourth** aim: **Investigate the pharmacological and functional properties of $A_{2A}R$ in the $A_{2A}R$-CB_1R heteromer.**

- Adenosine $A_{2A}R$ changes its G-protein coupling from stimulatory G_s to inhibitory G_i when it forms heteromer with CB_1R and a synergistic cross-talk in G-protein activation is observed when both receptors are coactivated.

- CB_1R mainly controls the $ERK_{1/2}$ signaling under the $A_{2A}R$-CB_1R heteromer.

- The $A_{2A}R$-CB_1R heteromer does not show allosteric effects at the ligand binding level.

Conclusions derived from the **fifth** aim: **Compound screening of different $A_{2A}R$ antagonists in stable CHO cell lines expressing $A_{2A}R$, A_1R-$A_{2A}R$, $A_{2A}R$-D_2R or $A_{2A}R$-CB_1R heteromers.**

- Compound number 9 could be a good candidate to treat Parkinson's disease due to its preferential binding to $A_{2A}R$ forming $A_{2A}R$-D_2R heteromer.

VI. BIBLIOGRAPHY

AbdAlla, S., Lother, H., and Quitterer, U. (2000). AT1-receptor heterodimers show enhanced G-protein activation and altered receptor sequestration. Nature *407*, 94–98.

Agnati, L.F., Ferré, S., Lluis, C., Franco, R., and Fuxe, K. (2003). Molecular mechanisms and therapeutical implications of intramembrane receptor/receptor interactions among heptahelical receptors with examples from the striatopallidal GABA neurons. Pharmacol. Rev. *55*, 509–550.

Agnati, L.F., Guidolin, D., Vilardaga, J.P., Ciruela, F., and Fuxe, K. (2010). On the expanding terminology in the GPCR field: the meaning of receptor mosaics and receptor heteromers. J. Recept. Signal Transduct. Res. *30*, 287–303.

Albin, R.L. (2006). Neurobiology of basal ganglia and Tourette syndrome: striatal and dopamine function. Adv Neurol *99*, 99–106.

Albin, R.L., Young, A.B., and Penney, J.B. (1989). The functional anatomy of basal ganglia disorders. Trends Neurosci. *12*, 366–375.

Albin, R.L., Reiner, A., Anderson, K.D., Dure, L.S., 4th, Handelin, B., Balfour, R., Whetsell, W.O., Jr, Penney, J.B., and Young, A.B. (1992). Preferential loss of striato-external pallidal projection neurons in presymptomatic Huntington's disease. Ann. Neurol. *31*, 425–430.

Albizu, L., Cottet, M., Kralikova, M., Stoev, S., Seyer, R., Brabet, I., Roux, T., Bazin, H., Bourrier, E., Lamarque, L., et al. (2010). Time-resolved FRET between GPCR ligands reveals oligomers in native tissues. Nat Chem Biol *6*, 587–594.

D' Alcantara, P., Ledent, C., Swillens, S., and Schiffmann, S.N. (2001). Inactivation of adenosine A2A receptor impairs long term potentiation in the accumbens nucleus without altering basal synaptic transmission. Neuroscience *107*, 455–464.

Amara, S.G., and Kuhar, M.J. (1993). Neurotransmitter transporters: recent progress. Annu. Rev. Neurosci. *16*, 73–93.

Ameri, A. (1999). The effects of cannabinoids on the brain. Prog. Neurobiol. *58*, 315–348.

Andersson, M., Usiello, A., Borgkvist, A., Pozzi, L., Dominguez, C., Fienberg, A.A., Svenningsson, P., Fredholm, B.B., Borrelli, E., Greengard, P., et al. (2005a). Cannabinoid action depends on phosphorylation of dopamine- and cAMP-regulated phosphoprotein of 32 kDa at the protein kinase A site in striatal projection neurons. J. Neurosci. *25*, 8432–8438.

Andersson, M., Terasmaa, A., Fuxe, K., and Strömberg, I. (2005b). Subchronic haloperidol increases CB(1) receptor binding and G protein coupling in discrete regions of the basal ganglia. J. Neurosci. Res. *82*, 264–272.

Angers, S., Salahpour, A., Joly, E., Hilairet, S., Chelsky, D., Dennis, M., and Bouvier, M. (2000). Detection of beta 2-adrenergic receptor dimerization in living cells using bioluminescence resonance energy transfer (BRET). Proc. Natl. Acad. Sci. U.S.A. *97*, 3684–3689.

Antle, M.C., Steen, N.M., and Mistlberger, R.E. (2001). Adenosine and caffeine modulate circadian rhythms in the Syrian hamster. Neuroreport *12*, 2901–2905.

Arch, J.R., and Newsholme, E.A. (1978). Activities and some properties of 5'-nucleotidase, adenosine kinase and adenosine deaminase in tissues from vertebrates and invertebrates in relation to the control of the concentration and the physiological role of adenosine. Biochem. J. *174*, 965–977.

Armentero, M.T., Pinna, A., Ferré, S., Lanciego, J.L., Müller, C.E., and Franco, R. (2011). Past, present and future of A2A adenosine receptor antagonists in the therapy of Parkinson's disease. Pharmacol Ther *132*, 280–299.

Arrasate, M., Mitra, S., Schweitzer, E.S., Segal, M.R., and Finkbeiner, S. (2004). Inclusion body formation reduces levels of mutant huntingtin and the risk of neuronal death. Nature *431*, 805–810.

Artola, A., and Singer, W. (1987). Long-term potentiation and NMDA receptors in rat visual cortex. Nature *330*, 649–652.

Ashton, J.C., Friberg, D., Darlington, C.L., and Smith, P.F. (2006). Expression of the cannabinoid CB2 receptor in the rat cerebellum: an immunohistochemical study. Neurosci. Lett. *396*, 113–116.

Attwood, T.K., and Findlay, J.B. (1994). Fingerprinting G-protein-coupled receptors. Protein Eng. *7*, 195–203.

Awad, J.A., Johnson, R.A., Jakobs, K.H., and Schultz, G. (1983). Interactions of forskolin and adenylate cyclase. Effects on substrate kinetics and protection against inactivation by heat and N-ethylmaleimide. J. Biol. Chem. *258*, 2960–2965.

Azdad, K., Gall, D., Woods, A.S., Ledent, C., Ferré, S., and Schiffmann, S.N. (2009). Dopamine D2 and adenosine A2A receptors regulate NMDA-mediated excitation in accumbens neurons through A2A-D2 receptor heteromerization. Neuropsychopharmacology *34*, 972–986.

Baik, J.H., Picetti, R., Saiardi, A., Thiriet, G., Dierich, A., Depaulis, A., Le Meur, M., and Borrelli, E. (1995). Parkinsonian-like locomotor impairment in mice lacking dopamine D2 receptors. Nature *377*, 424–428.

Baldwin, J.M. (1994). Structure and function of receptors coupled to G proteins. Curr. Opin. Cell Biol. *6*, 180–190.

Banères, J.-L., and Parello, J. (2003). Structure-based Analysis of GPCR Function: Evidence for a Novel Pentameric Assembly between the Dimeric Leukotriene B4 Receptor BLT1 and the G-protein. Journal of Molecular Biology *329*, 815–829.

Bankowski, B.J., and Zacur, H.A. (2003). Dopamine agonist therapy for hyperprolactinemia. Clin Obstet Gynecol *46*, 349–362.

Bara-Jimenez, W., Sherzai, A., Dimitrova, T., Favit, A., Bibbiani, F., Gillespie, M., Morris, M.J., Mouradian, M.M., and Chase, T.N. (2003). Adenosine A(2A) receptor antagonist treatment of Parkinson's disease. Neurology *61*, 293–296.

Bayburt, T.H., Leitz, A.J., Xie, G., Oprian, D.D., and Sligar, S.G. (2007). Transducin activation by nanoscale lipid bilayers containing one and two rhodopsins. J. Biol. Chem. *282*, 14875–14881.

Beal, M.F., Kowall, N.W., Ellison, D.W., Mazurek, M.F., Swartz, K.J., and Martin, J.B. (1986). Replication of the neurochemical characteristics of Huntington's disease by quinolinic acid. Nature *321*, 168–171.

Beaulieu, J.-M., Sotnikova, T.D., Marion, S., Lefkowitz, R.J., Gainetdinov, R.R., and Caron, M.G. (2005). An Akt/beta-arrestin 2/PP2A signaling complex mediates dopaminergic neurotransmission and behavior. Cell *122*, 261–273.

Beltramo, M., Stella, N., Calignano, A., Lin, S.Y., Makriyannis, A., and Piomelli, D. (1997). Functional role of high-affinity anandamide transport, as revealed by selective inhibition. Science *277*, 1094–1097.

Benito, C., Núñez, E., Tolón, R.M., Carrier, E.J., Rábano, A., Hillard, C.J., and Romero, J. (2003). Cannabinoid CB2 receptors and fatty acid amide hydrolase are selectively overexpressed in neuritic plaque-associated glia in Alzheimer's disease brains. J. Neurosci. *23*, 11136–11141.

Benito, C., Núñez, E., Pazos, M.R., Tolón, R.M., and Romero, J. (2007). The endocannabinoid system and Alzheimer's disease. Mol. Neurobiol. *36*, 75–81.

Benkirane, M., Jin, D.Y., Chun, R.F., Koup, R.A., and Jeang, K.T. (1997). Mechanism of transdominant inhibition of CCR5-mediated HIV-1 infection by ccr5delta32. J. Biol. Chem. *272*, 30603–30606.

Birdsall, N.J.M. (2010). Class A GPCR heterodimers: evidence from binding studies. Trends Pharmacol. Sci. *31*, 499–508.

Bisogno, T., Howell, F., Williams, G., Minassi, A., Cascio, M.G., Ligresti, A., Matias, I., Schiano-Moriello, A., Paul, P., Williams, E.-J., et al. (2003). Cloning of the first sn1-DAG lipases points to the spatial and temporal regulation of endocannabinoid signaling in the brain. J. Cell Biol. *163*, 463–468.

Bisogno, T., Martire, A., Petrosino, S., Popoli, P., and Di Marzo, V. (2008). Symptom-related changes of endocannabinoid and palmitoylethanolamide levels in brain areas of R6/2 mice, a transgenic model of Huntington's disease. Neurochem. Int. *52*, 307–313.

Blatow, M., Rozov, A., Katona, I., Hormuzdi, S.G., Meyer, A.H., Whittington, M.A., Caputi, A., and Monyer, H. (2003). A Novel Network of Multipolar Bursting Interneurons Generates Theta Frequency Oscillations in Neocortex. Neuron *38*, 805–817.

Blättermann, S., Peters, L., Ottersbach, P.A., Bock, A., Konya, V., Weaver, C.D., Gonzalez, A., Schröder, R., Tyagi, R., Luschnig, P., et al. (2012). A biased ligand for OXE-R uncouples Gα and Gβγ signaling within a heterotrimer. Nat. Chem. Biol. *8*, 631–638.

Blázquez, C., Chiarlone, A., Sagredo, O., Aguado, T., Pazos, M.R., Resel, E., Palazuelos, J., Julien, B., Salazar, M., Börner, C., et al. (2011). Loss of striatal type 1 cannabinoid receptors is a key pathogenic factor in Huntington's disease. Brain *134*, 119–136.

Blum, D., Galas, M.-C., Pintor, A., Brouillet, E., Ledent, C., Muller, C.E., Bantubungi, K., Galluzzo, M., Gall, D., Cuvelier, L., et al. (2003). A dual role of adenosine A2A receptors in 3-nitropropionic acid-induced striatal lesions: implications for the neuroprotective potential of A2A antagonists. J. Neurosci. *23*, 5361–5369.

Blum, K., Chen, A.L.C., Giordano, J., Borsten, J., Chen, T.J.H., Hauser, M., Simpatico, T., Femino, J., Braverman, E.R., and Barh, D. (2012). The addictive brain: all roads lead to dopamine. J Psychoactive Drugs *44*, 134–143.

Bockaert, J., Roussignol, G., Bécamel, C., Gavarini, S., Joubert, L., Dumuis, A., Fagni, L., and Marin, P. (2004). GPCR-interacting proteins (GIPs): nature and functions. Biochem. Soc. Trans. *32*, 851–855.

Böhm, S.K., Grady, E.F., and Bunnett, N.W. (1997). Regulatory mechanisms that modulate signalling by G-protein-coupled receptors. Biochem. J. *322 (Pt 1)*, 1–18.

Boison, D. (2012). Adenosine dysfunction in epilepsy. Glia *60*, 1234–1243.

Bokoch, G.M., and Gilman, A.G. (1984). Inhibition of receptor-mediated release of arachidonic acid by pertussis toxin. Cell *39*, 301–308.

Bonhaus, D.W., Chang, L.K., Kwan, J., and Martin, G.R. (1998). Dual activation and inhibition of adenylyl cyclase by cannabinoid receptor agonists: evidence for agonist-specific trafficking of intracellular responses. J. Pharmacol. Exp. Ther. *287*, 884–888.

Borroto-Escuela, D.O., Romero-Fernandez, W., Tarakanov, A.O., Gómez-Soler, M., Corrales, F., Marcellino, D., Narvaez, M., Frankowska, M., Flajolet, M., Heintz, N., et al. (2010). Characterization of the A2AR-D2R interface: focus on the role of the C-terminal tail and the transmembrane helices. Biochem. Biophys. Res. Commun. *402*, 801–807.

Bouaboula, M., Poinot-Chazel, C., Bourrié, B., Canat, X., Calandra, B., Rinaldi-Carmona, M., Le Fur, G., and Casellas, P. (1995). Activation of mitogen-activated protein kinases by stimulation of the central cannabinoid receptor CB1. Biochem. J. *312 (Pt 2)*, 637–641.

Bourne, H.R., Sanders, D.A., and McCormick, F. (1991). The GTPase superfamily: conserved structure and molecular mechanism. Nature *349*, 117–127.

Bouvier, M. (2001). Oligomerization of G-protein-coupled transmitter receptors. Nat. Rev. Neurosci. *2*, 274–286.

Bouvier, M., Loisel, T.P., and Hebert, T. (1995). Dynamic regulation of G-protein coupled receptor palmitoylation: potential role in receptor function. Biochem. Soc. Trans. *23*, 577–581.

Breit, A., Lagacé, M., and Bouvier, M. (2004). Hetero-oligomerization between beta2- and beta3-adrenergic receptors generates a beta-adrenergic signaling unit with distinct functional properties. J. Biol. Chem. *279*, 28756–28765.

Broch, O.J., and Ueland, P.M. (1980). Regional and subcellular distribution of S-adenosylhomocysteine hydrolase in the adult rat brain. J. Neurochem. *35*, 484–488.

Brog, J.S., Salyapongse, A., Deutch, A.Y., and Zahm, D.S. (1993). The patterns of afferent innervation of the core and shell in the "accumbens" part of the rat ventral striatum: immunohistochemical detection of retrogradely transported fluoro-gold. J. Comp. Neurol. *338*, 255–278.

Brown, R.M., and Short, J.L. (2008). Adenosine A(2A) receptors and their role in drug addiction. J. Pharm. Pharmacol. *60*, 1409–1430.

Brusco, A., Tagliaferro, P.A., Saez, T., and Onaivi, E.S. (2008a). Ultrastructural localization of neuronal brain CB2 cannabinoid receptors. Ann. N. Y. Acad. Sci. *1139*, 450–457.

Brusco, A., Tagliaferro, P., Saez, T., and Onaivi, E.S. (2008b). Postsynaptic localization of CB2 cannabinoid receptors in the rat hippocampus. Synapse *62*, 944–949.

Bulenger, S., Marullo, S., and Bouvier, M. (2005). Emerging role of homo- and heterodimerization in G-protein-coupled receptor biosynthesis and maturation. Trends Pharmacol. Sci. *26*, 131–137.

Burgueño, J., Enrich, C., Canela, E.I., Mallol, J., Lluis, C., Franco, R., and Ciruela, F. (2003a). Metabotropic glutamate type 1alpha receptor localizes in low-density caveolin-rich plasma membrane fractions. J. Neurochem. *86*, 785–791.

Burgueño, J., Blake, D.J., Benson, M.A., Tinsley, C.L., Esapa, C.T., Canela, E.I., Penela, P., Mallol, J., Mayor, F., Jr, Lluis, C., et al. (2003b). The adenosine A2A receptor interacts with the actin-binding protein alpha-actinin. J. Biol. Chem. *278*, 37545–37552.

Cabello, N., Gandía, J., Bertarelli, D.C.G., Watanabe, M., Lluís, C., Franco, R., Ferré, S., Luján, R., and Ciruela, F. (2009). Metabotropic glutamate type 5, dopamine D2 and adenosine A2a receptors form higher-order oligomers in living cells. J. Neurochem. *109*, 1497–1507.

Calebiro, D., Rieken, F., Wagner, J., Sungkaworn, T., Zabel, U., Borzi, A., Cocucci, E., Zürn, A., and Lohse, M.J. (2013). Single-molecule analysis of fluorescently labeled G-protein-coupled receptors reveals complexes with distinct dynamics and organization. Proc. Natl. Acad. Sci. U.S.A. *110*, 743–748.

Callén, L., Moreno, E., Barroso-Chinea, P., Moreno-Delgado, D., Cortés, A., Mallol, J., Casadó, V., Lanciego, J.L., Franco, R., Lluis, C., et al. (2012). Cannabinoid receptors CB1 and CB2 form functional heteromers in brain. J. Biol. Chem. *287*, 20851–20865.

Canals, M., Marcellino, D., Fanelli, F., Ciruela, F., Benedetti, P. de, Goldberg, S.R., Neve, K., Fuxe, K., Agnati, L.F., Woods, A.S., et al. (2003). Adenosine A2A-Dopamine D2 Receptor-Receptor Heteromerization QUALITATIVE AND QUANTITATIVE ASSESSMENT BY FLUORESCENCE AND BIOLUMINESCENCE ENERGY TRANSFER. J. Biol. Chem. *278*, 46741–46749.

Canals, M., Burgueño, J., Marcellino, D., Cabello, N., Canela, E.I., Mallol, J., Agnati, L., Ferré, S., Bouvier, M., Fuxe, K., et al. (2004). Homodimerization of adenosine A2A receptors: qualitative and quantitative assessment by fluorescence and bioluminescence energy transfer. Journal of Neurochemistry *88*, 726–734.

Canals, M., Angulo, E., Casadó, V., Canela, E.I., Mallol, J., Viñals, F., Staines, W., Tinner, B., Hillion, J., Agnati, L., et al. (2005). Molecular mechanisms involved in the adenosine A and A receptor-induced neuronal differentiation in neuroblastoma cells and striatal primary cultures. J. Neurochem. *92*, 337–348.

Canals, M., Sexton, P.M., and Christopoulos, A. (2011). Allostery in GPCRs: "MWC" revisited. Trends Biochem. Sci. *36*, 663–672.

Carriba, P., Ortiz, O., Patkar, K., Justinova, Z., Stroik, J., Themann, A., Müller, C., Woods, A.S., Hope, B.T., Ciruela, F., et al. (2007). Striatal adenosine A2A and cannabinoid CB1 receptors form functional heteromeric complexes that mediate the motor effects of cannabinoids. Neuropsychopharmacology *32*, 2249–2259.

Carriba, P., Navarro, G., Ciruela, F., Ferré, S., Casadó, V., Agnati, L., Cortés, A., Mallol, J., Fuxe, K., Canela, E.I., et al. (2008). Detection of heteromerization of more than two proteins by sequential BRET-FRET. Nat. Methods *5*, 727–733.

Carrillo, J.J., Pediani, J., and Milligan, G. (2003). Dimers of class A G protein-coupled receptors function via agonist-mediated trans-activation of associated G proteins. J. Biol. Chem. *278*, 42578–42587.

Carswell, H.V., Graham, D.I., and Stone, T.W. (1997). Kainate-evoked release of adenosine from the hippocampus of the anaesthetised rat: possible involvement of free radicals. J. Neurochem. *68*, 240–247.

Carús-Cadavieco, M., and de Andrés, I. (2012). [Adenosine and homeostatic control of sleep. Actions in target structures of the sleep-wake circuits]. Rev Neurol *55*, 413–420.

Casadó, V., Martí, T., Franco, R., Lluis, C., Mallol, J., and Canela, E.I. (1990). A method for binding parameters estimation of A1 adenosine receptor subtype: A practical approach. Analytical Biochemistry *184*, 117–123.

Casadó, V., Cortés, A., Ciruela, F., Mallol, J., Ferré, S., Lluis, C., Canela, E.I., and Franco, R. (2007). Old and new ways to calculate the affinity of agonists and antagonists interacting with G-protein-coupled monomeric and dimeric receptors: The receptor–dimer cooperativity index. Pharmacology & Therapeutics *116*, 343–354.

Casadó, V., Cortés, A., Mallol, J., Pérez-Capote, K., Ferré, S., Lluis, C., Franco, R., and Canela, E.I. (2009a). GPCR homomers and heteromers: A better choice as targets for drug development than GPCR monomers? Pharmacology & Therapeutics *124*, 248–257.

Casadó, V., Ferrada, C., Bonaventura, J., Gracia, E., Mallol, J., Canela, E.I., Lluís, C., Cortés, A., and Franco, R. (2009b). Useful pharmacological parameters for G-protein-coupled receptor homodimers obtained from competition experiments. Agonist-antagonist binding modulation. Biochem. Pharmacol. *78*, 1456–1463.

Cattaneo, E., Rigamonti, D., Goffredo, D., Zuccato, C., Squitieri, F., and Sipione, S. (2001). Loss of normal huntingtin function: new developments in Huntington's disease research. Trends Neurosci. *24*, 182–188.

Cepeda, C., Ariano, M.A., Calvert, C.R., Flores-Hernández, J., Chandler, S.H., Leavitt, B.R., Hayden, M.R., and Levine, M.S. (2001). NMDA receptor function in mouse models of Huntington disease. J. Neurosci. Res. *66*, 525–539.

Cha, J.H., Frey, A.S., Alsdorf, S.A., Kerner, J.A., Kosinski, C.M., Mangiarini, L., Penney, J.B., Jr, Davies, S.W., Bates, G.P., and Young, A.B. (1999). Altered neurotransmitter receptor expression in transgenic mouse models of Huntington's disease. Philos. Trans. R. Soc. Lond., B, Biol. Sci. *354*, 981–989.

Chen, J.-F., Moratalla, R., Impagnatiello, F., Grandy, D.K., Cuellar, B., Rubinstein, M., Beilstein, M.A., Hackett, E., Fink, J.S., Low, M.J., et al. (2001). The role of the D2 dopamine receptor (D2R) in A2A adenosine receptor (A2AR)-mediated behavioral and cellular responses as revealed by A2A and D2 receptor knockout mice. Proc Natl Acad Sci U S A *98*, 1970–1975.

Chen, J.-F., Eltzschig, H.K., and Fredholm, B.B. (2013). Adenosine receptors as drug targets--what are the challenges? Nat Rev Drug Discov *12*, 265–286.

Chen, X.P., Yang, W., Fan, Y., Luo, J.S., Hong, K., Wang, Z., Yan, J.F., Chen, X., Lu, J.X., Benovic, J.L., et al. (2010). Structural determinants in the second intracellular loop of the human cannabinoid CB1 receptor mediate selective coupling to G(s) and G(i). Br. J. Pharmacol. *161*, 1817–1834.

Chou, S.-Y., Lee, Y.-C., Chen, H.-M., Chiang, M.-C., Lai, H.-L., Chang, H.-H., Wu, Y.-C., Sun, C.-N., Chien, C.-L., Lin, Y.-S., et al. (2005). CGS21680 attenuates symptoms of Huntington's disease in a transgenic mouse model. J. Neurochem. *93*, 310–320.

Chrościńska-Krawczyk, M., Jargiełło-Baszak, M., Wałek, M., Tylus, B., and Czuczwar, S.J. (2011). Caffeine and the anticonvulsant potency of antiepileptic drugs: experimental and clinical data. Pharmacol Rep *63*, 12–18.

Chu, J., Zhang, Z., Zheng, Y., Yang, J., Qin, L., Lu, J., Huang, Z.-L., Zeng, S., and Luo, Q. (2009). A novel far-red bimolecular fluorescence complementation system that allows for efficient visualization of protein interactions under physiological conditions. Biosens Bioelectron *25*, 234–239.

Chun, M., Liyanage, U.K., Lisanti, M.P., and Lodish, H.F. (1994). Signal transduction of a G protein-coupled receptor in caveolae: colocalization of endothelin and its receptor with caveolin. Proc. Natl. Acad. Sci. U.S.A. *91*, 11728–11732.

Chung, K.Y., Rasmussen, S.G.F., Liu, T., Li, S., DeVree, B.T., Chae, P.S., Calinski, D., Kobilka, B.K., Woods, V.L., and Sunahara, R.K. (2011). β2 adrenergic receptor-induced conformational changes in the heterotrimeric G protein Gs. Nature *477*, 611–615.

Cipriani, S., Bizzoco, E., Gianfriddo, M., Melani, A., Vannucchi, M.G., and Pedata, F. (2008). Adenosine A2A receptor antagonism increases nNOS-immunoreactive neurons in the striatum of Huntington transgenic mice. Exp. Neurol. *213*, 163–170.

Ciruela, F., Casadó, V., Mallol, J., Canela, E.I., Lluis, C., and Franco, R. (1995). Immunological identification of A1 adenosine receptors in brain cortex. J. Neurosci. Res. *42*, 818–828.

Ciruela, F., Escriche, M., Burgueno, J., Angulo, E., Casado, V., Soloviev, M.M., Canela, E.I., Mallol, J., Chan, W.Y., Lluis, C., et al. (2001). Metabotropic glutamate 1alpha and adenosine A1 receptors assemble into functionally interacting complexes. J. Biol. Chem. *276*, 18345–18351.

Ciruela, F., Burgueño, J., Casadó, V., Canals, M., Marcellino, D., Goldberg, S.R., Bader, M., Fuxe, K., Agnati, L.F., Lluis, C., et al. (2004). Combining Mass Spectrometry and Pull-Down Techniques for the Study of Receptor Heteromerization. Direct Epitope–Epitope Electrostatic Interactions between Adenosine A2A and Dopamine D2 Receptors. Anal. Chem. *76*, 5354–5363.

Ciruela, F., Casadó, V., Rodrigues, R.J., Luján, R., Burgueño, J., Canals, M., Borycz, J., Rebola, N., Goldberg, S.R., Mallol, J., et al. (2006a). Presynaptic control of striatal glutamatergic neurotransmission by adenosine A1-A2A receptor heteromers. J. Neurosci. *26*, 2080–2087.

Ciruela, F., Ferré, S., Casadó, V., Cortés, A., Cunha, R.A., Lluis, C., and Franco, R. (2006b). Heterodimeric adenosine receptors: a device to regulate neurotransmitter release. Cell. Mol. Life Sci. *63*, 2427–2431.

Civelli, O., Bunzow, J.R., and Grandy, D.K. (1993). Molecular diversity of the dopamine receptors. Annu. Rev. Pharmacol. Toxicol. *33*, 281–307.

Claing, A., Perry, S.J., Achiriloaie, M., Walker, J.K., Albanesi, J.P., Lefkowitz, R.J., and Premont, R.T. (2000). Multiple endocytic pathways of G protein-coupled receptors delineated by GIT1 sensitivity. Proc. Natl. Acad. Sci. U.S.A. *97*, 1119–1124.

Cobbin, L.B., Einstein, R., and Maguire, M.H. (1974). Studies on the coronary dilator actions of some adenosine analogues. Br. J. Pharmacol. *50*, 25–33.

Coleman, P.D., and Riesen, A.H. (1968). Evironmental effects on cortical dendritic fields. I. Rearing in the dark. J. Anat. *102*, 363–374.

Colquhoun, D., Rang, H.P., and Ritchie, J.M. (1973). The binding of labelled tetrodotoxin and cobra toxin by the rat diaphragm. Br. J. Pharmacol. *47*, 632P–633P.

Coney, A.M., and Marshall, J.M. (1998). Role of adenosine and its receptors in the vasodilatation induced in the cerebral cortex of the rat by systemic hypoxia. J. Physiol. (Lond.) *509 (Pt 2)*, 507–518.

Conn, P.J., and Pin, J.P. (1997). Pharmacology and functions of metabotropic glutamate receptors. Annu. Rev. Pharmacol. Toxicol. *37*, 205–237.

Consroe, P., Laguna, J., Allender, J., Snider, S., Stern, L., Sandyk, R., Kennedy, K., and Schram, K. (1991). Controlled clinical trial of cannabidiol in Huntington's disease. Pharmacol. Biochem. Behav. *40*, 701–708.

Cooper, J.K., Schilling, G., Peters, M.F., Herring, W.J., Sharp, A.H., Kaminsky, Z., Masone, J., Khan, F.A., Delanoy, M., Borchelt, D.R., et al. (1998). Truncated N-terminal fragments of huntingtin with expanded glutamine repeats form nuclear and cytoplasmic aggregates in cell culture. Hum. Mol. Genet. *7*, 783–790.

Cooper, R.L., Winslow, J.L., Govind, C.K., and Atwood, H.L. (1996). Synaptic structural complexity as a factor enhancing probability of calcium-mediated transmitter release. J. Neurophysiol. *75*, 2451–2466.

Correia-de-Sá, P., and Ribeiro, J.A. (1994). Tonic adenosine A2A receptor activation modulates nicotinic autoreceptor function at the rat neuromuscular junction. Eur. J. Pharmacol. *271*, 349–355.

Van Corven, E.J., Hordijk, P.L., Medema, R.H., Bos, J.L., and Moolenaar, W.H. (1993). Pertussis toxin-sensitive activation of p21ras by G protein-coupled receptor agonists in fibroblasts. Proc. Natl. Acad. Sci. U.S.A. *90*, 1257–1261.

Costa, T., and Herz, A. (1989). Antagonists with negative intrinsic activity at delta opioid receptors coupled to GTP-binding proteins. Proc. Natl. Acad. Sci. U.S.A. *86*, 7321–7325.

Cowan, R.L., Wilson, C.J., Emson, P.C., and Heizmann, C.W. (1990). Parvalbumin-containing GABAergic interneurons in the rat neostriatum. J. Comp. Neurol. *302*, 197–205.

Coyle, J.T., and Schwarcz, R. (1976). Lesion of striatal neurones with kainic acid provides a model for Huntington's chorea. Nature *263*, 244–246.

Cristalli, G., Cacciari, B., Dal Ben, D., Lambertucci, C., Moro, S., Spalluto, G., and Volpini, R. (2007). Highlights on the development of A(2A) adenosine receptor agonists and antagonists. ChemMedChem *2*, 260–281.

Cristalli, G., Müller, C.E., and Volpini, R. (2009). Recent developments in adenosine A2A receptor ligands. Handb Exp Pharmacol 59–98.

Cunha, R.A. (2005). Neuroprotection by adenosine in the brain: From A(1) receptor activation to A (2A) receptor blockade. Purinergic Signal. *1*, 111–134.

Cunha, R.A., Johansson, B., van der Ploeg, I., Sebastião, A.M., Ribeiro, J.A., and Fredholm, B.B. (1994). Evidence for functionally important adenosine A2a receptors in the rat hippocampus. Brain Res. *649*, 208–216.

Curtis, A., Mitchell, I., Patel, S., Ives, N., and Rickards, H. (2009). A pilot study using nabilone for symptomatic treatment in Huntington's disease. Mov. Disord. *24*, 2254–2259.

Cvejic, S., and Devi, L.A. (1997). Dimerization of the delta opioid receptor: implication for a role in receptor internalization. J. Biol. Chem. *272*, 26959–26964.

Daaka, Y., Luttrell, L.M., Ahn, S., Della Rocca, G.J., Ferguson, S.S., Caron, M.G., and Lefkowitz, R.J. (1998). Essential role for G protein-coupled receptor endocytosis in the activation of mitogen-activated protein kinase. J. Biol. Chem. *273*, 685–688.

Dai, J.-P., Li, W.-Z., Zhao, X.-F., Wang, G.-F., Yang, J.-C., Zhang, L., Chen, X.-X., Xu, Y.-X., and Li, K.-S. (2012). A Drug Screening Method Based on the Autophagy Pathway and Studies of the Mechanism of Evodiamine against Influenza A Virus. PLoS One *7*.

Dasgupta, S., Ferré, S., Kull, B., Hedlund, P.B., Finnman, U.B., Ahlberg, S., Arenas, E., Fredholm, B.B., and Fuxe, K. (1996). Adenosine A2A receptors modulate the binding characteristics of dopamine D2 receptors in stably cotransfected fibroblast cells. Eur. J. Pharmacol. *316*, 325–331.

Davis, F.B., Davis, P.J., Blas, S.D., and Gombas, D.Z. (1995). Inositol phosphates modulate human red blood cell Ca(2+)-adenosine triphosphatase activity in vitro by a guanine nucleotide regulatory protein. Metab. Clin. Exp. *44*, 865–868.

Day, J.J. (2008). Extracellular signal-related kinase activation during natural reward learning: a physiological role for phasic nucleus accumbens dopamine? J. Neurosci. *28*, 4295–4297.

Décaillot, F.M., Kazmi, M.A., Lin, Y., Ray-Saha, S., Sakmar, T.P., and Sachdev, P. (2011). CXCR7/CXCR4 Heterodimer Constitutively Recruits β-Arrestin to Enhance Cell Migration. J Biol Chem *286*, 32188–32197.

DeFea, K.A., Zalevsky, J., Thoma, M.S., Déry, O., Mullins, R.D., and Bunnett, N.W. (2000). beta-arrestin-dependent endocytosis of proteinase-activated receptor 2 is required for intracellular targeting of activated ERK1/2. J. Cell Biol. *148*, 1267–1281.

Delaney, S.M., and Geiger, J.D. (1996). Brain regional levels of adenosine and adenosine nucleotides in rats killed by high-energy focused microwave irradiation. J. Neurosci. Methods *64*, 151–156.

Delaney, S.M., Shepel, P.N., and Geiger, J.D. (1998). Levels of endogenous adenosine in rat striatum. I. Regulation by ionotropic glutamate receptors, nitric oxide and free radicals. J. Pharmacol. Exp. Ther. *285*, 561–567.

DeLong, M.R. (1990). Primate models of movement disorders of basal ganglia origin. Trends Neurosci. *13*, 281–285.

DeLong, M.R., and Wichmann, T. (2007). Circuits and circuit disorders of the basal ganglia. Arch. Neurol. *64*, 20–24.

Denovan-Wright, E.M., and Robertson, H.A. (2000). Cannabinoid receptor messenger RNA levels decrease in a subset of neurons of the lateral striatum, cortex and hippocampus of transgenic Huntington's disease mice. Neuroscience *98*, 705–713.

Derkinderen, P., Valjent, E., Toutant, M., Corvol, J.-C., Enslen, H., Ledent, C., Trzaskos, J., Caboche, J., and Girault, J.-A. (2003). Regulation of extracellular signal-regulated kinase by cannabinoids in hippocampus. J. Neurosci. *23*, 2371–2382.

Devane, W.A., Hanus, L., Breuer, A., Pertwee, R.G., Stevenson, L.A., Griffin, G., Gibson, D., Mandelbaum, A., Etinger, A., and Mechoulam, R. (1992). Isolation and structure of a brain constituent that binds to the cannabinoid receptor. Science *258*, 1946–1949.

Devi, L.A. (2001). Heterodimerization of G-protein-coupled receptors: pharmacology, signaling and trafficking. Trends Pharmacol. Sci. *22*, 532–537.

DeWire, S.M., Ahn, S., Lefkowitz, R.J., and Shenoy, S.K. (2007). Beta-arrestins and cell signaling. Annu. Rev. Physiol. *69*, 483–510.

DiFiglia, M., Sapp, E., Chase, K., Schwarz, C., Meloni, A., Young, C., Martin, E., Vonsattel, J.P., Carraway, R., and Reeves, S.A. (1995). Huntingtin is a cytoplasmic protein associated with vesicles in human and rat brain neurons. Neuron *14*, 1075–1081.

Dinh, T.P., Carpenter, D., Leslie, F.M., Freund, T.F., Katona, I., Sensi, S.L., Kathuria, S., and Piomelli, D. (2002). Brain monoglyceride lipase participating in endocannabinoid inactivation. Proc. Natl. Acad. Sci. U.S.A. *99*, 10819–10824.

Dohlman, H.G., Caron, M.G., DeBlasi, A., Frielle, T., and Lefkowitz, R.J. (1990). Role of extracellular disulfide-bonded cysteines in the ligand binding function of the beta 2-adrenergic receptor. Biochemistry *29*, 2335–2342.

Domenici, M.R., Scattoni, M.L., Martire, A., Lastoria, G., Potenza, R.L., Borioni, A., Venerosi, A., Calamandrei, G., and Popoli, P. (2007). Behavioral and electrophysiological effects of the adenosine A2A receptor antagonist SCH 58261 in R6/2 Huntington's disease mice. Neurobiol. Dis. *28*, 197–205.

Dorsch, S., Klotz, K.-N., Engelhardt, S., Lohse, M.J., and Bünemann, M. (2009). Analysis of receptor oligomerization by FRAP microscopy. Nat. Methods *6*, 225–230.

Dragatsis, I., Dietrich, P., and Zeitlin, S. (2000). Expression of the Huntingtin-associated protein 1 gene in the developing and adult mouse. Neurosci. Lett. *282*, 37–40.

Dragunow, M. (1996). A role for immediate-early transcription factors in learning and memory. Behav. Genet. *26*, 293–299.

Dubach, M., Schmidt, R., Kunkel, D., Bowden, D.M., Martin, R., and German, D.C. (1987). Primate neostriatal neurons containing tyrosine hydroxylase: immunohistochemical evidence. Neurosci. Lett. *75*, 205–210.

Dunwiddie, T.V., Diao, L., and Proctor, W.R. (1997). Adenine nucleotides undergo rapid, quantitative conversion to adenosine in the extracellular space in rat hippocampus. J. Neurosci. *17*, 7673–7682.

Egertová, M., Cravatt, B.F., and Elphick, M.R. (2003). Comparative analysis of fatty acid amide hydrolase and cb(1) cannabinoid receptor expression in the mouse brain: evidence of a widespread role for fatty acid amide hydrolase in regulation of endocannabinoid signaling. Neuroscience *119*, 481–496.

El Moustaine, D., Granier, S., Doumazane, E., Scholler, P., Rahmeh, R., Bron, P., Mouillac, B., Banères, J.-L., Rondard, P., and Pin, J.-P. (2012). Distinct roles of metabotropic glutamate receptor dimerization in agonist activation and G-protein coupling. Proc. Natl. Acad. Sci. U.S.A. *109*, 16342–16347.

Enjalbert, A., and Bockaert, J. (1983). Pharmacological characterization of the D2 dopamine receptor negatively coupled with adenylate cyclase in rat anterior pituitary. Mol. Pharmacol. *23*, 576–584.

Faber, P.W., Alter, J.R., MacDonald, M.E., and Hart, A.C. (1999). Polyglutamine-mediated dysfunction and apoptotic death of a Caenorhabditis elegans sensory neuron. Proc. Natl. Acad. Sci. U.S.A. *96*, 179–184.

Faure, M., Voyno-Yasenetskaya, T.A., and Bourne, H.R. (1994). cAMP and beta gamma subunits of heterotrimeric G proteins stimulate the mitogen-activated protein kinase pathway in COS-7 cells. J. Biol. Chem. *269*, 7851–7854.

Fenu, S., Pinna, A., Ongini, E., and Morelli, M. (1997). Adenosine A2A receptor antagonism potentiates L-DOPA-induced turning behaviour and c-fos expression in 6-hydroxydopamine-lesioned rats. Eur. J. Pharmacol. *321*, 143–147.

Ferguson, S.S. (2001). Evolving concepts in G protein-coupled receptor endocytosis: the role in receptor desensitization and signaling. Pharmacol. Rev. *53*, 1–24.

Fernández, P., Trzaska, S., Wilder, T., Chiriboga, L., Blackburn, M.R., Cronstein, B.N., and Chan, E.S.L. (2008). Pharmacological blockade of A2A receptors prevents dermal fibrosis in a model of elevated tissue adenosine. Am. J. Pathol. *172*, 1675–1682.

Ferrada, C., Ferré, S., Casadó, V., Cortés, A., Justinova, Z., Barnes, C., Canela, E.I., Goldberg, S.R., Leurs, R., Lluis, C., et al. (2008). Interactions between histamine H3 and dopamine D2 receptors and the implications for striatal function. Neuropharmacology *55*, 190–197.

Ferrada, C., Moreno, E., Casadó, V., Bongers, G., Cortés, A., Mallol, J., Canela, E.I., Leurs, R., Ferré, S., Lluís, C., et al. (2009). Marked changes in signal transduction upon heteromerization of dopamine D1 and histamine H3 receptors. Br J Pharmacol *157*, 64–75.

Ferrante, R.J., Kowall, N.W., and Richardson, E.P., Jr (1991). Proliferative and degenerative changes in striatal spiny neurons in Huntington's disease: a combined study using the section-Golgi method and calbindin D28k immunocytochemistry. J. Neurosci. *11*, 3877–3887.

Ferrante, R.J., Gutekunst, C.A., Persichetti, F., McNeil, S.M., Kowall, N.W., Gusella, J.F., MacDonald, M.E., Beal, M.F., and Hersch, S.M. (1997). Heterogeneous topographic and cellular distribution of huntingtin expression in the normal human neostriatum. J. Neurosci. *17*, 3052–3063.

Ferre, S., and Franco, R. (2010). Oligomerization of G protein-coupled receptors: A reality. Curr Opin Pharmacol *10*, 1–5.

Ferre, S., von Euler, G., Johansson, B., Fredholm, B.B., and Fuxe, K. (1991). Stimulation of high-affinity adenosine A2 receptors decreases the affinity of dopamine D2 receptors in rat striatal membranes. Proc. Natl. Acad. Sci. U.S.A. *88*, 7238–7241.

Ferré, S., Fuxe, K., von Euler, G., Johansson, B., and Fredholm, B.B. (1992). Adenosine-dopamine interactions in the brain. Neuroscience *51*, 501–512.

Ferré, S., Snaprud, P., and Fuxe, K. (1993). Opposing actions of an adenosine A2 receptor agonist and a GTP analogue on the regulation of dopamine D2 receptors in rat neostriatal membranes. Eur. J. Pharmacol. *244*, 311–315.

Ferré, S., Fredholm, B.B., Morelli, M., Popoli, P., and Fuxe, K. (1997). Adenosine-dopamine receptor-receptor interactions as an integrative mechanism in the basal ganglia. Trends Neurosci. *20*, 482–487.

Ferré, S., Popoli, P., Giménez-Llort, L., Rimondini, R., Müller, C.E., Strömberg, I., Ögren, S.O., and Fuxe, K. (2001). Adenosine/dopamine interaction: implications for the treatment of Parkinson's disease. Parkinsonism Relat. Disord. *7*, 235–241.

Ferré, S., Karcz-Kubicha, M., Hope, B.T., Popoli, P., Burgueño, J., Gutiérrez, M.A., Casadó, V., Fuxe, K., Goldberg, S.R., Lluis, C., et al. (2002). Synergistic interaction between adenosine A2A and glutamate mGlu5 receptors: implications for striatal neuronal function. Proc. Natl. Acad. Sci. U.S.A. *99*, 11940–11945.

Ferré, S., Ciruela, F., Canals, M., Marcellino, D., Burgueno, J., Casadó, V., Hillion, J., Torvinen, M., Fanelli, F., Benedetti Pd, P. de, et al. (2004). Adenosine A2A-dopamine D2 receptor-receptor heteromers. Targets for neuro-psychiatric disorders. Parkinsonism Relat. Disord. *10*, 265–271.

Ferré, S., Borycz, J., Goldberg, S.R., Hope, B.T., Morales, M., Lluis, C., Franco, R., Ciruela, F., and Cunha, R. (2005). Role of adenosine in the control of homosynaptic plasticity in striatal excitatory synapses. J. Integr. Neurosci. *4*, 445–464.

Ferré, S., Ciruela, F., Woods, A.S., Lluis, C., and Franco, R. (2007a). Functional relevance of neurotransmitter receptor heteromers in the central nervous system. Trends in Neurosciences *30*, 440–446.

Ferré, S., Ciruela, F., Quiroz, C., Luján, R., Popoli, P., Cunha, R.A., Agnati, L.F., Fuxe, K., Woods, A.S., Lluis, C., et al. (2007b). Adenosine receptor heteromers and their integrative role in striatal function. ScientificWorldJournal *7*, 74–85.

Ferré, S., Agnati, L.F., Ciruela, F., Lluis, C., Woods, A.S., Fuxe, K., and Franco, R. (2007c). Neurotransmitter receptor heteromers and their integrative role in "local modules": the striatal spine module. Brain Res Rev *55*, 55–67.

Ferré, S., Quiroz, C., Woods, A.S., Cunha, R., Popoli, P., Ciruela, F., Lluis, C., Franco, R., Azdad, K., and Schiffmann, S.N. (2008). An Update on Adenosine A2A-Dopamine D2 receptor interactions. Implications for the Function of G Protein-Coupled Receptors. Curr Pharm Des *14*, 1468–1474.

Ferré, S., Baler, R., Bouvier, M., Caron, M.G., Devi, L.A., Durroux, T., Fuxe, K., George, S.R., Javitch, J.A., Lohse, M.J., et al. (2009a). Building a new conceptual framework for receptor heteromers. Nat Chem Biol *5*, 131–134.

Ferré, S., Goldberg, S.R., Lluis, C., and Franco, R. (2009b). Looking for the role of cannabinoid receptor heteromers in striatal function. Neuropharmacology *56*, 226–234.

Ferré, S., Navarro, G., Casadó, V., Cortés, A., Mallol, J., Canela, E.I., Lluís, C., and Franco, R. (2010a). G protein-coupled receptor heteromers as new targets for drug development. Prog Mol Biol Transl Sci *91*, 41–52.

Ferré, S., Lluís, C., Justinova, Z., Quiroz, C., Orru, M., Navarro, G., Canela, E.I., Franco, R., and Goldberg, S.R. (2010b). Adenosine–cannabinoid receptor interactions. Implications for striatal function. Br J Pharmacol *160*, 443–453.

Ferrer, B., Asbrock, N., Kathuria, S., Piomelli, D., and Giuffrida, A. (2003). Effects of levodopa on endocannabinoid levels in rat basal ganglia: implications for the treatment of levodopa-induced dyskinesias. Eur. J. Neurosci. *18*, 1607–1614.

Fields, R.D., and Burnstock, G. (2006). Purinergic signalling in neuron–glia interactions. Nat Rev Neurosci *7*, 423–436.

Fields, H.L., Hjelmstad, G.O., Margolis, E.B., and Nicola, S.M. (2007). Ventral tegmental area neurons in learned appetitive behavior and positive reinforcement. Annu. Rev. Neurosci. *30*, 289–316.

Fink, J.S., Weaver, D.R., Rivkees, S.A., Peterfreund, R.A., Pollack, A.E., Adler, E.M., and Reppert, S.M. (1992). Molecular cloning of the rat A2 adenosine receptor: selective co-expression with D2 dopamine receptors in rat striatum. Brain Res. Mol. Brain Res. *14*, 186–195.

Flower, D.R. (1999). Modelling G-protein-coupled receptors for drug design. Biochim. Biophys. Acta *1422*, 207–234.

Fotiadis, D., Liang, Y., Filipek, S., Saperstein, D.A., Engel, A., and Palczewski, K. (2003). Atomic-force microscopy: Rhodopsin dimers in native disc membranes. Nature *421*, 127–128.

Fotiadis, D., Liang, Y., Filipek, S., Saperstein, D.A., Engel, A., and Palczewski, K. (2004). The G protein-coupled receptor rhodopsin in the native membrane. FEBS Lett. *564*, 281–288.

Franco, R., Casadó, V., Ciruela, F., Mallol, J., Lluis, C., and Canela, E.I. (1996). The cluster-arranged cooperative model: a model that accounts for the kinetics of binding to A1 adenosine receptors. Biochemistry *35*, 3007–3015.

Franco, R., Canals, M., Marcellino, D., Ferré, S., Agnati, L., Mallol, J., Casadó, V., Ciruela, F., Fuxe, K., Lluis, C., et al. (2003). Regulation of heptaspanning-membrane-receptor function by dimerization and clustering. Trends Biochem. Sci. *28*, 238–243.

Franco, R., Casadó, V., Mallol, J., Ferré, S., Fuxe, K., Cortés, A., Ciruela, F., Lluis, C., and Canela, E.I. (2005a). Dimer-based model for heptaspanning membrane receptors. Trends in Biochemical Sciences *30*, 360–366.

Franco, R., Ciruela, F., Casadó, V., Cortes, A., Canela, E.I., Mallol, J., Agnati, L.F., Ferré, S., Fuxe, K., and Lluis, C. (2005b). Partners for adenosine A1 receptors. J. Mol. Neurosci. *26*, 221–232.

Franco, R., Casadó, V., Mallol, J., Ferrada, C., Ferré, S., Fuxe, K., Cortés, A., Ciruela, F., Lluis, C., and Canela, E.I. (2006). The two-state dimer receptor model: a general model for receptor dimers. Mol. Pharmacol. *69*, 1905–1912.

Franco, R., Casadó, V., Cortés, A., Pérez-Capote, K., Mallol, J., Canela, E., Ferré, S., and Lluis, C. (2008). Novel pharmacological targets based on receptor heteromers. Brain Res Rev *58*, 475–482.

Fredholm, B.B., Lindström, K., and Wallman-Johansson, A. (1994). Propentofylline and other adenosine transport inhibitors increase the efflux of adenosine following electrical or metabolic stimulation of rat hippocampal slices. J. Neurochem. *62*, 563–573.

Fredholm, B.B., Irenius, E., Kull, B., and Schulte, G. (2001a). Comparison of the potency of adenosine as an agonist at human adenosine receptors expressed in Chinese hamster ovary cells. Biochem. Pharmacol. *61*, 443–448.

Fredholm, B.B., IJzerman, A.P., Jacobson, K.A., Klotz, K.N., and Linden, J. (2001b). International Union of Pharmacology. XXV. Nomenclature and classification of adenosine receptors. Pharmacol. Rev. *53*, 527–552.

Fredholm, B.B., Chen, J.-F., Masino, S.A., and Vaugeois, J.-M. (2005). Actions of adenosine at its receptors in the CNS: insights from knockouts and drugs. Annu. Rev. Pharmacol. Toxicol. *45*, 385–412.

Fredholm, B.B., Chern, Y., Franco, R., and Sitkovsky, M. (2007). Aspects of the general biology of adenosine A2A signaling. Prog. Neurobiol. *83*, 263–276.

Fredriksson, R., Lagerström, M.C., Lundin, L.-G., and Schiöth, H.B. (2003). The G-protein-coupled receptors in the human genome form five main families. Phylogenetic analysis, paralogon groups, and fingerprints. Mol. Pharmacol. *63*, 1256–1272.

Freund, T.F., Katona, I., and Piomelli, D. (2003). Role of endogenous cannabinoids in synaptic signaling. Physiol. Rev. *83*, 1017–1066.

Fung, J.J., Deupi, X., Pardo, L., Yao, X.J., Velez-Ruiz, G.A., DeVree, B.T., Sunahara, R.K., and Kobilka, B.K. (2009). Ligand-regulated oligomerization of β2-adrenoceptors in a model lipid bilayer. EMBO J *28*, 3315–3328.

Fusco, F.R., Chen, Q., Lamoreaux, W.J., Figueredo-Cardenas, G., Jiao, Y., Coffman, J.A., Surmeier, D.J., Honig, M.G., Carlock, L.R., and Reiner, A. (1999). Cellular localization of huntingtin in striatal and cortical neurons in rats: lack of correlation with neuronal vulnerability in Huntington's disease. J. Neurosci. *19*, 1189–1202.

Fusco, F.R., Martorana, A., Giampà, C., De March, Z., Farini, D., D'Angelo, V., Sancesario, G., and Bernardi, G. (2004). Immunolocalization of CB1 receptor in rat striatal neurons: a confocal microscopy study. Synapse *53*, 159–167.

Fuxe, K., and Owman, C. (1965). Cellular localization of monoamines in the area postrema of certain mammals. J. Comp. Neurol. *125*, 337–353.

Fuxe, K., Goldstein, M., Hökfelt, T., Jonsson, G., and Lidbrink, P. (1974). Dopaminergic involvement in hypothalamic function: extrahypothalamic and hypothalamic control. A neuroanatomical analysis. Adv Neurol *5*, 405–419.

Fuxe, K., Strömberg, I., Popoli, P., Rimondini-Giorgini, R., Torvinen, M., Ogren, S.O., Franco, R., Agnati, L.F., and Ferré, S. (2001). Adenosine receptors and Parkinson's disease. Relevance of antagonistic adenosine and dopamine receptor interactions in the striatum. Adv Neurol *86*, 345–353.

Fuxe, K., Marcellino, D., Borroto-Escuela, D.O., Frankowska, M., Ferraro, L., Guidolin, D., Ciruela, F., and Agnati, L.F. (2010). The changing world of G protein-coupled receptors: from monomers to dimers and receptor mosaics with allosteric receptor-receptor interactions. J. Recept. Signal Transduct. Res. *30*, 272–283.

Gafni, J., and Ellerby, L.M. (2002). Calpain activation in Huntington's disease. J. Neurosci. *22*, 4842–4849.

Galés, C., Rebois, R.V., Hogue, M., Trieu, P., Breit, A., Hébert, T.E., and Bouvier, M. (2005). Real-time monitoring of receptor and G-protein interactions in living cells. Nat. Methods *2*, 177–184.

Galve-Roperh, I., Aguado, T., Palazuelos, J., and Guzmán, M. (2008). Mechanisms of control of neuron survival by the endocannabinoid system. Curr. Pharm. Des. *14*, 2279–2288.

Gandia, J., Galino, J., Amaral, O.B., Soriano, A., Lluís, C., Franco, R., and Ciruela, F. (2008). Detection of higher-order G protein-coupled receptor oligomers by a combined BRET-BiFC technique. FEBS Lett. *582*, 2979–2984.

Gaoni, Y., and Mechoulam, R. (1971). The isolation and structure of delta-1-tetrahydrocannabinol and other neutral cannabinoids from hashish. J. Am. Chem. Soc. *93*, 217–224.

Gehl, C., Waadt, R., Kudla, J., Mendel, R.-R., and Hänsch, R. (2009). New GATEWAY vectors for high throughput analyses of protein-protein interactions by bimolecular fluorescence complementation. Mol Plant *2*, 1051–1058.

George, S.R., Lee, S.P., Varghese, G., Zeman, P.R., Seeman, P., Ng, G.Y., and O'Dowd, B.F. (1998). A transmembrane domain-derived peptide inhibits D1 dopamine receptor function without affecting receptor oligomerization. J. Biol. Chem. *273*, 30244–30248.

George, S.R., Fan, T., Xie, Z., Tse, R., Tam, V., Varghese, G., and O'Dowd, B.F. (2000). Oligomerization of mu- and delta-opioid receptors. Generation of novel functional properties. J. Biol. Chem. *275*, 26128–26135.

George, S.R., O'Dowd, B.F., and Lee, S.P. (2002). G-protein-coupled receptor oligomerization and its potential for drug discovery. Nat Rev Drug Discov *1*, 808–820.

Gerfen, C.R. (1992). The neostriatal mosaic: multiple levels of compartmental organization. Trends Neurosci. *15*, 133–139.

Gervais, F.G., Singaraja, R., Xanthoudakis, S., Gutekunst, C.-A., Leavitt, B.R., Metzler, M., Hackam, A.S., Tam, J., Vaillancourt, J.P., Houtzager, V., et al. (2002). Recruitment and activation of caspase-8 by the Huntingtin-interacting protein Hip-1 and a novel partner Hippi. Nat. Cell Biol. *4*, 95–105.

Gianfriddo, M., Melani, A., Turchi, D., Giovannini, M.G., and Pedata, F. (2004). Adenosine and glutamate extracellular concentrations and mitogen-activated protein kinases in the striatum of Huntington transgenic mice. Selective antagonism of adenosine A2A receptors reduces transmitter outflow. Neurobiol. Dis. *17*, 77–88.

Gill, D.M., and Meren, R. (1978). ADP-ribosylation of membrane proteins catalyzed by cholera toxin: basis of the activation of adenylate cyclase. Proc Natl Acad Sci U S A *75*, 3050–3054.

Ginés, S., Hillion, J., Torvinen, M., Le Crom, S., Casadó, V., Canela, E.I., Rondin, S., Lew, J.Y., Watson, S., Zoli, M., et al. (2000). Dopamine D1 and adenosine A1 receptors form functionally interacting heteromeric complexes. Proc. Natl. Acad. Sci. U.S.A. *97*, 8606–8611.

Giuffrida, A., Parsons, L.H., Kerr, T.M., Rodríguez de Fonseca, F., Navarro, M., and Piomelli, D. (1999). Dopamine activation of endogenous cannabinoid signaling in dorsal striatum. Nat. Neurosci. *2*, 358–363.

Glass, M., and Dragunow, M. (1995). Induction of the Krox 24 transcription factor in striosomes by a cannabinoid agonist. Neuroreport *6*, 241–244.

Glass, M., and Felder, C.C. (1997). Concurrent stimulation of cannabinoid CB1 and dopamine D2 receptors augments cAMP accumulation in striatal neurons: evidence for a Gs linkage to the CB1 receptor. J. Neurosci. *17*, 5327–5333.

Glass, M., Dragunow, M., and Faull, R.L. (1997). Cannabinoid receptors in the human brain: a detailed anatomical and quantitative autoradiographic study in the fetal, neonatal and adult human brain. Neuroscience *77*, 299–318.

Glass, M., Dragunow, M., and Faull, R.L. (2000). The pattern of neurodegeneration in Huntington's disease: a comparative study of cannabinoid, dopamine, adenosine and GABA(A) receptor alterations in the human basal ganglia in Huntington's disease. Neuroscience *97*, 505–519.

Gomes, I., IJzerman, A.P., Ye, K., Maillet, E.L., and Devi, L.A. (2011). G Protein-Coupled Receptor Heteromerization: A Role in Allosteric Modulation of Ligand Binding. Mol Pharmacol *79*, 1044–1052.

Gómez del Pulgar, T., Velasco, G., and Guzmán, M. (2000). The CB1 cannabinoid receptor is coupled to the activation of protein kinase B/Akt. Biochem. J. *347*, 369–373.

Gong, J.-P., Onaivi, E.S., Ishiguro, H., Liu, Q.-R., Tagliaferro, P.A., Brusco, A., and Uhl, G.R. (2006). Cannabinoid CB2 receptors: immunohistochemical localization in rat brain. Brain Res. *1071*, 10–23.

Gorinski, N., Kowalsman, N., Renner, U., Wirth, A., Reinartz, M.T., Seifert, R., Zeug, A., Ponimaskin, E., and Niv, M.Y. (2012). Computational and experimental analysis of the transmembrane domain 4/5 dimerization interface of the serotonin 5-HT(1A) receptor. Mol. Pharmacol. *82*, 448–463.

Goudet, C., Kniazeff, J., Hlavackova, V., Malhaire, F., Maurel, D., Acher, F., Blahos, J., Prézeau, L., and Pin, J.-P. (2005). Asymmetric functioning of dimeric metabotropic glutamate receptors disclosed by positive allosteric modulators. J. Biol. Chem. *280*, 24380–24385.

Gouldson, P.R., Higgs, C., Smith, R.E., Dean, M.K., Gkoutos, G.V., and Reynolds, C.A. (2000). Dimerization and domain swapping in G-protein-coupled receptors: a computational study. Neuropsychopharmacology *23*, S60–77.

Gracia, E., Cortés, A., Meana, J.J., García-Sevilla, J., Herhsfield, M.S., Canela, E.I., Mallol, J., Lluís, C., Franco, R., and Casadó, V. (2008). Human adenosine deaminase as an allosteric modulator of human A(1) adenosine receptor: abolishment of negative cooperativity for [H](R)-pia binding to the caudate nucleus. J. Neurochem. *107*, 161–170.

Gracia, E., Pérez-Capote, K., Moreno, E., Barkešová, J., Mallol, J., Lluís, C., Franco, R., Cortés, A., Casadó, V., and Canela, E.I. (2011). A $_{2A}$ adenosine receptor ligand binding and signalling is allosterically modulated by adenosine deaminase. Biochemical Journal *435*, 701–709.

Graveland, G.A., and DiFiglia, M. (1985). The frequency and distribution of medium-sized neurons with indented nuclei in the primate and rodent neostriatum. Brain Res. *327*, 307–311.

Graveland, G.A., Williams, R.S., and DiFiglia, M. (1985). Evidence for degenerative and regenerative changes in neostriatal spiny neurons in Huntington's disease. Science *227*, 770–773.

Gubellini, P., Saulle, E., Centonze, D., Costa, C., Tropepi, D., Bernardi, G., Conquet, F., and Calabresi, P. (2003). Corticostriatal LTP requires combined mGluR1 and mGluR5 activation. Neuropharmacology *44*, 8–16.

Gubitz, A.K., Widdowson, L., Kurokawa, M., Kirkpatrick, K.A., and Richardson, P.J. (1996). Dual signalling by the adenosine A2a receptor involves activation of both N- and P-type calcium channels by different G proteins and protein kinases in the same striatal nerve terminals. J. Neurochem. *67*, 374–381.

Gudermann, T., Schöneberg, T., and Schultz, G. (1997). Functional and structural complexity of signal transduction via G-protein-coupled receptors. Annu. Rev. Neurosci. *20*, 399–427.

Guo, W., Shi, L., and Javitch, J.A. (2003). The fourth transmembrane segment forms the interface of the dopamine D2 receptor homodimer. J. Biol. Chem. *278*, 4385–4388.

Guo, W., Shi, L., Filizola, M., Weinstein, H., and Javitch, J.A. (2005). Crosstalk in G protein-coupled receptors: Changes at the transmembrane homodimer interface determine activation. Proc Natl Acad Sci U S A *102*, 17495–17500.

Guo, W., Urizar, E., Kralikova, M., Mobarec, J.C., Shi, L., Filizola, M., and Javitch, J.A. (2008). Dopamine D2 receptors form higher order oligomers at physiological expression levels. EMBO J *27*, 2293–2304.

Gurevich, V.V., and Gurevich, E.V. (2008). GPCR monomers and oligomers: it takes all kinds. Trends Neurosci *31*, 74–81.

Guttman, M., Boileau, I., Warsh, J., Saint-Cyr, J.A., Ginovart, N., McCluskey, T., Houle, S., Wilson, A., Mundo, E., Rusjan, P., et al. (2007). Brain serotonin transporter binding in non-depressed patients with Parkinson's disease. Eur. J. Neurol. *14*, 523–528.

Hackam, A.S., Singaraja, R., Wellington, C.L., Metzler, M., McCutcheon, K., Zhang, T., Kalchman, M., and Hayden, M.R. (1998). The influence of huntingtin protein size on nuclear localization and cellular toxicity. J. Cell Biol. *141*, 1097–1105.

Håkansson, K., Galdi, S., Hendrick, J., Snyder, G., Greengard, P., and Fisone, G. (2006). Regulation of phosphorylation of the GluR1 AMPA receptor by dopamine D2 receptors. Journal of Neurochemistry *96*, 482–488.

Hall, D.A. (2000). Modeling the functional effects of allosteric modulators at pharmacological receptors: an extension of the two-state model of receptor activation. Mol. Pharmacol. *58*, 1412–1423.

Hamilton, N.B., and Attwell, D. (2010). Do astrocytes really exocytose neurotransmitters? Nat. Rev. Neurosci. *11*, 227–238.

Hamm, H.E. (1998). The many faces of G protein signaling. J. Biol. Chem. *273*, 669–672.

Han, Y., Moreira, I.S., Urizar, E., Weinstein, H., and Javitch, J.A. (2009). Allosteric communication between protomers of dopamine Class A GPCR dimers modulates activation. Nat Chem Biol *5*, 688–695.

Hanus, L., Abu-Lafi, S., Fride, E., Breuer, A., Vogel, Z., Shalev, D.E., Kustanovich, I., and Mechoulam, R. (2001). 2-arachidonyl glyceryl ether, an endogenous agonist of the cannabinoid CB1 receptor. Proc. Natl. Acad. Sci. U.S.A. *98*, 3662–3665.

Harjes, P., and Wanker, E.E. (2003). The hunt for huntingtin function: interaction partners tell many different stories. Trends Biochem. Sci. *28*, 425–433.

Harms, G.S., Cognet, L., Lommerse, P.H.M., Blab, G.A., Kahr, H., Gamsjäger, R., Spaink, H.P., Soldatov, N.M., Romanin, C., and Schmidt, T. (2001). Single-Molecule Imaging of L-Type Ca2+ Channels in Live Cells. Biophysical Journal *81*, 2639–2646.

Harvey, J., and Lacey, M.G. (1997). A postsynaptic interaction between dopamine D1 and NMDA receptors promotes presynaptic inhibition in the rat nucleus accumbens via adenosine release. J. Neurosci. *17*, 5271–5280.

Hashimotodani, Y., Ohno-Shosaku, T., and Kano, M. (2007). Presynaptic monoacylglycerol lipase activity determines basal endocannabinoid tone and terminates retrograde endocannabinoid signaling in the hippocampus. J. Neurosci. *27*, 1211–1219.

Hausdorff, W.P., Bouvier, M., O'Dowd, B.F., Irons, G.P., Caron, M.G., and Lefkowitz, R.J. (1989). Phosphorylation sites on two domains of the beta 2-adrenergic receptor are involved in distinct pathways of receptor desensitization. J. Biol. Chem. *264*, 12657–12665.

Hauser, R.A., Hubble, J.P., and Truong, D.D. (2003). Randomized trial of the adenosine A(2A) receptor antagonist istradefylline in advanced PD. Neurology *61*, 297–303.

Hebert, T.E., Moffett, S., Morello, J.P., Loisel, T.P., Bichet, D.G., Barret, C., and Bouvier, M. (1996). A peptide derived from a beta2-adrenergic receptor transmembrane domain inhibits both receptor dimerization and activation. J. Biol. Chem. *271*, 16384–16392.

Herkenham, M., Lynn, A.B., Little, M.D., Johnson, M.R., Melvin, L.S., de Costa, B.R., and Rice, K.C. (1990). Cannabinoid receptor localization in brain. Proc Natl Acad Sci U S A *87*, 1932–1936.

Herkenham, M., Groen, B.G., Lynn, A.B., De Costa, B.R., and Richfield, E.K. (1991). Neuronal localization of cannabinoid receptors and second messengers in mutant mouse cerebellum. Brain Res. *552*, 301–310.

Hermans, E., Vanisberg, M.A., Geurts, M., and Maloteaux, J.M. (1997). Down-regulation of neurotensin receptors after ligand-induced internalization in rat primary cultured neurons. Neurochem. Int. *31*, 291–299.

Hern, J.A., Baig, A.H., Mashanov, G.I., Birdsall, B., Corrie, J.E.T., Lazareno, S., Molloy, J.E., and Birdsall, N.J.M. (2010). Formation and dissociation of M1 muscarinic receptor dimers seen by total internal reflection fluorescence imaging of single molecules. Proc. Natl. Acad. Sci. U.S.A. *107*, 2693–2698.

Herrera, C., Casadó, V., Ciruela, F., Schofield, P., Mallol, J., Lluis, C., and Franco, R. (2001). Adenosine A2B receptors behave as an alternative anchoring protein for cell

surface adenosine deaminase in lymphocytes and cultured cells. Mol. Pharmacol. *59*, 127–134.

Herrick-Davis, K., Weaver, B.A., Grinde, E., and Mazurkiewicz, J.E. (2006). Serotonin 5-HT2C receptor homodimer biogenesis in the endoplasmic reticulum: real-time visualization with confocal fluorescence resonance energy transfer. J. Biol. Chem. *281*, 27109–27116.

Hertz, L., Yu, A.C., and Schousboe, A. (1992). Uptake and metabolism of malate in neurons and astrocytes in primary cultures. J. Neurosci. Res. *33*, 289–296.

Hettinger, B.D., Lee, A., Linden, J., and Rosin, D.L. (2001). Ultrastructural localization of adenosine A2A receptors suggests multiple cellular sites for modulation of GABAergic neurons in rat striatum. J. Comp. Neurol. *431*, 331–346.

Hibert, M.F., Trumpp-Kallmeyer, S., Bruinvels, A., and Hoflack, J. (1991). Three-dimensional models of neurotransmitter G-binding protein-coupled receptors. Mol. Pharmacol. *40*, 8–15.

Hickey, P., and Stacy, M. (2012). Adenosine A2A antagonists in Parkinson's disease: what's next? Curr Neurol Neurosci Rep *12*, 376–385.

Higley, M.J., and Sabatini, B.L. (2010). Competitive regulation of synaptic Ca influx by D2 dopamine and A2A adenosine receptors. Nat Neurosci *13*, 958–966.

Hillard, C.J., Edgemond, W.S., Jarrahian, A., and Campbell, W.B. (1997). Accumulation of N-arachidonoylethanolamine (anandamide) into cerebellar granule cells occurs via facilitated diffusion. J. Neurochem. *69*, 631–638.

Hillion, J., Canals, M., Torvinen, M., Casado, V., Scott, R., Terasmaa, A., Hansson, A., Watson, S., Olah, M.E., Mallol, J., et al. (2002). Coaggregation, cointernalization, and codesensitization of adenosine A2A receptors and dopamine D2 receptors. J. Biol. Chem. *277*, 18091–18097.

Hlavackova, V., Goudet, C., Kniazeff, J., Zikova, A., Maurel, D., Vol, C., Trojanova, J., Prézeau, L., Pin, J.-P., and Blahos, J. (2005). Evidence for a single heptahelical domain being turned on upon activation of a dimeric GPCR. EMBO J. *24*, 499–509.

Hohmann, A.G., and Herkenham, M. (2000). Localization of cannabinoid CB(1) receptor mRNA in neuronal subpopulations of rat striatum: a double-label in situ hybridization study. Synapse *37*, 71–80.

Von Hörsten, S., Schmitt, I., Nguyen, H.P., Holzmann, C., Schmidt, T., Walther, T., Bader, M., Pabst, R., Kobbe, P., Krotova, J., et al. (2003). Transgenic rat model of Huntington's disease. Hum. Mol. Genet. *12*, 617–624.

Howlett, A.C., Qualy, J.M., and Khachatrian, L.L. (1986). Involvement of Gi in the inhibition of adenylate cyclase by cannabimimetic drugs. Mol. Pharmacol. *29*, 307–313.

Hu, C.-D., Chinenov, Y., and Kerppola, T.K. (2002). Visualization of interactions among bZIP and Rel family proteins in living cells using bimolecular fluorescence complementation. Mol. Cell *9*, 789–798.

Hu, J., Thor, D., Zhou, Y., Liu, T., Wang, Y., McMillin, S.M., Mistry, R., Challiss, R.A.J., Costanzi, S., and Wess, J. (2012). Structural aspects of M3 muscarinic acetylcholine receptor dimer formation and activation. FASEB J *26*, 604–616.

Huang, C., Hepler, J.R., Chen, L.T., Gilman, A.G., Anderson, R.G., and Mumby, S.M. (1997). Organization of G proteins and adenylyl cyclase at the plasma membrane. Mol. Biol. Cell *8*, 2365–2378.

Huang, C.-C., Chen, Y.-L., Lo, S.-W., and Hsu, K.-S. (2002). Activation of cAMP-dependent protein kinase suppresses the presynaptic cannabinoid inhibition of glutamatergic transmission at corticostriatal synapses. Mol. Pharmacol. *61*, 578–585.

Huang, N.-K., Lin, J.-H., Lin, J.-T., Lin, C.-I., Liu, E.M., Lin, C.-J., Chen, W.-P., Shen, Y.-C., Chen, H.-M., Chen, J.-B., et al. (2011). A new drug design targeting the adenosinergic system for Huntington's disease. PLoS ONE *6*, e20934.

Hughes, P.E., Young, D., Preston, K.M., Yan, Q., and Dragunow, M. (1998). Differential regulation by MK801 of immediate-early genes, brain-derived neurotrophic factor and trk receptor mRNA induced by a kindling after-discharge. Brain Res. Mol. Brain Res. *53*, 138–151.

Humbert, S., Bryson, E.A., Cordelières, F.P., Connors, N.C., Datta, S.R., Finkbeiner, S., Greenberg, M.E., and Saudou, F. (2002). The IGF-1/Akt pathway is neuroprotective in Huntington's disease and involves Huntingtin phosphorylation by Akt. Dev. Cell *2*, 831–837.

Ikemoto, K., Satoh, K., Kitahama, K., and Maeda, T. (1996). Demonstration of a new dopamine-containing cell group in the primate rostral telencephalon. Neurosci. Lett. *220*, 69–71.

Jaakola, V.-P., Griffith, M.T., Hanson, M.A., Cherezov, V., Chien, E.Y.T., Lane, J.R., Ijzerman, A.P., and Stevens, R.C. (2008). The 2.6 angstrom crystal structure of a human A2A adenosine receptor bound to an antagonist. Science *322*, 1211–1217.

Jacobsen, J.C., Bawden, C.S., Rudiger, S.R., McLaughlan, C.J., Reid, S.J., Waldvogel, H.J., MacDonald, M.E., Gusella, J.F., Walker, S.K., Kelly, J.M., et al. (2010). An ovine transgenic Huntington's disease model. Hum. Mol. Genet. *19*, 1873–1882.

Jacobson, K.A., and Gao, Z.-G. (2006). Adenosine receptors as therapeutic targets. Nat Rev Drug Discov *5*, 247–264.

Jacoby, E., Bouhelal, R., Gerspacher, M., and Seuwen, K. (2006). The 7 TM G-protein-coupled receptor target family. ChemMedChem *1*, 761–782.

Jarabek, B.R., Yasuda, R.P., and Wolfe, B.B. (2004). Regulation of proteins affecting NMDA receptor-induced excitotoxicity in a Huntington's mouse model. Brain *127*, 505–516.

Jarrahian, A., Watts, V.J., and Barker, E.L. (2004). D2 dopamine receptors modulate Galpha-subunit coupling of the CB1 cannabinoid receptor. J. Pharmacol. Exp. Ther. *308*, 880–886.

Jarvis, M.F., Jackson, R.H., and Williams, M. (1989). Autoradiographic characterization of high-affinity adenosine A2 receptors in the rat brain. Brain Res. *484*, 111–118.

Jarvis, M.F., Wismer, C.T., Schweitzer, E., Yu, H., van Biesen T, Lynch, K.J., Burgard, E.C., and Kowaluk, E.A. (2001). Modulation of BzATP and formalin induced nociception: attenuation by the P2X receptor antagonist, TNP-ATP and enhancement by the P2X(3) allosteric modulator, cibacron blue. Br. J. Pharmacol. *132*, 259–269.

Jenner, P. (2003). A2A antagonists as novel non-dopaminergic therapy for motor dysfunction in PD. Neurology *61*, S32–38.

Jenner, P. (2005). Istradefylline, a novel adenosine A2A receptor antagonist, for the treatment of Parkinson's disease. Expert Opin Investig Drugs *14*, 729–738.

Jenner, P., Mori, A., Hauser, R., Morelli, M., Fredholm, B.B., and Chen, J.F. (2009). Adenosine, adenosine A 2A antagonists, and Parkinson's disease. Parkinsonism Relat. Disord. *15*, 406–413.

De Jesús, M.L., Sallés, J., Meana, J.J., and Callado, L.F. (2006). Characterization of CB1 cannabinoid receptor immunoreactivity in postmortem human brain homogenates. Neuroscience *140*, 635–643.

Ji, X.-D., and Jacobson, K.A. (1999). Use of the Triazolotriazine [3H]ZM 241385 as a Radioligand at Recombinant Human A2B Adenosine Receptors. Drug Des Discov *16*, 217–226.

Jockers, R., Angers, S., Da Silva, A., Benaroch, P., Strosberg, A.D., Bouvier, M., and Marullo, S. (1999). Beta(2)-adrenergic receptor down-regulation. Evidence for a pathway that does not require endocytosis. J. Biol. Chem. *274*, 28900–28908.

Johansson, B., Halldner, L., Dunwiddie, T.V., Masino, S.A., Poelchen, W., Giménez-Llort, L., Escorihuela, R.M., Fernández-Teruel, A., Wiesenfeld-Hallin, Z., Xu, X.J., et al. (2001). Hyperalgesia, anxiety, and decreased hypoxic neuroprotection in mice lacking the adenosine A1 receptor. Proc. Natl. Acad. Sci. U.S.A. *98*, 9407–9412.

Johnson, R., and Buckley, N.J. (2009). Gene dysregulation in Huntington's disease: REST, microRNAs and beyond. Neuromolecular Med. *11*, 183–199.

Jones, K.A., Borowsky, B., Tamm, J.A., Craig, D.A., Durkin, M.M., Dai, M., Yao, W.J., Johnson, M., Gunwaldsen, C., Huang, L.Y., et al. (1998). GABA(B) receptors

function as a heteromeric assembly of the subunits GABA(B)R1 and GABA(B)R2. Nature *396*, 674–679.

Jones, R.W., Green, D.G., and Pinter, R.B. (1962). Mathematical simulation of certain receptor and effector organs. Fed. Proc. *21*, 97–102.

Jordan, B.A., and Devi, L.A. (1999). G-protein-coupled receptor heterodimerization modulates receptor function. Nature *399*, 697–700.

Jordan, B.A., Trapaidze, N., Gomes, I., Nivarthi, R., and Devi, L.A. (2001). Oligomerization of opioid receptors with β2-adrenergic receptors: A role in trafficking and mitogen-activated protein kinase activation. Proc Natl Acad Sci U S A *98*, 343–348.

Jordan, B.A., Gomes, I., Rios, C., Filipovska, J., and Devi, L.A. (2003). Functional interactions between mu opioid and alpha 2A-adrenergic receptors. Mol. Pharmacol. *64*, 1317–1324.

Joyce, J.N., Lexow, N., Bird, E., and Winokur, A. (1988). Organization of dopamine D1 and D2 receptors in human striatum: receptor autoradiographic studies in Huntington's disease and schizophrenia. Synapse *2*, 546–557.

Kaasinen, V., Ruottinen, H.M., Någren, K., Lehikoinen, P., Oikonen, V., and Rinne, J.O. (2000). Upregulation of putaminal dopamine D2 receptors in early Parkinson's disease: a comparative PET study with [11C] raclopride and [11C]N-methylspiperone. J. Nucl. Med. *41*, 65–70.

Kaasinen, V., Aalto, S., Någren, K., and Rinne, J.O. (2004a). Dopaminergic effects of caffeine in the human striatum and thalamus. Neuroreport *15*, 281–285.

Kaasinen, V., Aalto, S., Någren, K., and Rinne, J.O. (2004b). Expectation of caffeine induces dopaminergic responses in humans. European Journal of Neuroscience *19*, 2352–2356.

Kachroo, A., Orlando, L.R., Grandy, D.K., Chen, J.-F., Young, A.B., and Schwarzschild, M.A. (2005). Interactions between metabotropic glutamate 5 and adenosine A2A receptors in normal and parkinsonian mice. J. Neurosci. *25*, 10414–10419.

Kamal, M., and Jockers, R. (2011). Biological Significance of GPCR Heteromerization in the Neuro-Endocrine System. Front Endocrinol (Lausanne) *2*.

Kamiya, T., Saitoh, O., Yoshioka, K., and Nakata, H. (2003). Oligomerization of adenosine A2A and dopamine D2 receptors in living cells. Biochem. Biophys. Res. Commun. *306*, 544–549.

Kanda, T., Jackson, M.J., Smith, L.A., Pearce, R.K., Nakamura, J., Kase, H., Kuwana, Y., and Jenner, P. (1998). Adenosine A2A antagonist: a novel antiparkinsonian agent that does not provoke dyskinesia in parkinsonian monkeys. Ann. Neurol. *43*, 507–513.

Kanda, T., Jackson, M.J., Smith, L.A., Pearce, R.K., Nakamura, J., Kase, H., Kuwana, Y., and Jenner, P. (2000). Combined use of the adenosine A(2A) antagonist KW-6002 with L-DOPA or with selective D1 or D2 dopamine agonists increases antiparkinsonian activity but not dyskinesia in MPTP-treated monkeys. Exp. Neurol. *162*, 321–327.

Kang, D.S., Tian, X., and Benovic, J.L. (2013). β-Arrestins and G protein-coupled receptor trafficking. Meth. Enzymol. *521*, 91–108.

Karcz-Kubicha, M., Ferré, S., Díaz-Ruiz, O., Quiroz-Molina, C., Goldberg, S.R., Hope, B.T., and Morales, M. (2006). Stimulation of adenosine receptors selectively activates gene expression in striatal enkephalinergic neurons. Neuropsychopharmacology *31*, 2173–2179.

Kasai, R.S., Suzuki, K.G.N., Prossnitz, E.R., Koyama-Honda, I., Nakada, C., Fujiwara, T.K., and Kusumi, A. (2011). Full characterization of GPCR monomer–dimer dynamic equilibrium by single molecule imaging. J Cell Biol *192*, 463–480.

Kase, H. (2001). New aspects of physiological and pathophysiological functions of adenosine A2A receptor in basal ganglia. Biosci. Biotechnol. Biochem. *65*, 1447–1457.

Katona, I., and Freund, T.F. (2008). Endocannabinoid signaling as a synaptic circuit breaker in neurological disease. Nat. Med. *14*, 923–930.

Katona, I., Urbán, G.M., Wallace, M., Ledent, C., Jung, K.-M., Piomelli, D., Mackie, K., and Freund, T.F. (2006). Molecular Composition of the Endocannabinoid System at Glutamatergic Synapses. J Neurosci *26*, 5628–5637.

Kaupmann, K., Malitschek, B., Schuler, V., Heid, J., Froestl, W., Beck, P., Mosbacher, J., Bischoff, S., Kulik, A., Shigemoto, R., et al. (1998). GABA(B)-receptor subtypes assemble into functional heteromeric complexes. Nature *396*, 683–687.

Kawaguchi, Y. (1993). Physiological, morphological, and histochemical characterization of three classes of interneurons in rat neostriatum. J. Neurosci. *13*, 4908–4923.

Kawaguchi, Y., Wilson, C.J., Augood, S.J., and Emson, P.C. (1995). Striatal interneurones: chemical, physiological and morphological characterization. Trends Neurosci. *18*, 527–535.

Kearn, C.S., Blake-Palmer, K., Daniel, E., Mackie, K., and Glass, M. (2005). Concurrent stimulation of cannabinoid CB1 and dopamine D2 receptors enhances heterodimer formation: a mechanism for receptor cross-talk? Mol. Pharmacol. *67*, 1697–1704.

Kebabian, J.W., and Greengard, P. (1971). Dopamine-sensitive adenyl cyclase: possible role in synaptic transmission. Science *174*, 1346–1349.

Kegel, K.B., Meloni, A.R., Yi, Y., Kim, Y.J., Doyle, E., Cuiffo, B.G., Sapp, E., Wang, Y., Qin, Z.-H., Chen, J.D., et al. (2002). Huntingtin is present in the nucleus, interacts

with the transcriptional corepressor C-terminal binding protein, and represses transcription. J. Biol. Chem. *277*, 7466–7476.

Kelleher, R.J., 3rd, Govindarajan, A., Jung, H.-Y., Kang, H., and Tonegawa, S. (2004). Translational control by MAPK signaling in long-term synaptic plasticity and memory. Cell *116*, 467–479.

Kemp, J.M., and Powell, T.P. (1971). The structure of the caudate nucleus of the cat: light and electron microscopy. Philos. Trans. R. Soc. Lond., B, Biol. Sci. *262*, 383–401.

Kendall, R.T., and Luttrell, L.M. (2009). Diversity in arrestin function. Cell. Mol. Life Sci. *66*, 2953–2973.

Kerppola, T.K. (2006). VISUALIZATION OF MOLECULAR INTERACTIONS BY FLUORESCENCE COMPLEMENTATION. Nat Rev Mol Cell Biol *7*, 449–456.

Klinger, M., Kuhn, M., Just, H., Stefan, E., Palmer, T., Freissmuth, M., and Nanoff, C. (2002). Removal of the carboxy terminus of the A2A-adenosine receptor blunts constitutive activity: differential effect on cAMP accumulation and MAP kinase stimulation. Naunyn Schmiedebergs Arch. Pharmacol. *366*, 287–298.

Klotz, K.N., and Lohse, M.J. (1986). The glycoprotein nature of A1 adenosine receptors. Biochem. Biophys. Res. Commun. *140*, 406–413.

Klotz, K.N., Hessling, J., Hegler, J., Owman, C., Kull, B., Fredholm, B.B., and Lohse, M.J. (1998). Comparative pharmacology of human adenosine receptor subtypes - characterization of stably transfected receptors in CHO cells. Naunyn Schmiedebergs Arch. Pharmacol. *357*, 1–9.

Koch, W.J., Hawes, B.E., Allen, L.F., and Lefkowitz, R.J. (1994). Direct evidence that Gi-coupled receptor stimulation of mitogen-activated protein kinase is mediated by G beta gamma activation of p21ras. Proc. Natl. Acad. Sci. U.S.A. *91*, 12706–12710.

Köfalvi, A., Rodrigues, R.J., Ledent, C., Mackie, K., Vizi, E.S., Cunha, R.A., and Sperlágh, B. (2005). Involvement of cannabinoid receptors in the regulation of neurotransmitter release in the rodent striatum: a combined immunochemical and pharmacological analysis. J. Neurosci. *25*, 2874–2884.

Kolakowski, L.F., Jr (1994). GCRDb: a G-protein-coupled receptor database. Recept. Channels *2*, 1–7.

Kreitzer, A.C. (2009). Physiology and pharmacology of striatal neurons. Annu. Rev. Neurosci. *32*, 127–147.

Kreitzer, A.C., and Malenka, R.C. (2007). Endocannabinoid-mediated rescue of striatal LTD and motor deficits in Parkinson's disease models. Nature *445*, 643–647.

Kreitzer, A.C., and Regehr, W.G. (2001). Retrograde inhibition of presynaptic calcium influx by endogenous cannabinoids at excitatory synapses onto Purkinje cells. Neuron *29*, 717–727.

Krishnaraju, K., Nguyen, H.Q., Liebermann, D.A., and Hoffman, B. (1995). The zinc finger transcription factor Egr-1 potentiates macrophage differentiation of hematopoietic cells. Mol. Cell. Biol. *15*, 5499–5507.

Krueger, K.M., Daaka, Y., Pitcher, J.A., and Lefkowitz, R.J. (1997). The role of sequestration in G protein-coupled receptor resensitization. Regulation of beta2-adrenergic receptor dephosphorylation by vesicular acidification. J. Biol. Chem. *272*, 5–8.

Krupnick, J.G., and Benovic, J.L. (1998). The role of receptor kinases and arrestins in G protein-coupled receptor regulation. Annu. Rev. Pharmacol. Toxicol. *38*, 289–319.

Kuemmerle, S., Gutekunst, C.A., Klein, A.M., Li, X.J., Li, S.H., Beal, M.F., Hersch, S.M., and Ferrante, R.J. (1999). Huntington aggregates may not predict neuronal death in Huntington's disease. Ann. Neurol. *46*, 842–849.

Kull, B., Ferré, S., Arslan, G., Svenningsson, P., Fuxe, K., Owman, C., and Fredholm, B.B. (1999). Reciprocal interactions between adenosine A2A and dopamine D2 receptors in Chinese hamster ovary cells co-transfected with the two receptors. Biochem. Pharmacol. *58*, 1035–1045.

Kull, B., Svenningsson, P., and Fredholm, B.B. (2000). Adenosine A(2A) receptors are colocalized with and activate g(olf) in rat striatum. Mol. Pharmacol. *58*, 771–777.

Kumar, P., Kalonia, H., and Kumar, A. (2010). Huntington's disease: pathogenesis to animal models. Pharmacol Rep *62*, 1–14.

Künzle, H. (1975). Bilateral projections from precentral motor cortex to the putamen and other parts of the basal ganglia. An autoradiographic study in Macaca fascicularis. Brain Res. *88*, 195–209.

Kusumi, A., Nakada, C., Ritchie, K., Murase, K., Suzuki, K., Murakoshi, H., Kasai, R.S., Kondo, J., and Fujiwara, T. (2005). Paradigm shift of the plasma membrane concept from the two-dimensional continuum fluid to the partitioned fluid: high-speed single-molecule tracking of membrane molecules. Annu Rev Biophys Biomol Struct *34*, 351–378.

Lambert, D.M., and Fowler, C.J. (2005). The endocannabinoid system: drug targets, lead compounds, and potential therapeutic applications. J. Med. Chem. *48*, 5059–5087.

Lastres-Becker, I., Berrendero, F., Lucas, J.J., Martín-Aparicio, E., Yamamoto, A., Ramos, J.A., and Fernández-Ruiz, J.J. (2002). Loss of mRNA levels, binding and activation of GTP-binding proteins for cannabinoid CB1 receptors in the basal ganglia of a transgenic model of Huntington's disease. Brain Res. *929*, 236–242.

Latini, S., and Pedata, F. (2001). Adenosine in the central nervous system: release mechanisms and extracellular concentrations. J. Neurochem. *79*, 463–484.

Law, P.-Y., Erickson-Herbrandson, L.J., Zha, Q.Q., Solberg, J., Chu, J., Sarre, A., and Loh, H.H. (2005). Heterodimerization of mu- and delta-opioid receptors occurs at the cell surface only and requires receptor-G protein interactions. J. Biol. Chem. *280*, 11152–11164.

De Lean, A., Stadel, J.M., and Lefkowitz, R.J. (1980). A ternary complex model explains the agonist-specific binding properties of the adenylate cyclase-coupled beta-adrenergic receptor. J. Biol. Chem. *255*, 7108–7117.

Leavitt, B.R., van Raamsdonk, J.M., Shehadeh, J., Fernandes, H., Murphy, Z., Graham, R.K., Wellington, C.L., Raymond, L.A., and Hayden, M.R. (2006). Wild-type huntingtin protects neurons from excitotoxicity. J. Neurochem. *96*, 1121–1129.

Leck, K.J., Blaha, C.D., Matthaei, K.I., Forster, G.L., Holgate, J., and Hendry, I.A. (2006). Gz proteins are functionally coupled to dopamine D2-like receptors in vivo. Neuropharmacology *51*, 597–605.

Ledent, C., Vaugeois, J.M., Schiffmann, S.N., Pedrazzini, T., El Yacoubi, M., Vanderhaeghen, J.J., Costentin, J., Heath, J.K., Vassart, G., and Parmentier, M. (1997). Aggressiveness, hypoalgesia and high blood pressure in mice lacking the adenosine A2a receptor. Nature *388*, 674–678.

Lee, K.-W., Hong, J.-H., Choi, I.Y., Che, Y., Lee, J.-K., Yang, S.-D., Song, C.-W., Kang, H.S., Lee, J.-H., Noh, J.S., et al. (2002). Impaired D2 dopamine receptor function in mice lacking type 5 adenylyl cyclase. J. Neurosci. *22*, 7931–7940.

Lee, Y.I., Kang-Park, S., Do, S.I., and Lee, Y.I. (2001). The hepatitis B virus-X protein activates a phosphatidylinositol 3-kinase-dependent survival signaling cascade. J. Biol. Chem. *276*, 16969–16977.

Leenders, A.G.M., and Sheng, Z.-H. (2005). Modulation of neurotransmitter release by the second messenger-activated protein kinases: implications for presynaptic plasticity. Pharmacol. Ther. *105*, 69–84.

Leff, P. (1995). The two-state model of receptor activation. Trends Pharmacol. Sci. *16*, 89–97.

Lefkowitz, R.J. (1998). G protein-coupled receptors. III. New roles for receptor kinases and beta-arrestins in receptor signaling and desensitization. J. Biol. Chem. *273*, 18677–18680.

Lefkowitz, R.J., Cotecchia, S., Kjelsberg, M.A., Pitcher, J., Koch, W.J., Inglese, J., and Caron, M.G. (1993). Adrenergic receptors: recent insights into their mechanism of activation and desensitization. Adv. Second Messenger Phosphoprotein Res. *28*, 1–9.

Lerner, T.N., Horne, E.A., Stella, N., and Kreitzer, A.C. (2010). Endocannabinoid signaling mediates psychomotor activation by adenosine A2A antagonists. J. Neurosci. *30*, 2160–2164.

Levac, B.A.R., O'Dowd, B.F., and George, S.R. (2002). Oligomerization of opioid receptors: generation of novel signaling units. Curr Opin Pharmacol *2*, 76–81.

Levitt, M., Spector, S., Sjoerdsma, A., and Udenfriend, S. (1965). Elucidation of the rate-limiting step in norepinephrine biosynthesis in the perfused guinea-pig heart. J. Pharmacol. Exp. Ther. *148*, 1–8.

LeWitt, P.A., Guttman, M., Tetrud, J.W., Tuite, P.J., Mori, A., Chaikin, P., and Sussman, N.M. (2008). Adenosine A2A receptor antagonist istradefylline (KW-6002) reduces "off" time in Parkinson's disease: a double-blind, randomized, multicenter clinical trial (6002-US-005). Ann. Neurol. *63*, 295–302.

Li, S.-H., and Li, X.-J. (2004). Huntingtin-protein interactions and the pathogenesis of Huntington's disease. Trends Genet. *20*, 146–154.

Li, H., Wyman, T., Yu, Z.-X., Li, S.-H., and Li, X.-J. (2003a). Abnormal association of mutant huntingtin with synaptic vesicles inhibits glutamate release. Hum. Mol. Genet. *12*, 2021–2030.

Li, S.-H., Yu, Z.-X., Li, C.-L., Nguyen, H.-P., Zhou, Y.-X., Deng, C., and Li, X.-J. (2003b). Lack of huntingtin-associated protein-1 causes neuronal death resembling hypothalamic degeneration in Huntington's disease. J. Neurosci. *23*, 6956–6964.

Ligresti, A., Morera, E., Van Der Stelt, M., Monory, K., Lutz, B., Ortar, G., and Di Marzo, V. (2004). Further evidence for the existence of a specific process for the membrane transport of anandamide. Biochem. J. *380*, 265–272.

Liles, S.L., and Updyke, B.V. (1985). Projection of the digit and wrist area of precentral gyrus to the putamen: relation between topography and physiological properties of neurons in the putamen. Brain Res. *339*, 245–255.

Lin, R., Karpa, K., Kabbani, N., Goldman-Rakic, P., and Levenson, R. (2001). Dopamine D2 and D3 receptors are linked to the actin cytoskeleton via interaction with filamin A. Proc. Natl. Acad. Sci. U.S.A. *98*, 5258–5263.

Linden, J., Thai, T., Figler, H., Jin, X., and Robeva, A.S. (1999). Characterization of human A(2B) adenosine receptors: radioligand binding, western blotting, and coupling to G(q) in human embryonic kidney 293 cells and HMC-1 mast cells. Mol. Pharmacol. *56*, 705–713.

Lindgren, N., Usiello, A., Goiny, M., Haycock, J., Erbs, E., Greengard, P., Hokfelt, T., Borrelli, E., and Fisone, G. (2003). Distinct roles of dopamine D2L and D2S receptor isoforms in the regulation of protein phosphorylation at presynaptic and postsynaptic sites. Proc. Natl. Acad. Sci. U.S.A. *100*, 4305–4309.

Liu, W., Chun, E., Thompson, A.A., Chubukov, P., Xu, F., Katritch, V., Han, G.W., Roth, C.B., Heitman, L.H., IJzerman, A.P., et al. (2012). Structural basis for allosteric regulation of GPCRs by sodium ions. Science *337*, 232–236.

Lloyd, H.G., and Fredholm, B.B. (1995). Involvement of adenosine deaminase and adenosine kinase in regulating extracellular adenosine concentration in rat hippocampal slices. Neurochem. Int. *26*, 387–395.

Loening, A.M., Fenn, T.D., and Gambhir, S.S. (2007). Crystal Structures of the Luciferase and Green Fluorescent Protein from Renilla reniformis. Journal of Molecular Biology *374*, 1017–1028.

Lohse, M.J., Benovic, J.L., Codina, J., Caron, M.G., and Lefkowitz, R.J. (1990). beta-Arrestin: a protein that regulates beta-adrenergic receptor function. Science *248*, 1547–1550.

Lommerse, P.H.M., Blab, G.A., Cognet, L., Harms, G.S., Snaar-Jagalska, B.E., Spaink, H.P., and Schmidt, T. (2004). Single-Molecule Imaging of the H-Ras Membrane-Anchor Reveals Domains in the Cytoplasmic Leaflet of the Cell Membrane. Biophysical Journal *86*, 609–616.

Lopes, L.V., Cunha, R.A., and Ribeiro, J.A. (1999). Cross talk between A(1) and A(2A) adenosine receptors in the hippocampus and cortex of young adult and old rats. J. Neurophysiol. *82*, 3196–3203.

Lopes, L.V., Cunha, R.A., Kull, B., Fredholm, B.B., and Ribeiro, J.A. (2002). Adenosine A(2A) receptor facilitation of hippocampal synaptic transmission is dependent on tonic A(1) receptor inhibition. Neuroscience *112*, 319–329.

V. Lopes, L., M. Sebastiao, A., and A. Ribeiro, J. (2011). Adenosine and Related Drugs in Brain Diseases: Present and Future in Clinical Trials. Current Topics in Medicinal Chemistry *11*, 1087–1101.

Lopez-Gimenez, J.F., Canals, M., Pediani, J.D., and Milligan, G. (2007). The alpha1b-adrenoceptor exists as a higher-order oligomer: effective oligomerization is required for receptor maturation, surface delivery, and function. Mol. Pharmacol. *71*, 1015–1029.

Lorenzen, A., Beukers, M.W., van der Graaf, P.H., Lang, H., van Muijlwijk-Koezen, J., de Groote, M., Menge, W., Schwabe, U., and IJzerman, A.P. (2002). Modulation of agonist responses at the A(1) adenosine receptor by an irreversible antagonist, receptor-G protein uncoupling and by the G protein activation state. Biochem. Pharmacol. *64*, 1251–1265.

Lunkes, A., and Mandel, J.L. (1998). A cellular model that recapitulates major pathogenic steps of Huntington's disease. Hum. Mol. Genet. *7*, 1355–1361.

Luttrell, L.M., and Gesty-Palmer, D. (2010). Beyond desensitization: physiological relevance of arrestin-dependent signaling. Pharmacol. Rev. *62*, 305–330.

Luttrell, L.M., and Lefkowitz, R.J. (2002). The role of beta-arrestins in the termination and transduction of G-protein-coupled receptor signals. J. Cell. Sci. *115*, 455–465.

Luttrell, L.M., Ferguson, S.S., Daaka, Y., Miller, W.E., Maudsley, S., Della Rocca, G.J., Lin, F., Kawakatsu, H., Owada, K., Luttrell, D.K., et al. (1999). Beta-arrestin-dependent formation of beta2 adrenergic receptor-Src protein kinase complexes. Science *283*, 655–661.

Maccarrone, M., Battista, N., and Centonze, D. (2007). The endocannabinoid pathway in Huntington's disease: a comparison with other neurodegenerative diseases. Prog. Neurobiol. *81*, 349–379.

Maggio, R., Vogel, Z., and Wess, J. (1993). Coexpression studies with mutant muscarinic/adrenergic receptors provide evidence for intermolecular "cross-talk" between G-protein-linked receptors. Proc. Natl. Acad. Sci. U.S.A. *90*, 3103–3107.

Maia, L., and de Mendonça, A. (2002). Does caffeine intake protect from Alzheimer's disease? Eur. J. Neurol. *9*, 377–382.

Mangiarini, L., Sathasivam, K., Seller, M., Cozens, B., Harper, A., Hetherington, C., Lawton, M., Trottier, Y., Lehrach, H., Davies, S.W., et al. (1996). Exon 1 of the HD gene with an expanded CAG repeat is sufficient to cause a progressive neurological phenotype in transgenic mice. Cell *87*, 493–506.

Manglik, A., Kruse, A.C., Kobilka, T.S., Thian, F.S., Mathiesen, J.M., Sunahara, R.K., Pardo, L., Weis, W.I., Kobilka, B.K., and Granier, S. (2012). Crystal structure of the μ-opioid receptor bound to a morphinan antagonist. Nature *485*, 321–326.

Marcellino, D., Ferré, S., Casadó, V., Cortés, A., Le Foll, B., Mazzola, C., Drago, F., Saur, O., Stark, H., Soriano, A., et al. (2008). Identification of dopamine D1-D3 receptor heteromers. Indications for a role of synergistic D1-D3 receptor interactions in the striatum. J. Biol. Chem. *283*, 26016–26025.

Marchese, A., Paing, M.M., Temple, B.R.S., and Trejo, J. (2008). G protein-coupled receptor sorting to endosomes and lysosomes. Annu. Rev. Pharmacol. Toxicol. *48*, 601–629.

Margeta-Mitrovic, M., Jan, Y.N., and Jan, L.Y. (2000). A trafficking checkpoint controls GABA(B) receptor heterodimerization. Neuron *27*, 97–106.

Marinissen, M.J., and Gutkind, J.S. (2001). G-protein-coupled receptors and signaling networks: emerging paradigms. Trends Pharmacol. Sci. *22*, 368–376.

Marques, S., Batalha, V.L., Lopes, L.V., and Outeiro, T.F. (2011). Modulating Alzheimer's disease through caffeine: a putative link to epigenetics. J. Alzheimers Dis. *24 Suppl 2*, 161–171.

Marsh, J.L., Pallos, J., and Thompson, L.M. (2003). Fly models of Huntington's disease. Hum. Mol. Genet. *12 Spec No 2*, R187–193.

Marshall, G.R. (2001). Peptide interactions with G-protein coupled receptors. Biopolymers *60*, 246–277.

Marsicano, G., Goodenough, S., Monory, K., Hermann, H., Eder, M., Cannich, A., Azad, S.C., Cascio, M.G., Gutiérrez, S.O., van der Stelt, M., et al. (2003). CB1 cannabinoid receptors and on-demand defense against excitotoxicity. Science *302*, 84–88.

Martín, A.B., Fernandez-Espejo, E., Ferrer, B., Gorriti, M.A., Bilbao, A., Navarro, M., Rodriguez de Fonseca, F., and Moratalla, R. (2008). Expression and function of CB1 receptor in the rat striatum: localization and effects on D1 and D2 dopamine receptor-mediated motor behaviors. Neuropsychopharmacology *33*, 1667–1679.

Martinez-Mir, M.I., Probst, A., and Palacios, J.M. (1991). Adenosine A2 receptors: selective localization in the human basal ganglia and alterations with disease. Neuroscience *42*, 697–706.

Martire, A., Calamandrei, G., Felici, F., Scattoni, M.L., Lastoria, G., Domenici, M.R., Tebano, M.T., and Popoli, P. (2007). Opposite effects of the A2A receptor agonist CGS21680 in the striatum of Huntington's disease versus wild-type mice. Neurosci. Lett. *417*, 78–83.

Martire, A., Tebano, M.T., Chiodi, V., Ferreira, S.G., Cunha, R.A., Köfalvi, A., and Popoli, P. (2011). Pre-synaptic adenosine A2A receptors control cannabinoid CB1 receptor-mediated inhibition of striatal glutamatergic neurotransmission. J. Neurochem. *116*, 273–280.

Mary, S., Damian, M., Louet, M., Floquet, N., Fehrentz, J.-A., Marie, J., Martinez, J., and Banères, J.-L. (2012). Ligands and signaling proteins govern the conformational landscape explored by a G protein-coupled receptor. Proc Natl Acad Sci U S A *109*, 8304–8309.

Di Marzo, V., Bifulco, M., and De Petrocellis, L. (2004). The endocannabinoid system and its therapeutic exploitation. Nat Rev Drug Discov *3*, 771–784.

Matsuda, L.A., Lolait, S.J., Brownstein, M.J., Young, A.C., and Bonner, T.I. (1990). Structure of a cannabinoid receptor and functional expression of the cloned cDNA. Nature *346*, 561–564.

Mattera, R., Pitts, B.J., Entman, M.L., and Birnbaumer, L. (1985). Guanine nucleotide regulation of a mammalian myocardial muscarinic receptor system. Evidence for homo- and heterotropic cooperativity in ligand binding analyzed by computer-assisted curve fitting. J. Biol. Chem. *260*, 7410–7421.

Mátyás, F., Yanovsky, Y., Mackie, K., Kelsch, W., Misgeld, U., and Freund, T.F. (2006). Subcellular localization of type 1 cannabinoid receptors in the rat basal ganglia. Neuroscience *137*, 337–361.

Maurice, P., Daulat, A.M., Turecek, R., Ivankova-Susankova, K., Zamponi, F., Kamal, M., Clement, N., Guillaume, J.-L., Bettler, B., Galès, C., et al. (2010). Molecular organization and dynamics of the melatonin MT1 receptor/RGS20/Gi protein complex reveal asymmetry of receptor dimers for RGS and Gi coupling. EMBO J *29*, 3646–3659.

Maurice, P., Kamal, M., and Jockers, R. (2011). Asymmetry of GPCR oligomers supports their functional relevance. Trends Pharmacol. Sci. *32*, 514–520.

McAllister, S.D., and Glass, M. (2002). CB(1) and CB(2) receptor-mediated signalling: a focus on endocannabinoids. Prostaglandins Leukot. Essent. Fatty Acids *66*, 161–171.

McCaw, E.A., Hu, H., Gomez, G.T., Hebb, A.L.O., Kelly, M.E.M., and Denovan-Wright, E.M. (2004). Structure, expression and regulation of the cannabinoid receptor gene (CB1) in Huntington's disease transgenic mice. Eur. J. Biochem. *271*, 4909–4920.

McVey, M., Ramsay, D., Kellett, E., Rees, S., Wilson, S., Pope, A.J., and Milligan, G. (2001). Monitoring receptor oligomerization using time-resolved fluorescence resonance energy transfer and bioluminescence resonance energy transfer. The human delta -opioid receptor displays constitutive oligomerization at the cell surface, which is not regulated by receptor occupancy. J. Biol. Chem. *276*, 14092–14099.

Mende-Mueller, L.M., Toneff, T., Hwang, S.R., Chesselet, M.F., and Hook, V.Y. (2001). Tissue-specific proteolysis of Huntingtin (htt) in human brain: evidence of enhanced levels of N- and C-terminal htt fragments in Huntington's disease striatum. J. Neurosci. *21*, 1830–1837.

Mercuri, N.B., Saiardi, A., Bonci, A., Picetti, R., Calabresi, P., Bernardi, G., and Borrelli, E. (1997). Loss of autoreceptor function in dopaminergic neurons from dopamine D2 receptor deficient mice. Neuroscience *79*, 323–327.

Mievis, S., Blum, D., and Ledent, C. (2011). A2A receptor knockout worsens survival and motor behaviour in a transgenic mouse model of Huntington's disease. Neurobiol. Dis. *41*, 570–576.

Millan, M.J. (2010). From the cell to the clinic: a comparative review of the partial D_2/D_3receptor agonist and α2-adrenoceptor antagonist, piribedil, in the treatment of Parkinson's disease. Pharmacol. Ther. *128*, 229–273.

Milligan, G., and Bouvier, M. (2005). Methods to monitor the quaternary structure of G protein-coupled receptors. FEBS J. *272*, 2914–2925.

Milligan, G., and Kostenis, E. (2006). Heterotrimeric G-proteins: a short history. Br. J. Pharmacol. *147 Suppl 1*, S46–55.

Minelli, A., Brecha, N.C., Karschin, C., DeBiasi, S., and Conti, F. (1995). GAT-1, a high-affinity GABA plasma membrane transporter, is localized to neurons and astroglia in the cerebral cortex. J. Neurosci. *15*, 7734–7746.

Minelli, A., DeBiasi, S., Brecha, N.C., Zuccarello, L.V., and Conti, F. (1996). GAT-3, a high-affinity GABA plasma membrane transporter, is localized to astrocytic processes, and it is not confined to the vicinity of GABAergic synapses in the cerebral cortex. J. Neurosci. *16*, 6255–6264.

Minghetti, L., Greco, A., Potenza, R.L., Pezzola, A., Blum, D., Bantubungi, K., and Popoli, P. (2007). Effects of the adenosine A2A receptor antagonist SCH 58621 on cyclooxygenase-2 expression, glial activation, and brain-derived neurotrophic factor availability in a rat model of striatal neurodegeneration. J. Neuropathol. Exp. Neurol. *66*, 363–371.

Missale, C., Nash, S.R., Robinson, S.W., Jaber, M., and Caron, M.G. (1998). Dopamine receptors: from structure to function. Physiol. Rev. *78*, 189–225.

Mizuno, Y., Hasegawa, K., Kondo, T., Kuno, S., and Yamamoto, M. (2010). Clinical efficacy of istradefylline (KW-6002) in Parkinson's disease: a randomized, controlled study. Mov. Disord. *25*, 1437–1443.

Monory, K., Blaudzun, H., Massa, F., Kaiser, N., Lemberger, T., Schütz, G., Wotjak, C.T., Lutz, B., and Marsicano, G. (2007). Genetic Dissection of Behavioural and Autonomic Effects of Δ9-Tetrahydrocannabinol in Mice. PLoS Biol *5*.

Moreau, J.L., and Huber, G. (1999). Central adenosine A(2A) receptors: an overview. Brain Res. Brain Res. Rev. *31*, 65–82.

Moreno, E., Hoffmann, H., Gonzalez-Sepúlveda, M., Navarro, G., Casadó, V., Cortés, A., Mallol, J., Vignes, M., McCormick, P.J., Canela, E.I., et al. (2011). Dopamine D1-histamine H3 Receptor Heteromers Provide a Selective Link to MAPK Signaling in GABAergic Neurons of the Direct Striatal Pathway. J Biol Chem *286*, 5846–5854.

Muller, C., and Ferre, S. (2007). Blocking Striatal Adenosine A2A Receptors: A New Strategy for Basal Ganglia Disorders. Recent Patents on CNS Drug Discovery *2*, 1–21.

Mundell, S., and Kelly, E. (2011). Adenosine receptor desensitization and trafficking. Biochim. Biophys. Acta *1808*, 1319–1328.

Munro, S., Thomas, K.L., and Abu-Shaar, M. (1993). Molecular characterization of a peripheral receptor for cannabinoids. Nature *365*, 61–65.

Murakami, M., and Kouyama, T. (2008). Crystal structure of squid rhodopsin. Nature *453*, 363–367.

Nasir, J., Floresco, S.B., O'Kusky, J.R., Diewert, V.M., Richman, J.M., Zeisler, J., Borowski, A., Marth, J.D., Phillips, A.G., and Hayden, M.R. (1995). Targeted disruption of the Huntington's disease gene results in embryonic lethality and behavioral and morphological changes in heterozygotes. Cell *81*, 811–823.

Navarro, G., Carriba, P., Gandía, J., Ciruela, F., Casadó, V., Cortés, A., Mallol, J., Canela, E.I., Lluis, C., and Franco, R. (2008). Detection of heteromers formed by

cannabinoid CB1, dopamine D2, and adenosine A2A G-protein-coupled receptors by combining bimolecular fluorescence complementation and bioluminescence energy transfer. ScientificWorldJournal *8*, 1088–1097.

Navarro, G., Aymerich, M.S., Marcellino, D., Cortés, A., Casadó, V., Mallol, J., Canela, E.I., Agnati, L., Woods, A.S., Fuxe, K., et al. (2009). Interactions between Calmodulin, Adenosine A2A, and Dopamine D2 Receptors. J Biol Chem *284*, 28058–28068.

Navarro, G., Ferré, S., Cordomi, A., Moreno, E., Mallol, J., Casadó, V., Cortés, A., Hoffmann, H., Ortiz, J., Canela, E.I., et al. (2010a). Interactions between Intracellular Domains as Key Determinants of the Quaternary Structure and Function of Receptor Heteromers. J Biol Chem *285*, 27346–27359.

Navarro, G., Moreno, E., Aymerich, M., Marcellino, D., McCormick, P.J., Mallol, J., Cortés, A., Casadó, V., Canela, E.I., Ortiz, J., et al. (2010b). Direct involvement of σ-1 receptors in the dopamine D1 receptor-mediated effects of cocaine. Proc Natl Acad Sci U S A *107*, 18676–18681.

Neuwald, A.F., and Hirano, T. (2000). HEAT repeats associated with condensins, cohesins, and other complexes involved in chromosome-related functions. Genome Res. *10*, 1445–1452.

Ng, G.Y., O'Dowd, B.F., Lee, S.P., Chung, H.T., Brann, M.R., Seeman, P., and George, S.R. (1996). Dopamine D2 receptor dimers and receptor-blocking peptides. Biochem. Biophys. Res. Commun. *227*, 200–204.

Nicola, S.M. (2007). The nucleus accumbens as part of a basal ganglia action selection circuit. Psychopharmacology (Berl.) *191*, 521–550.

Nicola, S.M., Surmeier, J., and Malenka, R.C. (2000). Dopaminergic modulation of neuronal excitability in the striatum and nucleus accumbens. Annu. Rev. Neurosci. *23*, 185–215.

Nie, J., and Lewis, D.L. (2001). Structural domains of the CB1 cannabinoid receptor that contribute to constitutive activity and G-protein sequestration. J. Neurosci. *21*, 8758–8764.

Nishi, A., Bibb, J.A., Snyder, G.L., Higashi, H., Nairn, A.C., and Greengard, P. (2000). Amplification of dopaminergic signaling by a positive feedback loop. Proc. Natl. Acad. Sci. U.S.A. *97*, 12840–12845.

Nishi, A., Liu, F., Matsuyama, S., Hamada, M., Higashi, H., Nairn, A.C., and Greengard, P. (2003). Metabotropic mGlu5 receptors regulate adenosine A2A receptor signaling. Proc. Natl. Acad. Sci. U.S.A. *100*, 1322–1327.

Nobles, M., Benians, A., and Tinker, A. (2005). Heterotrimeric G proteins precouple with G protein-coupled receptors in living cells. Proc Natl Acad Sci U S A *102*, 18706–18711.

Núñez, E., Benito, C., Pazos, M.R., Barbachano, A., Fajardo, O., González, S., Tolón, R.M., and Romero, J. (2004). Cannabinoid CB2 receptors are expressed by perivascular microglial cells in the human brain: an immunohistochemical study. Synapse *53*, 208–213.

O'Hara, P.J., Sheppard, P.O., Thøgersen, H., Venezia, D., Haldeman, B.A., McGrane, V., Houamed, K.M., Thomsen, C., Gilbert, T.L., and Mulvihill, E.R. (1993). The ligand-binding domain in metabotropic glutamate receptors is related to bacterial periplasmic binding proteins. Neuron *11*, 41–52.

O'Kane, E.M., and Stone, T.W. (1998). Interaction between adenosine A1 and A2 receptor-mediated responses in the rat hippocampus in vitro. Eur. J. Pharmacol. *362*, 17–25.

Obeso, J.A., and Lanciego, J.L. (2011). Past, present, and future of the pathophysiological model of the Basal Ganglia. Front Neuroanat *5*, 39.

Obeso, J.A., Rodríguez-Oroz, M.C., Rodríguez, M., Arbizu, J., and Giménez-Amaya, J.M. (2002). The basal ganglia and disorders of movement: pathophysiological mechanisms. News Physiol. Sci. *17*, 51–55.

Ohno-Shosaku, T., Maejima, T., and Kano, M. (2001). Endogenous cannabinoids mediate retrograde signals from depolarized postsynaptic neurons to presynaptic terminals. Neuron *29*, 729–738.

Ohrt, T., Staroske, W., Mütze, J., Crell, K., Landthaler, M., and Schwille, P. (2011). Fluorescence Cross-Correlation Spectroscopy Reveals Mechanistic Insights into the Effect of 2′-O-Methyl Modified siRNAs in Living Cells. Biophys J *100*, 2981–2990.

Okada, M., Nutt, D.J., Murakami, T., Zhu, G., Kamata, A., Kawata, Y., and Kaneko, S. (2001). Adenosine receptor subtypes modulate two major functional pathways for hippocampal serotonin release. J. Neurosci. *21*, 628–640.

Okamoto, Y., Morishita, J., Tsuboi, K., Tonai, T., and Ueda, N. (2004). Molecular characterization of a phospholipase D generating anandamide and its congeners. J. Biol. Chem. *279*, 5298–5305.

Olah, M.E. (1997). Identification of A2a adenosine receptor domains involved in selective coupling to Gs. Analysis of chimeric A1/A2a adenosine receptors. J. Biol. Chem. *272*, 337–344.

Onaran, H.O., Costa, T., and Rodbard, D. (1993). Beta gamma subunits of guanine nucleotide-binding proteins and regulation of spontaneous receptor activity: thermodynamic model for the interaction between receptors and guanine nucleotide-binding protein subunits. Mol. Pharmacol. *43*, 245–256.

Ongini, E., Dionisotti, S., Gessi, S., Irenius, E., and Fredholm, B.B. (1999). Comparison of CGS 15943, ZM 241385 and SCH 58261 as antagonists at human adenosine receptors. Naunyn Schmiedebergs Arch. Pharmacol. *359*, 7–10.

Orban, T., Jastrzebska, B., Gupta, S., Wang, B., Miyagi, M., Chance, M.R., and Palczewski, K. (2012). Conformational dynamics of activation for the pentameric complex of dimeric G protein-coupled receptor and heterotrimeric G protein. Structure *20*, 826–840.

Orru, M., Bakešová, J., Brugarolas, M., Quiroz, C., Beaumont, V., Goldberg, S.R., Lluís, C., Cortés, A., Franco, R., Casadó, V., et al. (2011). Striatal Pre- and Postsynaptic Profile of Adenosine A2A Receptor Antagonists. PLoS ONE *6*, e16088.

Ossowska, K., Konieczny, J., Wolfarth, S., Wierońska, J., and Pilc, A. (2001). Blockade of the metabotropic glutamate receptor subtype 5 (mGluR5) produces antiparkinsonian-like effects in rats. Neuropharmacology *41*, 413–420.

Pak, Y., O'Dowd, B.F., Wang, J.B., and George, S.R. (1999). Agonist-induced, G protein-dependent and -independent down-regulation of the mu opioid receptor. The receptor is a direct substrate for protein-tyrosine kinase. J. Biol. Chem. *274*, 27610–27616.

Palczewski, K., Kumasaka, T., Hori, T., Behnke, C.A., Motoshima, H., Fox, B.A., Le Trong, I., Teller, D.C., Okada, T., Stenkamp, R.E., et al. (2000). Crystal structure of rhodopsin: A G protein-coupled receptor. Science *289*, 739–745.

Palmer, T.M., and Stiles, G.L. (1995). Adenosine receptors. Neuropharmacology *34*, 683–694.

Palmer, T.M., Gettys, T.W., Jacobson, K.A., and Stiles, G.L. (1994). Desensitization of the canine A2a adenosine receptor: delineation of multiple processes. Mol. Pharmacol. *45*, 1082–1094.

Paulmurugan, R., and Gambhir, S.S. (2003). Monitoring protein-protein interactions using split synthetic renilla luciferase protein-fragment-assisted complementation. Anal. Chem. *75*, 1584–1589.

Pazos, M.R., Sagredo, O., and Fernández-Ruiz, J. (2008). The endocannabinoid system in Huntington's disease. Curr. Pharm. Des. *14*, 2317–2325.

Pedata, F., Gianfriddo, M., Turchi, D., and Melani, A. (2005). The protective effect of adenosine A2A receptor antagonism in cerebral ischemia. Neurol. Res. *27*, 169–174.

Penney, J.B., Jr, and Young, A.B. (1986). Striatal inhomogeneities and basal ganglia function. Mov. Disord. *1*, 3–15.

Perreault, M.L., O'Dowd, B.F., and George, S.R. (2011). Dopamine receptor homooligomers and heterooligomers in schizophrenia. CNS Neurosci Ther *17*, 52–57.

Pertwee, R.G. (1997). Pharmacology of cannabinoid CB1 and CB2 receptors. Pharmacol. Ther. *74*, 129–180.

Perutz, M.F., Johnson, T., Suzuki, M., and Finch, J.T. (1994). Glutamine repeats as polar zippers: their possible role in inherited neurodegenerative diseases. Proc. Natl. Acad. Sci. U.S.A. *91*, 5355–5358.

Peterfreund, R.A., MacCollin, M., Gusella, J., and Fink, J.S. (1996). Characterization and expression of the human A2a adenosine receptor gene. J. Neurochem. *66*, 362–368.

Pfeiffer, M., Kirscht, S., Stumm, R., Koch, T., Wu, D., Laugsch, M., Schröder, H., Höllt, V., and Schulz, S. (2003). Heterodimerization of substance P and mu-opioid receptors regulates receptor trafficking and resensitization. J. Biol. Chem. *278*, 51630–51637.

Pfleger, K.D.G., and Eidne, K.A. (2005). Monitoring the formation of dynamic G-protein-coupled receptor-protein complexes in living cells. Biochem. J. *385*, 625–637.

Phelps, P.E., Houser, C.R., and Vaughn, J.E. (1985). Immunocytochemical localization of choline acetyltransferase within the rat neostriatum: a correlated light and electron microscopic study of cholinergic neurons and synapses. J. Comp. Neurol. *238*, 286–307.

Phillis, J.W., Edstrom, J.P., Kostopoulos, G.K., and Kirkpatrick, J.R. (1979). Effects of adenosine and adenine nucleotides on synaptic transmission in the cerebral cortex. Can. J. Physiol. Pharmacol. *57*, 1289–1312.

Pickel, V.M., Chan, J., Kash, T.L., Rodríguez, J.J., and MacKie, K. (2004). Compartment-specific localization of cannabinoid 1 (CB1) and mu-opioid receptors in rat nucleus accumbens. Neuroscience *127*, 101–112.

Pickel, V.M., Chan, J., Kearn, C.S., and Mackie, K. (2006). Targeting dopamine D2 and cannabinoid-1 (CB1) receptors in rat nucleus accumbens. J. Comp. Neurol. *495*, 299–313.

Pierce, K.L., and Lefkowitz, R.J. (2001). Classical and new roles of beta-arrestins in the regulation of G-protein-coupled receptors. Nat. Rev. Neurosci. *2*, 727–733.

Pignatelli, M., Cortés-Canteli, M., Santos, A., and Perez-Castillo, A. (1999). Involvement of the NGFI-A gene in the differentiation of neuroblastoma cells. FEBS Lett. *461*, 37–42.

Pignatelli, M., Luna-Medina, R., Pérez-Rendón, A., Santos, A., and Perez-Castillo, A. (2003). The transcription factor early growth response factor-1 (EGR-1) promotes apoptosis of neuroblastoma cells. Biochem. J. *373*, 739–746.

Pin, J.-P., Neubig, R., Bouvier, M., Devi, L., Filizola, M., Javitch, J.A., Lohse, M.J., Milligan, G., Palczewski, K., Parmentier, M., et al. (2007). International Union of Basic and Clinical Pharmacology. LXVII. Recommendations for the recognition and nomenclature of G protein-coupled receptor heteromultimers. Pharmacol. Rev. *59*, 5–13.

Pinna, A. (2009). Novel investigational adenosine A 2A receptor antagonists for Parkinson's disease. Expert Opinion on Investigational Drugs *18*, 1619–1631.

Pinna, A., Corsi, C., Carta, A.R., Valentini, V., Pedata, F., and Morelli, M. (2002). Modification of adenosine extracellular levels and adenosine A(2A) receptor mRNA by dopamine denervation. Eur. J. Pharmacol. *446*, 75–82.

Piomelli, D. (2003). The molecular logic of endocannabinoid signalling. Nat. Rev. Neurosci. *4*, 873–884.

Pittenger, C., Fasano, S., Mazzocchi-Jones, D., Dunnett, S.B., Kandel, E.R., and Brambilla, R. (2006). Impaired bidirectional synaptic plasticity and procedural memory formation in striatum-specific cAMP response element-binding protein-deficient mice. J. Neurosci. *26*, 2808–2813.

Pivonello, R., Ferone, D., Lombardi, G., Colao, A., Lamberts, S.W.J., and Hofland, L.J. (2007). Novel insights in dopamine receptor physiology. Eur. J. Endocrinol. *156 Suppl 1*, S13–21.

Popoli, P., Pèzzola, A., Domenici, M.R., Sagratella, S., Diana, G., Caporali, M.G., Bronzetti, E., Vega, J., and Scotti de Carolis, A. (1994). Behavioral and electrophysiological correlates of the quinolinic acid rat model of Huntington's disease in rats. Brain Res. Bull. *35*, 329–335.

Popoli, P., Pèzzola, A., Torvinen, M., Reggio, R., Pintor, A., Scarchilli, L., Fuxe, K., and Ferré, S. (2001). The selective mGlu(5) receptor agonist CHPG inhibits quinpirole-induced turning in 6-hydroxydopamine-lesioned rats and modulates the binding characteristics of dopamine D(2) receptors in the rat striatum: interactions with adenosine A(2a) receptors. Neuropsychopharmacology *25*, 505–513.

Popoli, P., Pintor, A., Domenici, M.R., Frank, C., Tebano, M.T., Pèzzola, A., Scarchilli, L., Quarta, D., Reggio, R., Malchiodi-Albedi, F., et al. (2002). Blockade of striatal adenosine A2A receptor reduces, through a presynaptic mechanism, quinolinic acid-induced excitotoxicity: possible relevance to neuroprotective interventions in neurodegenerative diseases of the striatum. J. Neurosci. *22*, 1967–1975.

Popoli, P., Minghetti, L., Tebano, M.T., Pintor, A., Domenici, M.R., and Massotti, M. (2004). Adenosine A2A receptor antagonism and neuroprotection: mechanisms, lights, and shadows. Crit Rev Neurobiol *16*, 99–106.

Popoli, P., Pepponi, R., Martire, A., Armida, M., Pèzzola, A., Galluzzo, M., Domenici, M.R., Potenza, R.L., Tebano, M.T., Mollinari, C., et al. (2007a). Neuroprotective effects of thymosin beta4 in experimental models of excitotoxicity. Ann. N. Y. Acad. Sci. *1112*, 219–224.

Popoli, P., Blum, D., Martire, A., Ledent, C., Ceruti, S., and Abbracchio, M.P. (2007b). Functions, dysfunctions and possible therapeutic relevance of adenosine A2A receptors in Huntington's disease. Prog. Neurobiol. *81*, 331–348.

Porter, A.C., Sauer, J.-M., Knierman, M.D., Becker, G.W., Berna, M.J., Bao, J., Nomikos, G.G., Carter, P., Bymaster, F.P., Leese, A.B., et al. (2002). Characterization of a novel endocannabinoid, virodhamine, with antagonist activity at the CB1 receptor. J. Pharmacol. Exp. Ther. *301*, 1020–1024.

Pourcher, E., Fernandez, H.H., Stacy, M., Mori, A., Ballerini, R., and Chaikin, P. (2012). Istradefylline for Parkinson's disease patients experiencing motor fluctuations: results of the KW-6002-US-018 study. Parkinsonism Relat. Disord. *18*, 178–184.

Prinster, S.C., Hague, C., and Hall, R.A. (2005). Heterodimerization of g protein-coupled receptors: specificity and functional significance. Pharmacol. Rev. *57*, 289–298.

Probst, W.C., Snyder, L.A., Schuster, D.I., Brosius, J., and Sealfon, S.C. (1992). Sequence alignment of the G-protein coupled receptor superfamily. DNA Cell Biol. *11*, 1–20.

Pull, I., and McIlwain, H. (1972). Adenine derivatives as neurohumoral agents in the brain. The quantities liberated on excitation of superfused cerebral tissues. Biochem. J. *130*, 975–981.

Quarta, D., Ferré, S., Solinas, M., You, Z.-B., Hockemeyer, J., Popoli, P., and Goldberg, S.R. (2004a). Opposite modulatory roles for adenosine A1 and A2A receptors on glutamate and dopamine release in the shell of the nucleus accumbens. Effects of chronic caffeine exposure. Journal of Neurochemistry *88*, 1151–1158.

Quarta, D., Borycz, J., Solinas, M., Patkar, K., Hockemeyer, J., Ciruela, F., Lluís, C., Franco, R., Woods, A.S., Goldberg, S.R., et al. (2004b). Adenosine receptor-mediated modulation of dopamine release in the nucleus accumbens depends on glutamate neurotransmission and N-methyl-D-aspartate receptor stimulation. J. Neurochem. *91*, 873–880.

Quiroz, C., Luján, R., Uchigashima, M., Simoes, A.P., Lerner, T.N., Borycz, J., Kachroo, A., Canas, P.M., Orru, M., Schwarzschild, M.A., et al. (2009). Key Modulatory Role of Presynaptic Adenosine A2A Receptors in Cortical Neurotransmission to the Striatal Direct Pathway. ScientificWorldJournal *9*, 1321–1344.

Quiroz, C., Pearson, V., Gulyani, S., Allen, R., Earley, C., and Ferré, S. (2010). Up-regulation of striatal adenosine A2A receptors with iron deficiency in rats. Effects on locomotion and cortico-striatal neurotransmission. Exp Neurol *224*, 292–298.

Ramkumar, V., Olah, M.E., Jacobson, K.A., and Stiles, G.L. (1991). Distinct pathways of desensitization of A1- and A2-adenosine receptors in DDT1 MF-2 cells. Mol. Pharmacol. *40*, 639–647.

Rashid, A.J., So, C.H., Kong, M.M.C., Furtak, T., El-Ghundi, M., Cheng, R., O'Dowd, B.F., and George, S.R. (2007). D1–D2 dopamine receptor heterooligomers with unique pharmacology are coupled to rapid activation of Gq/11 in the striatum. Proc Natl Acad Sci U S A *104*, 654–659.

Rasmussen, S.G.F., DeVree, B.T., Zou, Y., Kruse, A.C., Chung, K.Y., Kobilka, T.S., Thian, F.S., Chae, P.S., Pardon, E., Calinski, D., et al. (2011). Crystal Structure of the β2Adrenergic Receptor-Gs protein complex. Nature *477*, 549–555.

Rebola, N., Porciúncula, L.O., Lopes, L.V., Oliveira, C.R., Soares-da-Silva, P., and Cunha, R.A. (2005a). Long-term effect of convulsive behavior on the density of adenosine A1 and A 2A receptors in the rat cerebral cortex. Epilepsia *46 Suppl 5*, 159–165.

Rebola, N., Canas, P.M., Oliveira, C.R., and Cunha, R.A. (2005b). Different synaptic and subsynaptic localization of adenosine A2A receptors in the hippocampus and striatum of the rat. Neuroscience *132*, 893–903.

Reggio, R., Pèzzola, A., and Popoli, P. (1999). The intrastratial injection of an adenosine A(2) receptor antagonist prevents frontal cortex EEG abnormalities in a rat model of Huntington's disease. Brain Res. *831*, 315–318.

Reiner, A., Albin, R.L., Anderson, K.D., D'Amato, C.J., Penney, J.B., and Young, A.B. (1988). Differential loss of striatal projection neurons in Huntington disease. Proc. Natl. Acad. Sci. U.S.A. *85*, 5733–5737.

Reiner, A., Arant, R.J., and Isacoff, E.Y. (2012). Assembly Stoichiometry of the GluK2/GluK5 Kainate Receptor Complex. Cell Reports *1*, 234–240.

Rekas, A., Alattia, J.-R., Nagai, T., Miyawaki, A., and Ikura, M. (2002). Crystal structure of venus, a yellow fluorescent protein with improved maturation and reduced environmental sensitivity. J. Biol. Chem. *277*, 50573–50578.

Ribeiro, J.A., and Sebastião, A.M. (1987). On the role, inactivation and origin of endogenous adenosine at the frog neuromuscular junction. J Physiol *384*, 571–585.

Richfield, E.K., Maguire-Zeiss, K.A., Vonkeman, H.E., and Voorn, P. (1995). Preferential loss of preproenkephalin versus preprotachykinin neurons from the striatum of Huntington's disease patients. Ann. Neurol. *38*, 852–861.

Rigamonti, D., Bauer, J.H., De-Fraja, C., Conti, L., Sipione, S., Sciorati, C., Clementi, E., Hackam, A., Hayden, M.R., Li, Y., et al. (2000). Wild-type huntingtin protects from apoptosis upstream of caspase-3. J. Neurosci. *20*, 3705–3713.

Van Rijn, R.M., Whistler, J.L., and Waldhoer, M. (2010). Novel pharmaco-types and trafficking-types induced by opioid receptor heteromerization. Curr Opin Pharmacol *10*, 73–79.

Rivero-Müller, A., Chou, Y.-Y., Ji, I., Lajic, S., Hanyaloglu, A.C., Jonas, K., Rahman, N., Ji, T.H., and Huhtaniemi, I. (2010). Rescue of defective G protein-coupled receptor function in vivo by intermolecular cooperation. Proc. Natl. Acad. Sci. U.S.A. *107*, 2319–2324.

Rivkees, S.A. (1995). The ontogeny of cardiac and neural A1 adenosine receptor expression in rats. Brain Res. Dev. Brain Res. *89*, 202–213.

Rivkees, S.A., Barbhaiya, H., and IJzerman, A.P. (1999). Identification of the adenine binding site of the human A1 adenosine receptor. J. Biol. Chem. *274*, 3617–3621.

Robbins, M.J., Ciruela, F., Rhodes, A., and McIlhinney, R.A. (1999). Characterization of the dimerization of metabotropic glutamate receptors using an N-terminal truncation of mGluR1alpha. J. Neurochem. *72*, 2539–2547.

Robitaille, M., Héroux, I., Baragli, A., and Hébert, T.E. (2009). Novel tools for use in bioluminescence resonance energy transfer (BRET) assays. Methods Mol. Biol. *574*, 215–234.

Rocheville, M., Lange, D.C., Kumar, U., Sasi, R., Patel, R.C., and Patel, Y.C. (2000a). Subtypes of the somatostatin receptor assemble as functional homo- and heterodimers. J. Biol. Chem. *275*, 7862–7869.

Rocheville, M., Lange, D.C., Kumar, U., Patel, S.C., Patel, R.C., and Patel, Y.C. (2000b). Receptors for dopamine and somatostatin: formation of hetero-oligomers with enhanced functional activity. Science *288*, 154–157.

Rodriguez, J.J., Mackie, K., and Pickel, V.M. (2001). Ultrastructural localization of the CB1 cannabinoid receptor in mu-opioid receptor patches of the rat Caudate putamen nucleus. J. Neurosci. *21*, 823–833.

Romano, C., Yang, W.L., and O'Malley, K.L. (1996). Metabotropic glutamate receptor 5 is a disulfide-linked dimer. J. Biol. Chem. *271*, 28612–28616.

Romano, C., Miller, J.K., Hyrc, K., Dikranian, S., Mennerick, S., Takeuchi, Y., Goldberg, M.P., and O'Malley, K.L. (2001). Covalent and noncovalent interactions mediate metabotropic glutamate receptor mGlu5 dimerization. Mol. Pharmacol. *59*, 46–53.

Rosin, D.L., Robeva, A., Woodard, R.L., Guyenet, P.G., and Linden, J. (1998). Immunohistochemical localization of adenosine A2A receptors in the rat central nervous system. J. Comp. Neurol. *401*, 163–186.

Rosin, D.L., Hettinger, B.D., Lee, A., and Linden, J. (2003). Anatomy of adenosine A2A receptors in brain: morphological substrates for integration of striatal function. Neurology *61*, S12–18.

Rouge-Pont, F., Usiello, A., Benoit-Marand, M., Gonon, F., Piazza, P.V., and Borrelli, E. (2002). Changes in extracellular dopamine induced by morphine and cocaine: crucial control by D2 receptors. J. Neurosci. *22*, 3293–3301.

Sakmar, T.P. (1998). Rhodopsin: a prototypical G protein-coupled receptor. Prog. Nucleic Acid Res. Mol. Biol. *59*, 1–34.

Salim, H., Ferré, S., Dalal, A., Peterfreund, R.A., Fuxe, K., Vincent, J.D., and Lledo, P.M. (2000). Activation of adenosine A1 and A2A receptors modulates dopamine D2 receptor-induced responses in stably transfected human neuroblastoma cells. J. Neurochem. *74*, 432–439.

Samama, P., Cotecchia, S., Costa, T., and Lefkowitz, R.J. (1993). A mutation-induced activated state of the beta 2-adrenergic receptor. Extending the ternary complex model. J. Biol. Chem. *268*, 4625–4636.

Samama, P., Pei, G., Costa, T., Cotecchia, S., and Lefkowitz, R.J. (1994). Negative antagonists promote an inactive conformation of the beta 2-adrenergic receptor. Mol. Pharmacol. *45*, 390–394.

Sánchez, C., de Ceballos, M.L., Gomez del Pulgar, T., Rueda, D., Corbacho, C., Velasco, G., Galve-Roperh, I., Huffman, J.W., Ramón y Cajal, S., and Guzmán, M. (2001). Inhibition of glioma growth in vivo by selective activation of the CB(2) cannabinoid receptor. Cancer Res. *61*, 5784–5789.

Sarrió, S., Casadó, V., Escriche, M., Ciruela, F., Mallol, J., Canela, E.I., Lluis, C., and Franco, R. (2000). The Heat Shock Cognate Protein hsc73 Assembles with A1 Adenosine Receptors To Form Functional Modules in the Cell Membrane. Mol. Cell. Biol. *20*, 5164–5174.

Sauer, R., Maurinsh, J., Reith, U., Fülle, F., Klotz, K.N., and Müller, C.E. (2000). Water-soluble phosphate prodrugs of 1-propargyl-8-styrylxanthine derivatives, A(2A)-selective adenosine receptor antagonists. J. Med. Chem. *43*, 440–448.

Saura, C., Ciruela, F., Casadó, V., Canela, E.I., Mallol, J., Lluis, C., and Franco, R. (1996). Adenosine Deaminase Interacts with A1 Adenosine Receptors in Pig Brain Cortical Membranes. Journal of Neurochemistry *66*, 1675–1682.

Saura, C.A., Mallol, J., Canela, E.I., Lluis, C., and Franco, R. (1998). Adenosine deaminase and A1 adenosine receptors internalize together following agonist-induced receptor desensitization. J. Biol. Chem. *273*, 17610–17617.

Scarselli, M., Armogida, M., Chiacchio, S., DeMontis, M.G., Colzi, A., Corsini, G.U., and Maggio, R. (2000). Reconstitution of functional dopamine D(2s) receptor by co-expression of amino- and carboxyl-terminal receptor fragments. Eur. J. Pharmacol. *397*, 291–296.

Scarselli, M., Annibale, P., and Radenovic, A. (2012). Cell type-specific β2-adrenergic receptor clusters identified using photoactivated localization microscopy are not lipid raft related, but depend on actin cytoskeleton integrity. J. Biol. Chem. *287*, 16768–16780.

Scattoni, M.L., Valanzano, A., Pezzola, A., March, Z.D., Fusco, F.R., Popoli, P., and Calamandrei, G. (2007). Adenosine A2A receptor blockade before striatal excitotoxic lesions prevents long term behavioural disturbances in the quinolinic rat model of Huntington's disease. Behav. Brain Res. *176*, 216–221.

Schiffmann, S.N., and Vanderhaeghen, J.J. (1991). Does the absence of clinical expression of choreoathetosis, despite severe striatal atrophy, correlate with plasticity of neuropeptide synthesis? J. Neural Transm. Suppl. *33*, 99–103.

Schiffmann, S.N., Dassesse, D., d' Alcantara, P., Ledent, C., Swillens, S., and Zoli, M. (2003). A2A receptor and striatal cellular functions: regulation of gene expression, currents, and synaptic transmission. Neurology *61*, S24–29.

Schiffmann, S.N., Fisone, G., Moresco, R., Cunha, R.A., and Ferré, S. (2007). Adenosine A2A receptors and basal ganglia physiology. Prog Neurobiol *83*, 277–292.

Schmidt, T., Schütz, G.J., Baumgartner, W., Gruber, H.J., and Schindler, H. (1996). Imaging of single molecule diffusion. Proc Natl Acad Sci U S A *93*, 2926–2929.

Schousboe, A., and Waagepetersen, H.S. (2007). GABA: homeostatic and pharmacological aspects. Prog. Brain Res. *160*, 9–19.

Schröder, R., Janssen, N., Schmidt, J., Kebig, A., Merten, N., Hennen, S., Müller, A., Blättermann, S., Mohr-Andrä, M., Zahn, S., et al. (2010). Deconvolution of complex G protein-coupled receptor signaling in live cells using dynamic mass redistribution measurements. Nat. Biotechnol. *28*, 943–949.

Schubert, P., Reddington, M., and Kreutzberg, G.W. (1979). On the possible role of adenosine as a modulatory messenger in the hippocampus and other regions of the CNS. Prog. Brain Res. *51*, 149–165.

Schütz, G.J., Schindler, H., and Schmidt, T. (1997). Single-molecule microscopy on model membranes reveals anomalous diffusion. Biophysical Journal *73*, 1073–1080.

Schwarzschild, M.A., Chen, J.-F., and Ascherio, A. (2002). Caffeinated clues and the promise of adenosine A(2A) antagonists in PD. Neurology *58*, 1154–1160.

Schwarzschild, M.A., Agnati, L., Fuxe, K., Chen, J.-F., and Morelli, M. (2006). Targeting adenosine A2A receptors in Parkinson's disease. Trends Neurosci. *29*, 647–654.

Scotter, E.L., Goodfellow, C.E., Graham, E.S., Dragunow, M., and Glass, M. (2010). Neuroprotective potential of CB1 receptor agonists in an in vitro model of Huntington's disease. Br. J. Pharmacol. *160*, 747–761.

Sebastião, A.M., and Ribeiro, J.A. (2000). Fine-tuning neuromodulation by adenosine. Trends Pharmacol. Sci. *21*, 341–346.

Seeman, P., and Niznik, H.B. (1990). Dopamine receptors and transporters in Parkinson's disease and schizophrenia. FASEB J. *4*, 2737–2744.

Seidel, M.G., Klinger, M., Freissmuth, M., and Höller, C. (1999). Activation of mitogen-activated protein kinase by the A(2A)-adenosine receptor via a rap1-dependent and via a p21(ras)-dependent pathway. J. Biol. Chem. *274*, 25833–25841.

Seifert, R., Wenzel-Seifert, K., and Kobilka, B.K. (1999). GPCR-Galpha fusion proteins: molecular analysis of receptor-G-protein coupling. Trends Pharmacol. Sci. *20*, 383–389.

Sfakianos, M.K., Eisman, A., Gourley, S.L., Bradley, W.D., Scheetz, A.J., Settleman, J., Taylor, J.R., Greer, C.A., Williamson, A., and Koleske, A.J. (2007). Inhibition of Rho via Arg and p190RhoGAP in the postnatal mouse hippocampus regulates dendritic spine maturation, synapse and dendrite stability, and behavior. J. Neurosci. *27*, 10982–10992.

Shen, H.-Y., Singer, P., Lytle, N., Wei, C.J., Lan, J.-Q., Williams-Karnesky, R.L., Chen, J.-F., Yee, B.K., and Boison, D. (2012). Adenosine augmentation ameliorates psychotic and cognitive endophenotypes of schizophrenia. J. Clin. Invest. *122*, 2567–2577.

Shen, W., Flajolet, M., Greengard, P., and Surmeier, D.J. (2008). Dichotomous dopaminergic control of striatal synaptic plasticity. Science *321*, 848–851.

Sheng, M., and Kim, E. (2000). The Shank family of scaffold proteins. J. Cell. Sci. *113 (Pt 11)*, 1851–1856.

Shenoy, S.K., and Lefkowitz, R.J. (2003). Multifaceted roles of beta-arrestins in the regulation of seven-membrane-spanning receptor trafficking and signalling. Biochem. J. *375*, 503–515.

Shenoy, S.K., Drake, M.T., Nelson, C.D., Houtz, D.A., Xiao, K., Madabushi, S., Reiter, E., Premont, R.T., Lichtarge, O., and Lefkowitz, R.J. (2006). beta-arrestin-dependent, G protein-independent ERK1/2 activation by the beta2 adrenergic receptor. J. Biol. Chem. *281*, 1261–1273.

Shiflett, M.W., and Balleine, B.W. (2011). Contributions of ERK signaling in the striatum to instrumental learning and performance. Behav. Brain Res. *218*, 240–247.

Shimamura, T., Shiroishi, M., Weyand, S., Tsujimoto, H., Winter, G., Katritch, V., Abagyan, R., Cherezov, V., Liu, W., Han, G.W., et al. (2011). Structure of the human histamine H1 receptor complex with doxepin. Nature *475*, 65–70.

Shindou, T., Nonaka, H., Richardson, P.J., Mori, A., Kase, H., and Ichimura, M. (2002). Presynaptic adenosine A2A receptors enhance GABAergic synaptic transmission via a cyclic AMP dependent mechanism in the rat globus pallidus. Br. J. Pharmacol. *136*, 296–302.

Shire, D., Calandra, B., Delpech, M., Dumont, X., Kaghad, M., Le Fur, G., Caput, D., and Ferrara, P. (1996). Structural features of the central cannabinoid CB1 receptor involved in the binding of the specific CB1 antagonist SR 141716A. J. Biol. Chem. *271*, 6941–6946.

Smith, N.J., and Milligan, G. (2010). Allostery at G Protein-Coupled Receptor Homo- and Heteromers: Uncharted Pharmacological Landscapes. Pharmacol Rev *62*, 701–725.

Smith, R., Petersén, A., Bates, G.P., Brundin, P., and Li, J.-Y. (2005). Depletion of rabphilin 3A in a transgenic mouse model (R6/1) of Huntington's disease, a possible culprit in synaptic dysfunction. Neurobiol. Dis. *20*, 673–684.

Smith, R.J., Sam, L.M., Justen, J.M., Bundy, G.L., Bala, G.A., and Bleasdale, J.E. (1990). Receptor-coupled signal transduction in human polymorphonuclear neutrophils: effects of a novel inhibitor of phospholipase C-dependent processes on cell responsiveness. J. Pharmacol. Exp. Ther. *253*, 688–697.

Snel, J., and Lorist, M.M. (2011). Effects of caffeine on sleep and cognition. Prog. Brain Res. *190*, 105–117.

Sohy, D., Yano, H., de Nadai, P., Urizar, E., Guillabert, A., Javitch, J.A., Parmentier, M., and Springael, J.-Y. (2009). Hetero-oligomerization of CCR2, CCR5, and CXCR4 and the Protean Effects of "Selective" Antagonists. J Biol Chem *284*, 31270–31279.

Song, M.S., Shin, K.A., Kang, J.S., Lee, C.H., Shin, I.C., Lee, S., and Koh, H.C. (2002). The involvement of nitric oxide on the adenosine A(2) receptor-induced cardiovascular inhibitory responses in the posterior hypothalamus of rats. Neurosci. Lett. *326*, 41–45.

Soria, G., Castañé, A., Berrendero, F., Ledent, C., Parmentier, M., Maldonado, R., and Valverde, O. (2004). Adenosine A2A receptors are involved in physical dependence and place conditioning induced by THC. Eur. J. Neurosci. *20*, 2203–2213.

Soriano, A., Ventura, R., Molero, A., Hoen, R., Casadó, V., Cortés, A., Fanelli, F., Albericio, F., Lluís, C., Franco, R., et al. (2009). Adenosine A2A receptor-antagonist/dopamine D2 receptor-agonist bivalent ligands as pharmacological tools to detect A2A-D2 receptor heteromers. J. Med. Chem. *52*, 5590–5602.

Spano, P.F., Govoni, S., and Trabucchi, M. (1978). Studies on the pharmacological properties of dopamine receptors in various areas of the central nervous system. Adv. Biochem. Psychopharmacol. *19*, 155–165.

Stacy, M., Silver, D., Mendis, T., Sutton, J., Mori, A., Chaikin, P., and Sussman, N.M. (2008). A 12-week, placebo-controlled study (6002-US-006) of istradefylline in Parkinson disease. Neurology *70*, 2233–2240.

Steeves, T.D.L., and Fox, S.H. (2008). Neurobiological basis of serotonin-dopamine antagonists in the treatment of Gilles de la Tourette syndrome. Prog. Brain Res. *172*, 495–513.

Steffan, J.S., Agrawal, N., Pallos, J., Rockabrand, E., Trotman, L.C., Slepko, N., Illes, K., Lukacsovich, T., Zhu, Y.-Z., Cattaneo, E., et al. (2004). SUMO modification of Huntingtin and Huntington's disease pathology. Science *304*, 100–104.

Stehle, J.H., Rivkees, S.A., Lee, J.J., Weaver, D.R., Deeds, J.D., and Reppert, S.M. (1992). Molecular cloning and expression of the cDNA for a novel A2-adenosine receptor subtype. Mol. Endocrinol. *6*, 384–393.

Steindel, F., Lerner, R., Häring, M., Ruehle, S., Marsicano, G., Lutz, B., and Monory, K. (2013). Neuron-type specific cannabinoid-mediated G protein signalling in mouse hippocampus. J. Neurochem. *124*, 795–807.

Stella, N., and Piomelli, D. (2001). Receptor-dependent formation of endogenous cannabinoids in cortical neurons. Eur. J. Pharmacol. *425*, 189–196.

Stella, N., Schweitzer, P., and Piomelli, D. (1997). A second endogenous cannabinoid that modulates long-term potentiation. Nature *388*, 773–778.

Stone, T.W., Ceruti, S., and Abbracchio, M.P. (2009). Adenosine receptors and neurological disease: neuroprotection and neurodegeneration. Handb Exp Pharmacol 535–587.

Strömberg, I., Popoli, P., Müller, C.E., Ferré, S., and Fuxe, K. (2000). Electrophysiological and behavioural evidence for an antagonistic modulatory role of adenosine A2A receptors in dopamine D2 receptor regulation in the rat dopamine-denervated striatum. Eur. J. Neurosci. *12*, 4033–4037.

Stryer, L. (1978). Fluorescence energy transfer as a spectroscopic ruler. Annu. Rev. Biochem. *47*, 819–846.

Sugiura, T., Kondo, S., Sukagawa, A., Nakane, S., Shinoda, A., Itoh, K., Yamashita, A., and Waku, K. (1995). 2-Arachidonoylglycerol: a possible endogenous cannabinoid receptor ligand in brain. Biochem. Biophys. Res. Commun. *215*, 89–97.

Sukhatme, V.P., Cao, X.M., Chang, L.C., Tsai-Morris, C.H., Stamenkovich, D., Ferreira, P.C., Cohen, D.R., Edwards, S.A., Shows, T.B., and Curran, T. (1988). A zinc finger-encoding gene coregulated with c-fos during growth and differentiation, and after cellular depolarization. Cell *53*, 37–43.

Sun, Y., Savanenin, A., Reddy, P.H., and Liu, Y.F. (2001). Polyglutamine-expanded huntingtin promotes sensitization of N-methyl-D-aspartate receptors via post-synaptic density 95. J. Biol. Chem. *276*, 24713–24718.

Sunahara, R.K., Seeman, P., Van Tol, H.H., and Niznik, H.B. (1993). Dopamine receptors and antipsychotic drug response. Br J Psychiatry Suppl 31–38.

Svenningsson, P., Nergårdh, R., and Fredholm, B.B. (1998). Regional differences in the ability of caffeine to affect haloperidol-induced striatal c-fos mRNA expression in the rat. Neuropharmacology *37*, 331–337.

Svenningsson, P., Le Moine, C., Fisone, G., and Fredholm, B.B. (1999). Distribution, biochemistry and function of striatal adenosine A2A receptors. Prog. Neurobiol. *59*, 355–396.

Svenningsson, P., Lindskog, M., Ledent, C., Parmentier, M., Greengard, P., Fredholm, B.B., and Fisone, G. (2000). Regulation of the phosphorylation of the dopamine- and

cAMP-regulated phosphoprotein of 32 kDa in vivo by dopamine D1, dopamine D2, and adenosine A2A receptors. Proc Natl Acad Sci U S A *97*, 1856–1860.

Tadagaki, K., Jockers, R., and Kamal, M. (2012). History and Biological Significance of GPCR Heteromerization in the Neuroendocrine System. Neuroendocrinology *95*, 223–231.

Tarditi, A., Camurri, A., Varani, K., Borea, P.A., Woodman, B., Bates, G., Cattaneo, E., and Abbracchio, M.P. (2006). Early and transient alteration of adenosine A2A receptor signaling in a mouse model of Huntington disease. Neurobiol. Dis. *23*, 44–53.

Tebano, M.T., Martire, A., Chiodi, V., Pepponi, R., Ferrante, A., Domenici, M.R., Frank, C., Chen, J.-F., Ledent, C., and Popoli, P. (2009). Adenosine A2A receptors enable the synaptic effects of cannabinoid CB1 receptors in the rodent striatum. J. Neurochem. *110*, 1921–1930.

Temussi, P.A., Masino, L., and Pastore, A. (2003). From Alzheimer to Huntington: why is a structural understanding so difficult? EMBO J. *22*, 355–361.

Tepper, J.M., Tecuapetla, F., Koós, T., and Ibáñez-Sandoval, O. (2010). Heterogeneity and diversity of striatal GABAergic interneurons. Front Neuroanat *4*, 150.

Terrillon, S., and Bouvier, M. (2004a). Roles of G-protein-coupled receptor dimerization. EMBO Rep *5*, 30–34.

Terrillon, S., and Bouvier, M. (2004b). Receptor activity-independent recruitment of betaarrestin2 reveals specific signalling modes. EMBO J. *23*, 3950–3961.

Thaker, G.K. (2007). Schizophrenia endophenotypes as treatment targets. Expert Opinion on Therapeutic Targets *11*, 1189–1206.

Thompson, R.E., Larson, D.R., and Webb, W.W. (2002). Precise Nanometer Localization Analysis for Individual Fluorescent Probes. Biophysical Journal *82*, 2775–2783.

Thron, C.D. (1973). On the analysis of pharmacological experiments in terms of an allosteric receptor model. Mol. Pharmacol. *9*, 1–9.

Tomassini, N., Renaud, F.L., Roy, S., and Loh, H.H. (2003). Mu and delta receptors mediate morphine effects on phagocytosis by murine peritoneal macrophages. J. Neuroimmunol. *136*, 9–16.

Trejo, J., Hammes, S.R., and Coughlin, S.R. (1998). Termination of signaling by protease-activated receptor-1 is linked to lysosomal sorting. Proc. Natl. Acad. Sci. U.S.A. *95*, 13698–13702.

Trifilieff, P., Rives, M.-L., Urizar, E., Piskorowski, R.A., Vishwasrao, H.D., Castrillon, J., Schmauss, C., Slättman, M., Gullberg, M., and Javitch, J.A. (2011). Detection of

antigen interactions ex vivo by proximity ligation assay: endogenous dopamine D2-adenosine A2A receptor complexes in the striatum. BioTechniques *51*, 111–118.

Truant, R., Atwal, R.S., Desmond, C., Munsie, L., and Tran, T. (2008). Huntington's disease: revisiting the aggregation hypothesis in polyglutamine neurodegenerative diseases. FEBS J. *275*, 4252–4262.

Tucek, S., and Proska, J. (1995). Allosteric modulation of muscarinic acetylcholine receptors. Trends Pharmacol. Sci. *16*, 205–212.

Tucker, A.L., Jia, L.G., Holeton, D., Taylor, A.J., and Linden, J. (2000). Dominance of G(s) in doubly G(s)/G(i)-coupled chimaeric A(1)/A(2A) adenosine receptors in HEK-293 cells. Biochem. J. *352 Pt 1*, 203–210.

Uchigashima, M., Narushima, M., Fukaya, M., Katona, I., Kano, M., and Watanabe, M. (2007). Subcellular arrangement of molecules for 2-arachidonoyl-glycerol-mediated retrograde signaling and its physiological contribution to synaptic modulation in the striatum. J. Neurosci. *27*, 3663–3676.

Ulrich, C.D., 2nd, Holtmann, M., and Miller, L.J. (1998). Secretin and vasoactive intestinal peptide receptors: members of a unique family of G protein-coupled receptors. Gastroenterology *114*, 382–397.

Valjent, E., Corvol, J.C., Pages, C., Besson, M.J., Maldonado, R., and Caboche, J. (2000). Involvement of the extracellular signal-regulated kinase cascade for cocaine-rewarding properties. J. Neurosci. *20*, 8701–8709.

Valjent, E., Pagès, C., Rogard, M., Besson, M.J., Maldonado, R., and Caboche, J. (2001). Delta 9-tetrahydrocannabinol-induced MAPK/ERK and Elk-1 activation in vivo depends on dopaminergic transmission. Eur. J. Neurosci. *14*, 342–352.

Vallone, D., Picetti, R., and Borrelli, E. (2000). Structure and function of dopamine receptors. Neurosci Biobehav Rev *24*, 125–132.

Varani, K., Rigamonti, D., Sipione, S., Camurri, A., Borea, P.A., Cattabeni, F., Abbracchio, M.P., and Cattaneo, E. (2001). Aberrant amplification of A(2A) receptor signaling in striatal cells expressing mutant huntingtin. FASEB J. *15*, 1245–1247.

Varani, K., Abbracchio, M.P., Cannella, M., Cislaghi, G., Giallonardo, P., Mariotti, C., Cattabriga, E., Cattabeni, F., Borea, P.A., Squitieri, F., et al. (2003). Aberrant A2A receptor function in peripheral blood cells in Huntington's disease. FASEB J. *17*, 2148–2150.

Varani, K., Vincenzi, F., Tosi, A., Gessi, S., Casetta, I., Granieri, G., Fazio, P., Leung, E., MacLennan, S., Granieri, E., et al. (2010). A2A adenosine receptor overexpression and functionality, as well as TNF-alpha levels, correlate with motor symptoms in Parkinson's disease. FASEB J. *24*, 587–598.

Vaz, S.H., Jørgensen, T.N., Cristóvão-Ferreira, S., Duflot, S., Ribeiro, J.A., Gether, U., and Sebastião, A.M. (2011). Brain-derived neurotrophic factor (BDNF) enhances GABA transport by modulating the trafficking of GABA transporter-1 (GAT-1) from the plasma membrane of rat cortical astrocytes. J. Biol. Chem. *286*, 40464–40476.

Venkatakrishnan, A.J., Deupi, X., Lebon, G., Tate, C.G., Schertler, G.F., and Babu, M.M. (2013). Molecular signatures of G-protein-coupled receptors. Nature *494*, 185–194.

Vonsattel, J.P., and DiFiglia, M. (1998). Huntington disease. J. Neuropathol. Exp. Neurol. *57*, 369–384.

Vossler, M.R., Yao, H., York, R.D., Pan, M.G., Rim, C.S., and Stork, P.J. (1997). cAMP activates MAP kinase and Elk-1 through a B-Raf- and Rap1-dependent pathway. Cell *89*, 73–82.

Wager-Miller, J., Westenbroek, R., and Mackie, K. (2002). Dimerization of G protein-coupled receptors: CB1 cannabinoid receptors as an example. Chem. Phys. Lipids *121*, 83–89.

Waldhoer, M., Fong, J., Jones, R.M., Lunzer, M.M., Sharma, S.K., Kostenis, E., Portoghese, P.S., and Whistler, J.L. (2005). A heterodimer-selective agonist shows in vivo relevance of G protein-coupled receptor dimers. Proc Natl Acad Sci U S A *102*, 9050–9055.

Walker, F.O. (2007). Huntington's disease. Lancet *369*, 218–228.

Walter, L., Franklin, A., Witting, A., Wade, C., Xie, Y., Kunos, G., Mackie, K., and Stella, N. (2003). Nonpsychotropic cannabinoid receptors regulate microglial cell migration. J. Neurosci. *23*, 1398–1405.

Wan, W., Sutherland, G.R., and Geiger, J.D. (1990). Binding of the adenosine A2 receptor ligand [3H]CGS 21680 to human and rat brain: evidence for multiple affinity sites. J. Neurochem. *55*, 1763–1771.

Wang, L.Y., Salter, M.W., and MacDonald, J.F. (1991). Regulation of kainate receptors by cAMP-dependent protein kinase and phosphatases. Science *253*, 1132–1135.

Wei, C.J., Singer, P., Coelho, J., Boison, D., Feldon, J., Yee, B.K., and Chen, J.-F. (2011). Selective inactivation of adenosine A(2A) receptors in striatal neurons enhances working memory and reversal learning. Learn. Mem. *18*, 459–474.

Weiss, J., Mägert, H.J., Cieslak, A., and Forssmann, W.G. (1996). Association between different psychotic disorders and the DRD4 polymorphism, but no differences in the main ligand binding region of the DRD4 receptor protein compared to controls. Eur. J. Med. Res. *1*, 439–445.

Wellington, C.L., Ellerby, L.M., Hackam, A.S., Margolis, R.L., Trifiro, M.A., Singaraja, R., McCutcheon, K., Salvesen, G.S., Propp, S.S., Bromm, M., et al. (1998).

Caspase cleavage of gene products associated with triplet expansion disorders generates truncated fragments containing the polyglutamine tract. J. Biol. Chem. *273*, 9158–9167.

Wellington, C.L., Singaraja, R., Ellerby, L., Savill, J., Roy, S., Leavitt, B., Cattaneo, E., Hackam, A., Sharp, A., Thornberry, N., et al. (2000). Inhibiting caspase cleavage of huntingtin reduces toxicity and aggregate formation in neuronal and nonneuronal cells. J. Biol. Chem. *275*, 19831–19838.

Wexler, N.S., Young, A.B., Tanzi, R.E., Travers, H., Starosta-Rubinstein, S., Penney, J.B., Snodgrass, S.R., Shoulson, I., Gomez, F., and Ramos Arroyo, M.A. (1987). Homozygotes for Huntington's disease. Nature *326*, 194–197.

White, J.H., Wise, A., Main, M.J., Green, A., Fraser, N.J., Disney, G.H., Barnes, A.A., Emson, P., Foord, S.M., and Marshall, F.H. (1998). Heterodimerization is required for the formation of a functional GABA(B) receptor. Nature *396*, 679–682.

Whorton, M.R., Bokoch, M.P., Rasmussen, S.G.F., Huang, B., Zare, R.N., Kobilka, B., and Sunahara, R.K. (2007). A monomeric G protein-coupled receptor isolated in a high-density lipoprotein particle efficiently activates its G protein. Proc Natl Acad Sci U S A *104*, 7682–7687.

Wilson, R.I., and Nicoll, R.A. (2001). Endogenous cannabinoids mediate retrograde signalling at hippocampal synapses. Nature *410*, 588–592.

Winters, B.D., Krüger, J.M., Huang, X., Gallaher, Z.R., Ishikawa, M., Czaja, K., Krueger, J.M., Huang, Y.H., Schlüter, O.M., and Dong, Y. (2012). Cannabinoid receptor 1-expressing neurons in the nucleus accumbens. Proc. Natl. Acad. Sci. U.S.A. *109*, E2717–2725.

Wirkner, K., Assmann, H., Köles, L., Gerevich, Z., Franke, H., Nörenberg, W., Boehm, R., and Illes, P. (2000). Inhibition by adenosine A(2A) receptors of NMDA but not AMPA currents in rat neostriatal neurons. Br. J. Pharmacol. *130*, 259–269.

Woehler, A., and Ponimaskin, E.G. (2009). G protein--mediated signaling: same receptor, multiple effectors. Curr Mol Pharmacol *2*, 237–248.

Wong, A.K., Cavalieri, E., and Rogan, E. (1986). Regioselectivity in rat microsomal metabolism of benzo[a]pyrene: evidence for involvement of two distinct binding sites. Chem. Biol. Interact. *59*, 113–126.

Woods, A.S., and Huestis, M.A. (2001). A study of peptide--peptide interaction by matrix-assisted laser desorption/ionization. J. Am. Soc. Mass Spectrom. *12*, 88–96.

Wreggett, K.A., and Wells, J.W. (1995). Cooperativity manifest in the binding properties of purified cardiac muscarinic receptors. J. Biol. Chem. *270*, 22488–22499.

Wu, K., Aoki, C., Elste, A., Rogalski-Wilk, A.A., and Siekevitz, P. (1997). The synthesis of ATP by glycolytic enzymes in the postsynaptic density and the effect of endogenously generated nitric oxide. Proc. Natl. Acad. Sci. U.S.A. *94*, 13273–13278.

Wu, Y., Pearl, S.M., Zigmond, M.J., and Michael, A.C. (2000). Inhibitory glutamatergic regulation of evoked dopamine release in striatum. Neuroscience *96*, 65–72.

Xia, J., Lee, D.H., Taylor, J., Vandelft, M., and Truant, R. (2003). Huntingtin contains a highly conserved nuclear export signal. Hum. Mol. Genet. *12*, 1393–1403.

Xiong, L., Shuhendler, A.J., and Rao, J. (2012). Self-luminescing BRET-FRET near-infrared dots for in vivo lymph-node mapping and tumour imaging. Nat Commun *3*, 1193.

Xu, F., Wu, H., Katritch, V., Han, G.W., Jacobson, K.A., Gao, Z.-G., Cherezov, V., and Stevens, R.C. (2011). Structure of an agonist-bound human A2A adenosine receptor. Science *332*, 322–327.

Yang, S.-H., Cheng, P.-H., Banta, H., Piotrowska-Nitsche, K., Yang, J.-J., Cheng, E.C.H., Snyder, B., Larkin, K., Liu, J., Orkin, J., et al. (2008). Towards a transgenic model of Huntington's disease in a non-human primate. Nature *453*, 921–924.

Yang, W., Dunlap, J.R., Andrews, R.B., and Wetzel, R. (2002). Aggregated polyglutamine peptides delivered to nuclei are toxic to mammalian cells. Hum. Mol. Genet. *11*, 2905–2917.

Yao, L., McFarland, K., Fan, P., Jiang, Z., Ueda, T., and Diamond, I. (2006). Adenosine A2a blockade prevents synergy between mu-opiate and cannabinoid CB1 receptors and eliminates heroin-seeking behavior in addicted rats. Proc. Natl. Acad. Sci. U.S.A. *103*, 7877–7882.

Yawo, H., and Chuhma, N. (1993). Preferential inhibition of omega-conotoxin-sensitive presynaptic Ca2+ channels by adenosine autoreceptors. Nature *365*, 256–258.

Yesilaltay, A., and Jenness, D.D. (2000). Homo-oligomeric complexes of the yeast alpha-factor pheromone receptor are functional units of endocytosis. Mol. Biol. Cell *11*, 2873–2884.

Yin, H.H., and Knowlton, B.J. (2006). The role of the basal ganglia in habit formation. Nat. Rev. Neurosci. *7*, 464–476.

Zeron, M.M., Hansson, O., Chen, N., Wellington, C.L., Leavitt, B.R., Brundin, P., Hayden, M.R., and Raymond, L.A. (2002). Increased sensitivity to N-methyl-D-aspartate receptor-mediated excitotoxicity in a mouse model of Huntington's disease. Neuron *33*, 849–860.

Zhu, X., and Wess, J. (1998). Truncated V2 vasopressin receptors as negative regulators of wild-type V2 receptor function. Biochemistry *37*, 15773–15784.

Zimmermann, G., Zhou, D., and Taussig, R. (1998). Mutations uncover a role for two magnesium ions in the catalytic mechanism of adenylyl cyclase. J. Biol. Chem. *273*, 19650–19655.

Zuccato, E., Castiglioni, S., Bagnati, R., Chiabrando, C., Grassi, P., and Fanelli, R. (2008). Illicit drugs, a novel group of environmental contaminants. Water Res. *42*, 961–968.

VI. RESUM DE LA TESI DOCTORAL

Els receptors acoblats a proteïna G han estat clàssicament classificats coma unitat individuals capaces de produir una senyal intracel·lular. Avui en dia és acceptat que aquests receptors poden interaccionar entre ells formant dímers, trímers o oligòmers de major ordre. Aquestes interaccions han de ser considerades com a noves entitats ja que produeixen canvis importants a la farmacologia i funcionalitat d'aquests receptors, el qual s'ha de tenir en compte a l'hora d'entendre processos com la transmissió neuronal o de cara a la recerca de nous compostos en la indústria farmacèutica. En aquest context, l'objectiu general d'aquesta tesi és investigar les conseqüències farmacològiques i funcionals de la interacció del receptor d'adenosina A2A amb altres receptors. Per tal d'assolir aquest objectiu, cinc objectius particulars van ser formulats.

Degut al paper que juguen els astròcits en el transport de GABA, un primer objectiu parcial va ser clarificar si els heteròmers A1R-A2AR modulaven els transportadors de GABA GAT-1 i/o GAT-3 als astròcits. Ja que l'estequiometria molecular i la dinàmica de formació d'aquests heteròmers i el nombre de proteïnes G unides romanen desconeguts un segon objectiu parcial va ser analitzar el comportament de les poblacions d'heteròmers A1R-A2AR a la membrana plasmàtica en absència de lligands. Per tal de trobar una resposta a aquestes preguntes el primer objectiu va ser:

Objectiu 1. Implicacions de l'heteròmer A1R-A2AR a les cèl·lules glials i el seu estudi a nivell molecular.

En el moment en el que la formació de l'heteròmer entre els receptors de dopamina D2 i el receptor d'adenosina A2A va ser descrit, aquests complexes han estat de gran interès en el desenvolupament de noves teràpies per a diferents patologies. En els últims anys s'han desenvolupat nous fàrmacs amb diferents afinitats per aquests receptors i han estat usats com

a teràpia i en recerca científica. Aquestes teràpies estan basades en la regulació negativa que els agonistes del receptor d'adenosina A2A produeixen sobre la unió d'agonistes en els receptors de dopamina D2, però no es coneix com aquesta modulació es porta a terme i si la unió de lligands als receptors A2A modifiquen la unió d'antagonistes al receptor D2. Considerant aquests antecedents, el segon objectiu de la tesi va ser:

Objectiu 2. Trobar evidències de modulacions al·lostèriques entre receptors a l'heteròmer A2AD-D2R que confereixen característiques farmacològiques específiques a l'heteròmer.

Els receptors d'adenosina A2A han emergit com a atractives dianes no-dopaminèrgiques en la recerca d'una millorada teràpia per a la malaltia de Parkinson, basat en part per la seva característica distribució al sistema nerviós central. És molt abundant en neurones estriato-palidals i poden formar complexes heteromèrics amb altres GPCR. El bloqueig de A2AR a neurones estriato-palidals redueix els efectes postsinàptics de la manca de dopamina, i a la seva vegada redueix els dèficits motos de la malaltia de Parkinson. D'altra banda, els receptors d'adenosina A2A localitzats presinàpticament es creu que poden ser responsables de la mort neuronal a la malaltia de Huntington ja que la presència d'adenosina endògena provoca un alliberament massiu de glutamat que porta a la mort per exitotoxicitat de les neurones espinoses mitjanes de l'estriat. Amb aquestes hipòtesi, el tercer objectiu és:

Objectiu 3. Recerca d'antagonistes selectius de A2AR per a heteròmers presinàptics A1R-A2AR versus heteròmers postsinàptics A2AR-D2R que poden ser útils en el tractament de malalties neurològiques, particularment en la malaltia de Huntington.

A més de formar heteròmers amb A1R i D2R, el receptor d'adenosina A2A també interacciona amb els receptors de cannabinoids CB1. CB1R es troben pre- i postsinàpticament tant en la via directa com indirecta dels circuits estriatals i és possible que

siguin els responsables de modular les funcions del receptor A2A a l'estriat. Els heteròmer A2AR-CB1R van ser prèviament descrits en aquest grup de recerca i tot i que se sabia que l'activació de A2AR era necessària per tal de que CB1R fos capaç de senyalitzar en línies cel·lulars de neuroblastomes transfectats, les característiques farmacològiques i funcionals de l'heteròmer són desconegudes. Amb això el quart objectiu és:

Objectiu 4. Investigar les propietats funcionals i farmacològiques de A2AR en l'heteròmer A2AR-CB1R.

Una vegada demostrat que els antagonistes poden mostrar diferents comportaments davant un receptor depenent de amb quin altre receptor es troba oligomeritzat, és de gran interès testar una bateria d'antagonistes del receptor A2A a les diferents línies cel·lulars estables usades en els anteriors objectius per tal de trobar compostos específics per a diferents heteròmers. Això seria de gran interès donada la implicació dels heteròmers de receptors d'adenosina A2A en malalties neurodegeneratives, adiccions i altres desordres. Per tant, el cinquè objectiu va ser:

Objectiu 5. Anàlisi de diferents compostos antagonistes de A2AR en línies cel·lulars estables CHO expressant A2AR, A1R-A2AR, A2AR-D2R o A2AR-CB1R.

RESULTATS I DISCUSSIÓ.

CAPÍTOL 1.1.

Heteròmers A1R-A2AR acoblats a proteïnes Gs i Gi/o modulen el transport de GABA als astròcits.

Els astròcits modulen la transmissió sinàptica ja que poden alliberar i capturar neurotransmissors i, per tant, regular amb precisió la balança entre excitació i inhibició. GABA és el neurotransmissor inhibidor principal al SNC, a on juga un paper clau en el control d'excitabilitat, plasticitat i sincronització. Aquestes accions depenen de canvis en les concentracions extracel·lulars de GABA, les quals estan sota el control de transportadors de GABA (GATs) expressats a ambdues neurones i als astròcits. Els astròcits corticals expressen GAT-1 i GAT-3 i ha estat estimat que aproximadament el 20% de GABA extracel·lular és capturada pels astròcits.

Els astròcits alliberen gran quantitats d'ATP, el qual és llavors hidrolitzat en adenosina per acció de les ecto-nucleotidases. L'adenosina extracel·lular opera a través de GPCR. En el cas de les cèl·lules neurals, els subtipus A1R i A2AR són els que s'activen a nivells basals d'adenosina extracel·lular. El A1R és sovint inhibitori i s'acobla a proteïnes Gi/o, mentre que A2AR normalment s'acobla a proteïnes Gs, estimulant l'acumulació d'AMPc i l'activitat de PKA. A1R i A2AR podrien interaccionar de manera que l'activació de A2AR porta a la inhibició de respostes mediades per A1R. Algunes interaccions podrien ocórrer a nivell funcional i de sistema de transducció però assajos de transferència d'energia han identificat la presència d'heteròmers A1R-A2AR en línies cel·lulars transfectades. Aquestes dades suggereixen un possible rol dels heteròmers A1R-A2AR a les neurones. De tota manera encara manquen evidències directes d'heteromerització de A1R-A2AR a cèl·lules neurals.

Donat el paper que juguen els astròcits en tot el transport de GABA, el primer objectiu va ser clarificar si A1R i A2AR modulaven el transport de GABA mediat per GAT-1 i/o GAT-3 als astròcits. Es va detectar una forta interacció entre A1R i A2AR, a més d'evidències de cross-antagonisme, una propietat bioquímica que s'utilitza sovint per demostrar la presència d'heteròmers. A més es va trobar la presència d'heteròmers 1R-A2AR en astròcits. Es va trobar que aquests heteròmers s'acoblen a dues proteïnes G diferents, Gs i Gi/o, totes dues regulant els transport de GABA de forma oposada, amb A1R mediant la inhibició del transport de GABA i A2AR mediant el transport de GABA per part dels astròcits. Aquesta unitat funcional A1R-A2AR, opera com un amplificador dual controlant els nivells de GABA a les sinapsi.

Discussió.

Aquest treball clarament demostra que la captació de GABA per part dels astròcits està sota la modulació de l'adenosina extracel·lular, la qual, interaccionant amb la unitat funcional constituïda per A1R-A2AR acoblats a dues proteïnes G diferents, Gi/o i Gs, poden tant incrementar com reduir la quantitat de neurotransmissor inhibidor disponible a l'espai sinàptic.

Utilitzant anàlegs d'adenosina, CADO, es va observar que a concentracions submicromolar hi ha un increment de transport de GABA. Considerant que l'afinitat de l'adenosina per A1R és lleugerament superior que per A2AR probablement la inhibició es mediada per A1R i facilitada per A2AR. D'acord amb això, l'agonista selectiu de A1R CPS va inhibir el recaptament de GABA als astròcits, mentre que l'agonista selectiu de A2AR CGS 21680 el va facilitar. Sorprenentment, el bloqueig de qualsevol dels dos receptors amb antagonistes selectius va prevenir els efectes mediats per qualsevol dels dos agonistes, una forta evidència de que A1R i A2AR es troben interaccionant a nivell molecular en els astròcits. Es va detectar transferència d'energia en astròcits transfectats amb els DNAc A2A-

Rluc i A1R-YFP. En aquests assajos es va detectar una senyal de BRET positiva i saturable en astròcits. A més aquest heteròmer es va detectar en els mateixos astròcits amb mètodes d'unió de radiolligand a on les propietats d'unió dels lligands de A1R canviaven quan el receptor A2AR estava activat. Aquests resultats complementen i enforteixen la evidència d'heteromerització a astròcits no transfectats.

Assajos de biotinilització van mostrar que en presència d'un dels dos agonistes específics de l'heteròmer era suficient per provocar la internalització d'ambdós receptors. El bloqueig previ amb un dels dos antagonistes de l'heteròmer evitava així mateix la internalització de l'heteròmer. Imatges de confocal de cèl·lules HEK-293T transfectades van confirmar aquests experiments.

La unió d'agonista no afectava als resultats de BRET, suggerint que la unió d'agonista no indueix modificacions al·lostèriques als receptors. D'aquesta manera sembla que l'heteròmer citat es comporta com a una entitat integrada que probablement arribi a la membrana extracel·lular ja com a heteròmer. A més a més, com que els antagonistes no van modificar els nivells de recptor a la membrana o la senyal de BRET, la pèrdua d'efecte d'un agonista amb el bloqueig previ de l'altre receptor no pot ser atribuït a la disrupció de l'heteròmer . El cross-antagonisme és considerat una empremta bioquímica, i és atribuïble a canvis conformacionals induïts per antagonistes que porten a un estat no-funcional de l'aparell senyalitzador del receptor desacoblant-lo de la proteïna G senyalitzadora.

Com que els heteròmers poden acoblar-se a diferents proteïnes G de les que originalment es trobarien units en forma monomèrica es va realitzar assajos label-free en combinació amb toxines que específicament bloquegen proteïnes G. Amb aquests experiments es va arribar a la conclusió que sota l'heteròmer A1R-A2AR s'hi troben unides dues proteïnes G, Gs i Gi/o, que en presència d'agonista de A1R senyalitza a través de Gi/o i en presència d'agonista de A2AR senyalitza mitjançant Gs, i sorprenentment el fet de bloquejar una de les unitats de l'heteròmer aconseguia bloquejar l'activitat de tot l'heteròmer.

Com que dos GPCR no poden trobar-se units a més d'una proteïna G per motius estequiomètrics, aquest heteròmer ha de trobar-se en forma de tetràmer A1R-A1R-A2AR-A2AR. Fent possible que s'hi acomodin dues proteïnes G.

A l'incrementar 10 vegades la concentració del lligand no selectiu CADO va ser suficient per canviar la modulació de recaptació de GABA. Assumint això es pot aproximar que el canvi de inhibició a potenciació del recaptament de GABA pot ocórrer a concentracions d'adenosina extracel·lular de l'ordre de micromolar. Aquestes concentracions són fàcilment aconseguibles a les sinapsi neuronals a on s'alliberen grans quantitats d'ATP. Com més gran és l'alliberament d'ATP, més gran és la concentració d'adenosina a l'espai sinàptic. Per tant és esperable que després de grans activacions neuronals es promogui l'activació de A2AR en l'heteròmer facilitant el recaptament de GABA. L'activació del recaptament de GABA per part dels astròcits portarà a una disminució de GABA extracel·lular. D'altra banda, a concentracions submicromolar d'adenosina, hi ha una activació preferent de A1R en l'heteròmer, i el recaptament de GABA pels astròcits serà inhibit. Per tant l'acció de l'adenosina a aquests heteròmers és com la d'un amplificador dual, facilitant l'excitació o inhibint-la. Aquest mecanisme necessita un control eficient per evitar canvis sobtats en la transició. De fet, amb una sobreestimulació de només un dels dos receptors promou la internalització de tot l'heteròmer, essent així un sistema de frenada per evitar canvis bruscos entre excitació i inhibició.

CAPÍTOL 1.2.

Heteròmers d'adenosina A1R-A2AR formen complexes tetramèrics dinàmics però estables amb dues proteïnes G diferents.

La idea controvertida de dimerització de GPCR està avui dia recolzada per moltes dades bioquímiques i estructurals. Aquest debat s'ha mogut a la qüestió dels heterocomplexes, a on un gran nombre d'estudis contemplen la presència d'heterodímers i heteròmers d'ordre superior en una gran quantitat de GPCR. Un exemple molt estudiat és la de l'heteròmer A1R-A2AR. De tota manera l'estequiometria i les dinàmiques de formació d'aquest heteròmer no han estat encara estudiades.

Discussió.

Una observació interessant dels experiments de "single particle tracking (SPT)" va ser que A1R i A2AR formen complexes dinàmics però estables a la membrana plasmàtica a on la forma més comú és el tetràmer consistent en dos A1R i dos A2AR. A més aquests complexes semblen ser molt estables al llarg del temps poden arribar a l'ordre de minuts.

Considerant aquests heteròmers com a tetràmers estables es va voler saber com s'estabilitzaven les proteïnes G en aquest tetràmer, com s'orientaven aquestes proteïnes i com seria l'arquitectura d'aquesta unitat senyalitzadora. En el cas dels tetràmers requereix que hi hagi més d'un lloc d'interacció per protomer. Assajos de BRET juntament amb models moleculars d'oligomerització de receptors indiquen que el lloc d'interacció per a l'homodimerització és el TM4, mentre que per a l'heteromerització és el TM5. Un altre aspecte interessant és la presència de les proteïnes G unides constitutivament al tetràmer. Aquest concepte de pre-acoblament de les proteïnes G abans de que es produeixi unió de lligand està reforçada per la davallada de transferència d'energia en experiments de BRETamb la presència de toxines específiques de les diferents proteïnes G. Com que la

màxima transferència d'energia és una funció del nombre de protomers formats, aquests resultats indiquen que les proteïnes G podrien induir i/o estabilitzar la dimerització dels receptors.

CAPÍTOL 2.

Interaccions al·lostèriques entre receptors a l'heteròmer A2AR-D2R induïdes per agonistes i antagonistes.

Els receptors D2 de dopamina s'expressen a les neurones estriatals GABAèrgiques encefalinèrgiques on també s'expressen els receptors A2A d'adenosina i on ambdós col·localitzen. De fet, els receptors D2 estan sota el control dels receptors A2A i, almenys en part, aquest control s'exerceix a través d'un fet altament descrit en els darrers anys que és la modulació de la funció a través de la formació d'hereròmers de receptors. Un heteròmer és un complex macromolecular format almenys per dos receptors funcionals i que mostra propietats bioquímiques que són diferents de les dels receptors individuals. Els heteròmers entre els receptors A2A d'adenosina i D2 de dopamina van ser uns dels primers heteròmers de GPCR descrits. La interacció molecular entre ambdós receptors es va demostrar mitjançant estudis de coimmunoprecipitació i col·localització, i per tècniques de FRET i BRET. L'existència dels heteròmers A2A-D2 a l'estriat de xai ha estat recentment descoberta emprant lligands bivalents i l'expressió d'aquests heteròmers a l'estriat de ratolí s'ha descrit en estudis de PLA. Els heteròmers de receptors A2A-D2 són molt rellevants per al control de l'activitat motora ja que estan presents en la via indirecta estriatal i el balanç en l'estimulació de les vies directa i indirecta resulta en el control del moviment.

La interacció al·lostèrica és una de les propietats habituals dels heteròmers de receptors i es defineix com una interacció intramolecular per la qual la unió d'un lligand a un receptor de l'heteròmer canvia les propietats d'unió de lligands a l'altre receptor de l'heteròmer. Les interaccions al·lostèriques en l'heteròmer A2A-D2 han rebut molta atenció de la comunitat científica però aquesta s'ha restringit a les interaccions al·lostèriques agonista-agonista. Aquestes s'han considerat com el principal responsable dels efectes antiparkinsonians dels antagonistes del receptor A2A i sembla que mitjançant heteròmers els

agonistes dels receptors A2A contraresten la inhibició produïda pels agonistes del receptor D2 de la estimulació mitjançada per receptors NMDA en neurones estriatals de la via indirecta. La interacció al·lostèrica també s'ha suggerit com el principal mecanisme responsable dels efectes de depressió o activació motora que causen els agonistes o antagonistes del receptor A2A, respectivament. En tots aquests casos, els antagonistes del receptor A2A juguen només un paper com a desplaçant de l'agonista endogen. De totes maneres, mai ha estat considerat el possible efecte exercit directament pels antagonistes del receptor A2A en la modulació de les propietats farmacològiques dels receptors D2. En aquest capítol s'ha demostrat que, mitjançant interaccions al·lostèriques no només l'agonista del receptor A2A CGS 21680 sinó també l'antagonista no-selectiu cafeïna redueixen la unió tant de l'agonista ([3H]quinpirole) com de l'antagonista ([3H]raclopride) del receptor D2 en membranes tant de cèl·lules transfectades com d'estriat de xai. Emprant aquestes interaccions al·lostèriques com a empremta dactilar de l'heteròmer A2A-D2, hem demostrat l'expressió del heteròmer a l'estriat humà.

Discussió.

Una propietat important dels heteròmers de receptors és la capacitat per establir interaccions al·lostèriques entre els monòmers i aquesta capacitat confereix característiques farmacològiques i funcionals específiques de l'heteròmer. En aquest estudi ens hem focalitzat en aquestes propietats per als heteròmers de receptors d'adenosina i de dopamina A2A-D2. En cultius cel·lulars, primer s'ha demostrat que la unió de qualsevol lligand (agonista o antagonista) al receptor A2A pot fer disminuïr la unió de qualsevol lligand (agonista o antagonista) al receptor D2. En segon lloc, s'ha establit que aquestes interaccions són conseqüència de les interaccions al·lostèriques entre ambdós receptors en l'heteròmer A2A-D2 i que constitueixen propietats bioquímiques característiques d'aquest heteròmer. Seguidament en teixits ex vivo, s'ha demostrat que la unió dels agonistes i els antagonistes del

receptor A2A –però no del receptor A1– redueixen l'afinitat tant dels agonistes com dels antagonistes del receptor D2 en membranes estriatals de xai on prèviament s'havia descrit l'heteròmer A2A-D2 i usant aquestes interaccions al·lostèriques com a empremta dactilar de l'heteròmer, s'ha demostrat l'expressió de l'heteròmer de receptors A2A-D2 a l'estriat humà.

Tant l'agonista del receptor A2A CGS 21680 com l'antagonista no selectiu cafeïna, la droga psicoactiva més consumida del món, redueixen l'afinitat del receptor D2 per als seus agonista o antagonista tritiats [3H]quinpirole i [3H]raclopride. En aquest estudi s'ha demostrat que aquestes interaccions entre els receptors A2A i D2 són interaccions al·lostèriques entre les diferents unitats en l'heteròmer A2A-D2 i que en constitueixen una propietat bioquímica. De fet, s'ha descrit que trobar una correlació entre canvis significatius a l'estructura quaternària de l'heteròmer i canvis significatius en la farmacologia o la funció del receptor permet establir les propietats bioquímiques d'aquest heteròmer. Seguint aquest concepte, s'ha usat el receptor A2AA374 (amb una mutació puntual de la Ser374 localitzada al seu domini C-terminal). Aquesta mutació comporta una disminució en els valors de BRET que implica un canvi significatiu en l'estructura quaternària de l'heteròmer A2A-D2 disrompent la interacció electrostàtica intracel·lular de l'heteròmer. Tal com s'esperava, s'ha observat un descens en el BRET per a la parella A2AA374-RLuc/D2-YFP comparada a la parella la parella A2A-RLuc/D2-YFP i aquest canvi en l'estructura quaternària ha resultat en la inhibició de les interaccions al·lostèriques a l'heteròmer. Per tant, les interaccions al·lostèriques que s'han descrit en aquest estudi constitueixen una característica bioquímica de l'heteròmer de receptors A2A-D2. En aquest estudi hem usat aquesta característica per a detectar i caracteritzar els heteròmers A2A-D2 a l'estriat cerebral de xai, i el que és més important, al nucli caudat del cervell humà. En les membranes del nucli caudat humà, el CGS 21680 i la cafeïna redueixen l'afinitat del receptor D2 per al [3H]raclopride amb pràcticament el mateix rang concentració-resposta trobat en les preparacions de membranes de cèl·lules CHO que expressen els heteròmers A2A-D2. I per tant, el fet de trobar aquest

fingerprint en aquestes membranes dóna, per primer cop, una prova de l'existència dels receptors heteromèrics A2A-D2 al cervell humà.

Els resultats anteriorment comentats són rellevants considerant que els receptors A2A i D2 de l'estriat són diana de molts fàrmacs per combatre afeccions neurològiques humanes, com ara desordres psiquiàtrics, addicció a les drogues, o malalties neurodegeneratives i que són el focus primari de molta recerca biomèdica i farmacèutica. De fet, els heteròmers tenen característiques bioquímiques úniques que són diferents de les de les seves unitats individuals. Aquestes propietats, incloent les modulacions al·lostèriques entre unitats que es descriuen aquí, poden ser fonamentals en el descobriment de nous fàrmacs ja que els paràmetres farmacològics d'un fàrmac seleccionat, per exemple per estratègies HTS (High-throughput screening o cribratge d'alt rendiment) usant receptors expressats individualment en una línia cel·lular, poden ser molt diferents dels paràmetres farmacològics reals del receptor en teixits natius on el receptor s'expressa formant heteròmers amb un altre receptor i en presència o en absència de lligands d'aquest altre receptor. En aquest marc, un aspecte interessant és que una interacció al·lostèrica entre protòmers d'un heteròmer s'ha d'interpretar com una interacció intramolecular en la que la unió d'un lligand a una de les unitats de receptor del heteròmer canvia les propietats de la unió a l'altra unitat de receptor. Algunes troballes anteriors demostraven que l'agonista del receptor A2A disminuïa la unió d'agonistes al receptor D2 i es va suggerir que aquesta interacció al·lostèrica podia ser un mecanisme clau involucrat en els efectes depressius de l'aparell motor dels agonistes del receptor A2A i dels efectes estimulants dels antagonistes del receptor A2A com la cafeïna o en la depleció induïda pels agonistes del receptor A2A de la inhibició que media el receptor D2 sobre l'excitació neuronal per NMDA. Aquest interacció al·lostèrica agonista-agonista també s'ha considerat com el mecanisme principal responsable dels efectes antiparkinsonians dels antagonistes del receptor A2A. Fins ara, els antagonistes del receptor A2A no s'havien considerat capaços d'induir interaccions al·lostèriques directes en l'heteròmer A2A-D2 i eren

considerats només com a molècules que podien desplaçar la unió dels agonistes endògens i, conseqüentment, bloquejar les interaccions al·lostèriques agonista-agonista a l'heteròmer A2A-D2. Els nostres resultats demostren, per primer cop, que una interacció al·lostèrica a l'heteròmer no només implica unes interaccions agonista-agonista sinó també interaccions agonista-antagonista i antagonista-antagonista en membranes cel·lulars i cerebrals, incloent les d'estriat humà. Per tant, la unió d'un antagonista a la unitat A2A del heteromer també redueix la unió dels agonistes i antagonistes a la unitat D2. Aquest comportament, ha de ser tingut en compte quan s'analitzen els efectes funcionals i farmacològics dels lligands del receptor A2A, i en particular els dels antagonistes, en la funcionalitat dels receptors D2. A pesar d'això cal no oblidar que no només hi ha les interaccions al·lostèriques sinó que també s'ha de tenir en compte un complex cross-talk molecular entre receptors en l'heteròmer que pot tenir conseqüències a nivell de senyalització que poden ser independents de les interaccions al·lostèriques i poden explicar, al menys en part, el paper dels lligands del receptor A2A en la modulació del receptor D2.

D'altra banda, un altre aspecte important d'aquests resultats és que poden tenir implicacions en el camp de la neuroimatge humana per PET (Positron Emission Tomography). En la tècnica de PET, sovint s'usa el [11C]raclopride com a marcador dels receptors D2 i el consum de cafeïna no acostuma a ser controlat quan s'usa aquest lligand. S'han realitzat alguns estudis de l'efecte de la cafeïna en el PET amb [11C]raclopride i ja indicaven un descens en la unió de l'antagonista al receptor D2 induïda per la cafeïna. Tenint en compte els resultats que es descriuen aquí, aquest descens en la unió de [11C]raclopride pot ser interpretat com una acció de la cafeïna sobre els receptors heteromèrics A2A-D2 al cervell humà. De totes maneres, en els estudis de PET només s'avaluava l'efecte d'una dosi oral de cafeïna en bevedors habituals de cafè després de 24 hores d'abstinència de cafeïna i els resultats són difícils d'interpretar en quan que la unió de [11C]raclopride només es veu significativament modificada en àrees talàmiques i els efectes de la cafeïna en alguns casos

poden ser reproduïts per placebo. De totes maneres, els resultats descrits en el nostre estudi indiquen que s'ha de tenir en compte l'efecte de la cafeïna mediat pels heteròmers de receptors A2A-D2 en els experiments de PET amb [11C]raclopride i ressalten que paràmetres com el consum habitual de cafè, els períodes d'abstinència o les diferents dosis de cafeïna han de ser tingudes en consideració quan es realitzin aquest tipus d'estudis.

CAPÍTOL 3.

Perfil pre- i postsinàptic d'antagonistes del receptor d'adenosina A2A estriatal.

Més d'un 95% de les neurones estriatals són neurones espinoses mitjanes (MSN) GABAèrgiques. Aquestes neurones reben dues senyals principals: eferents glutamatèrgics provinents del còrtex, tàlem i àrees límbiques i eferents dopaminergics provinents de la substància nigra pars compacta i de l'àrea tegmental ventral. Les MSN són neurones eferents que donen lloc a dues vies, la directa i la indirecta. Està acceptat que l'estimulació de la via directa i indirecta dóna lloc a l'activació motora i inhibició motora respectivament. Les MSN de la via directa expressen receptors de dopamina D1, mentre que MSN de la via indirecta tenen nivells alts d'expressió de D2R i adenosina A2AR. Hi ha evidències clares de l'existència de mecanismes de control postsinàptic de neurotransmissió glutamatèrgica en MSN de la via indirecta per part d'interaccions antagonístiques entre A2AR i D2R. En un tipus d'interacció, A2AR i D2R formen heteròmers i mitjançant interaccions al·lostèriques, A2AR contraresta la modulació inhibitòria mediada per D2R dels efectes de la estimulació de receptors NMDA a les MSN de la via indirecta. Aquesta interacció ha estat suggerida que sigui la responsable dels efectes locomotors repressors i efectes activadors dels agonistes i antagonistes de A2AR respectivament.

A2AR estriatals no estan únicament localitzats postsinàpticament, també es troben presinàpticament a terminals glutamatèrgics, a on heteromeritzen amb A1R i a on la seva estimulació facilita la transmissió glutamatèrgica. Aquest A2AR presinàptic es troba preferentment localitzat a terminals eferents de la via directa. El bloqueig mitjançant antagonistes de A2AR postsinàptic localitzat a MSN de la via indirecta hauria de produir activació motora (potenciant efectes mediats per D2R mitjançant les interaccions en l'heteròmer A2AR-D2R). Per altra banda, el bloqueig de A2AR presinàptics localitzats a MSN de la via directa hauria de reduir l'activitat motora (inhibint l'alliberament de

glutamat). La potència en la inducció d'activació motora pot ser utilitzada con una mesura in vivo de la capacitat d'un antagonista de A2AR per bloquejar A2AR estriatal postsinàptic. Recentment s'ha establert un model in vivo que evalua l'eficàcia de la neurotransmissió cortico-estriatal glutamatèrgica de les MSN de la via directa quantificant la correlació entre el corrent subministrat al còrtex premotor orofacial i la resposta electromiogràfica de la musculatura de les mandíbules. En aquest model, antagonistes de A2AR o D1R eren capaços de contrarestar l'activitat motora induïda per l'estimulació elèctrica cortical, cosa que només pot ser explicada pel bloqueig de A2AR estriatal presinàptic o D1R postsinàptic respectivament.

Els receptors d'heteròmers es defineixen com a complexes macroestructurals formats per almenys dos receptors funcionals, les propietats bioquímiques dels quals són diferents de quan es troben en components individuals. En aquest capítol s'investiga l'existència d'antagonistes que uneixin preferentment pre- o postsinàpticament els A2AR i si aquestes diferències venen determinades per la formació d'heteròmers amb A1R i D2R respectivament.

Discussió.

El primer resultat important en aquest estudi és el fet de que diferents antagonistes de A2AR que es creia que tenien característiques farmacològiques similars presenten perfils pre- i postsinàptics similars. Sis compostos diferents van ser testats en models in vivo. L'activació locomotora va ser utilitzada per avaluar l'activitat postsinàptica, mentre que la reducció en l'activitat de la musculatura mandibular (PCC) va ser utilitzada per avaluar l'activitat presinàptica. Dos compostos, SCH 442416 i KW 6002, van mostrar perfils preferencialment pre- i postsinàptics, respectivament, i quatre compostos, MSX 3, SCH 420814, SCH 58261 i ZM 241385, van mostrar perfils mixtes.

Experiments d'unió de radiolligands van ser realitzats amb cèl·lules CHO expressant establement A2AR, A2AR-D2R heteròmers o A1R-A2AR heteròmers per determinar possibles diferències en afinitat per aquests compostos pels diferents heteròmers de A2AR. La co-expressió amb A1R no va modificar significativament l'afinitat, però la co-expressió amb D2R va disminuir l'afinitat de tots els compostos, amb exepció de KW 6002. Els canvis estructurals a A2AR induïts per l'heteromerització amb D2R pot ser detectada tant amb antagonistes com amb agonistes. De fet, l'afinitat de l'agonista selectiu de A2AR CGS 21680 es va veure reduïda en cèl·lules co-transfectades amb D2R. En testar les afinitats de SCH 442416 és interessant assenyalar que va mostrar una afinitat molt més alta per A2AR presinàptic que postsinàptic. La unió de SCH 442416 a l'heteròmer A2AR-D2R va mostrar una forta cooperativitat negativa, fenomen no observat a la unió de SCH 442416 a l'heteròmer A1R-A2AR. Aquesta cooperativitat negativa explica el pronunciat descens en afinitat de A2AR a les cèl·lules que expressen heteròmers A2AR-D2R.

La pèrdua d'afinitat de A2AR davant la seva co-expressió amb D2R va ser menys pronunciada amb ZM 241385, SCH 58261, MSX 2 o SCH 420814, amb els quals l'afinitat es va reduir entre dues i nou vegades. KW 6002 va ser l'únic antagonista l'afinitat del qual no va ser significativament diferent en cèl·lules que expressen A2AR, A1R-A2AR heteròmers o A2AR-D2R heteròmers. D'aquesta manera, KW 6002 va mostrar la millor afinitat relativa pels heteròmers A2AR-D2R, cosa que pot explicar en part el seu perfil preferentment postsinàptic.

Aquest estudi defensa la idea de que els heteròmers poden ser usat com a dianes selectives de fàrmacs. Les principals raons per fer-ho son la seva localització neuronal específica i la seva afinitat diferencial depenent de qui és el seu receptor acompanyant en l'heteròmer. A l'estriat, A2AR es una diana particularment interessant i eventualment útil donada la seva implicació en varis desordres neuropsiquiàtrics. Els heteròmers A2AR-D2R i A1R-A2AR es troben segregats en diferents elements neuronals estriatals. Mentre

l'heteròmer A2AR-D2R es troba localitzat postsinàpticament a les espines dendrítiques de les MSN de la via indirecta, els heteròmers A1R-A2AR es troben presinàpticament a les terminals glutamatèrgiques contactant les MSN de la via directa. El bloqueig postinàptic de A2AR a les MSN de la via indirecta hauria de potenciar l'activació motora mediada per D2R, el qual es aprofitat per al desenvolupament de fàrmacs anti-parkinsonians. Pel contrari, el bloqueig de A2AR a terminals glutamatèrgiques de MSN de la via directa podria ser potencialment útil en desordres discinètics com la malaltia de Huntington i potser en desordres obsessiu-compulsius i en addicció a les drogues. Aquests resultats donen una explicació mecanística a la ja reportada activitat anti-parkinsoniana de KW 6002 i suggereixen que SCH 442416 podria ser útil en un tractament contra la malaltia de Huntington.

CAPÍTOL 4.

Caracterització farmacològica i funcional de l'heteròmer A2AR-CB1R.

El receptor de cannabinoids CB1R és el GPCR més abundant del cervell i es troba densament distribuït a l'estriat. Allà es troba distribuït a totes dues classes de MSN, neurones encefalinèrgiques i dinorfinèrgiques de la via indirecta i directa, respectivament. En aquesta localització postsinàptica, CB1R modula negativament la locomoció. A més, CB1R estriatal es troba també localitzat a interneurones GABAèrgiques i presinàpticament a terminals GABAèrgiques i glutamatèrgiques. La funció fisiològica més important del CB1R presinàptic és la de regular l'alliberament de neurotransmissors. L'elevada expressió de A2AR i CB1R a l'estriat suggereix que interaccions directes o indirectes entre aquests receptors poden estar involucrades en la modulació de l'activitat motora. És ja conegut que A2AR regula l'acció de CB1R tant a nivell pre- com postsinàptic. Treballs recents demostren que A2AR presinàptic inhibiex efectes mediats per CB1R probablement via AMPc-PKA. Sembla ser que interaccions entre A2AR i CB1R localitzats a terminals glutamatèrgics que estan en contacte amb MSN dinorfinèrgiques es troben involucrades en els efectes hipolocomotors i de recompensa de THC. De tota manera també ha estat suggerit que mecanismes post-sinàptics estan involucrats en la funció estriatal de CB1R depenent de A2AR. Ha estat demostrat prèviament que A2AR i CB1R formen heteròmers a cèl·lules HEK i a neuroblastomes humans. També s'ha observat que tots dos receptors co-localitzen i co-immunoprecipiten en teixit estriatal de rata. Als neuroblastomes humans, la senyalització de CB1R es va trobar que era completament depenent de l'activació de A2AR. D'acord amb això, el bloqueig de A2AR contrarestava els efectes motor-repressius produïts per l'administració d'agonistes de CB1R. Tot i que l'efecte de l'activació de A2AR sobre la funció de CB1R va ser estudiat, l'efecte de CB1R sobre la funció de A2AR no ha estat estudiada.

Discussió.

Els GPCR no es poden considerar com a unitats singulars de senyalització, si no que formen part d'agregats multimoleculars localitzats a la membrana plasmàtica. Un heteròmer de recpeotrs és un complex macromolecular format per almenys dues unitats de receptor funcionals amb propietats bioquímiques diferents dels seus receptors individuals. En aquest capítol s'han reportat algunes conclusions sobre les característiques bioquímiques dels heteròmers A2AR-CB1R. Primer de tot, mesurant l'activació de la proteïna G mitjançant assajos "label-free" a on s'ha demostrat que tant A2AR com CB1R es troben acoblats a proteïna Gi en l'heteròmer. Segon, s'ha observat un "cross-talk" a l'activació de la proteïna G quan els dos receptors es troben co-activats i és majoritàriament el CB1R qui controla la senyalització via ERK1/2. Finalment, s'ha demostrat que no hi ha cap efecte al·lostèric en la unió de lligands a l'heteròmer A2AR-CB1R.

En aquest capítol també s'ha demostrat que A2AR quan es troba expressat sol es troba acoblat a proteïna Gs, mentre que quan es troba co-expressat amb CB1R canvia a proteïna Gi tant en absència com en presència d'agonistes de CB1R. Així, l'heteròmer A2AR-CB1R d'alguna manera el CB1R bloqueja la producció de AMPc mediada pel A2AR.

Freqüentment, l'activació d'una unitat del receptor a l'heteròmer implica un "cross-talk" intermolecular que inclou canvis conformacionals que afecten a l'altra unitat de l'heteròmer. Aquests canvis conformacionals provoquen una modulació en la unió de lligands i/o senyalització en l'altra unitat de l'heteròmer. En el cas de l'heteròmer A2AR-CB1R, la unió de lligand a CB1R no modificava la unió de lligands a A2AR i viceversa , indicant una manca d'interaccions al·lostèriques per aquest heteròmer. De tota manera, es va observar un increment sinergístic en l'activació de proteïna Gi quan els dos receptors es trobaven co-activats. Aquests resultats estan en concordança amb el fet de que l'activació de A2AR és

necessària per a la senyalització de CB1R a les línies cel·lulars de neuroblastoma descrit anteriorment. Aquests resultats impliquen un processament d'informació, a nivell de membrana, dels senyals implicats en els heteròmers A2AR-CB1R. En aquest cas, aquest heteròmer de receptors funciona com a un processadir que modula la senyalització mediada per proteïna G ja que la senyalització tant quantitativa com qualitativament generada per l'estimulació de qualsevol de les unitats de receptor en l'heteròmer són diferents de les obtingudes amb la co-activació.

A part de la senyalització mediada per proteïna G, molts GPCR són capaços de senyalitzar per vies alternatives. La fosforilació de ERK1/2 es una de les vies de les MAPK que ha estat descrita com a via alternativa de senyalització independent de proteïna G. Comprovant la fosforilació de ERK1/2 quan els dos receptors de l'heteròmer es troben co-activats sembla que CB1R és qui controla principalment la senyalització. Donat que la fosforilació de ERK1/2 es troba implicada en la plasticitat neural, sembla ser que els cannabinoids podrien controlar canvis en la plasticitat neuronal a les cèl·lules a on es trobi present aquest heteròmer.

Els receptors d'adenosina A2AR estriatals es troben altament expressats a MSN de la via indirecta eferent així com també presinàpticament a teminals glutamatèrgics cortico-estriatals que contacten amb MSN de la via directa eferent i a totes dues localitzacions A2AR es troba co-distribuït amb CB1R. S'ha hipotetitzat que antagonistes postsinàptics de A2AR podrien ser útils per al tractament de la malaltia de Parkinson, mentre que antagonistes presinàptics de A2AR podrien ser beneficiosos en desordre discinètics com la malaltia de Huntington, desordres obsessius-compulsius i addiccions a drogues. D'aquesta manera seria interessant en un futur proper trobar un antagonista selectiu per A2AR o per a A2AR en l'heteròmer A2AR-CB1R degut a la seva rellevància com a element terapèutic.

CAPÍTOL 5.

Anàlisi d'antagonistes de A2AR en línies cel·lulars estables que expressen A2AR, A1R-A2AR, A2AR-D2R o A2AR-CB1R.

Està àmpliament provada la implicació dels receptors d'adenosina en diferents malalties i desordres com l'epilèpsia, malaltia de Parkinson, Huntington i altres disfuncions. A més, quan es té en compte l'heteromerització tal i com s'ha discutit en capítols anteriors, és particularment interessant la possibilitat de tenir caracteritzats una bateria d'antagonistes que siguin diferencialment selectius per A2AR depenent de qui sigui el receptor acompanyant en l'heteròmer. Degut a les diferent implicacions d'aquests heteròmers en diferents malalties i disfuncions, aquests antagonistes serien candidats potencials per al seu tractament.

Per tal de testar aquests compostos es varen utilitzar les línies cel·lulars estables utilitzades per al desenvolupament dels capítols anteriors. Aquestes són cèl·lules CHO que expressen A2AR, heteròmer A1R-A2AR, heteròmer A2AR-D2R o heteròmer A2AR-CB1R. Els experiments de competició per tal de trobar les constants de dissociació dels compostos candidats es van realitzar usant l'antagonista típic de A2AR, [3H] ZM 241385, el qual en els diferents assajos de competició era desplaçat pels diferents compostos. En total fins a la data d'escriptura d'aquesta tesi, catorze compostos van ser provats.

Discussió.

Al comparar totes les constants de dissociació obtingudes, dos compostos sobresortien en interès per sobre dels altres. El primer, el compost número quatre, mostrava una afinitat vint vegades millor per A2AR quan es trobava expressat en solitari a les cèl·lules que quan es trobava co-expressat en forma d'heteròmer amb A1R-A2AR o amb A2AR-CB1R, i més de mil vegades millor que quan es trobava co-expressat amb A2AR-D2R.

El segon compost interessant va ser el compost número nou. La unió d'aquest compost a A2AR quan es troba formant heteròmers amb D2R (A2AR-D2R) va ser sorprenentment bona, de fins a quatre vegades millor que al comparar-la amb A1R-A2AR i amb A2AR-CB1R. Aquesta diferència tot i no ser tant marcada com l'anterior compost és de molta importància ja que al comparar aquest resultats amb els dels altres compostos, el receptor A2A quan es troba unit al receptor D2 (i tal com es va discutir al capítol 3) mostra sempre afinitats molt pitjors que amb la resta d'heteròmers degut a la interacció al·lostèrica negativa produïda pel receptor de dopamina D2 sobre el receptor d'adenosina A2A.

Aquest compost número nou podria ser un bon candidat per a tractar malalties parkinsonianes al ser selectiu per a l'heteròmer A2AR-D2R tal i com s'ha discutit tant en el capítol 3 com 4. Seria interessant buscar compostos de característiques químiques similars per mirar de trobar un compost que idealment fos encara més selectiu per aquest heteròmer i poder augmentar així l'eficiència del potencial tractament.

CONCLUSIONS.

Les conclusions derivades del primer objectiu són:

- En la recaptació de GABA, l'adenosina te un efecte bifàsic, el qual està mediat pels heteròmers A1R-A2AR que es troben acoblats a proteïnes Gi/o i Gs. L'adenosina extracel·lular actuant sobre aquests heteròmers opera en el balanç de recaptació de GABA depenent de l'activitat PKA. La senyalització neural serà inhibitòria a baixa activació neuronal i facilitadora a alta activitat neuronal.
- L'adenosina, actuant a través de receptors d'adenosina als astròcits, podria contribuir a la neurotransmissió de manera dual, depenent la concentració d'adenosina extracellular, que a la seva vegada depèn del nivel d'activacio neuronal.
- BRET i experiments de "single molecule tracking" amb microscopi TIRF demostren que l'expressió mínima d'aquest heteròmer consta de quatre protomers i dues proteïnes G. La gran similitud entre GPCR suggereix que aquest model molecular podria ser aplicable a altres receptors.
- Aquests heteròmers poden formar-se a la membrana plasmàtica i són estables durant minuts. Aquesta estabilitat suggereix que el disseny de fàrmacs dirigits contra aquests heteròmers és una estratègia viable.
- L'orientació de les subunitats α de les proteïnes G es troba a la part distal dels receptors, suggerint que el "cross-talk" de les proteïnes G podria ocórrer a través dels receptors en el complex heteromeric.
- La unitat heteromèrica descrita, amb les seves limitacions dinàmiques i estructurals, proporciona un nou marc molecular per entendre perquè els heteròmers son unitats funcionals diferents i no únicament un agregat de dues entitats amb funcions independents.

Les conclusions derivades del segon objectiu són:

- En cultius cel·lulars, la unió d'agonistes i antagonistes a A2AR fa disminuir l'afinitat d'agonistes i antagonistes per al D2R.
- Aquestes interaccions negatives entre lligands són conseqüència d'interaccions al·lostèriques entre ambdós receptors que conformen l'heteròmer A2AR-D2R i constitueixen una unitat bioquímica.
- En teixit ex vivo, utilitzant aquestes interaccions al·lostèriques com a empremta bioquímica, ha estat demostrada l'expressió de l'heteròmer A2AR-D2R a estriat humà.
- El fet de que els antagonistes de A2AR són capaços de modular la farmacologia de D2R ha de ser tingut en compte per poder entendre patologies com la malaltia de Parkinson i per a la neuroimatge per PET.

Conclusions derivades del tercer objectiu:

- La presència física de D2R en l'heteròmer A2AR-D2R indueix una forta cooperativitat negativa a A2AR la qual va ser detectada per SCH 442416. Aquesta cooperativitat indica que el homodimers A2AR-A2AR es troben presents a l'heteròmer A2AR-D2R.
- Basant-nos en experiments in vitro i in vivo, el compost SCH 442416 va ser classificat com a preferentment antagonista de receptor A2A presinàptic, i el compost KW 6002 va ser classificat com a antagonista preferentment postsinàptic. Considerant això, SCH 442416 pot ser utilitzat per al desenvolupament de fàrmacs antidiscinètics per al tractament de la malaltia de Huntington, mentre que KW 6002 pot ser beneficiós per a tractar la malaltia de Parkinson.

Consclusions derivades del quart objectiu:

- A2AR canvia el seu acoblament a protein Gs per Gi quan passa a formar heteròmers amb CB1R i un "cross-talk" sinergísitc en activació de protein G s'observa quan tots dos receptors es troben co-activats.
- CB1R controla principalment la senyalització a través de ERK1/2 en l'heteròmer A2AR-CB1R.
- L'heteròmer A2AR-CB1R no mostra interaccions al·lostèriques a nivell d'unió de lligands.

Conclusions derivades del cinquè objectiu:

- El compost número nou podria ser un bon candidat per tractar la malaltia de Parkinson degut a la seva unió preferencial al receptor A2A present a l'heteròmer A2AR-D2R.